

An Efficient Method for the Synthesis of π -Expanded Phosphonium Salts

Krzysztof Górski,^a Łukasz W. Ciszewski,^a Antoni Wrzosek,^b Adam Szewczyk,^{*b} Andrzej Sobolewski^{*c} and Daniel T. Gryko^{*a}

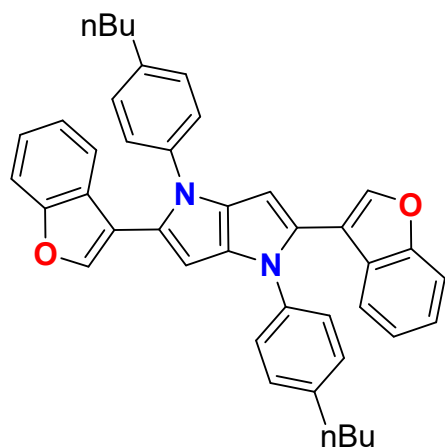
Table of context

1. Experimental.....	1
2. Synthetic procedures and compounds characterization data	2
3. NMR spectra	23
4. UV-Vis spectra.....	104
5. Electrochemistry.....	135
6. Computational studies.....	148
7. Bioimaging	166
8. X-ray analysis	168
9. References	175

1. Experimental

All chemicals were bought from Sigma Aldrich, TCI, Ambeed and AlfaAesar, and were used as received unless otherwise noted. All solvents used for the reaction were pure for analysis grade and were taken without further purification. 2-Bromo-4-*n*-butylaniline;¹ **1b**, **c** and (2-bromophenyl)diphenylphosphine oxide;² 2-(2-bromophenyl)-*N*-methylindole, **1f** and **1g**;³ 10,10,15,15-tetraethyl-5-oxatrxene;⁴ **1p**;⁵ **1q**;⁶ **1r**;⁷ 4,4,5,5-tetramethyl-2-(pyren-2-yl)-1,3,2-dioxaborolane;⁸ 9-(8-bromonaphthalen-1-yl)phenanthrene;⁹ and **1x**¹⁰ were synthesized according to literature procedures. All reactions requiring heating were carried out using an oil bath. All reported NMR spectra were recorded on a 400, 500 or 600 MHz spectrometer. Chemical shifts (δ ppm) for ^1H and ^{13}C { ^1H } NMR were determined vs solvent residual signal as the internal reference; J values are given in Hz. Due to C-F and C-P couplings, not all signals are visible in ^{13}C spectra. When C-P multiplets could be assigned, appropriate multiplicity was provided. UV-Vis absorption spectra were recorded in toluene, dichloromethane, tetrahydrofuran and acetonitrile in 1 cm quartz cuvettes at room temperature using dilute solutions ($C \approx 10^{-5}$ M) to avoid additional bands from aggregates and fluorescence reabsorption in emission spectra. Emission spectra were obtained upon excitation at 300 nm (for **2i,t,r,x**) or 350 nm (for rest salts). To determine the fluorescence quantum yield in solution, quinine sulphate solution in 0.5M H_2SO_4 ($\Phi=0.51$) was used as a standard. Solid state spectra as well as quantum yield were determined using an integrating sphere. Chromatography was performed on silica (Kieselgel 60, 200-400 mesh). Mass spectra were obtained with *an* EI ion source and the EBE double-focusing geometry mass analyzer or spectrometer equipped with an electrospray ion source with q-TOF type mass analyzer.

2. Synthetic procedures and compounds characterization data

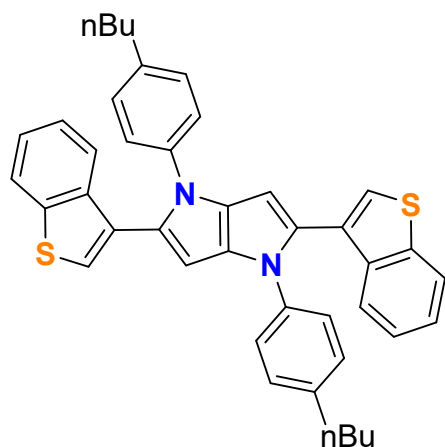


PP1: 4-n-Butylaniline (8 mmol) and 3-formylbenzo[b]furan (8 mmol) were dissolved in 6 mL of acetic acid, followed by heating up to 50 °C. After 1 h, butan-2,3-dione (4 mmol) and iron(III) perchlorate hydrate (0.024 mmol) were added. After 24 h, the reaction mixture was cooled to room temperature and filtrated. Afforded solid was washed with 2x10 mL of methanol and 2x10 mL of acetonitrile to obtain 318 mg (13.2 %) as a white solid.

¹H NMR: (500 MHz, CD₂Cl₂): δ 7.54 (d, *J* = 7.8 Hz, 2H), 7.48 (d, *J* = 8.2 Hz, 2H), 7.35 (d, *J* = 8.3 Hz, 4H), 7.30 (t, *J* = 7.7 Hz, 2H), 7.27 (s, 2H), 7.23 (d, *J* = 8.4 Hz, 4H), 7.18 (t, *J* = 7.5 Hz, 2H), 6.55 (s, 2H), 2.68 – 2.63 (m, 4H), 1.67 – 1.60 (m, 4H), 1.42 – 1.35 (m, 4H), 0.96 (t, *J* = 7.3 Hz, 6H).

¹³C {¹H} NMR: (126 MHz, CD₂Cl₂): δ 155.0, 141.7, 141.3, 137.4, 131.3, 129.2, 126.6, 125.7, 125.1, 124.1, 122.7, 120.9, 114.7, 111.2, 94.2, 35.1, 33.6, 22.3, 13.7..

HRMS (APCI) m/z: [M+H⁺] Calcd for C₄₂H₃₉N₂O₂ 603.3012; Found: 603.3016.

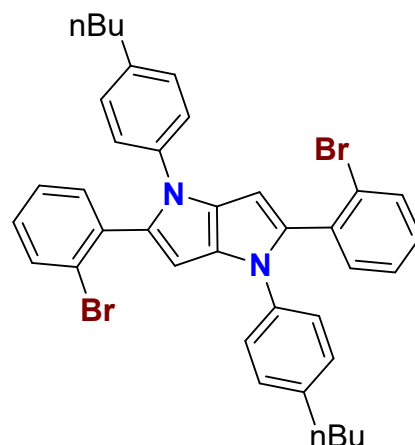


PP2: 4-n-Butylaniline (8 mmol) and 3-formylbenzo[b]thiophene (8 mmol) were dissolved in 6 mL of acetic acid, followed by heating up to 50 °C. After 1 h, butan-2,3-dione (4 mmol) and iron(III) perchlorate hydrate (0.024 mmol) were added. After 24 h, the reaction mixture was cooled to room temperature and filtrated. Afforded solid was washed with 2x10 mL of methanol and 2x10 mL of acetonitrile to obtain 1.05g (41.4 %) as a pale yellow solid.

¹H NMR: (500 MHz, CD₂Cl₂): δ 7.90 – 7.87 (m, 4H), 7.37 – 7.30 (m, 4H), 7.22 (d, *J* = 8.4 Hz, 4H), 7.13 (d, *J* = 8.4 Hz, 4H), 7.08 (s, 2H), 6.56 (s, 2H), 2.64 – 2.56 (m, 4H), 1.62 – 1.55 (m, 4H), 1.39 – 1.30 (m, 4H), 0.93 (t, *J* = 7.4 Hz, 6H).

¹³C {¹H} NMR: (126 MHz, CD₂Cl₂): δ 140.6, 139.8, 138.2, 137.5, 130.6, 129.4, 129.2, 128.9, 124.6, 124.3, 124.3, 124.2, 123.5, 122.5, 95.3, 35.0, 33.5, 22.3, 13.7.

HRMS (APCI) m/z: [M+H⁺] Calcd for C₄₂H₃₉N₂S₂ 632.2555; Found: 635.2549.

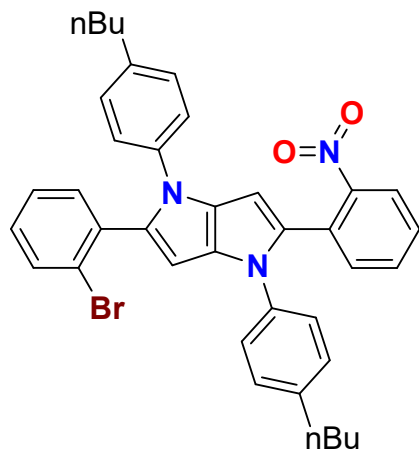


PP3: 4-n-Butylaniline (20 mmol) and 2-bromobenzaldehyde (20 mmol) were dissolved in 10 mL of acetic acid and 5 mL of toluene, followed by heating up to 50 °C. After 1 h, butan-2,3-dione (10 mmol) and iron(III) perchlorate hydrate (0.06 mmol) were added. After 24 h, the reaction mixture was cooled to room temperature and filtrated. Afforded solid was washed with 2x10 mL of methanol and 2x10 mL of acetonitrile to obtain 3.56g (52.3 %) as a white solid.

¹H NMR: (500 MHz, CD₂Cl₂): δ 7.59 (d, *J* = 8.0 Hz, 2H), 7.35 (dd, *J* = 7.6, 1.5 Hz, 2H), 7.30 – 7.25 (m, 2H), 7.17 (td, *J* = 7.9, 1.6 Hz, 2H), 7.15 – 7.11 (m, 8H), 6.43 (s, 2H), 2.63 – 2.58 (m, 4H), 1.64 – 1.56 (m, 4H), 1.41 – 1.34 (m, 4H), 0.95 (t, *J* = 7.4 Hz, 6H).

¹³C {¹H} NMR: (126 MHz, CD₂Cl₂): δ 140.1, 137.4, 135.1, 133.5, 133.1, 132.9, 129.7, 128.9, 128.8, 127.0, 124.5, 123.9, 96.0, 35.0, 33.5, 22.4, 13.7.

HRMS (APCI) m/z: [M+H⁺] Calcd for C₃₈H₃₇N₂Br₂ 679.1323; Found: 679.1328.

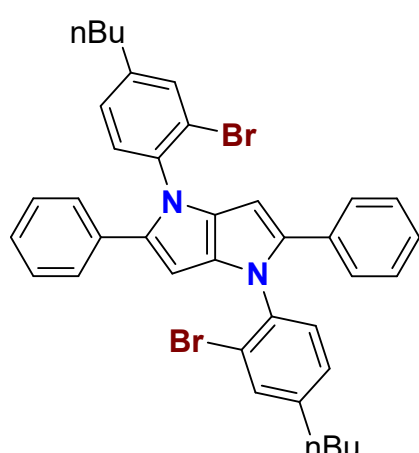


PP4: 4-n-Butylaniline (30 mmol), 2-bromobenzaldehyde (15 mmol) and 2-nitrobenzaldehyde (15 mmol) were dissolved in 15 mL of acetic acid, followed by heating up to 50 °C. After 1 h, butan-2,3-dione (15 mmol) and iron(III) perchlorate hydrate (0.09 mmol) were added. After 24 h, the reaction mixture was cooled to room temperature and filtrated. Crude mixture was dissolved in dichloromethane, adsorbed on celite, and purified via column chromatography using silica gel as stationary phase and hexane → 10% dichloromethane in hexane → 20% dichloromethane in hexane → 40% dichloromethane in hexane as eluent to obtain 1.39 g (14.3 %) of orange solid.

¹H NMR: (600 MHz, CD₂Cl₂): δ 7.74 (dd, *J* = 8.2, 0.9 Hz, 1H), 7.58 (d, *J* = 8.0 Hz, 1H), 7.54 (td, *J* = 7.6, 1.2 Hz, 1H), 7.48 (dd, *J* = 7.7, 1.3 Hz, 1H), 7.43 – 7.38 (m, 1H), 7.33 (dd, *J* = 7.6, 1.6 Hz, 1H), 7.26 (td, *J* = 7.5, 1.2 Hz, 1H), 7.16 (td, *J* = 7.8, 1.7 Hz, 1H), 7.12 (d, *J* = 3.6 Hz, 6H), 7.09 (d, *J* = 8.5 Hz, 2H), 6.39 (s, 1H), 6.38 (s, 1H), 2.59 (q, *J* = 7.8 Hz, 4H), 1.62 – 1.56 (m, 4H), 1.39 – 1.33 (m, 4H), 0.95 – 0.92 (m, 6H).

¹³C {¹H} NMR: (151 MHz, CD₂Cl₂): δ 148.9, 140.8, 140.3, 137.2, 136.4, 134.9, 134.4, 133.1, 133.0, 132.8, 132.3, 131.0, 130.0, 129.9, 129.1, 129.0, 128.8, 128.3, 127.8, 127.0, 124.4, 124.2, 124.1, 124.0, 95.7, 95.3, 35.0, 33.5, 33.5, 22.3, 22.2, 13.7.

HRMS (APCI) m/z: [M+H⁺] Calcd for C₃₈H₃₇N₃O₂Br 646.2069; Found: 646.2072.



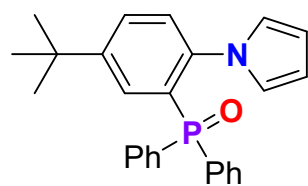
PP5: 2-Bromo-4-n-butylaniline (20 mmol) and benzaldehyde (20 mmol) were dissolved in 10 mL of acetic acid and 5 mL of toluene, followed by heating up to 50 °C. After 1 h, butan-2,3-dione (10 mmol) and iron(III) perchlorate hydrate (0.06 mmol) were added. After 24 h, to reaction mixture 25 mL of methanol was added and the solution was separated from gummy oil which was dissolved in dichloromethane and dried over MgSO₄. The crude mixture was adsorbed on silica gel, and purified via column chromatography using silica gel as stationary phase and hexane → 5% dichloromethane in hexane → 10% dichloromethane in hexane as eluent. Afforded solid was suspended in pentane and filtrated to obtain 1.14 g (16.8 %) as a white solid. (mixture of atropoisomers)

¹H NMR: (500 MHz, CD₂Cl₂): δ 7.60 – 7.56 (m, 2H), 7.25 – 7.15 (m, 10H), 7.14 – 7.08 (m, 3H), 7.05 (d, *J* = 8.0 Hz, 1H), 6.29 – 6.27 (m, 2H), 2.68 – 2.65 (m, 4H), 1.69 – 1.61 (m, 4H), 1.43 – 1.36 (m, 4H), 0.97 (t, *J* = 7.4 Hz, 6H).

¹³C {¹H} NMR: (126 MHz, CD₂Cl₂): δ 144.5, 144.4, 137.3, 137.1, 137.0, 133.6, 133.5, 133.4, 133.3, 132.4, 132.1, 129.94, 129.86, 128.3, 128.2, 128.1, 128.1, 127.3, 127.2, 125.9, 121.5, 121.4, 94.6, 94.1, 34.8, 33.2, 22.2, 13.6.

HRMS (APCI) m/z: [M+H⁺] Calcd for C₃₈H₃₇N₂Br₂ 679.1323; Found: 679.1324.

Synthetic procedures for phosphine oxides 1a-x:



1a: 1-(2-bromo-4-(*tert*-butyl)phenyl)-1*H*-pyrrole was synthesized according to Gross general procedure¹¹ from 1.20 g (5.26 mmol) of 2-bromo-4-(*tert*-butyl)aniline and 0.71 ml (5.52 mmol, 1.05 equiv.) of 2,5-dimethoxytetrahydrofuran to give 1.39 g (5.00 mmol, 95%) of crude pyrrole, which was used in the next step without further purification. To a solution of the latter (1.361 g, 4.89 mmol) in anhydrous THF (4 ml), stirred at -78 °C, 2.76 ml of 1.95 M solution of *n*-BuLi (5.38 mmol, 1.1 equiv.) was added dropwise. The mixture was stirred for 30 minutes after which 1.00 ml (5.28 mmol, 1.1 equiv.) of diphenylphosphinic chloride was added dropwise. The mixture was allowed to reach room temperature and was left to stir overnight. Then the mixture was quenched with water, the layers were separated and the aqueous phases was extracted with DCM three times. Combined organic phases were dried over Na₂SO₄, filtrated and evaporated in vacuo. Crude mixture was purified by column chromatography on silica gel using 2:1 AcOEt/hexane mixutre as eluent to give 239 mg (0.59 mmol, 12%) of (5-(*tert*-butyl)-2-(1*H*-pyrrol-1-yl)phenyl)diphenylphosphine oxide (**1a**) as a white solid.

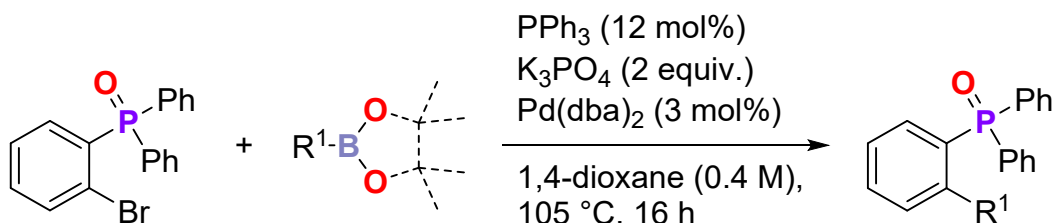
¹H NMR: (500 MHz, CDCl₃): δ 7.67 – 7.60 (m, 4H), 7.58 (ddd, *J* = 8.2, 2.3, 1.1 Hz, 1H), 7.46 – 7.31 (m, 7H), 7.27 (dd, *J* = 8.3, 4.9 Hz, 1H), 6.81 (t, *J* = 2.2 Hz, 2H), 5.86 (t, *J* = 2.1 Hz, 2H), 1.18 (s, 9H).

¹³C {¹H} NMR: (126 MHz, CDCl₃): δ 149.7 (d, *J* = 10.7 Hz), 142.2 (d, *J* = 4.4 Hz), 132.5 (d, *J* = 4.1 Hz), 132.1 (d, *J* = 91.7 Hz), 131.4 (d, *J* = 2.8 Hz), 131.2 (d, *J* = 9.6 Hz), 130.0 (d, *J* = 2.4 Hz), 128.1 (d, *J* = 12.2 Hz), 128.0 (d, *J* = 99.7 Hz), 127.7 (d, *J* = 7.8 Hz), 123.3, 109.2, 34.7, 31.0.

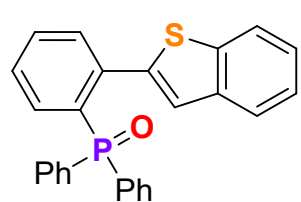
³¹P NMR (202 MHz, CDCl₃): δ 27.1.

HRMS (APCI) m/z: [M+H⁺] Calcd for C₂₆H₂₇NOP⁺ 400.1825; Found: 400.1829.

GP-1: General procedure for synthesis of phosphine oxides 1d-e, s-v:



A solution of (2-bromophenyl)diphenylphosphine oxide (1 equiv.), boronic acid or boronic pinacol ester (1 equiv.), triphenylphosphine (12 mol%), anhydrous tripotassium phosphate (2 equiv.) and bis(dibenzylideneacetone)palladium(0) (3 mol%) in anhydrous 1,4-dioxane (0.4 M), was stirred at 105 °C for 16 hours in a Schlenk vessel under argon atmosphere. The mixture was cooled down to room tempearature, diluted with water and extracted with DCM (x3). Combined organic layers were dried over Na₂SO₄, filtrated and evaporated in vacuo to give crude product which was purified by column chromatography.



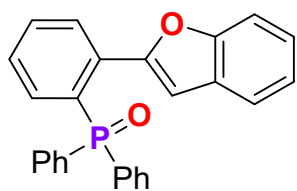
1d: Synthesised according to **GP-1** from 712 mg (2.00 mmol) of (2-bromophenyl)diphenylphosphine oxide and 355 mg (2.00 mmol) of benzo[*b*]thiophen-2-ylboronic acid. Crude product was purified by column chromatography on silica gel using 50-60% AcOEt/hexane mixture as eluent, giving 429 mg (1.05 mmol, 52%) of **1d** as a white solid.

¹H NMR: (400 MHz, CD₂Cl₂): δ 7.67 – 7.54 (m, 1H), 7.45 – 7.33 (m, 1H), 7.33 – 7.20 (m, 1H).

¹³C {¹H} NMR: (101 MHz, CD₂Cl₂): δ 141.7 (d, *J* = 4.5 Hz), 141.0, 140.3, 139.9 (d, *J* = 7.5 Hz), 135.1 (d, *J* = 11.9 Hz), 133.6 (d, *J* = 104.8 Hz), 133.5 (d, *J* = 101.5 Hz), 133.3 (d, *J* = 9.1 Hz), 132.4 (d, *J* = 2.5 Hz), 132.0 (d, *J* = 9.3 Hz), 131.7 (d, *J* = 2.8 Hz), 128.7 (d, *J* = 12.1 Hz), 128.3, 128.2, 127.9, 124.7 (d, *J* = 8.8 Hz), 124.5, 122.0.

³¹P NMR (162 MHz, CD₂Cl₂): δ 27.5.

HRMS (ESI) m/z: [M+H⁺] Calcd for C₂₆H₂₀OPS⁺ 411.0967; Found: 411.0969.



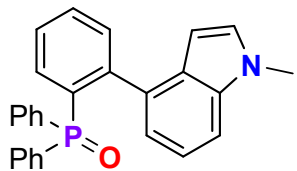
1e: Synthesised according to **GP-1** from 712 mg (2.00 mmol) of (2-bromophenyl)diphenylphosphine oxide and 355 mg (2.00 mmol) of benzofuran-2-ylboronic acid. Crude product was purified by column chromatography on silica gel using 60% AcOEt/hexane mixture as eluent, giving 481 mg (1.22 mmol, 61%) of **1e** as an off-white solid.

^1H NMR: (500 MHz, CD_2Cl_2): δ 7.89 (dd, $J = 7.8, 4.0$ Hz, 1H), 7.65 (td, $J = 12.1, 10.6, 5.1$ Hz, 5H), 7.51 – 7.27 (m, 10H), 7.25 – 7.07 (m, 3H).

$^{13}\text{C} \{^1\text{H}\}$ NMR: (126 MHz, CD_2Cl_2): δ 155.2, 154.1 (d, $J = 4.6$ Hz), 135.7, 135.6, 135.4 (d, $J = 11.2$ Hz), 133.9 (d, $J = 105.6$ Hz), 132.5 (d, $J = 2.5$ Hz), 132.1 (d, $J = 9.5$ Hz), 132.1 (d, $J = 99.4$ Hz), 131.9 (d, $J = 2.8$ Hz), 131.1 (d, $J = 9.3$ Hz), 129.3, 128.7 (d, $J = 12.1$ Hz), 124.9, 123.2, 121.9, 111.4, 108.9.

^{31}P NMR (202 MHz, CD_2Cl_2): δ 29.2.

HRMS (ESI) m/z: [$M+H^+$] Calcd for $\text{C}_{26}\text{H}_{20}\text{O}_2\text{P}^+$ 395.1195; Found: 395.1200.



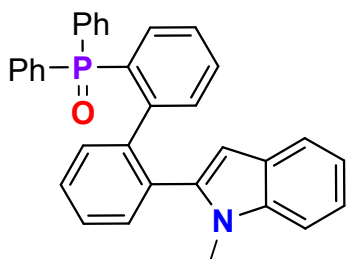
1h: (2-(1*H*-indol-4-yl)phenyl)diphenylphosphine oxide was synthesised according to **GP-1** from 712 mg (2.00 mmol) of (2-bromophenyl)diphenylphosphine oxide and 486 mg (2.00 mmol) of 4-(4,4,5,5-tetramethyl-1,3,2-dioxaborolan-2-yl)-1*H*-indole. 393 mg (1.00 mmol) of crude (2-(1*H*-indol-4-yl)phenyl)diphenylphosphine oxide was dissolved in anhydrous THF (5 ml), chilled to 0 °C, then 80 mg (2.00 mmol) of 60% (wt.) NaH suspension in mineral oil was added in one portion and the mixture was stirred for 1 hour, next 125 μl (2.00 mmol) of MeI was added to the reaction mixture. The solution was warmed to room temperature and stirred for additional 2 hours, then it was quenched with water, diluted with DCM and the layers were separated. Aqueous layer was extracted with DCM (3 times), combined organic phases were dried over Na_2SO_4 and concentrated *in vacuo*. Crude product was purified by column chromatography on silica gel using 3:2:1 AcOEt/hexane/DCM mixture as eluent, giving 350 mg (0.86 mmol, 43% over two steps) of **1h** as an off-white solid.

^1H NMR: (500 MHz, CD_2Cl_2): δ 7.70 – 7.48 (m, 5H), 7.47 – 7.18 (m, 6H), 7.13 – 6.86 (m, 7H), 6.05 (d, $J = 3.1$ Hz, 1H), 3.67 (s, 3H).

$^{13}\text{C} \{^1\text{H}\}$ NMR: (126 MHz, CD_2Cl_2): 146.5 (d, $J = 8.8$ Hz), 136.8, 134.9 (d, $J = 12.0$ Hz), 133.2 (d, $J = 4.0$ Hz), 133.0 (d, $J = 102.6$ Hz), 132.6 (d, $J = 9.7$ Hz), 131.8 (d, $J = 2.6$ Hz), 129.0, 128.3, 127.1 (d, $J = 12.3$ Hz), 122.7, 121.0, 109.3, 100.9, 33.2.

^{31}P NMR (202 MHz, CD_2Cl_2): δ 26.4.

HRMS (ESI) m/z: [$M+H^+$] Calcd for $\text{C}_{27}\text{H}_{23}\text{NOP}^+$ 408.1512; Found: 408.1516.



1i: Synthesised according to slightly modified literature procedure:¹² A round-bottom flask equipped with a stirring bar was charged with 2-(2-bromophenyl)-1-methyl-1*H*-indole (572 mg, 2.00 mmol), 4,4,4',4',5,5,5',5'-octamethyl-2,2'-bi(1,3,2-dioxaborolane) (533 mg, 2.10 mmol, 1.05 equiv.), potassium acetate (236 mg, 2.40 mmol, 1.2 equiv.) and bis(triphenylphosphine)palladium(II) dichloride (28 mg, 40 μmol , 2 mol%). To aid the stirring 3 ml of EtOH was added and the reaction vessel was transferred to a preheated oil bath (110 °C). During the reaction ethanol was allowed to evaporate. After full conversion of 2-(2-bromophenyl)-1-methyl-1*H*-indole

was observed by TLC (1 hour), potassium *tert*-butoxide (561 mg, 5.00 mmol, 2.5 equiv.), (2-bromophenyl)diphenylphosphine oxide (712 mg, 2.00 mmol, 1 equiv.) and ethanol (4 ml) was added and the mixture was refluxed for 16 hours. Then the reaction was cooled down, quenched with water, diluted with DCM and the aqueous layer was extracted with DCM (x3). Combined organic phases were dried over Na_2SO_4 and concentrated *in vacuo*. Crude product was purified by column chromatography on silica gel using 50%

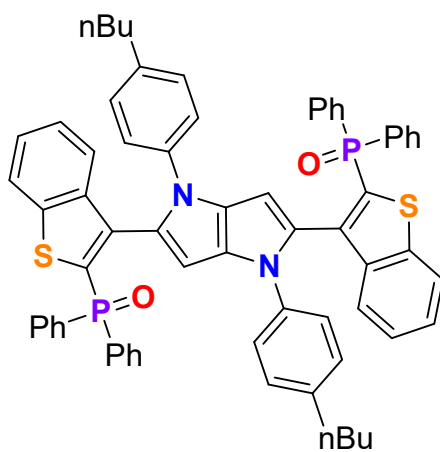
AcOEt/hexane mixture as eluent. Oily residue was then recrystallized from MeOH giving 675 mg (1.40 mmol, 70%) of **1i** as a white solid.

¹H NMR: (500 MHz, CD₂Cl₂): δ 7.63 – 7.52 (m, 3H), 7.51 – 7.29 (m, 9H), 7.28 – 7.10 (m, 8H), 7.06 – 7.00 (m, 1H), 7.00 – 6.91 (m, 1H), 6.20 (s, 1H), 3.59 (s, 3H).

¹³C {¹H} NMR: (126 MHz, CD₂Cl₂): δ 147.2 (d, *J* = 7.0 Hz), 142.0 (d, *J* = 3.4 Hz), 140.5, 138.0, 135.2 (d, *J* = 102.4 Hz), 134.6 (d, *J* = 104.2 Hz), 134.4, 134.3, 133.4 (d, *J* = 9.9 Hz), 132.4 (d, *J* = 4.1 Hz), 132.3 (d, *J* = 4.3 Hz), 132.1 (d, *J* = 2.8 Hz), 132.0 (d, *J* = 2.7 Hz), 131.4, 131.3, 131.3 (d, *J* = 2.5 Hz), 131.0 (d, *J* = 101.2 Hz), 129.0 (d, *J* = 12.0 Hz), 128.8 (d, *J* = 12.0 Hz), 128.4, 127.6, 127.4, 126.8 (d, *J* = 12.7 Hz), 121.5, 120.6, 119.8, 110.1, 104.2, 31.6.

³¹P NMR (202 MHz, CD₂Cl₂): δ 28.7.

HRMS (ESI) m/z: [M+Na⁺] Calcd for C₃₃H₂₆NOPNa⁺ 506.1644; Found: 506.1651.



1j: **PP2** (1 mmol) solution in 2 mL tetrahydrofuran was cooled to -78 °C under Ar atmosphere, followed by the addition of n-butyllithium solution in hexene (3 mmol, 2.5 M). Then obtained mixture was brought to room temperature - the mixture became dark - and once again cooled to -78 °C. After 1h at -78 °C, Ph₂POCl (3 mmol) was added and the solution was brought slowly to room temperature. Then 8 mL water, 8 mL dichloromethane were added, the organic layer was separated, the aqueous layer was extracted with dichloromethane, the combined extracts were dried over Na₂SO₄. The crude mixture was adsorbed on silica gel, and purified via column chromatography using silica gel as stationary phase and dichloromethane → 10% ethyl acetate in dichloromethane → 20% ethyl acetate in dichloromethane → 50% ethyl acetate in dichloromethane → 70% ethyl acetate in dichloromethane as eluent.

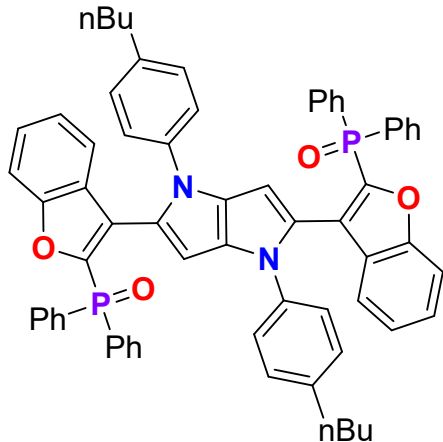
Then, the obtained residue was suspended in methanol and filtered to give 600 mg (58.0%) of a light yellow solid. (obtained as a mixture of atropoisomers)

¹H NMR: (600 MHz, CD₂Cl₂): δ 7.86 – 7.84 (m, 3H), 7.81 – 7.74 (m, 5H), 7.70 – 7.63 (m, 1H), 7.63 – 7.60 (m, 2H), 7.58 – 7.42 (m, 9H), 7.41 – 7.26 (m, 6H), 7.21 – 7.14 (m, 2H), 6.96 – 6.84 (m, 4H), 6.78 – 6.71 (m, 4H), 5.61 – 5.56 (m, 2H), 2.50 – 2.45 (m, 4H), 1.56 – 1.45 (m, 4H), 1.32 – 1.21 (m, 4H), 0.93 – 0.86 (m, 6H).

¹³C {¹H} NMR: (151 MHz, CD₂Cl₂): δ 141.4, 140.9, 139.8, 139.6, 137.2, 134.2, 133.4, 133.4, 132.6, 132.1, 132.0, 131.9, 131.8, 131.7, 131.6, 131.6, 129.5, 128.52, 128.49, 128.41, 128.39, 128.3, 126.4, 126.0, 124.7, 122.9, 122.8, 122.0, 121.9, 98.4, 34.8, 33.3, 22.1, 13.6.

³¹P NMR (243 MHz, CD₂Cl₂): δ 19.5.

HRMS (APCI) m/z: [M⁺] Calcd for C₆₇H₅₄N₂O₃S₃P₂F₃⁺ 1034.3258; Found: 1034.3242.



1k: **PP1** (0.5 mmol) solution in 2 mL tetrahydrofuran was cooled to -78 °C under Ar atmosphere, followed by the addition of n-butyllithium solution in hexene (1.5 mmol, 2.5 M). Then obtained mixture was brought to room temperature - the mixture became dark - and once again cooled to -78 °C. After 1 h at -78 °C, Ph₂POCl (1.5 mmol) was added and the solution was brought slowly to room temperature. Then 8 mL water, 8 mL dichloromethane were added, the organic layer was separated, the aqueous layer was extracted with dichloromethane, the combined extracts were dried over Na₂SO₄. The crude mixture was adsorbed on silica gel, and purified via column chromatography using silica gel as stationary phase and dichloromethane → 10% ethyl acetate in dichloromethane → 20% ethyl acetate in dichloromethane → 50% ethyl acetate in dichloromethane → 70% ethyl acetate in dichloromethane as eluent.

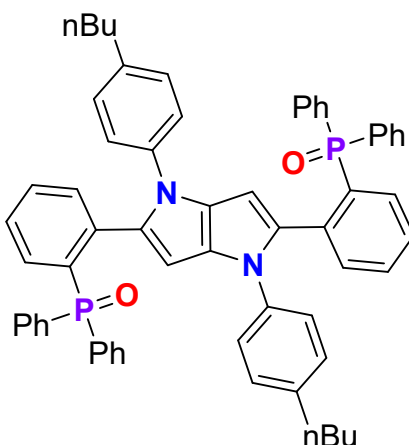
Then, the obtained residue was suspended in methanol and filtered to give 211 mg (42.1%) of a light yellow solid.

¹H NMR: (600 MHz, CD₂Cl₂): δ 7.67 (dd, *J* = 12.7, 7.6 Hz, 8H), 7.50 (t, *J* = 7.1 Hz, 4H), 7.48 – 7.44 (m, 2H), 7.42 – 7.36 (m, 8H), 7.36 – 7.33 (m, 4H), 7.16 (td, *J* = 7.4, 0.9 Hz, 2H), 7.07 (d, *J* = 8.4 Hz, 4H), 6.98 (d, *J* = 8.4 Hz, 4H), 6.16 (s, 2H), 2.54 – 2.49 (m, 4H), 1.56 – 1.51 (m, 4H), 1.34 – 1.27 (m, 4H), 0.91 (t, *J* = 7.4 Hz, 6H).

¹³C {¹H} NMR: (151 MHz, CD₂Cl₂): δ 156.3, 156.3, 140.1, 137.2, 131.92, 131.58, 131.51, 130.66, 128.76, 128.45, 128.40, 128.34, 128.3, 126.7, 123.6, 123.5, 122.7, 122.1, 111.7, 98.2, 34.9, 33.4, 22.2, 13.7.

³¹P NMR (243 MHz, CD₂Cl₂): δ 16.0.

HRMS (APCI) m/z: [M+H⁺] Calcd for C₆₆H₅₇N₂O₄P₂⁺ 1003.3794; Found: 1003.3786.



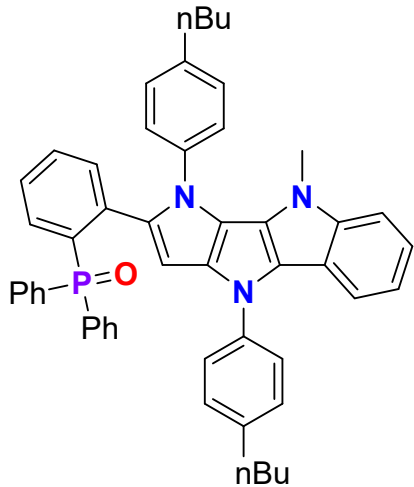
1l: The s-butyllithium solution in cyclohexane (12.5 mmol, 1.4 M) were mixed with 5 mL of dry tetrahydrafuran and cooled under Ar atmosphere to -75 °C followed by the addition of **PP3** (2.5 mmol) solution in 5 mL of tetrahydrofuran (made at reflux) - the cloudy mixture thickens and turns yellow. After 1 hour, Ph₂PCl (12.5 mmol) was added and the obtained solution was brought to room temperature. Then it was poured onto 100 mL of water and 100 mL of dichloromethane and 10 mL of saturated Na₂CO₃(aq) were added, the organic layer was separated and evaporated. Then it was dissolved in 10 mL of tetrahydrafuran and 1 mL of 30% H₂O₂ was added. After 20 min, 50 mL of dichloromethane and 50 mL of water were added, the organic layer was separated and dried over Na₂SO₄. The crude mixture was adsorbed on silica gel, and purified via column chromatography using silica gel as stationary phase and dichloromethane → 10% ethyl acetate in dichloromethane → 20% ethyl acetate in dichloromethane. The resulting solid was suspended in diethyl ether and filtered to give 1.30g (56.3%) of the product as a white solid. (mixture of atropoisomers)

¹H NMR: (500 MHz, CD₂Cl₂): δ 7.72 – 7.63 (m, 8H), 7.60 – 7.38 (m, 16H), 7.33 – 7.26 (m, 6H), 7.02 – 7.00 (m, *J* = 7.7, 4.2 Hz, 2H), 6.95 (d, *J* = 8.0 Hz, 4H), 6.74 (d, *J* = 7.8 Hz, 2H), 2.59 – 2.54 (m, 4H), 1.60 – 1.56 (m, 4H), 1.41 – 1.34 (m, 4H), 0.96 (t, *J* = 7.4 Hz, 6H).

¹³C {¹H} NMR: (126 MHz, CD₂Cl₂): δ 139.6, 136.9, 134.1, 134.0, 131.9, 131.8, 131.4, 129.4, 128.5, 128.4, 128.3, 124.2, 110.0, 97.8, 35.0, 33.5, 22.4, 13.7.

³¹P NMR (243 MHz, CD₂Cl₂): δ 28.4, 26.9.

HRMS (APCI) m/z: [M+H⁺] Calcd for C₆₂H₅₇N₂O₂P₂⁺ 923.3895; Found: 923.3887.



1m: STEP 1: **PP4** (2.75 mmol) was mixed with 14.5 mL triethyl phosphite, deaerated and heated to 160°C under an argon atmosphere. After 24 h, the excess triethyl phosphite was evaporated and the resulting oil was dissolved in hexane and quickly purified by chromatography using silica gel as a stationary phase and hexane → 20% dichloromethane in hexane as eluent. After evaporation, the obtained oil was dissolved in 5.5ml of dimethylformamide, cooled to 0 °C and deaerated, then KOH (5.5 mmol) was added. After 10 minutes to the orange solution CH₃I (5.5 mmol) was added. After 24 hours, 20 mL of water was added and extracted with diethyl ether 3x20 mL. The combined extracts were dried over MgSO₄ and evaporated. Due to the instability of the tripyrrole derivative, the raw product was used for the next step. STEP 2: Solution of s-butyllithium (6.1 mmol, 1.4 M in cyclohexane) [II] in 5ml of tetrahydrofuran was cooled under Ar atmosphere to -75 °C and solution of tripyrrole] in 5ml of tetrahydrofuran (prepared at boiling) was slowly added - the cloudy mixture thickens and turns yellow. After 1 h Ph₂PCl (6.1 mmol) was added and the obtained mixture was brought to room temperature. Then it was poured onto 100 mL of water and 100 mL of dichloromethane and 10 mL of saturated Na₂CO₃(aq) were added, the organic layer was separated and evaporated. Then it was dissolved in 10 mL of tetrahydrofuran and 0.5 mL of 30% H₂O₂ was added. After 20 min, 50 mL of dichloromethane and 50 mL of water were added, the organic layer was separated and evaporated. The obtained residue was suspended in diethyl ether and washed with hexane to obtain 1,00g (48.5%, after two steps) as a white solid.

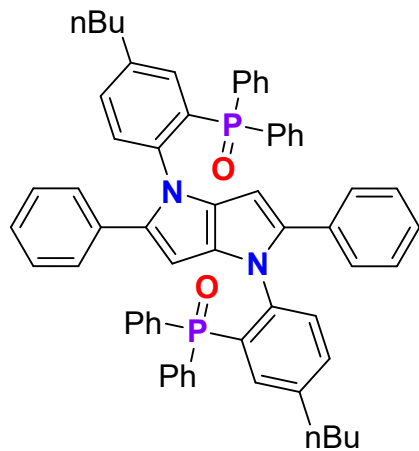
mixture thickens and turns yellow. After 1 h Ph₂PCl (6.1 mmol) was added and the obtained mixture was brought to room temperature. Then it was poured onto 100 mL of water and 100 mL of dichloromethane and 10 mL of saturated Na₂CO₃(aq) were added, the organic layer was separated and evaporated. Then it was dissolved in 10 mL of tetrahydrofuran and 0.5 mL of 30% H₂O₂ was added. After 20 min, 50 mL of dichloromethane and 50 mL of water were added, the organic layer was separated and evaporated. The obtained residue was suspended in diethyl ether and washed with hexane to obtain 1,00g (48.5%, after two steps) as a white solid.

¹H NMR: (500 MHz, CD₂Cl₂): δ 7.75 – 7.64 (m, 3H), 7.63 (d, *J* = 7.2 Hz, 2H), 7.54 (t, *J* = 8.0 Hz, 2H), 7.48 (dd, *J* = 12.9, 7.9 Hz, 1H), 7.44 – 7.41 (m, 4H), 7.33 – 7.26 (m, 10H), 7.18 (d, *J* = 8.2 Hz, 2H), 7.13 – 7.10 (m, 1H), 7.04 (bs, 1H), 5.69 (bs, 1H), 3.23 (bs, 3H), 2.73 (t, *J* = 7.8 Hz, 2H), 2.65 (t, *J* = 7.7 Hz, 2H), 1.77 – 1.70 (m, 2H), 1.66 – 1.59 (m, 2H), 1.53 – 1.45 (m, 2H), 1.40 – 1.32 (m, 2H), 1.04 (t, *J* = 7.3 Hz, 3H), 0.96 (t, *J* = 7.4 Hz, 3H).).

¹³C {¹H} NMR: (126 MHz, CD₂Cl₂): δ 142.7, 138.5, 137.7, 134.6, 133.9, 133.84, 133.80, 131.9, 131.8, 131.40, 131.38, 130.6, 129.2, 128.7, 128.4, 128.3, 128.2, 126.8, 126.7, 120.8, 97.9, 35.1, 33.9, 33.5, 32.1, 22.5, 22.2, 13.8, 13.7.

³¹P NMR (202 MHz, CD₂Cl₂): δ 27.9.

HRMS (APCI) m/z: [M+H⁺] Calcd for C₅₁H₄₉N₃OP⁺ 750.3613; Found: 750.3621.



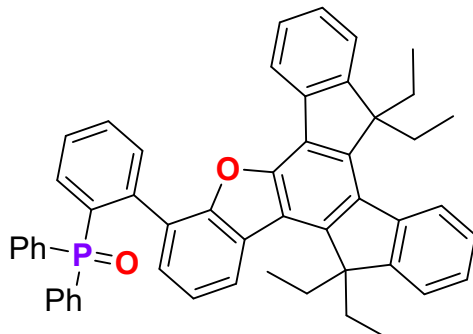
1n: The s-butyllithium solution in cyclohexane (7.5 mmol, 1.4 M) was mixed with 3 mL of dry tetrahydrofuran and cooled under Ar atmosphere to -75 °C followed by the addition of **PP5** (1.5 mmol) solution in 6 mL of tetrahydrofuran (made at reflux) - the cloudy mixture thickens and turns orange. After 1 hour, Ph₂PCl (7.5 mmol) was added and the obtained solution was brought to room temperature. Then it was poured onto 60 mL of water and 60 mL of dichloromethane and 6 mL of saturated Na₂CO₃(aq) were added, the organic layer was separated and evaporated. Then it was dissolved in 6 mL of tetrahydrofuran and 0.6 mL of 30% H₂O₂ was added. After 20 min, 50 mL of dichloromethane and 50 mL of water were added, the organic layer was separated and dried over Na₂SO₄, filtrated and evaporated. The resulting solid was suspended in diethyl ether and filtered to give 600mg (43.3%) of the product as a white solid.

¹H NMR: (500 MHz, CD₂Cl₂): δ 7.55 – 7.44 (m, 10H), 7.42 – 7.33 (m, 6H), 7.31 – 7.21 (m, 8H), 7.13 (dd, *J* = 8.2, 6.6 Hz, 4H), 7.09 – 7.05 (m, 2H), 7.01 (dd, *J* = 8.0, 4.8 Hz, 2H), 6.99 – 6.95 (m, 4H), 5.46 (s, 2H), 2.70 – 2.62 (m, 4H), 1.64 – 1.54 (m, 4H), 1.38 – 1.28 (m, 4H), 0.92 (t, *J* = 7.4 Hz, 6H).

^{13}C { ^1H } NMR: (126 MHz, CD_2Cl_2): δ 142.6, 142.5, 140.7, 140.7, 136.71, 135.17, 135.10, 133.82, 133.63, 132.98, 132.88, 132.85, 132.80, 132.0, 131.6, 131.5, 131.2, 131.2, 131.1, 131.0, 130.4, 127.8, 127.7, 127.7, 127.2, 125.3, 94.5, 35.0, 33.1, 22.1, 13.6.

^{31}P NMR (243 MHz, CD_2Cl_2): δ 24.8.

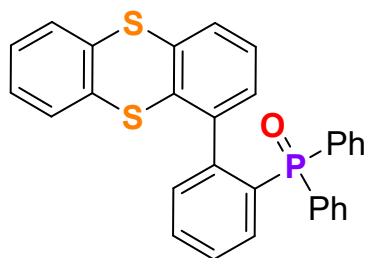
HRMS (APCI) m/z: [$M+\text{H}^+$] Calcd for $\text{C}_{62}\text{H}_{57}\text{N}_2\text{O}_2\text{P}_2^+$ 923.3895; Found: 923.3885.



1o: 10,10,15,15-tetraethyl-5-oxatruxene (1 mmol) was dissolved in 1ml of dry tetrahydrofuran at boiling, then cooled to 0 °C followed by the addition of n-butyllithium (1.2 mmol, 2.5 M in hexane) - the solution turned orange. After 1h at a constant temperature, trimethyl borate (1.2 mmol) was added and the mixture was brought to room temperature. After 1 h, (2-bromophenyl)diphenylphosphine oxide (1 mmol), tetrakis(triphenylphosphine)palladium(0) (0.02 mmol), 1 mL of dry tetrahydrofuran, and a solution of K_2CO_3 (6 mmol) in 1 mL of distilled water were added and the obtained mixture was heated up to 80 °C. After 24 h, 30 mL of water was added and extracted with

2x30mL of ethyl acetate. The combined extracts were dried over Na_2SO_4 . The crude mixture was adsorbed on silica gel, and purified via column chromatography using silica gel as stationary phase and 10% ethyl acetate in hexane → 20% ethyl acetate in hexane → 30% ethyl acetate in hexane as eluent. The resulting syellow oil was used without further purification.

HRMS (APCI) m/z: [$M+\text{H}^+$] Calcd for $\text{C}_{52}\text{H}_{46}\text{O}_2\text{P}^+$ 733.3235; Found: 733.3233.



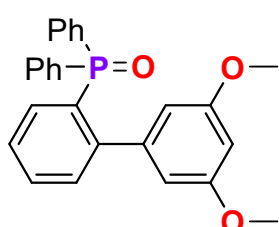
1s: Synthesised according to **GP-1** from 304 mg (0.85 mmol) of (2-bromophenyl)diphenylphosphine oxide and 221 mg (0.85 mmol) of thianthren-1-ylboronic acid. The crude product was purified via column chromatography using silica gel as stationary phase and hexane → 40% ethyl acetate in hexane → 80% ethyl acetate in hexane as eluent. Obtained residue was suspended in diethyl ether and filtered to give 134 mg (0.276 mmol, 33%) of a white solid.

^1H NMR: (500 MHz, CD_2Cl_2): δ 7.68 – 7.62 (m, 4H), 7.52 – 7.50 (m, 2H), 7.46 – 7.40 (m, 2H), 7.37 – 7.33 (m, 6H), 7.31 – 7.29 (m, 2H), 7.21 (dd, $J = 7.8, 1.3$ Hz, 1H), 7.05 (t, $J = 7.7$ Hz, 1H), 7.03 – 6.98 (m, 1H), 6.82 (td, $J = 7.7, 2.9$ Hz, 2H).

^{13}C { ^1H } NMR: (126 MHz, CD_2Cl_2): δ 135.9, 135.8, 135.2, 134.3, 134.1, 134.04, 133.97, 133.4, 132.53, 132.45, 132.0, 131.89, 131.82, 131.3, 131.1, 130.6, 130.5, 128.7, 128.6, 128.5, 128.3, 128.2, 128.1, 128.0, 127.8, 127.68, 127.66, 127.6, 127.4, 126.0.

^{31}P NMR (202 MHz, CD_2Cl_2): δ 25.7.

HRMS (ESI) m/z: [$M+\text{H}^+$] Calcd for $\text{C}_{30}\text{H}_{22}\text{S}_2\text{P}^+$ 493.0850; Found: 493.0852.



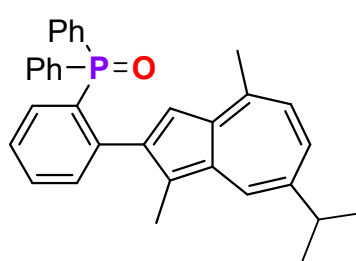
1t: Synthesised according to **GP-1** from 597 mg (1.67 mmol) of (2-bromophenyl)diphenylphosphine oxide and 304 mg (1.67 mmol) of (3,5-dimethoxyphenyl)boronic acid. Crude product was purified by column chromatography on silica gel using 60-70% AcOEt/hexane mixture as eluent, giving 525 mg (1.272 mmol, 76%) of **1t** as a white solid.

^1H NMR: (400 MHz, CD_2Cl_2): δ 7.63 – 7.50 (m, 5H), 7.47 – 7.29 (m, 9H), 6.40 (d, $J = 2.3$ Hz, 2H), 6.14 (t, $J = 2.3$ Hz, 1H), 3.63 (s, 6H).

^{13}C { ^1H } NMR: (101 MHz, CD_2Cl_2): δ 160.2, 147.9 (d, $J = 8.4$ Hz), 143.0 (d, $J = 4.2$ Hz), 134.7 (d, $J = 11.9$ Hz), 134.2 (d, $J = 104.1$ Hz), 132.3 (d, $J = 2.5$ Hz), 132.3 (d, $J = 101.8$ Hz), 132.1 (d, $J = 9.4$ Hz), 132.0 (d, $J = 9.7$ Hz), 131.6 (d, $J = 2.8$ Hz), 128.6 (d, $J = 12.0$ Hz), 127.4 (d, $J = 12.3$ Hz), 108.8, 100.7, 55.8.

^{31}P NMR (161 MHz, CD_2Cl_2): δ 27.1.

HRMS (ESI) m/z: [M+H⁺] Calcd for C₂₆H₂₄O₃P⁺ 415.1458; Found: 415.1461.



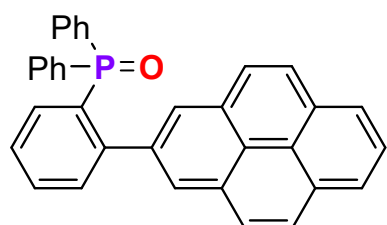
1u: Synthesised according to **GP-1** from 429 mg (1.20 mmol) of (2-bromophenyl)diphenylphosphine oxide and 410 mg (1.26 mmol) of 2-(7-isopropyl-1,4-dimethylazulen-2-yl)-4,4,5,5-tetramethyl-1,3,2-dioxaborolane. Crude product was purified by column chromatography on silica gel using 3:2:1 AcOEt/hexane/DCM mixture as eluent, giving 277 mg (0.584 mmol, 49%) of **1u** as a deep-blue solid.

¹H NMR: (600 MHz, CD₂Cl₂): δ 7.94 (d, *J* = 1.9 Hz, 1H), 7.72 (ddd, *J* = 13.5, 7.9, 1.4 Hz, 1H), 7.63 (tt, *J* = 7.5, 1.5 Hz, 1H), 7.45 (tdd, *J* = 7.7, 2.2, 1.3 Hz, 1H), 7.43 – 7.35 (m, 6H), 7.31 (t, *J* = 7.5 Hz, 2H), 7.22 – 7.16 (m, 4H), 6.96 (t, *J* = 5.3 Hz, 2H), 3.05 (hept, *J* = 6.9 Hz, 1H), 2.55 (s, 3H), 2.15 (s, 3H), 1.36 (d, *J* = 6.9 Hz, 6H).

¹³C {¹H} NMR: (151 MHz, CD₂Cl₂): δ 147.5 (d, *J* = 4.3 Hz), 144.9, 144.1 (d, *J* = 8.8 Hz), 140.9, 136.5, 136.1, 135.2, 134.5 (d, *J* = 11.3 Hz), 134.0 (d, *J* = 104.1 Hz), 133.9, 133.0 (d, *J* = 102.4 Hz), 132.5 (d, *J* = 9.9 Hz), 132.0 (d, *J* = 9.5 Hz), 131.7 (d, *J* = 2.6 Hz), 131.4 (d, *J* = 2.8 Hz), 128.2 (d, *J* = 12.0 Hz), 127.1 (d, *J* = 12.2 Hz), 125.9, 123.8, 117.5, 38.8, 25.1, 24.2, 11.2.

³¹P NMR (243 MHz, CD₂Cl₂): δ 26.5.

HRMS (ESI) m/z: [M+H⁺] Calcd for C₃₃H₃₂OP⁺ 475.2185; Found: 475.2194.



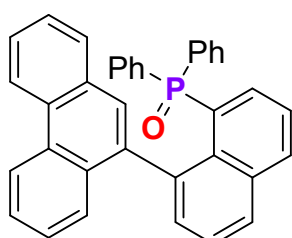
1v: Synthesised according to **GP-1** from 712 mg (2.00 mmol) of (2-bromophenyl)diphenylphosphine oxide and 656 mg (2.00 mmol) of 4,4,5,5-tetramethyl-2-(pyren-2-yl)-1,3,2-dioxaborolane. Crude product was purified by column chromatography on silica gel using 60-70% AcOEt/hexane mixture as eluent, giving 355 mg (0.743 mmol, 37%) of **1v** as a white solid.

¹H NMR: (400 MHz, CDCl₃): δ 8.15 (d, *J* = 7.6 Hz, 2H), 8.05 – 7.94 (m, 5H), 7.85 (d, *J* = 8.9 Hz, 2H), 7.70 – 7.41 (m, 9H), 7.19 – 7.12 (m, 2H), 7.10 – 7.00 (m, 4H).

¹³C {¹H} NMR: (101 MHz, CDCl₃): δ 147.8 (d, *J* = 8.6 Hz), 138.1 (d, *J* = 4.1 Hz), 134.2 (d, *J* = 11.8 Hz), 133.5, 132.7 (d, *J* = 102.0 Hz), 132.5 (d, *J* = 9.7 Hz), 132.5, 131.8 (d, *J* = 2.6 Hz), 131.6 (d, *J* = 9.4 Hz), 131.1 (d, *J* = 2.8 Hz), 130.7 (d, *J* = 111.2 Hz), 127.9 (d, *J* = 12.1 Hz), 127.7, 127.4, 127.0, 126.9 (d, *J* = 12.2 Hz), 125.9, 124.9, 124.4, 123.6.

³¹P NMR (161 MHz, CDCl₃): δ 27.5.

HRMS (ESI) m/z: [M+Na⁺] Calcd for C₃₄H₂₃OPNa⁺ 501.1379; Found: 501.1382.



1w: 9-(8-bromonaftalen-1-yl)phenanthrene (1 mmol) was dissolved in 2 mL of tetrahydrofuran and cooled to -78 °C in Ar atmosphere. After n-butyllithium (1.1 mmol, 2.5 M in hexane) was added - the mixture turned yellow, and after a while a yellow solid precipitated - the mixture was brought to room temperature. After 1h it was cooled again to -78 °C and Ph₂POCl (1.1 mmol) was added and the mixture was slowly warmed to room temperature. After 24 h 28 mL of dichloromethane was added, and the crude mixture was purified via chromatography on silica gel using hexane → 50% dichloromethane in hexane → dichloromethane → 40% ethyl acetate in hexane as eluent. The obtained solid residue was suspended in hexane and filtered off to give 173.5 mg (34.39%) of a light yellow solid.

¹H NMR: (500 MHz, CD₂Cl₂): δ 8.55 (s, 1H), 8.53 (s, 1H), 8.17 (d, *J* = 6.4 Hz, 1H), 8.07 (d, *J* = 8.2 Hz, 1H), 7.67 – 7.62 (m, 1H), 7.62 – 7.58 (m, 1H), 7.54 – 7.48 (m, 2H), 7.48 – 7.38 (m, 4H), 7.32 – 7.23 (m, 4H), 7.19 – 7.10 (m, 3H), 7.06 – 7.02 (m, 2H), 6.92 – 6.83 (m, 4H)..

¹³C {¹H} NMR: (126 MHz, CD₂Cl₂): δ 139.5, 138.0, 137.9, 135.4, 135.3, 133.9, 133.8, 133.8, 133.3, 133.0, 131.7, 130.93, 130.87, 130.85, 130.6, 130.5, 130.34, 130.28, 130.27, 130.2, 129.9, 129.19, 129.16, 127.9, 127.8, 127.6, 127.5, 127.3, 126.2, 125.9, 125.8, 125.7, 125.3, 123.7, 123.6, 122.3, 121.9.

^{31}P NMR (243 MHz, CD_2Cl_2): δ 31.7.

HRMS (APCI) m/z: $[M+\text{H}^+]$ Calcd for $\text{C}_{36}\text{H}_{26}\text{OP}^+$ 505.1721; Found: 505.1723.

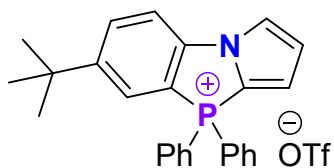
Synthesis of phosphonium salts 2a-x:

GP-2: General procedure for the synthesis of phosphonium salts at room temperature:

To a Schenk vessel charged with phosphine oxide (1 equiv.) and equipped with a stirring bar anhydrous DCM (0.1M) was added under argon atmosphere. Then Tf₂O (1.5 equiv. per reacting centre) was added and the mixture was stirred until complete conversion of the phosphine oxide was observed via TLC analysis. Upon reaction completion water and DCM was added, layers were separated and the aqueous phase was extracted with DCM (x2). Combined organic phases were concentrated *in vacuo*, and the residue was diluted with ethanol and evaporated (x2) to dispose traces of water. The crude product was purified by crystallization or column chromatography.

GP-3: General procedure for the synthesis of phosphonium salts from less active phosphine oxides:

To a Schenck vessel (*due to the high volatility of Tf₂O it is important to minimize available headspace in the reaction vessel to achieve efficient transformation*) charged with phosphine oxide (1 equiv.) and equipped with a stirring bar anhydrous toluene (0.1M) was added under argon atmosphere. Then 1.5 equiv. of Tf₂O was added and the mixture was stirred at 90 °C until complete conversion of the phosphine oxide was observed via TLC analysis. Upon reaction completion water and DCM was added, layers were separated and the aqueous phase was extracted with DCM (x2). Combined organic phases were concentrated *in vacuo*, and the residue was diluted with ethanol and evaporated (x2) to dispose traces of water. The crude product was purified by crystallization or column chromatography.



Salt 2a: Synthesised according to **GP-2** from phosphine oxide **1a** (101 mg, 0.252 mmol), no additional purification step was required to obtain 134 mg (0.252 mmol, quantitative) of **2a** as an off-white solid.

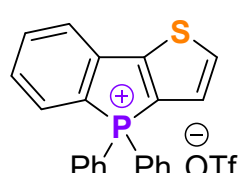
¹H NMR: (500 MHz, CDCl₃): δ 1H NMR (500 MHz, Chloroform-*d*) δ 7.99 (ddd, *J* = 3.6, 2.8, 1.1 Hz, 1H), 7.93 – 7.78 (m, 9H), 7.76 – 7.68 (m, 4H), 7.32 (ddd, *J* = 3.9, 1.9, 1.0 Hz, 1H), 6.68 (td, *J* = 3.8, 2.7 Hz, 1H), 1.34 (s, 9H).

¹³C {¹H} NMR: (126 MHz, CDCl₃): δ 152.0 (d, *J* = 10.6 Hz), 141.0 (d, *J* = 8.2 Hz), 136.0 (d, *J* = 3.2 Hz), 135.0 (d, *J* = 2.2 Hz), 133.4 (d, *J* = 12.5 Hz), 130.8 (d, *J* = 14.3 Hz), 128.5 (d, *J* = 7.7 Hz), 124.4 (d, *J* = 6.1 Hz), 123.5 (d, *J* = 12.8 Hz), 121.0 (q, *J* = 321.4 Hz), 118.2 (d, *J* = 11.4 Hz), 117.0 (d, *J* = 94.3 Hz), 114.4 (d, *J* = 7.1 Hz), 114.0 (d, *J* = 91.3 Hz), 109.9 (d, *J* = 128.4 Hz), 35.3, 31.2.

¹⁹F NMR (470 MHz, CDCl₃): δ -78.1.

³¹P NMR (202 MHz, CDCl₃): δ 4.8.

HRMS (ESI) m/z: [M⁺] Calcd for C₂₆H₂₅NP⁺ 382.1719; Found: 382.1729.



Salt 2b: Synthesised according to **GP-2** from phosphine oxide **1b** (90 mg, 0.250 mmol). Crude oily product was solubilized in minimal volume of EtOH, upon dropwise addition of Et₂O a yellowish solid precipitated. Filtration and washing with Et₂O yielded 69 mg (0.142 mmol, 57%) of **2b**.

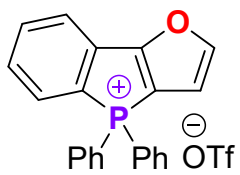
¹H NMR: (500 MHz, CD₂Cl₂): δ 8.16 (dd, *J* = 10.2, 7.6 Hz, 1H), 7.91 – 7.72 (m, 10H), 7.72 – 7.61 (m, 5H).

¹³C {¹H} NMR: (126 MHz, CDCl₃): δ 157.9 (d, *J* = 26.0 Hz), 139.0 (d, *J* = 15.6 Hz), 136.5 (d, *J* = 2.3 Hz), 136.1 (d, *J* = 3.3 Hz), 134.2 (d, *J* = 15.8 Hz), 133.4 (d, *J* = 12.1 Hz), 133.0 (d, *J* = 9.9 Hz), 131.0 (d, *J* = 13.8 Hz), 130.9 (d, *J* = 11.9 Hz), 126.7 (d, *J* = 14.7 Hz), 125.3 (d, *J* = 96.5 Hz), 123.6 (d, *J* = 8.8 Hz), 121.6 (d, *J* = 100.3 Hz), 121.0 (q, *J* = 320.8 Hz), 116.0 (d, *J* = 88.8 Hz).

¹⁹F NMR (470 MHz, CDCl₃): δ -78.1.

³¹P NMR (202 MHz, CDCl₃): δ 15.1

HRMS (ESI) m/z: [M⁺] Calcd for C₂₂H₁₆PS⁺ 343.0705; Found: 343.0714.



Salt 2c: Synthesised according to **GP-3** from phosphine oxide **1c** (86 mg, 0.250 mmol). Crude oily product was solubilized in minimal volume of *i*PrOH, upon dropwise addition of Et₂O a brownish solid precipitated. Filtration and washing with Et₂O yielded 81 mg (0.169 mmol, 68%) of **2c**.

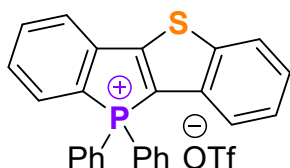
¹H NMR: (500 MHz, CD₂Cl₂): δ 8.08 (dd, *J* = 11.0, 7.6 Hz, 1H), 7.98 – 7.82 (m, 9H), 7.80 – 7.63 (m, 5H), 7.24 – 7.11 (m, 1H).

¹³C {¹H} NMR: (126 MHz, CD₂Cl₂): δ 168.5 (d, *J* = 33.5 Hz), 151.2 (d, *J* = 12.1 Hz), 136.8 (d, *J* = 3.3 Hz), 136.6 (d, *J* = 2.3 Hz), 134.3 (d, *J* = 11.0 Hz), 133.9 (d, *J* = 12.3 Hz), 133.6 (d, *J* = 9.1 Hz), 131.6 (d, *J* = 12.2 Hz), 131.3 (d, *J* = 14.1 Hz), 127.5 (d, *J* = 93.0 Hz), 122.4 (d, *J* = 8.5 Hz), 121.5 (q, *J* = 321.4 Hz), 115.9 (d, *J* = 91.2 Hz), 111.3 (d, *J* = 9.0 Hz), 105.7 (d, *J* = 118.2 Hz).

¹⁹F NMR (470 MHz, CD₂Cl₂): δ -78.9.

³¹P NMR (202 MHz, CD₂Cl₂): δ 12.4

HRMS (ESI) m/z: [M⁺] Calcd for C₂₂H₁₆OP⁺ 327.0933; Found: 327.0940.



Salt 2d: Synthesised according to **GP-2** from phosphine oxide **1d** (105 mg, 0.255 mmol). Crude oily product was solubilized in minimal volume of EtOH, upon dropwise addition of Et₂O a white solid precipitated. Filtration and washing with Et₂O yielded 81 mg (0.169 mmol, 68%) of **2d**.

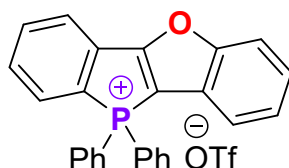
¹H NMR: (500 MHz, CDCl₃): δ 8.33 (dd, *J* = 10.5, 7.6 Hz, 1H), 8.07 (dt, *J* = 7.6, 1.9 Hz, 1H), 7.96 – 7.80 (m, 8H), 7.78 – 7.65 (m, 6H), 7.61 – 7.49 (m, 2H).

¹³C {¹H} NMR: (126 MHz, CDCl₃): δ 160.3 (d, *J* = 24.7 Hz), 143.5 (d, *J* = 13.9 Hz), 138.8 (d, *J* = 16.5 Hz), 136.6 (d, *J* = 2.2 Hz), 136.5 (d, *J* = 3.3 Hz), 134.7 (d, *J* = 13.5 Hz), 133.5 (d, *J* = 12.3 Hz), 133.2 (d, *J* = 10.3 Hz), 132.2 (d, *J* = 12.1 Hz), 131.3 (d, *J* = 14.0 Hz), 128.2, 127.4, 125.9 (d, *J* = 96.5 Hz), 125.0, 124.7 (d, *J* = 8.8 Hz), 122.3, 121.1 (d, *J* = 321.1 Hz), 115.7 (d, *J* = 99.6 Hz), 115.5 (d, *J* = 88.6 Hz).

¹⁹F NMR (470 MHz, CDCl₃): δ -78.1.

³¹P NMR (202 MHz, CDCl₃): δ 16.8.

HRMS (ESI) m/z: [M⁺] Calcd for C₂₆H₁₈PS⁺ 393.0861; Found: 393.0868.



Salt 2e: Synthesised according to **GP-2** from phosphine oxide **1e** (104 mg, 0.263 mmol). Crude oily product was solubilized in minimal volume of EtOH, upon dropwise addition of Et₂O a off-white solid precipitated. Filtration and washing with Et₂O yielded 93 mg (0.176 mmol, 68%) of **2e**

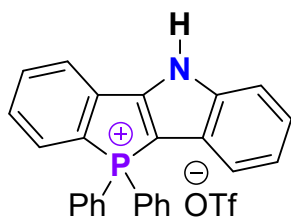
¹H NMR: (500 MHz, CDCl₃): δ 8.52 (dd, *J* = 11.1, 7.5 Hz, 1H), 8.03 – 7.92 (m, 5H), 7.92 – 7.86 (m, 1H), 7.85 – 7.77 (m, 4H), 7.72 (tt, *J* = 7.7, 4.0 Hz, 5H), 7.54 (dtd, *J* = 16.5, 7.4, 1.4 Hz, 2H).

¹³C {¹H} NMR: (126 MHz, CD₂Cl₂): δ 169.9 (d, *J* = 33.1 Hz), 159.8 (d, *J* = 11.6 Hz), 136.3 (d, *J* = 3.2 Hz), 136.0 (d, *J* = 2.3 Hz), 134.2 (d, *J* = 9.3 Hz), 133.3 (d, *J* = 12.4 Hz), 133.1 (d, *J* = 11.6 Hz), 132.9 (d, *J* = 12.3 Hz), 131.1 (d, *J* = 14.1 Hz), 127.8, 127.1 (d, *J* = 92.4 Hz), 126.9, 123.6 (d, *J* = 8.5 Hz), 122.9 (d, *J* = 8.6 Hz), 121.0 (q, *J* = 321.1 Hz), 120.3, 115.4 (d, *J* = 91.1 Hz), 113.7, 100.2 (d, *J* = 115.4 Hz).

¹⁹F NMR (470 MHz, CDCl₃): δ -78.1.

³¹P NMR (202 MHz, CDCl₃): δ 13.7.

HRMS (ESI) m/z: [M⁺] Calcd for C₂₆H₁₈OP⁺ 377.1090; Found: 377.1096.



Salt 2f: Synthesised according to **GP-2** from phosphine oxide **1f** (105 mg, 0.267 mmol). Crude oily product was solubilized in minimal volume of EtOH, upon dropwise addition of Et₂O a white solid precipitated. Filtration and washing with Et₂O yielded 96 mg (0.180 mmol, 68%) of **2f**.

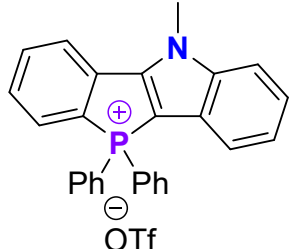
¹H NMR: (500 MHz, CD₂Cl₂): δ 12.61 (s, 1H), 8.34 (dd, *J* = 7.7, 3.6 Hz, 1H), 7.94 – 7.75 (m, 9H), 7.71 – 7.62 (m, 4H), 7.59 – 7.49 (m, 2H), 7.31 (dt, *J* = 29.1, 7.5 Hz, 2H).

¹³C {¹H} NMR: (126 MHz, CD₂Cl₂): δ 153.1 (d, *J* = 31.3 Hz), 142.4 (d, *J* = 12.1 Hz), 136.5 (d, *J* = 13.1 Hz), 135.8 (d, *J* = 2.2 Hz), 135.5 (d, *J* = 3.2 Hz), 133.0 (d, *J* = 12.1 Hz), 131.6 (d, *J* = 9.2 Hz), 130.5 (d, *J* = 13.6 Hz), 130.3 (d, *J* = 11.9 Hz), 128.4 (d, *J* = 94.6 Hz), 125.3 (d, *J* = 9.9 Hz), 125.0, 124.2 (d, *J* = 8.5 Hz), 123.8, 120.8 (q, *J* = 320.0 Hz), 118.6, 118.2 (d, *J* = 90.9 Hz), 115.2, 90.5 (d, *J* = 123.7 Hz).

¹⁹F NMR (470 MHz, CD₂Cl₂): δ -78.9.

³¹P NMR (202 MHz, CD₂Cl₂): δ 12.5.

HRMS (ESI) m/z: [M⁺] Calcd for C₂₆H₁₉NP⁺ 376.1250; Found: 376.1259.



Salt 2g: Synthesised according to **GP-2** from phosphine oxide **1g** 407.5 mg (1 mmol). The residue was suspended in 10 mL of 5% methanol in diethyl ether solution, and the yellow solid was filtrated to give 240mg (44%).

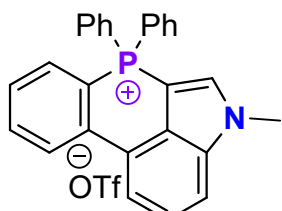
¹H NMR: (600 MHz, CD₂Cl₂): δ 8.17 (dd, *J* = 7.8, 3.9 Hz, 1H), 8.02 (dd, *J* = 11.1, 7.5 Hz, 1H), 7.91 (tt, *J* = 7.8, 1.1 Hz, 1H), 7.88 – 7.81 (m, 6H), 7.72 – 7.64 (m, 6H), 7.57 (d, *J* = 7.9 Hz, 1H), 7.52 – 7.47 (m, 1H), 7.40 – 7.36 (m, 1H), 4.28 (s, 3H).

¹³C {¹H} NMR: (151 MHz, CD₂Cl₂): δ 152.2 (d, *J_{P-C}* = 31.2 Hz), 143.5 (d, *J_{P-C}* = 11.4 Hz), 136.2 (d, *J_{P-C}* = 12.9 Hz), 135.8 (d, *J_{P-C}* = 2.1 Hz), 135.8 (d, *J_{P-C}* = 3.2 Hz), 133.1 (d, *J_{P-C}* = 12.2 Hz), 132.9 (d, *J_{P-C}* = 9.2 Hz), 130.7 (d, *J_{P-C}* = 12.1 Hz), 130.7 (d, *J_{P-C}* = 13.8 Hz), 128.9 (d, *J_{P-C}* = 94.0 Hz), 125.3, 124.9 (d, *J_{P-C}* = 9.5 Hz), 124.4, 123.8 (d, *J_{P-C}* = 9.0 Hz), 119.2, 117.6 (d, *J_{P-C}* = 91.4 Hz), 112.2 (d, *J_{P-C}* = 1.5 Hz), 91.5 (d, *J_{P-C}* = 122.6 Hz), 32.7.

¹⁹F NMR (470 MHz, CD₂Cl₂): δ -78.9.

³¹P NMR (243 MHz, CD₂Cl₂): δ 10.7.

HRMS (ESI) m/z: [M⁺] Calcd for C₂₇H₂₁NP⁺ 390.1412; Found: 390.1411.



Salt 2h: Synthesised according to **GP-2** from phosphine oxide **1h** (41 mg, 0.100 mmol) in the presence of 1.5 equiv of DIPEA. Crude oily product was solubilized in minimal volume of EtOH, upon dropwise addition of Et₂O brownish, needle-like crystals precipitated. Filtration and washing with Et₂O yielded 40 mg (0.075 mmol, 75%) of **2h**.

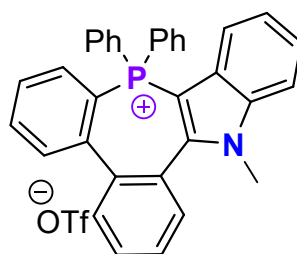
¹H NMR: (500 MHz, CDCl₃): δ 8.67 (d, *J* = 3.0 Hz, 1H), 8.53 (dd, *J* = 8.2, 5.8 Hz, 1H), 8.08 (d, *J* = 7.6 Hz, 1H), 7.88 (ddt, *J* = 8.6, 7.3, 1.4 Hz, 1H), 7.78 (ddd, *J* = 14.6, 7.8, 1.3 Hz, 1H), 7.75 – 7.66 (m, 6H), 7.65 – 7.58 (m, 6H), 7.54 (t, *J* = 7.9 Hz, 1H), 4.13 (s, 3H).

¹³C {¹H} NMR: (126 MHz, CDCl₃): δ 140.1 (d, *J* = 17.4 Hz), 139.1 (d, *J* = 4.3 Hz), 137.3 (d, *J* = 9.6 Hz), 134.7, 134.6 (d, *J* = 3.3 Hz), 133.3 (d, *J* = 11.8 Hz), 130.4 (d, *J* = 13.5 Hz), 128.9 (d, *J* = 13.3 Hz), 125.8 (d, *J* = 9.0 Hz), 125.4 (d, *J* = 6.9 Hz), 124.8, 123.4 (d, *J* = 93.1 Hz), 122.7, 122.7, 121.0 (q, *J* = 320.9 Hz), 118.3 (d, *J* = 1.7 Hz), 113.3, 113.1 (d, *J* = 91.4 Hz), 82.9 (d, *J* = 121.3 Hz), 34.7.

¹⁹F NMR (470 MHz, CDCl₃): δ -78.2.

³¹P NMR (202 MHz, CDCl₃): δ -1.3.

HRMS (ESI) m/z: [M⁺] Calcd for C₂₇H₂₁NP⁺ 390.1406; Found: 390.1410.



Salt 2i: Synthesised according to **GP-2** from phosphine oxide **1i** (146 mg, 0.302 mmol). Crude oily product was solubilized in minimal volume of EtOH, upon dropwise addition of Et₂O white solid precipitated. Filtration and washing with Et₂O yielded 110 mg (0.179 mmol, 59%) of **2i**.

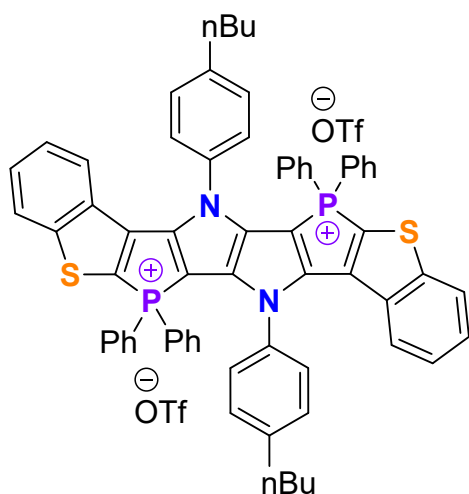
¹H NMR: (500 MHz, CD₂Cl₂): δ 8.07 (td, *J* = 7.6, 1.8 Hz, 1H), 7.95 – 7.80 (m, 4H), 7.74 – 7.52 (m, 6H), 7.52 – 7.21 (m, 9H), 7.11 (t, *J* = 7.7 Hz, 1H), 6.43 (d, *J* = 8.3 Hz, 1H), 3.98 (s, 3H).

¹³C {¹H} NMR: (126 MHz, CD₂Cl₂): δ 147.2 (d, *J* = 18.5 Hz), 144.1 (d, *J* = 8.3 Hz), 140.3 (d, *J* = 12.4 Hz), 138.3 (d, *J* = 3.1 Hz), 136.7 (d, *J* = 3.1 Hz), 136.5 (d, *J* = 10.9 Hz), 135.4 (d, *J* = 3.2 Hz), 135.0 (d, *J* = 2.7 Hz), 134.2 (d, *J* = 10.6 Hz), 133.6, 133.5 (d, *J* = 12.1 Hz), 132.1 (d, *J* = 10.7 Hz), 131.0 (d, *J* = 12.9 Hz), 131.0, 130.5, 130.2 (d, *J* = 13.7 Hz), 129.4, 129.0 (d, *J* = 12.7 Hz), 128.0 (d, *J* = 9.9 Hz), 127.3, 126.6 (d, *J* = 92.5 Hz), 125.1, 123.5, 121.6 (q, *J* = 320.9 Hz), 119.5, 117.8 (d, *J* = 91.4 Hz), 115.9 (d, *J* = 93.0 Hz), 112.3 (d, *J* = 1.5 Hz), 93.3 (d, *J* = 117.7 Hz), 33.7.

¹⁹F NMR (470 MHz, CD₂Cl₂): δ -78.0.

³¹P NMR (202 MHz, CD₂Cl₂): δ 10.7.

HRMS (ESI) m/z: [M⁺] Calcd for C₃₃H₂₅NP⁺ 466.1719; Found: 466.1726.



Salt 2j: Synthesised according to **GP-2** from phosphine oxide **1j** 517.6 mg (0.5 mmol) in the presence of 3 eq of DIPEA. The residue was suspended in 10 mL of 10% methanol in diethyl ether solution, and the obtained brick red solid was filtrated and washed with 10 mL of 10% methanol in diethyl ether solution to give 572mg (88%).

¹H NMR: (600 MHz, CD₂Cl₂): δ 7.91 – 7.88 (m, 6H), 7.69 – 7.66 (m, 8H), 7.59 (d, *J* = 7.4 Hz, 4H), 7.57 (d, *J* = 7.4 Hz, 4H), 7.52 (d, *J* = 8.1 Hz, 4H), 7.42 (t, *J* = 7.7 Hz, 2H), 7.25 (d, *J* = 8.0 Hz, 4H), 7.00 (t, *J* = 7.9 Hz, 2H), 5.95 (d, *J* = 8.5 Hz, 2H), 2.78 (t, *J* = 7.6 Hz, 4H), 1.69 – 1.64 (m, 4H), 1.39 – 1.33 (m, 4H), 1.00 (t, *J* = 7.4 Hz, 6H).

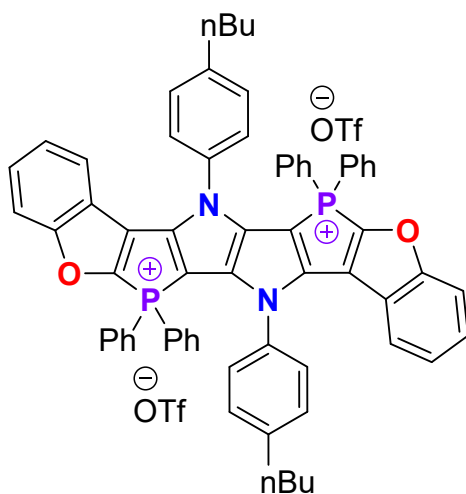
¹³C {¹H} NMR: (126 MHz, CD₂Cl₂): δ 149.3, 149.2, 147.3, 146.4, 146.18, 144.41, 144.33, 136.30, 135.00, 133.81, 133.77, 133.73,

130.8, 130.7, 130.7, 130.6, 130.6, 130.5, 128.3, 128.0, 126.2, 125.2, 123.9, 122.9, 122.2, 115.6, 115.0, 90.9, 90.1, 35.2, 33.8, 22.0, 13.6.

¹⁹F NMR (470 MHz, CD₂Cl₂): δ -78.9.

³¹P NMR (243 MHz, CD₂Cl₂): δ 9.4.

HRMS (APCI) m/z: [M⁺+CF₃SO₃⁺] Calcd for C₆₇H₅₄N₂O₃S₃P₂F₃⁺ 1149.2724; Found: 1149.2722.



Salt 2k: Synthesised according to **GP-2** from phosphine oxide **1k** 100.3 mg (0.1 mmol) in the presence of 3 eq of DIPEA. The residue was suspended in 10 mL of 10% methanol in diethyl ether solution, and the obtained orange solid was filtrated and washed with 10 mL of 10% methanol in diethyl ether solution to give 72mg (52%).

¹H NMR: (500 MHz, CD₂Cl₂): δ 7.95 – 7.90 (m, 4H), 7.73 – 7.69 (m, 8H), 7.66 – 7.58 (m, 10H), 7.55 (d, *J* = 7.9 Hz, 4H), 7.48 (t, *J* = 7.9 Hz, 2H), 7.28 (d, *J* = 7.7 Hz, 4H), 7.10 (t, *J* = 7.7 Hz, 2H), 6.03 (d, *J* = 8.1 Hz, 2H), 2.79 (t, *J* = 7.5 Hz, 4H), 1.69 – 1.63 (m, 4H), 1.34 (q, *J* = 7.5 Hz, 4H), 0.98 (t, *J* = 7.3 Hz, 6H).

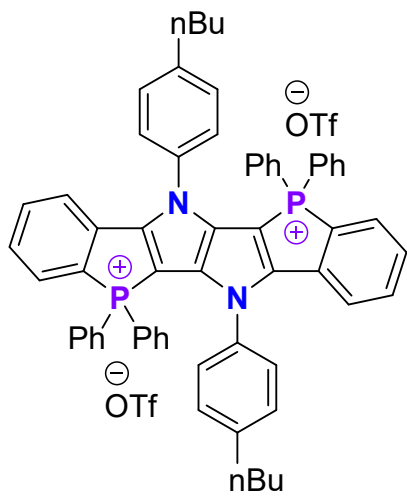
¹³C {¹H} NMR: (126 MHz, CD₂Cl₂): δ 163.5, 163.4, 147.1, 145.7, 144.7, 141.8, 141.6, 136.59, 136.58, 136.56, 133.98, 133.95, 133.9, 133.8, 133.7, 133.6, 132.43, 132.36, 132.3, 130.81, 130.75, 130.7,

130.4, 129.2, 127.6, 125.3, 122.3, 122.2, 120.12, 120.05, 119.7, 114.1, 113.4, 113.3, 85.6, 84.6, 35.1, 33.6, 21.9, 13.7.

¹⁹F NMR (470 MHz, CD₂Cl₂): δ -78.9.

³¹P NMR (243 MHz, CD₂Cl₂): δ 4.6.

HRMS (APCI) m/z: [M+OH⁺] Calcd for C₆₆H₅₅N₂O₃P₂⁺ 985.3688; Found: 985.3682.



Salt 2l: Synthesised according to **GP-2** from phosphine oxide **1l** 92.3 mg (0.1 mmol) in the presence of 3 eq of DIPEA. The residue was suspended in 10 mL of 10% methanol in diethyl ether solution, and the obtained yellow solid was filtrated and washed with 10 mL of 10% methanol in diethyl ether solution to give 75mg (63%).

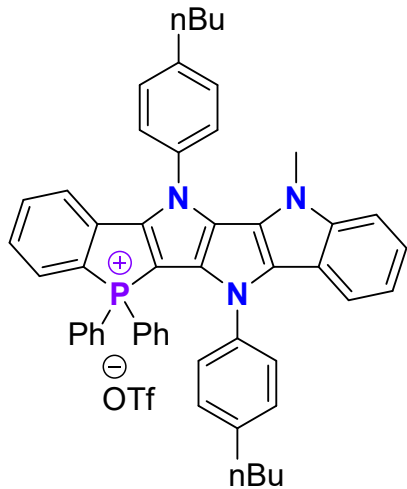
¹H NMR: (500 MHz, CD₂Cl₂): δ 7.90 – 7.85 (m, 4H), 7.72 – 7.67 (m, 2H), 7.67 – 7.63 (m, 8H), 7.50 – 7.41 (m, 16H), 7.20 (d, *J* = 7.9 Hz, 4H), 6.92 (dd, *J* = 7.9, 3.7 Hz, 2H), 2.73 (t, *J* = 7.7 Hz, 4H), 1.65 – 1.58 (m, 4H), 1.31 (q, *J* = 7.5 Hz, 4H), 0.96 (t, *J* = 7.4 Hz, 6H).

¹³C {¹H} NMR: (126 MHz, CD₂Cl₂): δ 148.1, 147.8, 146.6, 136.6, 136.5, 135.97, 135.95, 135.5, 134.2, 133.63, 133.58, 133.5, 133.2, 132.6, 132.5, 130.54, 130.49, 130.4, 130.3, 129.6, 129.5, 127.1, 126.3, 125.6, 122.34, 122.27, 122.2, 119.6, 116.2, 115.5, 35.1, 33.5, 22.1, 13.6.

¹⁹F NMR (470 MHz, CD₂Cl₂): δ -78.9.

³¹P NMR (243 MHz, CD₂Cl₂): δ 10.4.

HRMS (ESI) m/z: [M²⁺] Calcd for C₆₂H₅₄N₂P₂²⁺ 444.1876; Found: 444.1887.



Salt 2m: Synthesised according to **GP-2** from phosphine oxide **1m** 187.5 mg (0.25 mmol). The crude product was purified via column chromatography using silica gel as the stationary phase and dichloromethane → 50% ethyl acetate in dichloromethane → acetone as eluent. Obtained solid was dissolved in isopropanol and layered with pentane. After 24h orange solid was filtered to give 90 mg (41%).

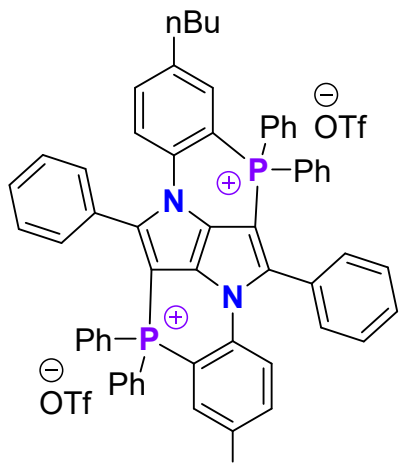
¹H NMR: (500 MHz, CD₂Cl₂): δ 7.85 (t, *J* = 7.5 Hz, 2H), 7.76 – 7.69 (m, 3H), 7.64 – 7.60 (m, 6H), 7.55 (d, *J* = 7.6 Hz, 2H), 7.52 (d, *J* = 7.1 Hz, 2H), 7.46 (t, *J* = 7.8 Hz, 1H), 7.41 (d, *J* = 8.0 Hz, 1H), 7.39 – 7.35 (m, 1H), 7.29 (d, *J* = 8.3 Hz, 1H), 7.24 – 7.21 (m, 3H), 7.08 (d, *J* = 7.9 Hz, 2H), 7.03 (t, *J* = 7.5 Hz, 1H), 6.76 (dd, *J* = 7.9, 3.7 Hz, 1H), 3.20 (s, 3H), 2.89 (t, *J* = 7.8 Hz, 2H), 2.66 (t, *J* = 7.6 Hz, 2H), 1.82 – 1.76 (m, 2H), 1.61 – 1.55 (m, 2H), 1.48 (q, *J* = 7.5 Hz, 2H), 1.33 (q, *J* = 7.5 Hz, 2H), 1.04 (t, *J* = 7.4 Hz, 3H), 0.96 (t, *J* = 7.4 Hz, 3H).

¹³C {¹H} NMR: (126 MHz, CD₂Cl₂): δ 146.8, 144.3, 144.1, 142.7, 140.5, 137.4, 137.3, 136.2, 135.63, 135.60, 135.4, 135.1, 133.5, 133.4, 132.6, 132.5, 130.6, 130.4, 130.3, 130.0, 129.7, 128.6, 128.5, 127.4, 126.8, 126.04, 125.95, 124.7, 124.6, 124.1, 122.1, 121.2, 121.1, 119.9, 118.7, 117.19, 117.10, 116.5, 115.1, 109.7, 35.4, 35.0, 33.7, 33.4, 31.8, 22.3, 22.1, 13.7, 13.7.

¹⁹F NMR (470 MHz, CD₂Cl₂): δ -78.9.

³¹P NMR (202 MHz, CD₂Cl₂): δ 9.5.

HRMS (ESI) m/z: [M⁺] Calcd for C₅₁H₄₇N₃P⁺ 732.3508; Found: 732.3493.



Salt 2n: Synthesised according to **GP-2** from phosphine oxide **1n** 92.3 mg (0.1 mmol) in the presence of 3 eq of DIPEA. The crude product was purified via column chromatography using silica gel as the stationary phase and ethyl acetate → 1% acetonitrile in ethyl acetate as eluent. The residue was suspended in 5% dichloromethane in ethyl acetate solution and the beige solid was filtered to give 41 mg (35%).

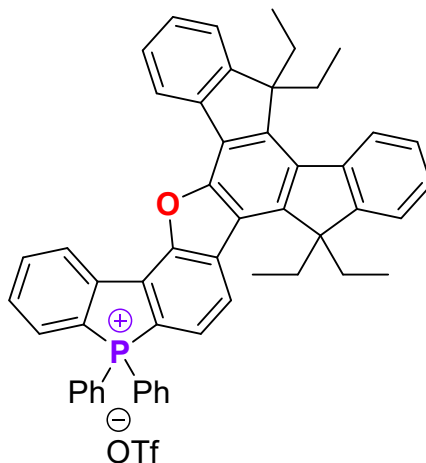
¹H NMR: (600 MHz, CD₂Cl₂): δ 7.82 – 7.80 (m, 4H), 7.65 – 7.60 (m, 14H), 7.60 – 7.57 (m, 3H), 7.44 – 7.39 (m, 9H), 7.36 – 7.35 (m, 3H), 7.33 – 7.30 (m, 2H), 2.56 (t, *J* = 7.7 Hz, 4H), 1.48 – 1.42 (m, 4H), 1.21 – 1.18 (m, 4H), 0.81 (t, *J* = 7.3 Hz, 6H).

¹³C {¹H} NMR: (151 MHz, CD₂Cl₂): δ 135.7, 135.48, 135.47, 135.3, 133.9, 133.8, 131.1, 130.3, 130.22, 130.15, 129.7, 129.6, 121.0, 120.4, 119.1, 34.5, 32.7, 21.9, 13.4.

¹⁹F NMR (470 MHz, CD₂Cl₂): δ -79.0.

³¹P NMR (243 MHz, CD₂Cl₂): δ 5.0.

HRMS (ESI) m/z: [M+CF₃SO₃⁺] Calcd for C₆₃H₅₄N₂O₃F₃SP₂⁺ 1037.3282; Found: 1037.3282.



Salt 2o: Synthesised according to **GP-3** from phosphine oxide **1o** 164.9 mg (0.225 mmol). The crude product was purified via column chromatography using silica gel as stationary phase and ethyl acetate → 10% acetonitrile in ethyl acetate → 50% acetonitrile in ethyl acetate as eluent. The residue was suspended in 10 mL of 10% isopropanol in a hexane solution and the white solid was filtered to give 87 mg (45%).

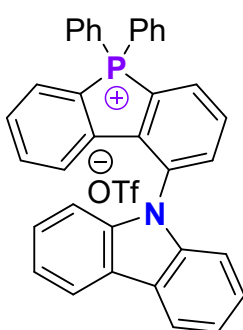
¹H NMR: (500 MHz, CD₂Cl₂): δ 9.05 (dd, *J* = 7.8, 3.3 Hz, 1H), 8.76 (dd, *J* = 8.1, 4.2 Hz, 1H), 8.46 (d, *J* = 7.5 Hz, 1H), 8.37 (d, *J* = 7.7 Hz, 1H), 8.25 (~t, *J* = 7.7 Hz, 1H), 8.20 (dd, *J* = 9.7, 7.9 Hz, 1H), 8.12 (dd, *J* = 9.5, 8.1 Hz, 1H), 7.96 – 7.84 (m, 7H), 7.80 – 7.76 (m, 4H), 7.68 (~td, *J* = 7.5, 1.3 Hz, 1H), 7.60 (d, *J* = 6.9 Hz, 1H), 7.57 (d, *J* = 7.0 Hz, 1H), 7.54 (d, *J* = 6.9 Hz, 1H), 7.50 (~td, *J* = 7.5, 1.4 Hz, 1H), 7.46 (~t, *J* = 6.9 Hz, 1H), 3.03 (dq, *J* = 14.5, 7.3 Hz, 2H), 2.81 (dq, *J* = 14.3, 7.1 Hz, 2H), 2.40 – 2.32 (m, 4H), 0.30 (t, *J* = 7.3 Hz, 6H), 0.23 (t, *J* = 7.3 Hz, 6H).

¹³C {¹H} NMR: (126 MHz, CD₂Cl₂): δ 152.5, 151.2, 150.7, 147.1, 146.2, 140.4, 138.1, 137.1, 136.5, 136.3, 133.5, 133.4, 132.4, 132.1, 131.3, 131.2, 131.0, 130.9, 127.9 127.5, 127.4, 127.3, 126.9, 126.2, 125.8, 125.7, 124.1, 122.6, 121.8, 118.1, 116.8, 116.1, 59.9, 57.2, 30.5, 29.7, 8.5, 8.1.

¹⁹F NMR (470 MHz, CD₂Cl₂): δ -78.9.

³¹P NMR (202 MHz, CD₂Cl₂): δ 24.1

HRMS (ESI) m/z: [M⁺] Calcd for C₅₂H₄₄OP⁺ 715.3130; Found: 715.3127.



Salt 2p: Synthesised according to **GP-3** from phosphine oxide **1p** (130 mg, 0.250 mmol). Crude oily product was solubilized in minimal volume of EtOH, upon dropwise addition of Et₂O a greenish solid precipitated. Filtration and washing with Et₂O yielded 123 mg (0.188 mmol, 75%) of **2p**.

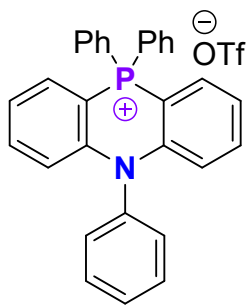
¹H NMR: (500 MHz, CD₂Cl₂): δ 8.36 (ddd, *J* = 10.2, 7.5, 1.2 Hz, 1H), 8.32 – 8.23 (m, 2H), 8.05 (dd, *J* = 10.4, 7.5 Hz, 1H), 8.00 – 7.87 (m, 8H), 7.85 – 7.74 (m, 4H), 7.55 (td, *J* = 7.6, 4.3 Hz, 1H), 7.39 (ddt, *J* = 10.8, 7.3, 3.8 Hz, 4H), 7.31 (tt, *J* = 7.8, 1.5 Hz, 1H), 7.09 (dd, *J* = 6.8, 2.0 Hz, 2H), 6.52 (dd, *J* = 8.1, 3.6 Hz, 1H).

¹³C {¹H} NMR: (126 MHz, CD₂Cl₂): δ 142.1 (d, *J* = 18.4 Hz), 141.8 (d, *J* = 19.2 Hz), 140.0, 138.9 (d, *J* = 2.6 Hz), 136.9 (d, *J* = 2.3 Hz), 136.4 (d, *J* = 3.2 Hz), 135.6 (d, *J* = 12.5 Hz), 133.6 (d, *J* = 11.7 Hz), 133.2, 133.1 (d, *J* = 5.1 Hz), 132.3 (d, *J* = 9.9 Hz), 131.5 (d, *J* = 12.0 Hz), 131.1 (d, *J* = 13.6 Hz), 127.0 (d, *J* = 9.9 Hz), 126.7, 123.9, 123.9 (d, *J* = 92.9 Hz), 121.1, 121.0 (q, *J* = 320.6 Hz), 120.9 (d, *J* = 93.5 Hz), 120.9, 115.9 (d, *J* = 88.1 Hz), 109.8.

¹⁹F NMR (470 MHz, CD₂Cl₂): δ -78.8.

³¹P NMR (202 MHz, CD₂Cl₂): δ 21.5.

HRMS (ESI) m/z: [M⁺] Calcd for C₃₆H₂₅NP⁺ 502.1719; Found: 502.1730.



Salt 2q: Synthesised according to **GP-3** from phosphine oxide **1q** 445.5 mg (1.0 mmol) in the presence of 3 eq of DIPEA. The crude product was purified via column chromatography using silica gel as stationary phase and dichloromethane → 10% acetone in dichloromethane → 20% acetone in dichloromethane → 40% acetone in dichloromethane as eluent. The residue was suspended in 10 mL of 10% isopropanol in diethyl ether solution and the white solid was filtered to give 495 mg (86%).

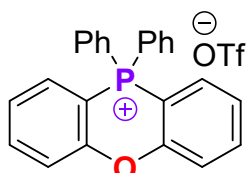
¹H NMR: (500 MHz, CD₂Cl₂): δ 7.89 (t, *J* = 7.5 Hz, 2H), 7.80 – 7.61 (m, 15H), 7.39 – 7.33 (m, 4H), 6.81 (dd, *J* = 8.8, 7.1 Hz, 2H).

¹³C {¹H} NMR: (126 MHz, CD₂Cl₂): δ 145.8 (d, *J_{P-C}* = 3.5 Hz), 138.9, 135.8, 135.3 (d, *J_{P-C}* = 3.1 Hz), 133.7 (d, *J_{P-C}* = 11.3 Hz), 132.4 (d, *J_{P-C}* = 7.1 Hz), 131.8, 130.5 (d, *J_{P-C}* = 13.5 Hz), 130.2, 130.0, 123.6 (d, *J_{P-C}* = 11.8 Hz), 120.7 (d, *J_{P-C}* = 93.6 Hz), 118.8 (d, *J_{P-C}* = 7.0 Hz), 96.4 (d, *J_{P-C}* = 92.2 Hz).

¹⁹F NMR (470 MHz, CD₂Cl₂): δ -78.9.

³¹P NMR (202 MHz, CD₂Cl₂): δ -2.3.

HRMS (APCI) m/z: [M⁺] Calcd for C₃₀H₂₃NP⁺ 428.1568; Found: 428.1566.



Salt 2r: Synthesised according to **GP-3** from phosphine oxide **1r** 370.4 mg (1.0 mmol). The crude product was purified via column chromatography using silica gel as stationary phase and dichloromethane → 10% acetone in dichloromethane → 20% acetone in dichloromethane → 40% acetone in dichloromethane as eluent. The residue was suspended in 10 mL of 10% isopropanol in diethyl ether solution and the white solid was filtered to give 316 mg (61%).

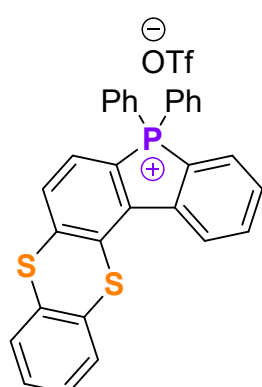
¹H NMR: (500 MHz, CD₂Cl₂): δ 7.97 (t, *J* = 8.3 Hz, 2H), 7.90 (t, *J* = 7.5 Hz, 2H), 7.77 – 7.65 (m, 12H), 7.60 – 7.57 (m, 2H).

¹³C {¹H} NMR: (126 MHz, CD₂Cl₂): δ 156.3 (d, *J_{P-C}* = 2.2 Hz), 137.7 (d, *J_{P-C}* = 1.9 Hz), 135.9 (d, *J_{P-C}* = 3.2 Hz), 133.7 (d, *J_{P-C}* = 11.7 Hz), 131.9 (d, *J_{P-C}* = 6.4 Hz), 130.7 (d, *J_{P-C}* = 13.8 Hz), 126.6 (d, *J_{P-C}* = 11.7 Hz), 120.1 (d, *J_{P-C}* = 6.1 Hz), 118.8 (d, *J_{P-C}* = 94.2 Hz), 98.9 (d, *J_{P-C}* = 92.6 Hz).

¹⁹F NMR (470 MHz, CD₂Cl₂): δ -78.9.

³¹P NMR (202 MHz, CD₂Cl₂): δ -8.3.

HRMS (ESI) m/z: [M⁺] Calcd for C₂₄H₁₈OP⁺ 353.1095; Found: 353.1096.



Salt 2s: Synthesised according to **GP-3** from phosphine oxide **1s** 24.6 mg (0.05 mmol). The crude product was purified via column chromatography using silica gel as the stationary phase and dichloromethane → 40% acetone in dichloromethane as eluent. The residue was dissolved in acetone and layered with hexane. After 24h, the formed pale yellow solid was filtrated to give 22mg (70%).

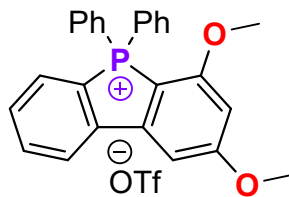
¹H NMR: (500 MHz, CD₂Cl₂): δ 9.52 (dd, *J* = 8.2, 3.9 Hz, 1H), 8.11 – 8.01 (m, 2H), 7.93 – 7.85 (m, 4H), 7.82 – 7.69 (m, 10H), 7.64 – 7.60 (m, 1H), 7.47 – 7.40 (m, 2H).

¹³C {¹H} NMR: (126 MHz, CD₂Cl₂): δ 136.7, 136.37, 136.35, 134.6, 133.5, 133.4, 132.53, 132.45, 131.3, 131.2, 131.0, 130.9, 130.8, 130.4, 130.3, 129.7, 129.4, 129.0, 128.9, 77.5.

¹⁹F NMR (470 MHz, CD₂Cl₂): δ -78.9.

³¹P NMR (202 MHz, CD₂Cl₂): δ 20.5.

HRMS (ESI) m/z: [M⁺] Calcd for C₃₀H₂₀S₂P⁺ 475.0744; Found: 475.0742.



Salt 2t: Synthesised according to **GP-2** from phosphine oxide **1t** (41 mg, 0.100 mmol). Crude oily product was solubilized in minimal volume of EtOH, upon dropwise addition of Et₂O white solid precipitated. Filtration and washing with Et₂O yielded 37 mg (0.067 mmol, 67%) of **2t**.

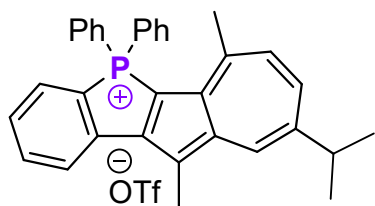
¹H NMR: (500 MHz, CDCl₃): δ 8.15 (dd, *J* = 7.9, 3.1 Hz, 1H), 7.96 – 7.90 (m, 1H), 7.87 (tt, *J* = 7.7, 1.4 Hz, 1H), 7.82 – 7.76 (m, 2H), 7.76 – 7.69 (m, 4H), 7.69 – 7.60 (m, 5H), 7.31 (t, *J* = 2.2 Hz, 1H), 6.66 (dd, *J* = 5.7, 1.8 Hz, 1H), 4.05 (s, 3H), 3.94 (s, 3H).

¹³C {¹H} NMR: (126 MHz, CDCl₃): δ 170.3, 164.1 (d, *J* = 4.9 Hz), 147.3 (d, *J* = 18.5 Hz), 143.7 (d, *J* = 19.3 Hz), 136.2, 135.7 (d, *J* = 3.2 Hz), 133.3 (d, *J* = 12.1 Hz), 131.7 (d, *J* = 4.2 Hz), 131.7 (d, *J* = 17.0 Hz), 130.6 (d, *J* = 13.9 Hz), 124.5 (d, *J* = 10.0 Hz), 122.8 (d, *J* = 93.6 Hz), 121.1 (d, *J* = 320.7 Hz), 117.2 (d, *J* = 90.3 Hz), 103.5 (d, *J* = 10.3 Hz), 99.7 (d, *J* = 7.6 Hz), 96.1 (d, *J* = 105.8 Hz), 57.1.

¹⁹F NMR (470 MHz, CDCl₃): δ -78.1.

³¹P NMR (202 MHz, CDCl₃): δ 23.2.

HRMS (ESI) m/z: [M⁺] Calcd for C₂₆H₂₂O₂P⁺ 397.1352; Found: 397.1356.



Salt 2u: Synthesised according to **GP-2** from phosphine oxide **1u** (48 mg, 0.100 mmol). Crude oily product was solubilized in minimal volume of EtOH, upon dropwise addition of Et₂O violet solid precipitated. Filtration and washing with Et₂O yielded 35 mg (0.058 mmol, 58%) of **2u**.

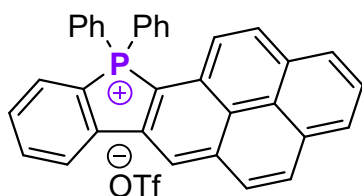
¹H NMR: (500 MHz, CDCl₃): δ 8.48 (t, *J* = 2.1 Hz, 1H), 8.21 (dd, *J* = 7.8, 3.4 Hz, 1H), 7.85 – 7.72 (m, 9H), 7.67 (td, *J* = 8.1, 3.6 Hz, 4H), 7.60 – 7.42 (m, 2H), 3.23 (hept, *J* = 6.9 Hz, 1H), 2.94 (s, 3H), 2.62 (s, 3H), 1.43 (d, *J* = 6.9 Hz, 6H).

¹³C {¹H} NMR: (126 MHz, CDCl₃): δ 153.9 (d, *J* = 23.1 Hz), 150.1, 148.8 (d, *J* = 12.9 Hz), 146.2, 143.0 (d, *J* = 9.0 Hz), 140.9 (d, *J* = 14.1 Hz), 139.0, 136.9, 135.5, 135.5, 134.0, 133.7 (d, *J* = 11.4 Hz), 132.4 (d, *J* = 97.4 Hz), 131.6 (d, *J* = 11.0 Hz), 131.3 (d, *J* = 12.3 Hz), 130.8 (d, *J* = 13.3 Hz), 125.7 (d, *J* = 8.7 Hz), 123.5 (d, *J* = 10.7 Hz), 121.1 (q, *J* = 321.1 Hz), 119.7 (d, *J* = 89.3 Hz), 96.9 (d, *J* = 114.8 Hz), 38.7, 28.5, 24.6, 12.1.

¹⁹F NMR (470 MHz, CDCl₃): δ -78.0.

³¹P NMR (202 MHz, CD₂Cl₃): δ 13.5.

HRMS (ESI) m/z: [M⁺] Calcd for C₃₃H₃₀P⁺ 457.2080; Found: 457.2089.



Salt 2v: Synthesised according to **GP-3** from phosphine oxide **1v** (120 mg, 0.250 mmol). Crude oily product was solubilized in minimal volume of EtOH, upon dropwise addition of toluene a yellow solid precipitated. Filtration and washing with toluene yielded 134 mg (0.220 mmol, 87%) of **2v**.

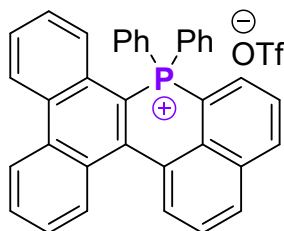
¹H NMR: (500 MHz, CD₂Cl₂): δ 8.95 (d, *J* = 2.9 Hz, 1H), 8.49 (dd, *J* = 7.8, 3.2 Hz, 1H), 8.46 – 8.35 (m, 4H), 8.31 (d, *J* = 8.9 Hz, 1H), 8.17 (t, *J* = 7.6 Hz, 1H), 8.10 – 7.99 (m, 2H), 7.98 – 7.86 (m, 6H), 7.73 (td, *J* = 7.8, 3.6 Hz, 5H), 7.31 – 7.14 (m, 1H).

¹³C {¹H} NMR: (126 MHz, CD₂Cl₂): δ 145.5 (d, *J* = 18.8 Hz), 142.7 (d, *J* = 19.7 Hz), 138.7, 138.5, 137.3, 136.7 (d, *J* = 3.3 Hz), 135.0 (d, *J* = 9.6 Hz), 134.3 (d, *J* = 11.8 Hz), 133.7, 133.2, 132.2 (d, *J* = 11.9 Hz), 132.0 (d, *J* = 10.4 Hz), 131.5 (d, *J* = 13.3 Hz), 130.7, 129.3 (d, *J* = 6.6 Hz), 129.1 (d, *J* = 101.8 Hz), 128.2 (d, *J* = 34.0 Hz), 125.9 (d, *J* = 10.8 Hz), 125.8, 124.7 (d, *J* = 10.0 Hz), 124.3, 124.0 (d, *J* = 95.7 Hz), 123.2 (d, *J* = 5.8 Hz), 121.6 (q, *J* = 320.9 Hz), 120.0 (d, *J* = 10.7 Hz), 116.9 (d, *J* = 86.7 Hz), 110.9 (d, *J* = 96.4 Hz).

¹⁹F NMR (470 MHz, CD₂Cl₂): δ -76.9.

³¹P NMR (202 MHz, CD₂Cl₂): δ 25.4.

HRMS (ESI) m/z: [M⁺] Calcd for C₃₄H₂₂P⁺ 461.1454; Found: 461.1462.



Salt 2w: Synthesised according to **GP-3** from phosphine oxide **1w** 151.4 mg (0.3 mmol). The crude product was purified via column chromatography using aluminum oxide as the stationary phase and ethyl acetate → acetonitrile as eluent. The residue was suspended in 10 mL of dichloromethane in diethyl ether and formed a pale yellow solid was filtrated to give 100mg (52%).

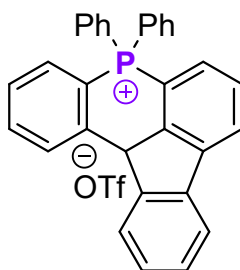
¹H NMR: (500 MHz, CD₂Cl₂): δ 8.91 (t, *J* = 8.4 Hz, 2H), 8.49 (d, *J* = 8.2 Hz, 1H), 8.34 (d, *J* = 7.4 Hz, 1H), 8.30 (d, *J* = 8.8 Hz, 2H), 8.07 – 7.88 (m, 5H), 7.86 – 7.73 (m, 8H), 7.64 (bs, 4H), 7.47 (t, *J* = 8.1 Hz, 1H).

¹³C {¹H} NMR: (126 MHz, CD₂Cl₂): δ 148.8 (d, *J_{P-C}* = 4.1 Hz), 138.7 (d, *J_{P-C}* = 3.4 Hz), 138.3 (d, *J_{P-C}* = 2.1 Hz), 138.0, 137.5 (d, *J_{P-C}* = 8.9 Hz), 137.3 (d, *J_{P-C}* = 2.3 Hz), 135.8 (d, *J_{P-C}* = 8.4 Hz), 134.6, 133.4 (d, *J_{P-C}* = 14.2 Hz), 133.2, 133.2 (d, *J_{P-C}* = 13.3 Hz), 132.0 (d, *J_{P-C}* = 11.8 Hz), 131.4, 131.3, 131.22, 131.16, 130.9, 130.3 (d, *J_{P-C}* = 1.2 Hz), 130.1 (d, *J_{P-C}* = 14.7 Hz), 130.1 (d, *J_{P-C}* = 15.0 Hz), 129.9, 129.2 (d, *J_{P-C}* = 8.1 Hz), 126.8 (d, *J_{P-C}* = 1.4 Hz), 126.4, 115.9 (d, *J_{P-C}* = 94.6 Hz), 111.2 (d, *J_{P-C}* = 88.8 Hz).

¹⁹F NMR (470 MHz, CD₂Cl₂): δ -78.9.

³¹P NMR (243 MHz, CD₂Cl₂): δ 1.7.

HRMS (ESI) m/z: [M⁺] Calcd for C₃₆H₂₄P⁺ 487.1616; Found: 487.1619.



Salt 2x: Synthesised according to **GP-3** from phosphine oxide **1x** (111 mg, 0.250 mmol). Crude oily product was solubilized in minimal volume of EtOH, upon dropwise addition of Et₂O a white solid precipitated. Filtration and washing with Et₂O yielded 109 mg (0.190 mmol, 76%) of **2x**.

¹H NMR: (500 MHz, CD₂Cl₂): δ 8.25 – 8.15 (m, 2H), 8.06 – 8.01 (m, 1H), 8.01 – 7.92 (m, 2H), 7.88 – 7.67 (m, 9H), 7.66 – 7.48 (m, 7H), 4.74 (d, *J* = 4.0 Hz, 1H).

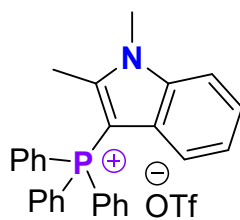
¹³C {¹H} NMR: (126 MHz, CDCl₃): δ 149.8 (d, *J* = 6.1 Hz), 142.0 (d, *J* = 5.8 Hz), 140.9 (d, *J* = 9.4 Hz), 140.4, 140.0, 136.6 (d, *J* = 3.2 Hz), 136.0 (d, *J* = 3.1 Hz), 135.1 (d, *J* = 2.3 Hz), 135.0 (d, *J* = 11.0 Hz), 134.5 (d, *J* = 10.3 Hz), 133.8 (d, *J* = 11.5 Hz), 131.1 (d, *J* = 13.4 Hz), 131.0 (d, *J* = 13.5 Hz), 130.6 (d, *J* = 12.0 Hz), 129.7 (d, *J* = 8.1 Hz), 129.1 (d, *J* = 7.0 Hz), 128.9 (d, *J* = 13.2 Hz), 127.7, 127.0 (d, *J* = 8.7 Hz), 126.1 (d, *J* = 3.1 Hz), 122.1, 121.1 (d, *J* = 321.5 Hz), 118.1 (d, *J* = 88.5 Hz), 115.7 (d, *J* = 88.9 Hz), 115.3 (d, *J* = 90.4 Hz), 114.6 (d, *J* = 88.5 Hz), 48.8 (d, *J* = 9.4 Hz).

¹⁹F NMR (470 MHz, CDCl₃): δ -78.0.

³¹P NMR (202 MHz, CDCl₃): δ 7.3.

HRMS (ESI) m/z: [M⁺] Calcd for C₃₁H₂₂P⁺ 425.1454; Found: 425.1458.

Intermolecular substitution



Salt 4a: N,2-dimethylindole (0.5 mmol) and triphenylphosphine oxide (0.5 mmol) were dissolved in dichloromethane under Ar atmosphere at room temperature. Then it was cooled to -78 °C, and trifluoromethanesulfonic anhydride (0.75 mmol) was added. After warming to room temperature, 50 mL of water and 50 mL of dichloromethane were added. The organic layer was separated and 50 mL of CHCl₃ was added and evaporated. The residue was suspended in a mixture of diethyl ether with propan-2-ol (19:1), and filtered, obtaining 126 mg (45.5 %) of a white solid.

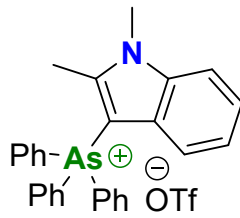
¹H NMR: (500 MHz, CD₂Cl₂): δ 7.90 – 7.86 (m, 3H), 7.79 – 7.69 (m, 12H), 7.56 (d, *J* = 8.4 Hz, 1H), 7.34 (t, *J* = 8.1 Hz, 1H), 6.98 (t, *J* = 7.7 Hz, 1H), 6.35 (d, *J* = 8.2, 1H), 3.86 (s, 3H), 1.95 (s, 3H).

¹³C {¹H} NMR: (126 MHz, CD₂Cl₂): δ 136.7, 136.37, 136.35, 134.6, 133.5, 133.4, 132.53, 132.45, 131.3, 131.2, 131.0, 130.9, 130.8, 130.4, 130.3, 129.7, 129.4, 129.0, 128.9, 77.5.

¹⁹F NMR (470 MHz, CD₂Cl₂): δ -79.0.

³¹P NMR (243 MHz, CD₂Cl₂): δ 11.4.

HRMS (ESI) m/z: [M⁺] Calcd for C₂₈H₂₅NP⁺ 406.1725; Found: 406.1722.



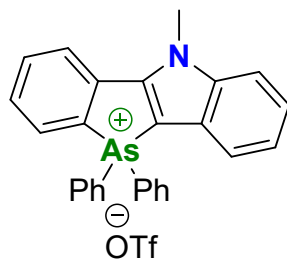
Salt 4b: N,2-dimethylindole (0.5 mmol) and triphenylarsine oxide (0.5 mmol) were dissolved in dichloromethane under Ar atmosphere at room temperature. Then it was cooled to -78 °C, and trifluoromethanesulfonic anhydride (0.75 mmol) was added. After warming to room temperature, 50 mL of water and 50 mL of dichloromethane were added. The organic layer was separated and 50 mL of CHCl₃ was added and evaporated. The residue was suspended in a mixture of diethyl ether with propan-2-ol (19:1), and filtered, obtaining 173 mg (57.7 %) of a white solid.

¹H NMR: (500 MHz, CD₂Cl₂): δ 7.88 – 7.83 (m, 3H), 7.75 – 7.71 (m, 12H), 7.56 (d, *J* = 8.4 Hz, 1H), 7.34 (t, *J* = 7.8 Hz, 1H), 7.00 (t, *J* = 8.1 Hz, 1H), 6.55 (d, *J* = 8.1 Hz, 1H), 3.86 (s, 3H), 2.11 (s, 3H).

¹³C {¹H} NMR: (126 MHz, CD₂Cl₂): δ 146.6, 138.2, 134.4, 132.6, 131.1, 128.0, 123.3, 122.7, 122.3, 118.4, 110.9, 30.8, 12.8.

¹⁹F NMR (470 MHz, CD₂Cl₂): δ -79.0.

HRMS (ESI) m/z: [M⁺] Calcd for C₂₈H₂₅NAs⁺ 450.1203; Found: 406.1201.



Salt 6: STEP 1 (AsBr₃ synthesis): Bromine (2.25 mmol) in 1 mL of pentane was added to arsenic (1.5 mmol) cooled to -78 °C under Ar atmosphere and then brought to room temperature. After 1 h solvent was evaporated under reduced pressure, and the solid residue (light yellow solid) was dissolved in 1 mL of dry tetrahydrofuran. STEP 2 (arsine synthesis): To a solution of s-butyllithium (2 mmol, 1.4 M in cyclohexane) in 1 mL of dry tetrahydrofuran cooled to -78 °C under Ar atmosphere, a mixture of 2-(2-bromophenyl)-N-methylindole (1 mmol) in 1mL of dry tetrahydrofuran was added. After 1 h phenylmagnesium bromide (3 mmol, 1 M in diethyl ether) was added, followed by the addition of AsBr₃ solution. The obtained mixture was warmed to room temperature - the solution became a cloudy light yellow color. After 24 h, 20 mL of water was added and extracted with 4x20mL of dichloromethane, the organic layer was separated, dried over MgSO₄ and evaporated. The crude arsine was dissolved in hexane and purified via column chromatography (to remove AsPh₃) using silica gel as stationary phase and hexane → 10% dichloromethane in hexane → 20% dichloromethane in hexane as eluent to obtain 93.1 mg of oil. Arsine undergoes decomposition, thus was used to immediately the next step. STEP 3: The obtained oil was dissolved in 2 mL of dry 1,2-dichloroethane, di-*t*-butylperoxide (1 mmol) was added followed by the addition of trifluoromethanesulfonic anhydride (1 mmol). Then, the mixture was heated to ~40 oC to initiate

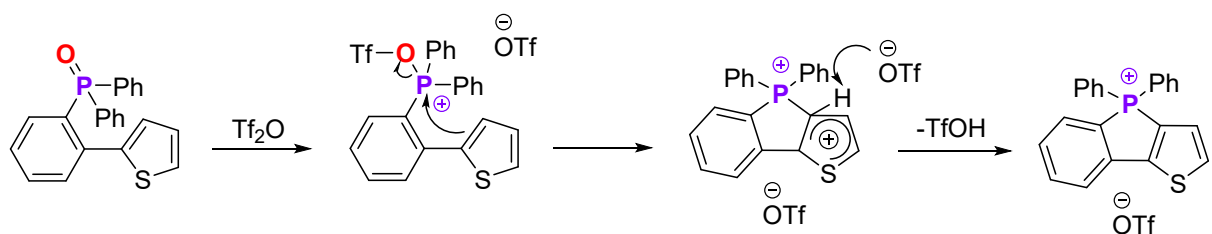
the reaction. After 0.5h, 10 mL of distilled water was added and extracted with 3x10 mL CHCl₃. The combined extracts were evaporated and the crude product was purified via chromatography using silica gel as stationary phase and dichloromethane → 10% acetone in dichloromethane → 20% acetone in dichloromethane → 50% acetone in dichloromethane as eluent. The brown residue was suspended in a mixture of diethyl ether with propane-2-ol (19:1), to give 72 mg (57.7%, after step 3, the overall yield is 12.3%) of a pale yellow solid.

¹H NMR: (500 MHz, CD₂Cl₂): δ 8.23 (d, *J* = 7.8 Hz, 1H), 8.07 (d, *J* = 7.6 Hz, 1H), 7.90 (t, *J* = 7.7 Hz, 1H), 7.86 – 7.79 (m, 6H), 7.74 – 7.69 (m, 4H), 7.68 (d, *J* = 9.9 Hz, 2H), 7.61 (d, *J* = 7.9 Hz, 1H), 7.50 (t, *J* = 8.2 Hz, 1H), 7.38 (t, *J* = 7.5 Hz, 1H), 4.31 (s, 3H).

¹³C {¹H} NMR: (126 MHz, CD₂Cl₂): δ 149.4, 142.9, 135.5, 135.0, 134.9, 132.9, 132.1, 131.3, 130.8, 130.6, 125.2, 125.1, 124.5, 123.9, 121.2, 119.0, 111.9, 94.4, 32.8.

¹⁹F NMR (470 MHz, CD₂Cl₂): δ -78.9.

HRMS (ESI) m/z: [M⁺] Calcd for C₂₇H₂₁NAs⁺ 434.0890; Found: 434.0892.



Scheme S1

3. NMR spectra

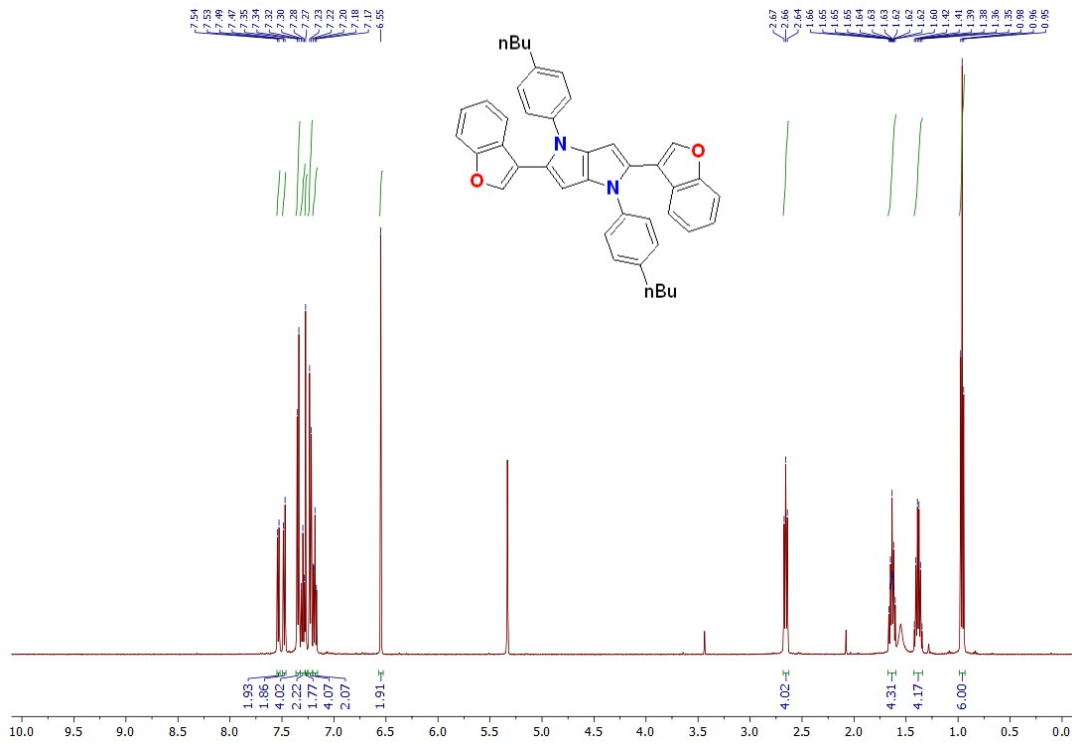


Figure S1: 500 MHz ^1H NMR spectrum of PP1 in CD_2Cl_2

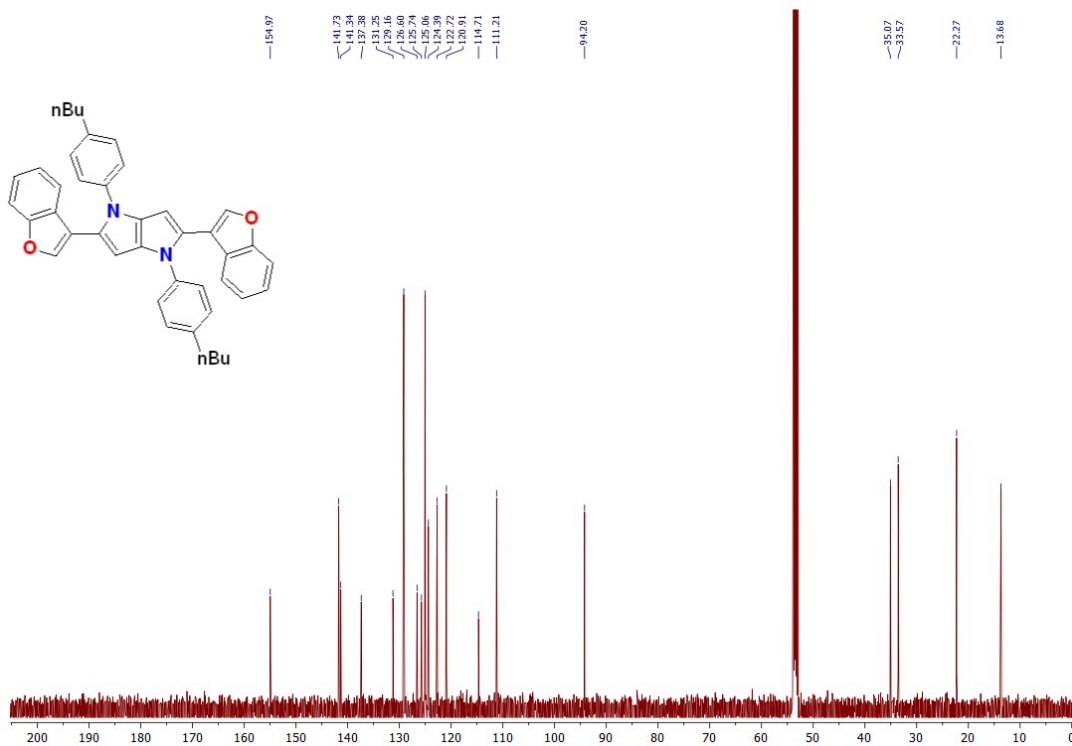


Figure S2: 126 MHz ^{13}C { ^1H } NMR spectrum of PP1 in CD_2Cl_2

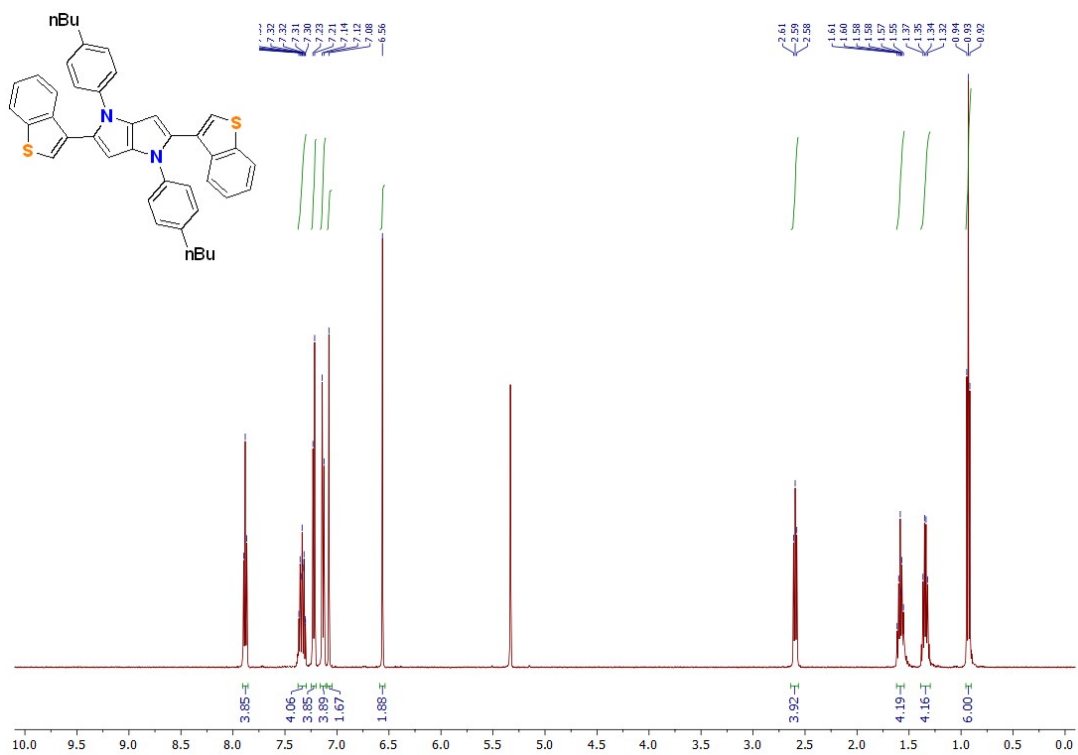


Figure S3: 500 MHz ^1H NMR spectrum of PP2 in CD_2Cl_2

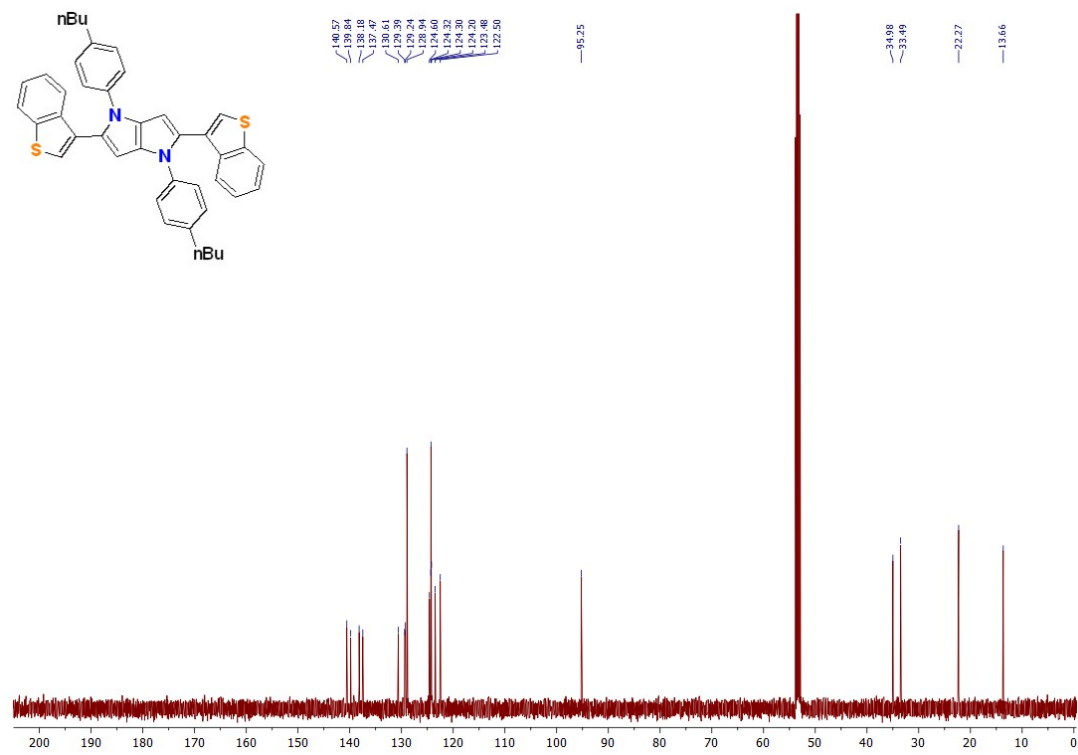


Figure S4: 126 MHz ^{13}C { ^1H } NMR spectrum of PP2 in CD_2Cl_2

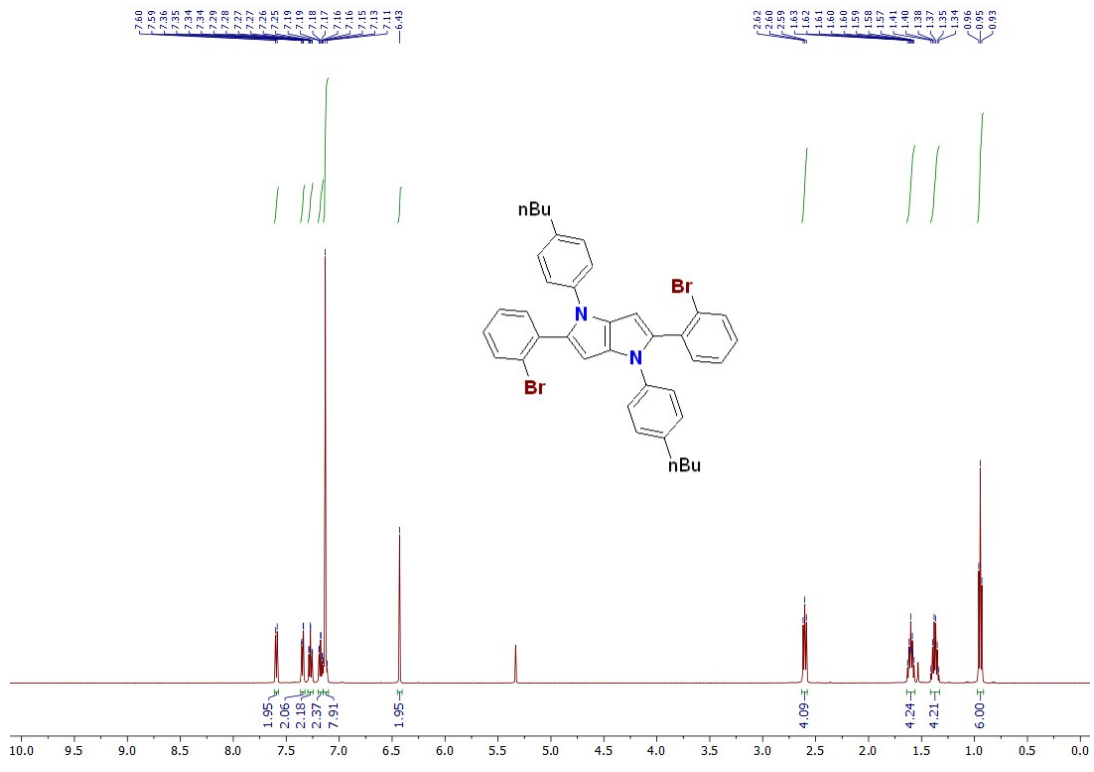


Figure S5: 500 MHz ^1H NMR spectrum of PP3 in CD_2Cl_2

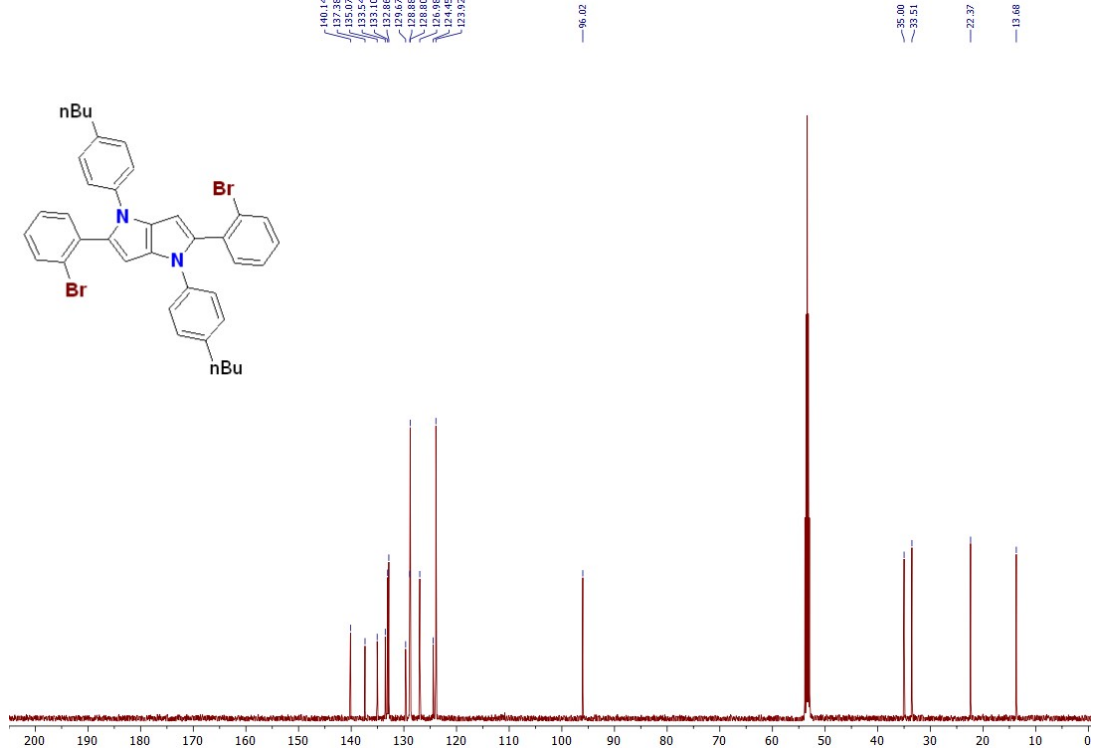


Figure S6: 126 MHz ^{13}C { ^1H } NMR spectrum of PP3 in CD_2Cl_2

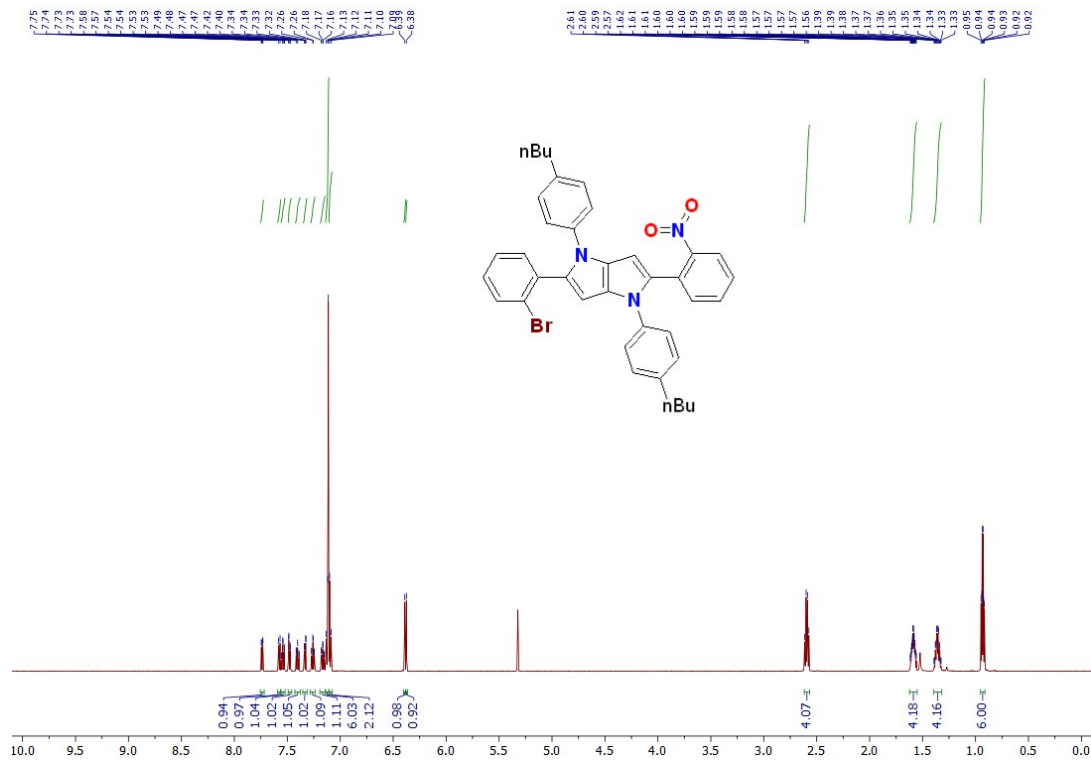


Figure S7: 600 MHz ^1H NMR spectrum of PP4 in CD_2Cl_2

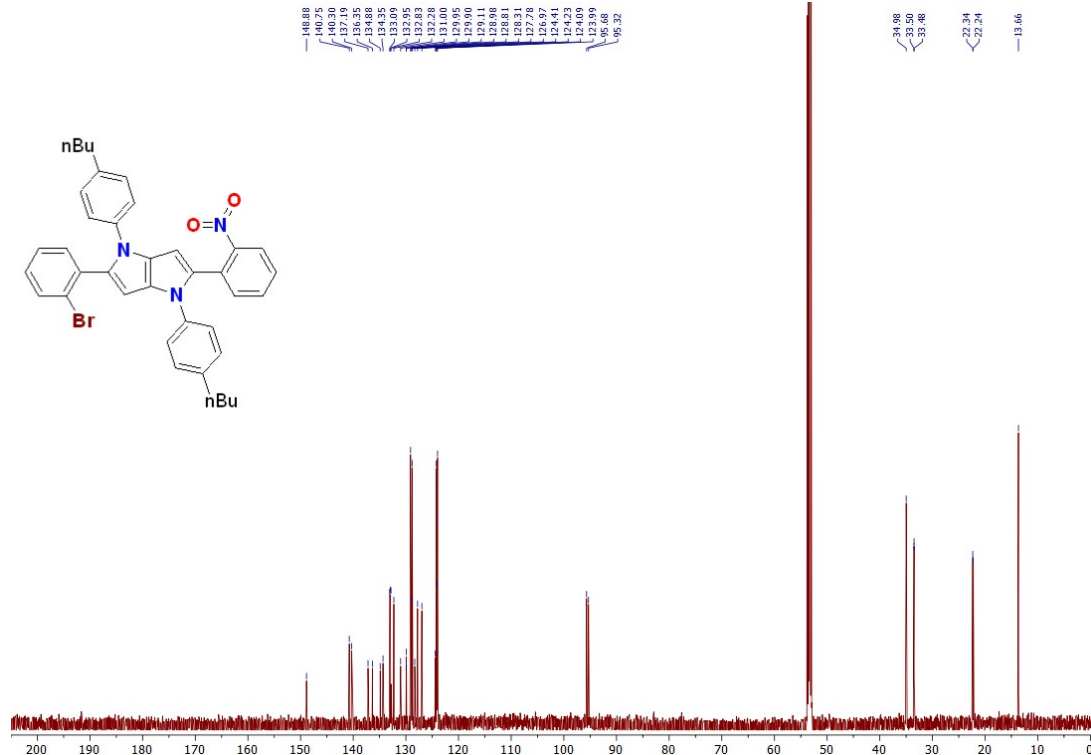


Figure S8: 151 MHz ^{13}C { ^1H } NMR spectrum of PP4 in CD_2Cl_2

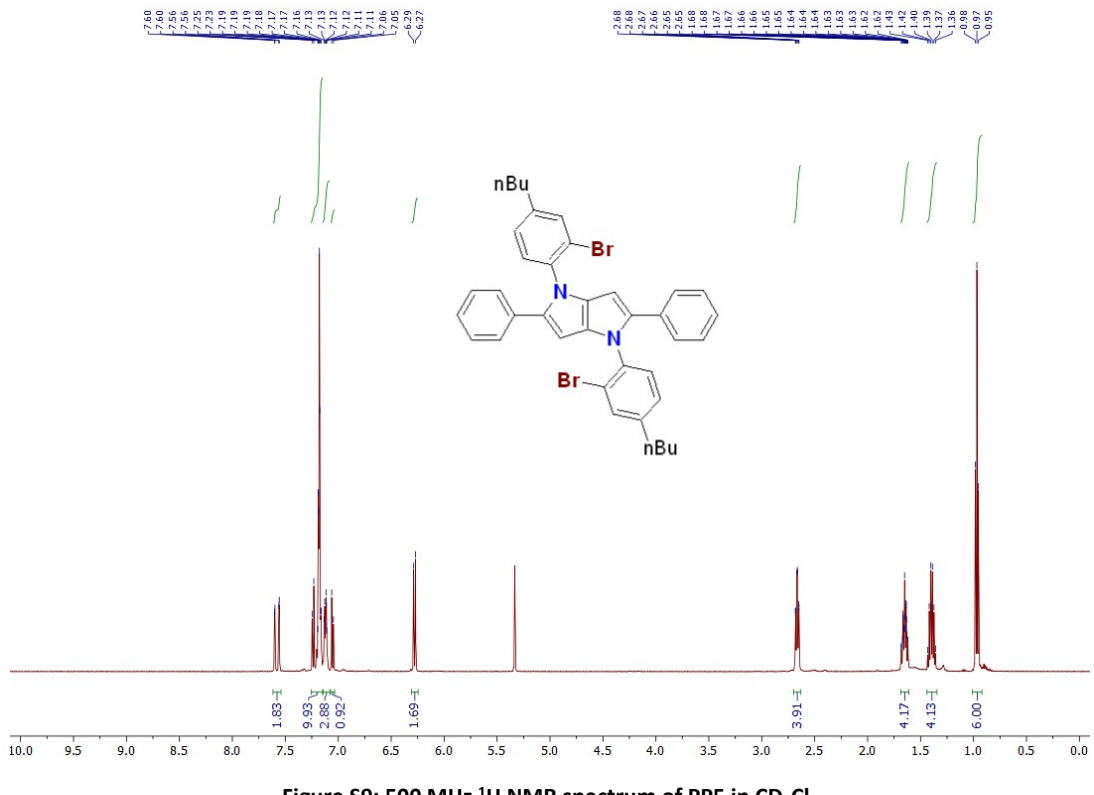


Figure S9: 500 MHz ^1H NMR spectrum of PP5 in CD_2Cl_2

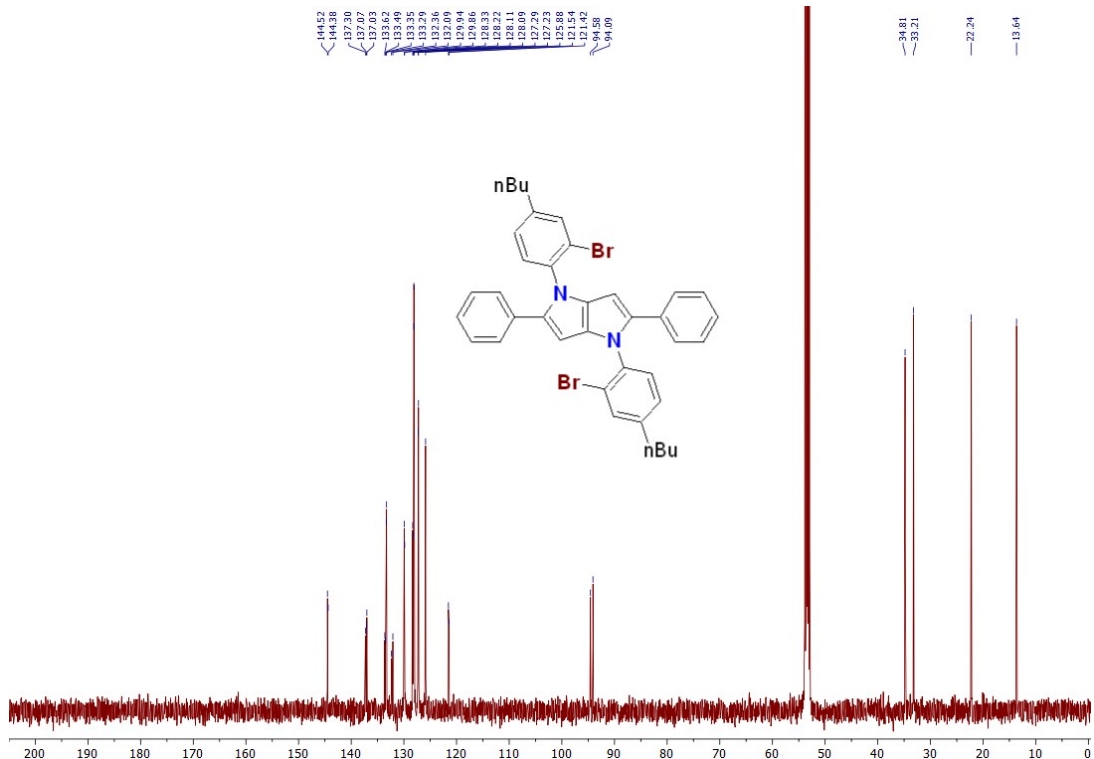


Figure S10: 126 MHz ^{13}C $\{{}^1\text{H}\}$ NMR spectrum of PP5 in CD_2Cl_2

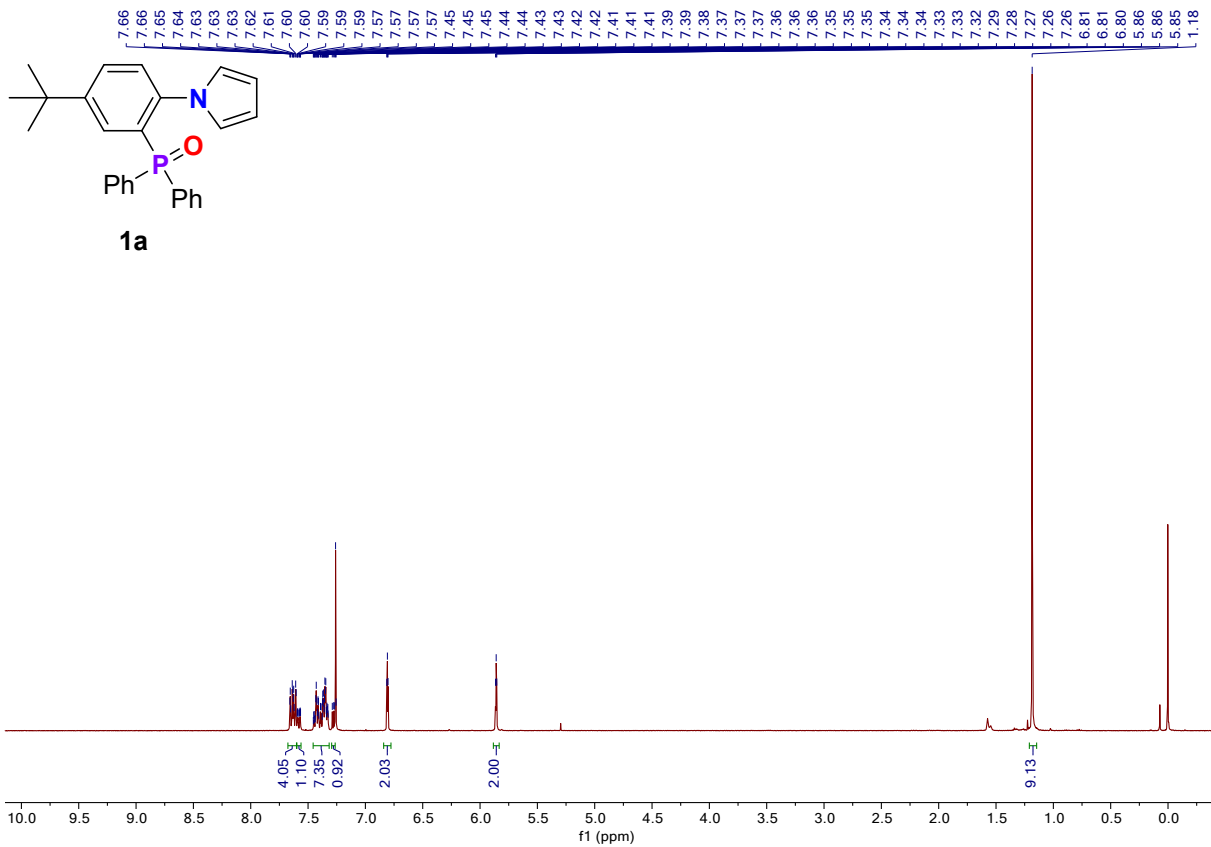


Figure S11: 500 MHz ^1H NMR spectrum of **1a** in CDCl_3

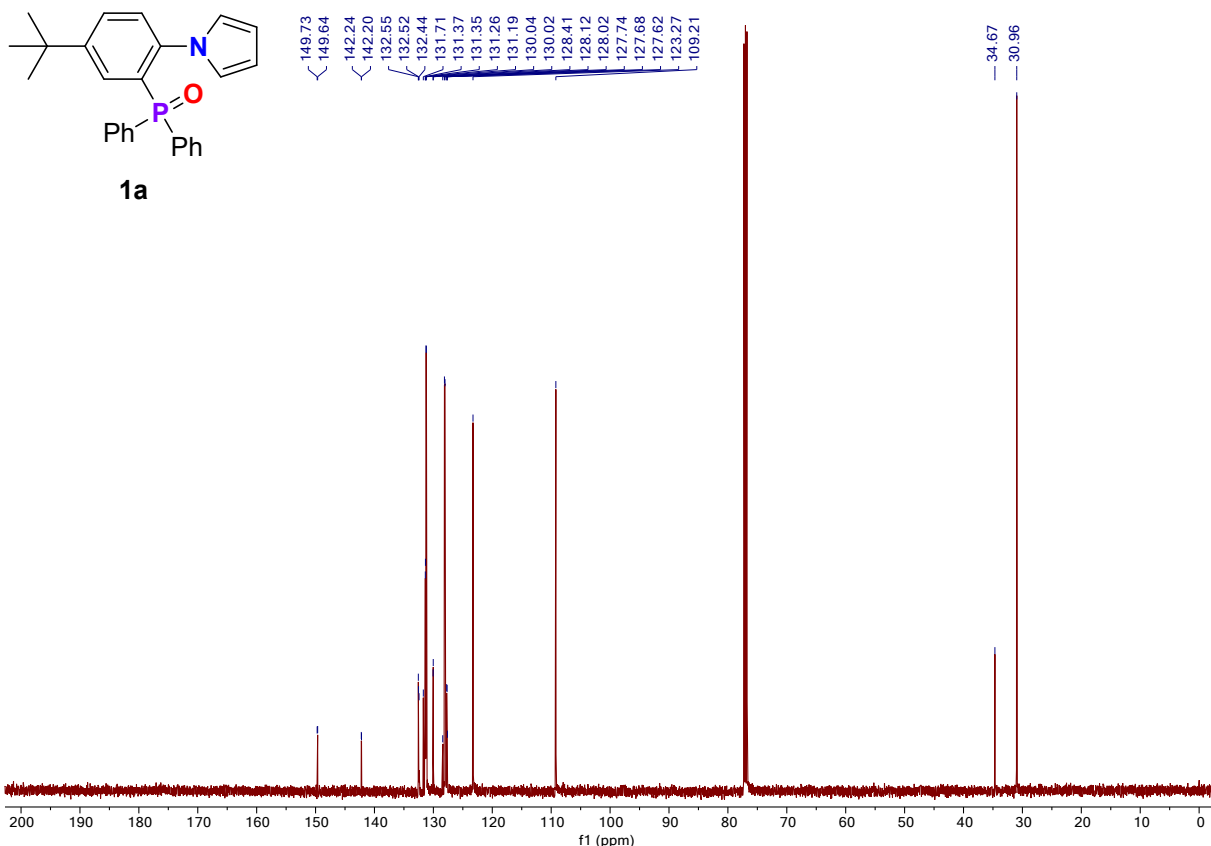


Figure S12: 126 MHz $^{13}\text{C}\{^1\text{H}\}$ NMR spectrum of **1a** in CDCl_3

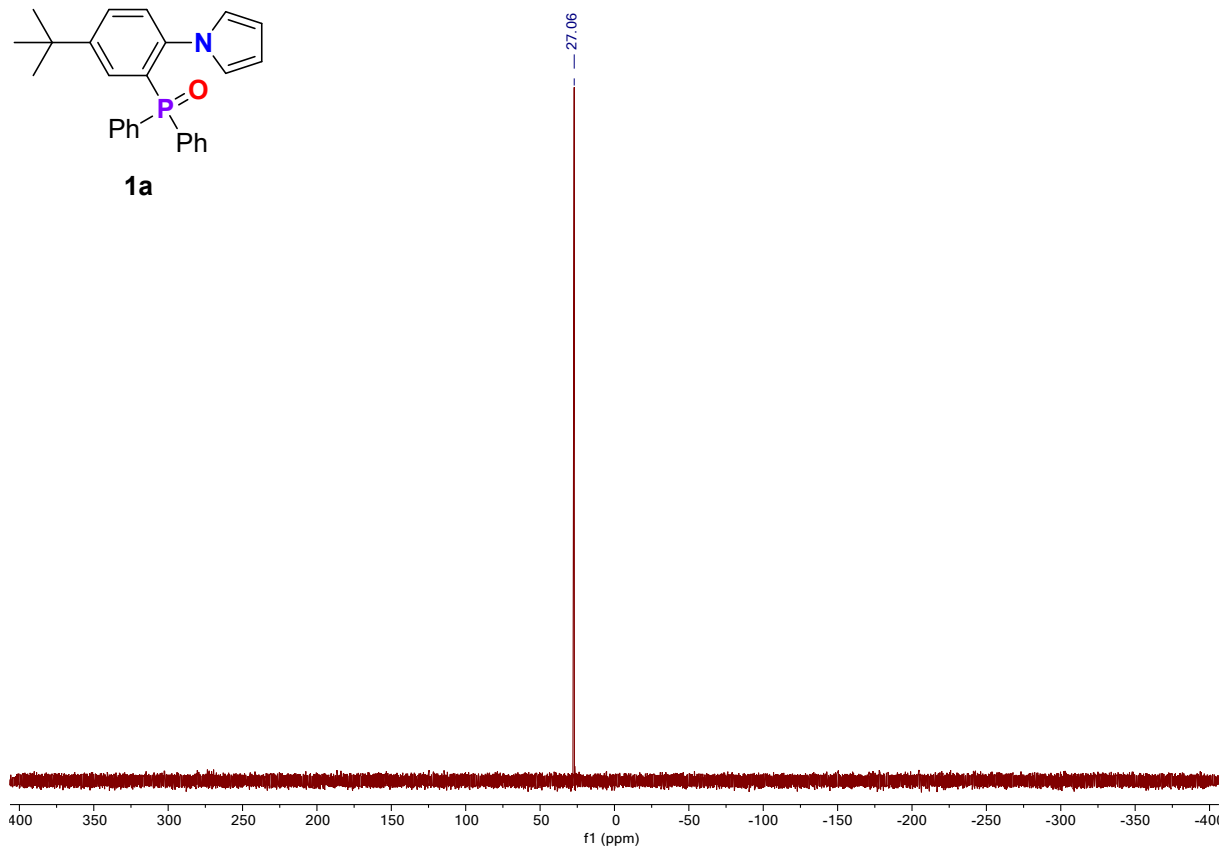
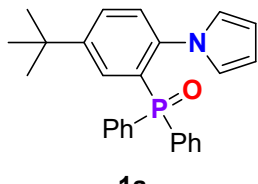


Figure S13: 202 MHz ^{31}P NMR spectrum of **1a** in CDCl_3

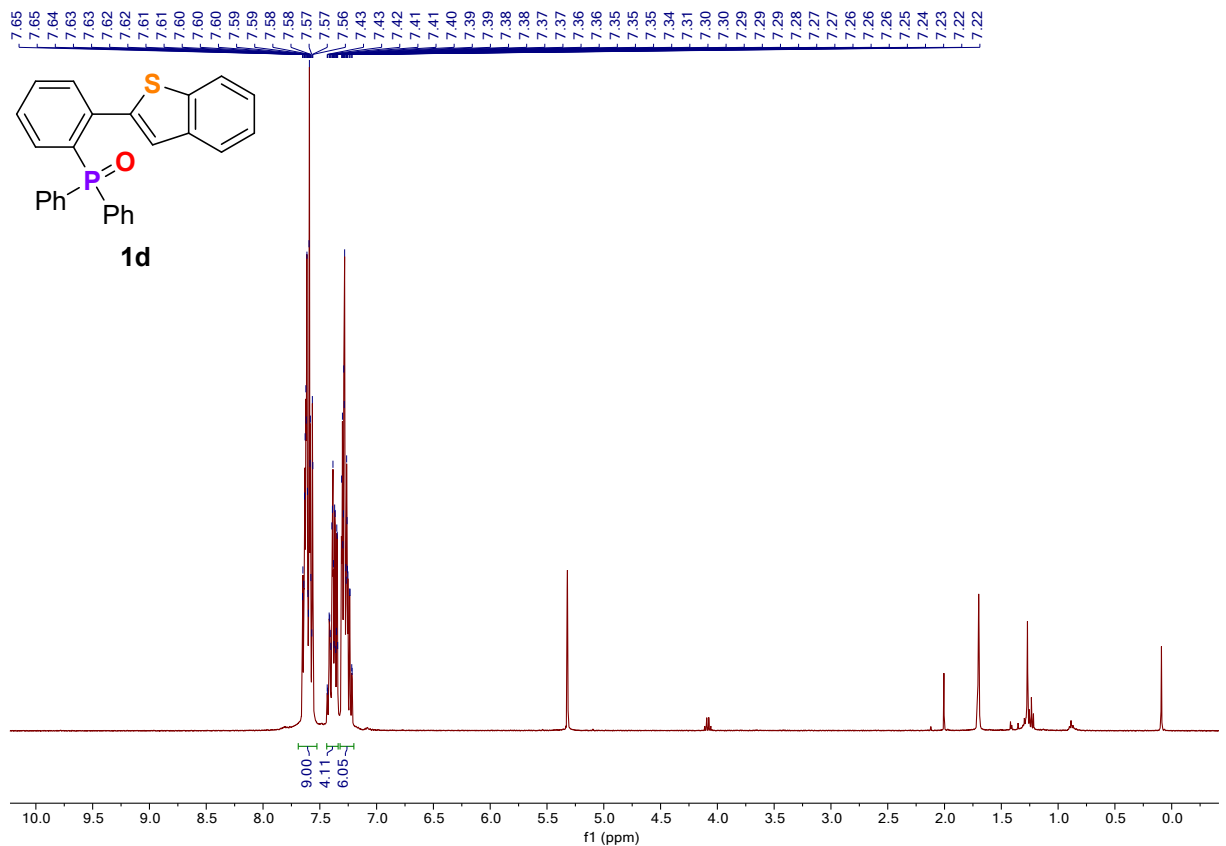
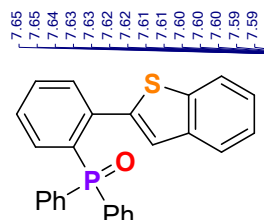


Figure S14: 400 MHz ^1H NMR spectrum of **1d** in CD_2Cl_2

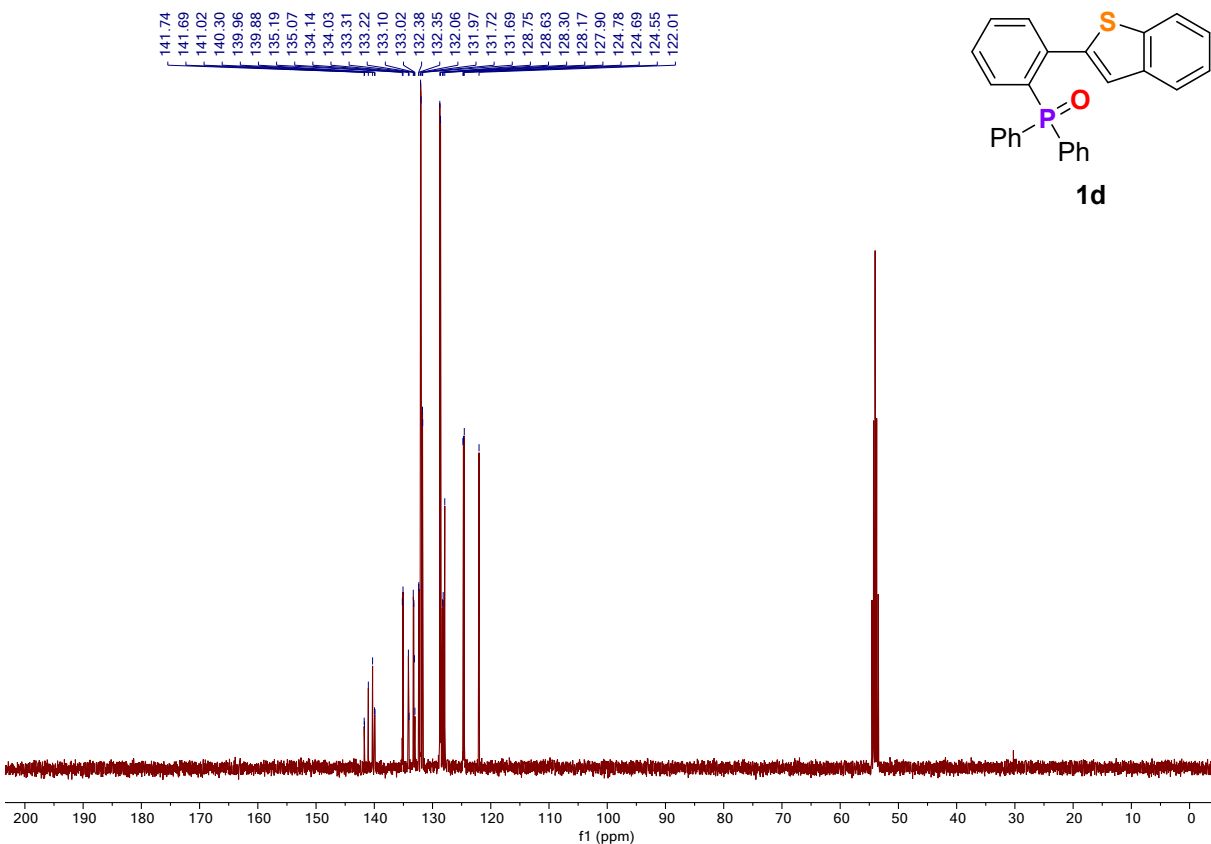


Figure S15: 101 MHz ^{13}C $\{^1\text{H}\}$ NMR spectrum of **1d** in CD_2Cl_2

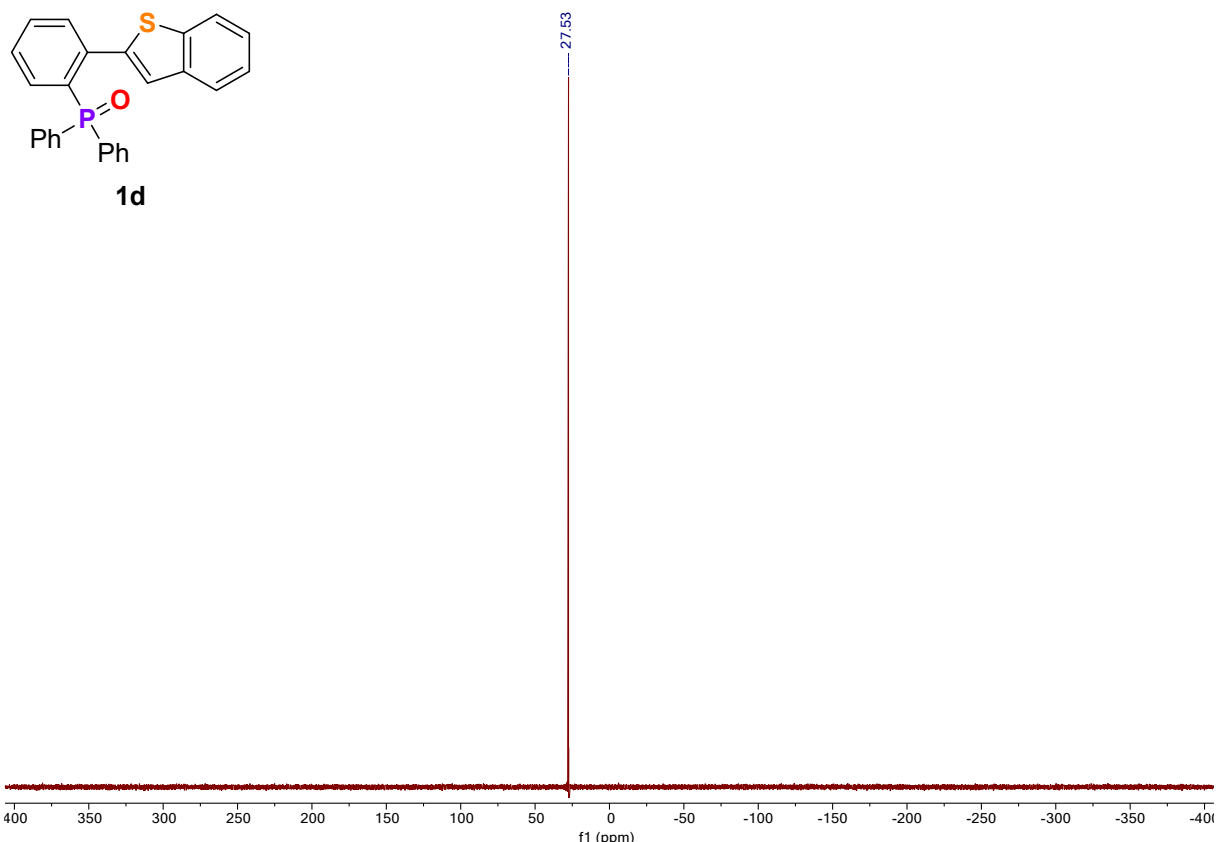


Figure S16: 162 MHz ^{31}P NMR spectrum of **1d** in CD_2Cl_2

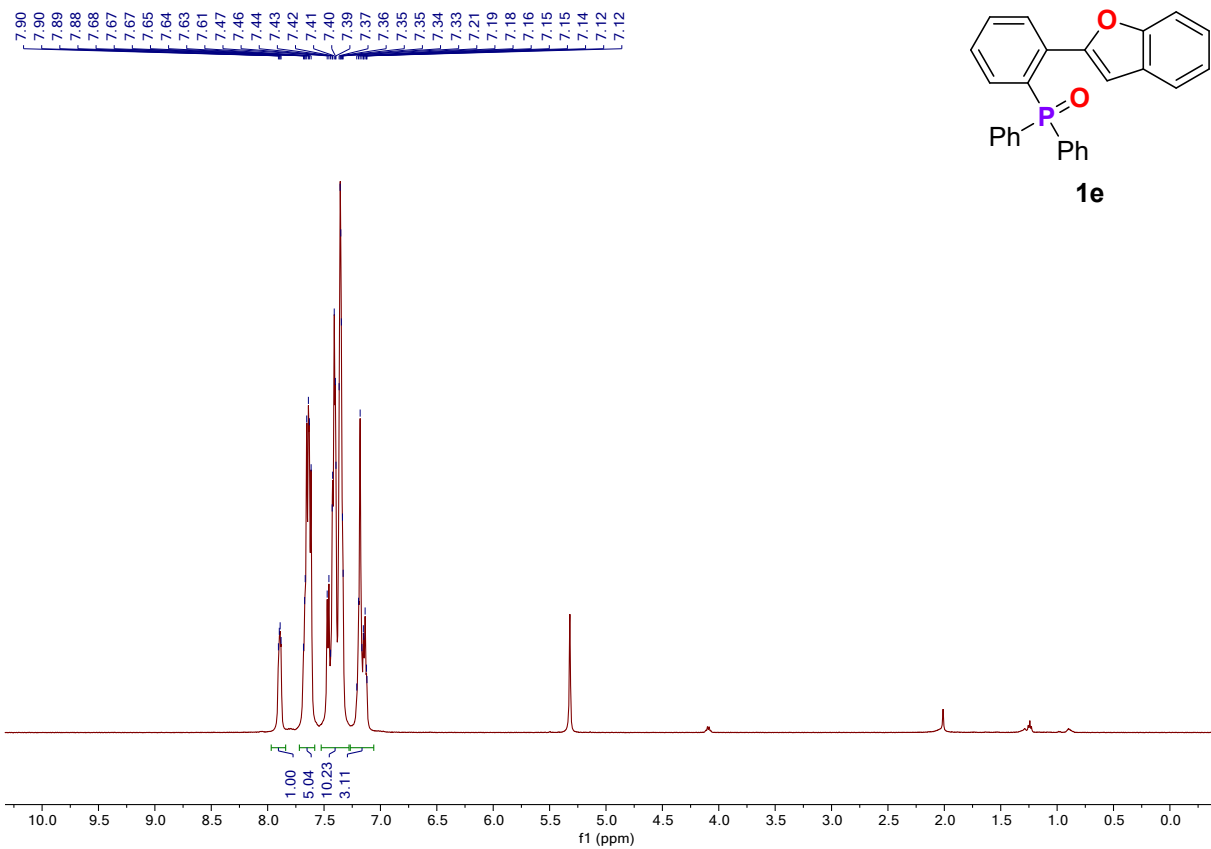


Figure S17: 500 MHz ^1H NMR spectrum of **1e** in CD_2Cl_2

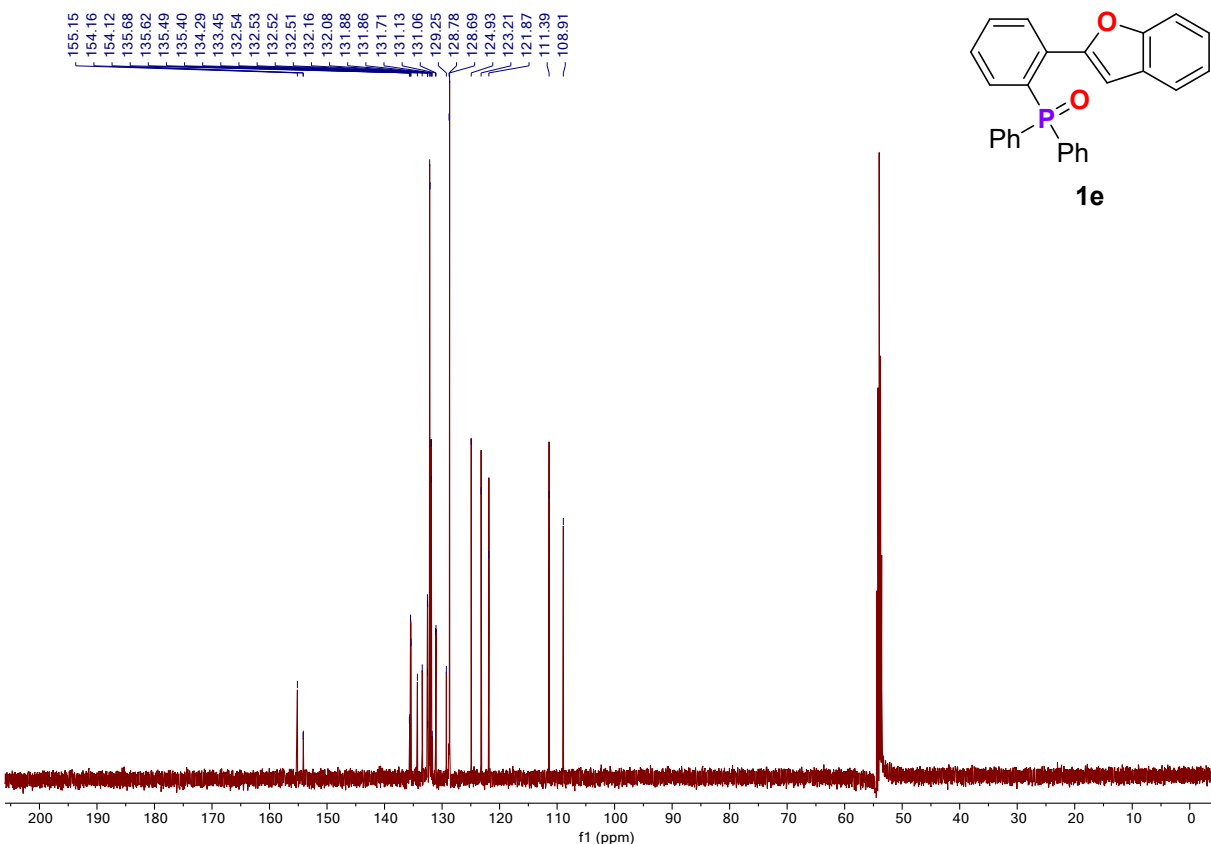


Figure S18: 126 MHz $^{13}\text{C}\{^1\text{H}\}$ NMR spectrum of **1e** in CD_2Cl_2

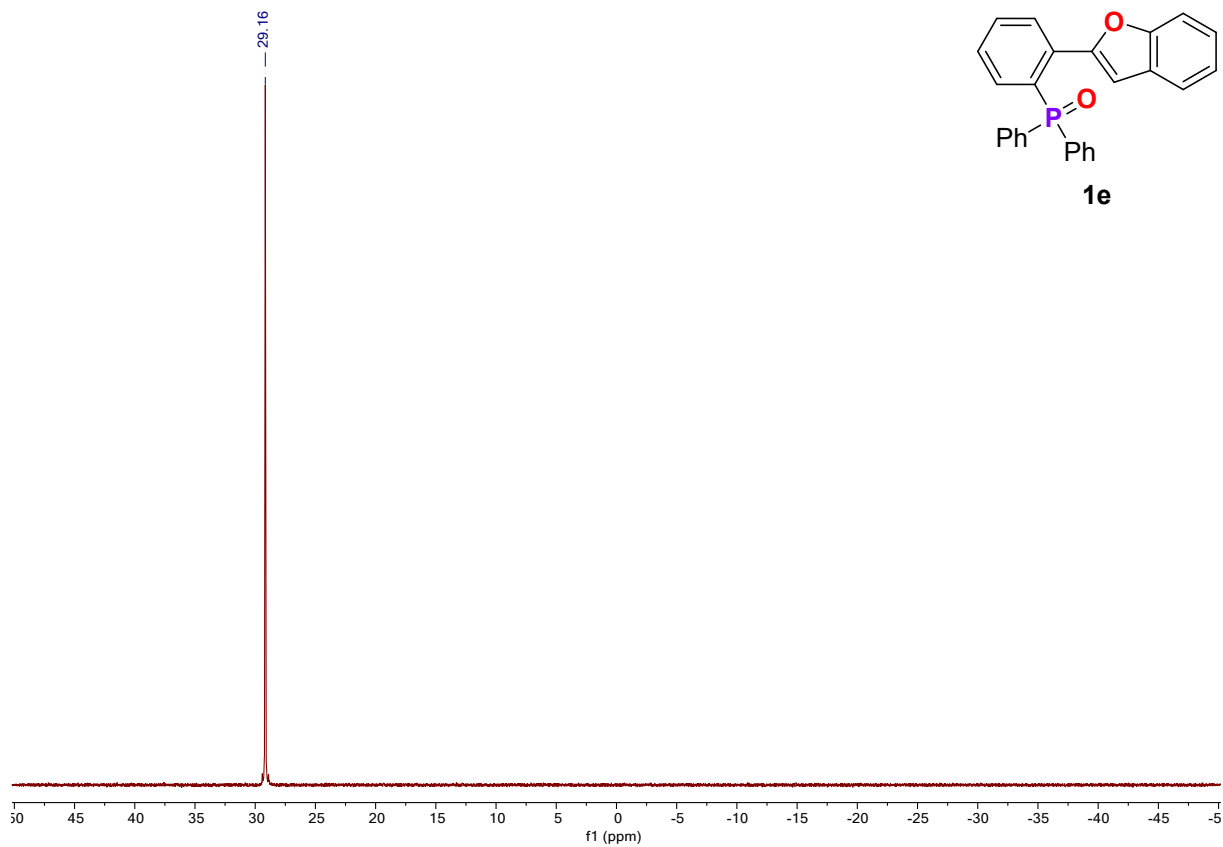


Figure S19: 202 MHz ^{31}P NMR spectrum of **1e** in CD_2Cl_2

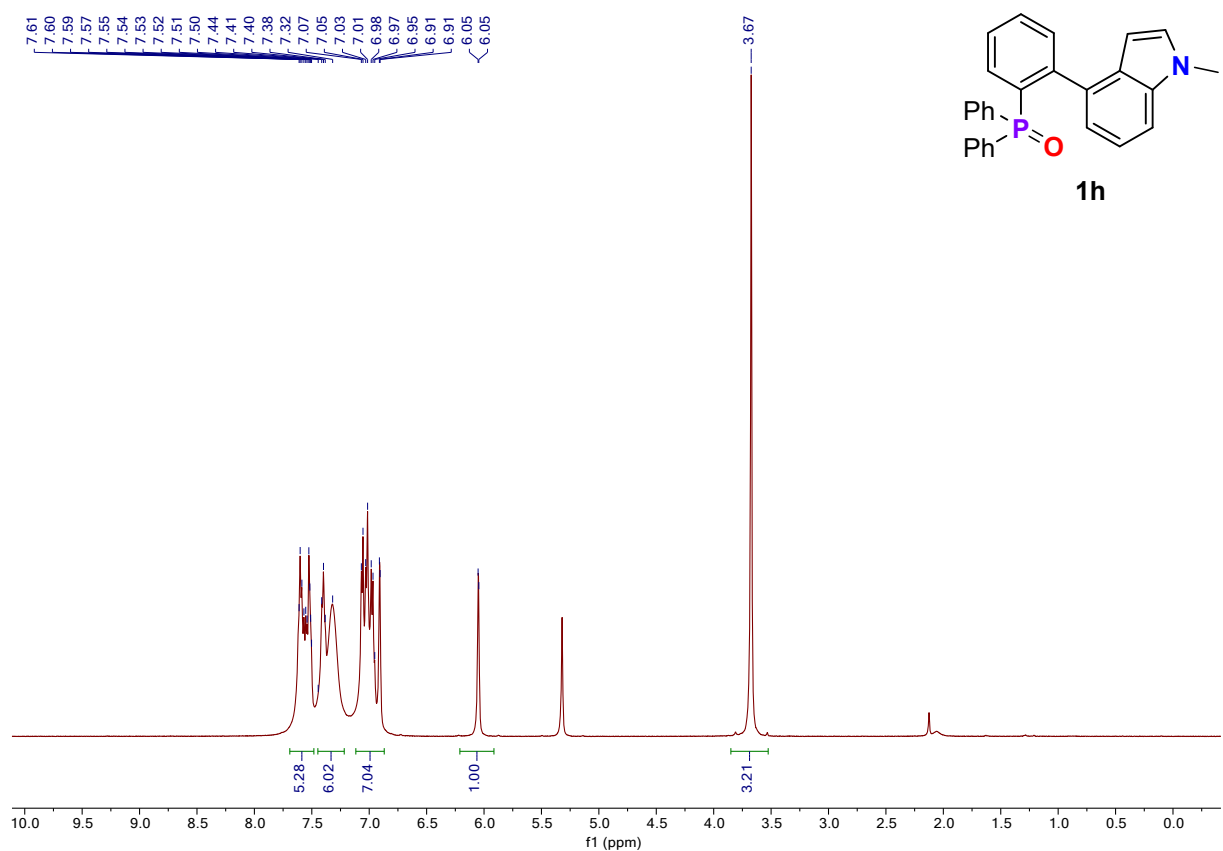


Figure S20: 500 MHz ^1H NMR spectrum of **1h** in CD_2Cl_2

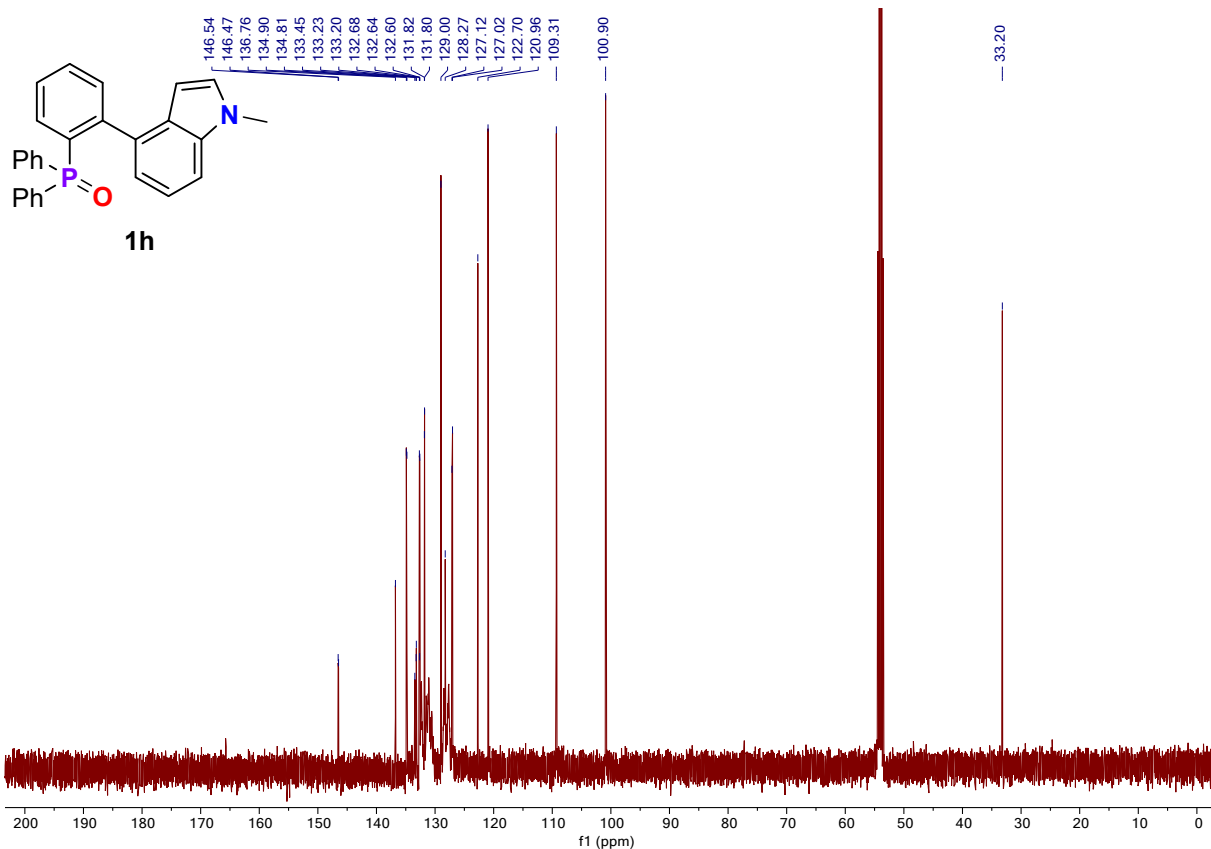


Figure S21: 126 MHz ^{13}C { ^1H } NMR spectrum of **1h** in CD_2Cl_2

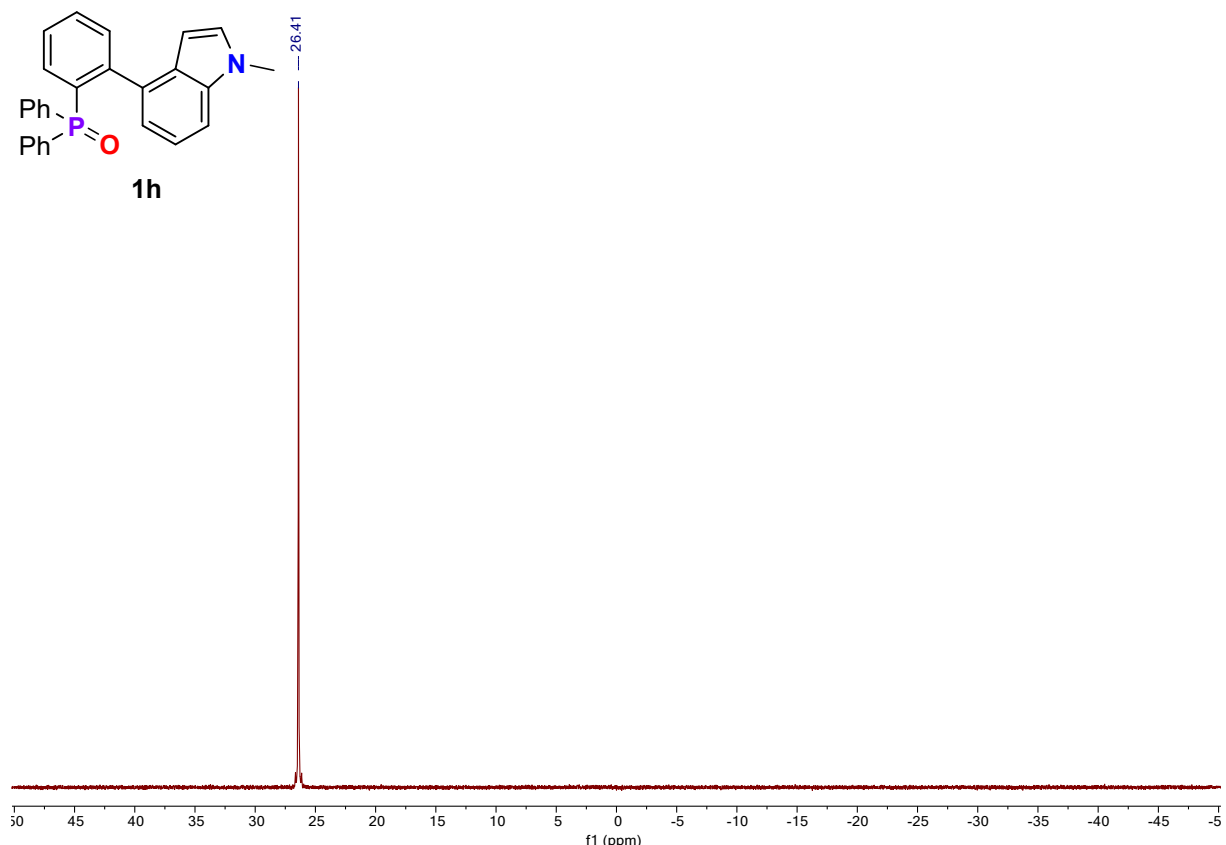


Figure S22: 202 MHz ^{31}P NMR spectrum of **1h** in CD_2Cl_2

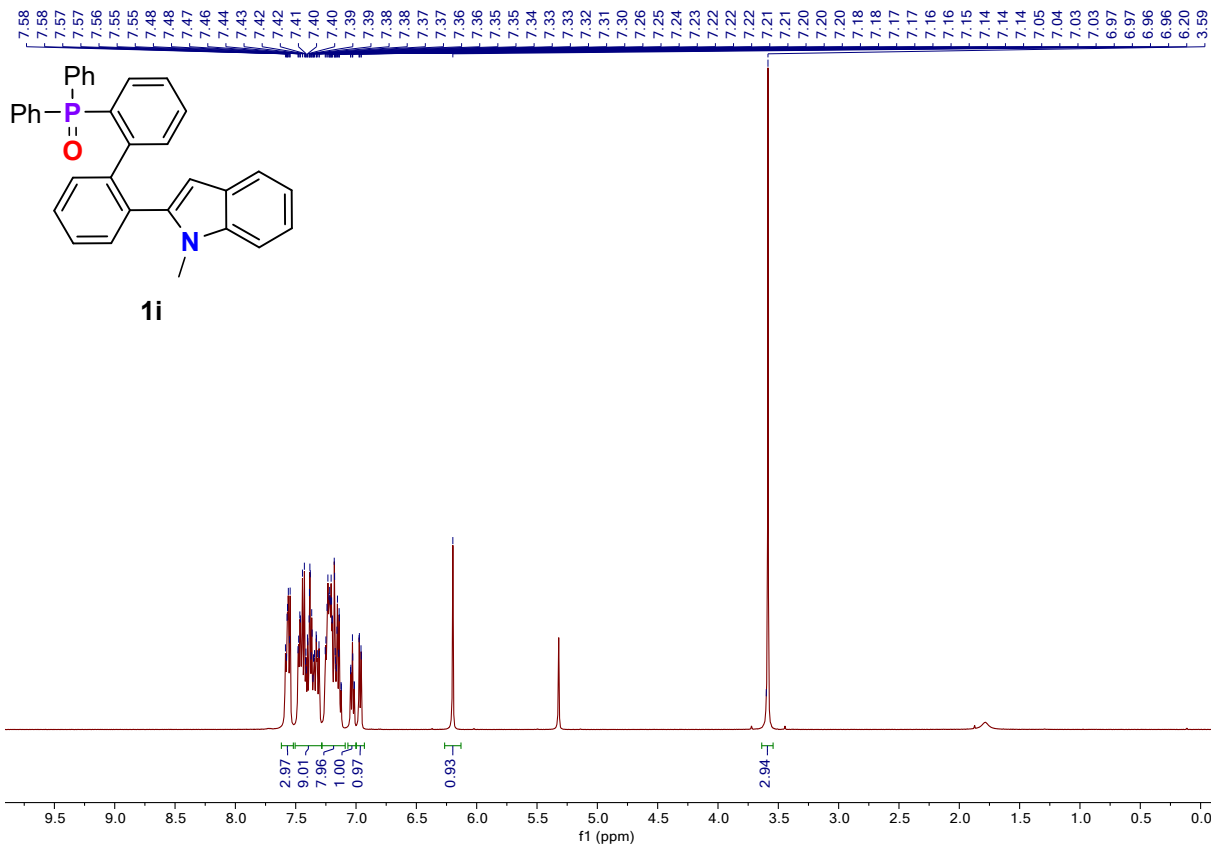


Figure S23: 500 MHz ^1H NMR spectrum of **1i** in CD_2Cl_2

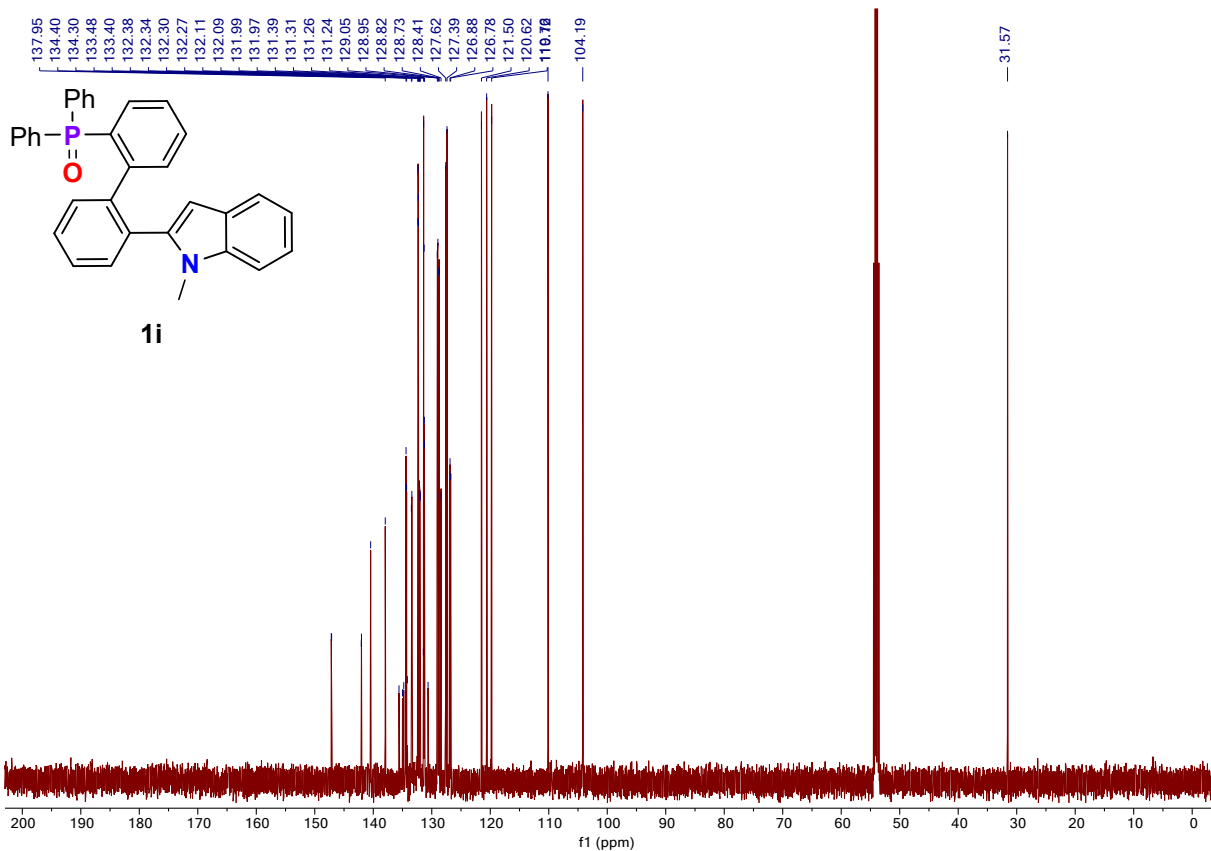


Figure S24: 126 MHz $^{13}\text{C}\{^1\text{H}\}$ NMR spectrum of **1i** in CD_2Cl_2

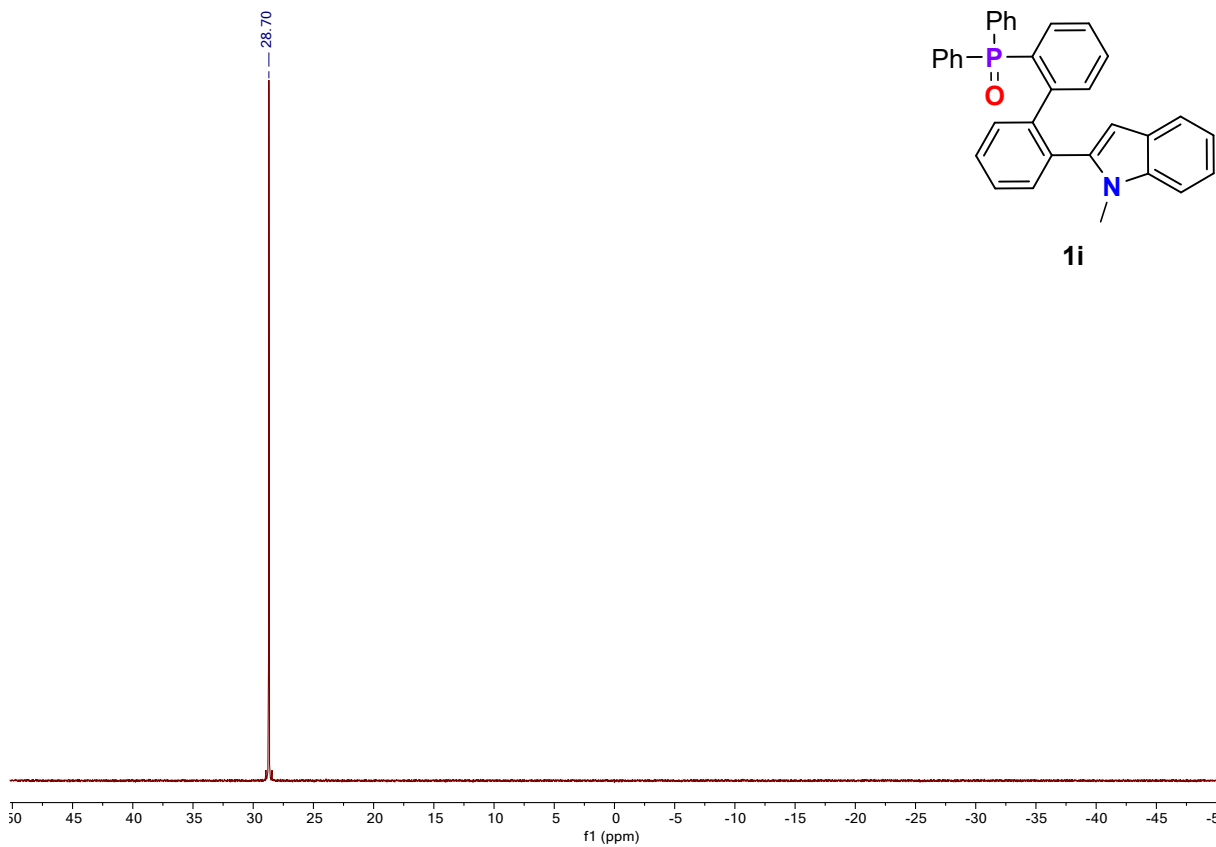


Figure S25: 202 MHz ^{31}P NMR spectrum of **1i** in CD_2Cl_2

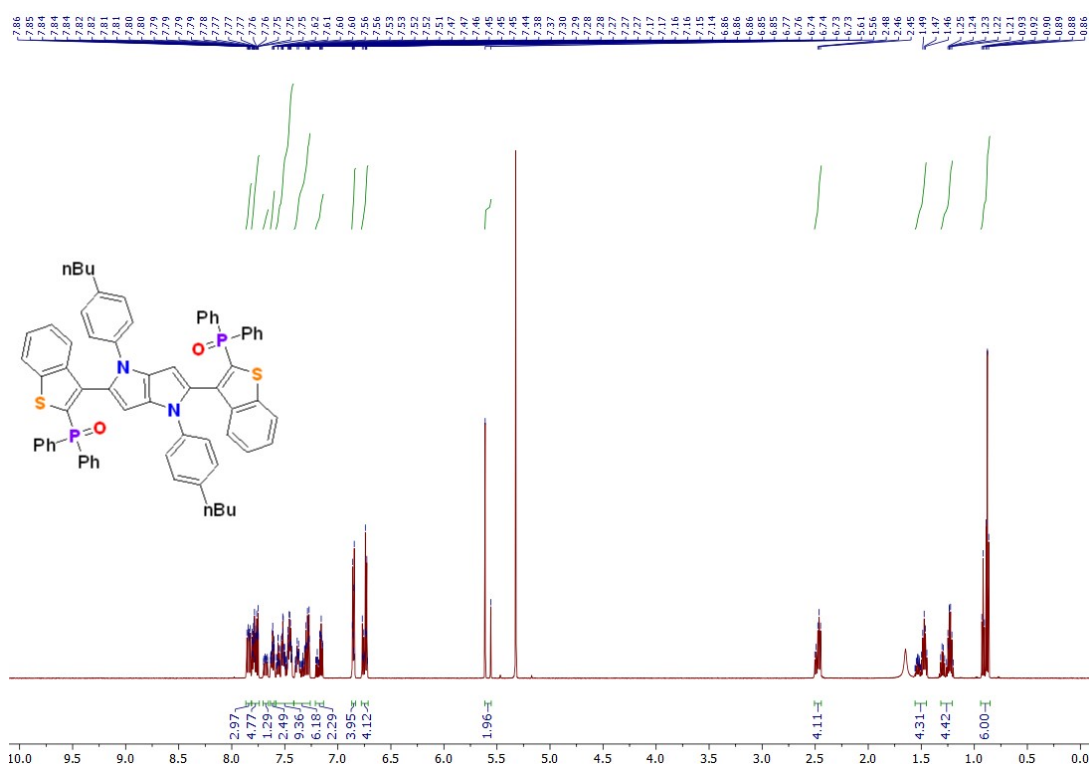


Figure S26: 600 MHz ^1H NMR spectrum of **1j** in CD_2Cl_2

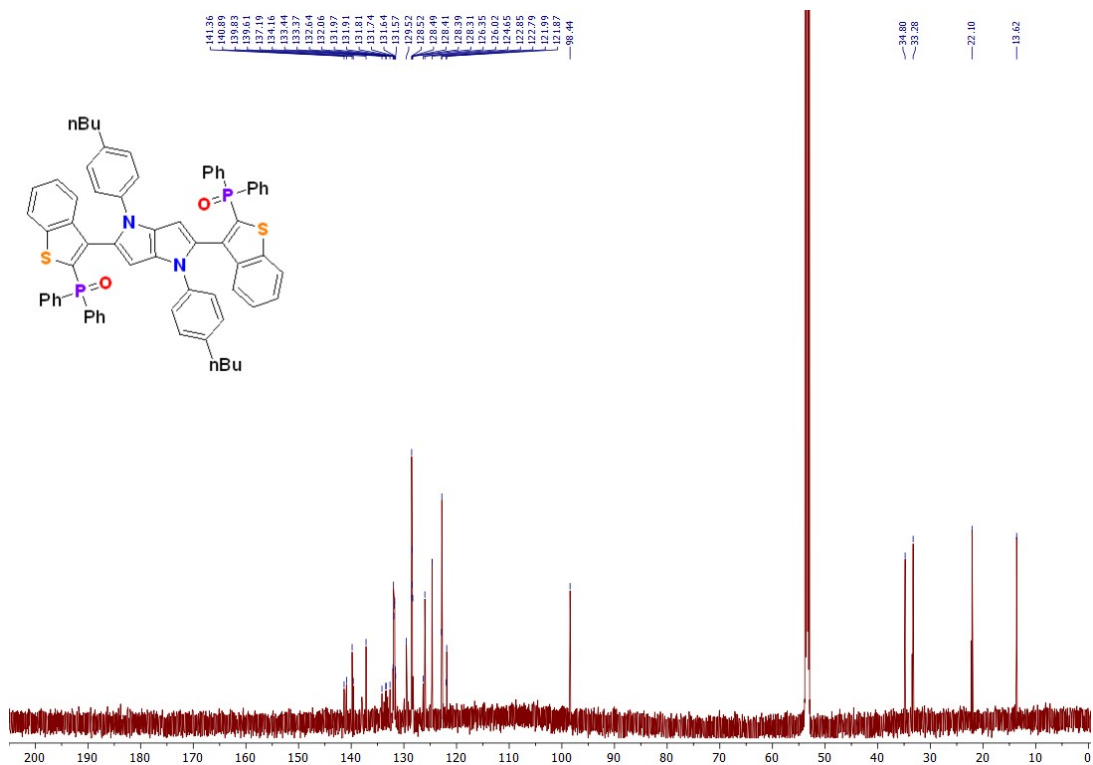


Figure S27: 151 MHz ^{13}C { ^1H } NMR spectrum of 1j in CD_2Cl_2

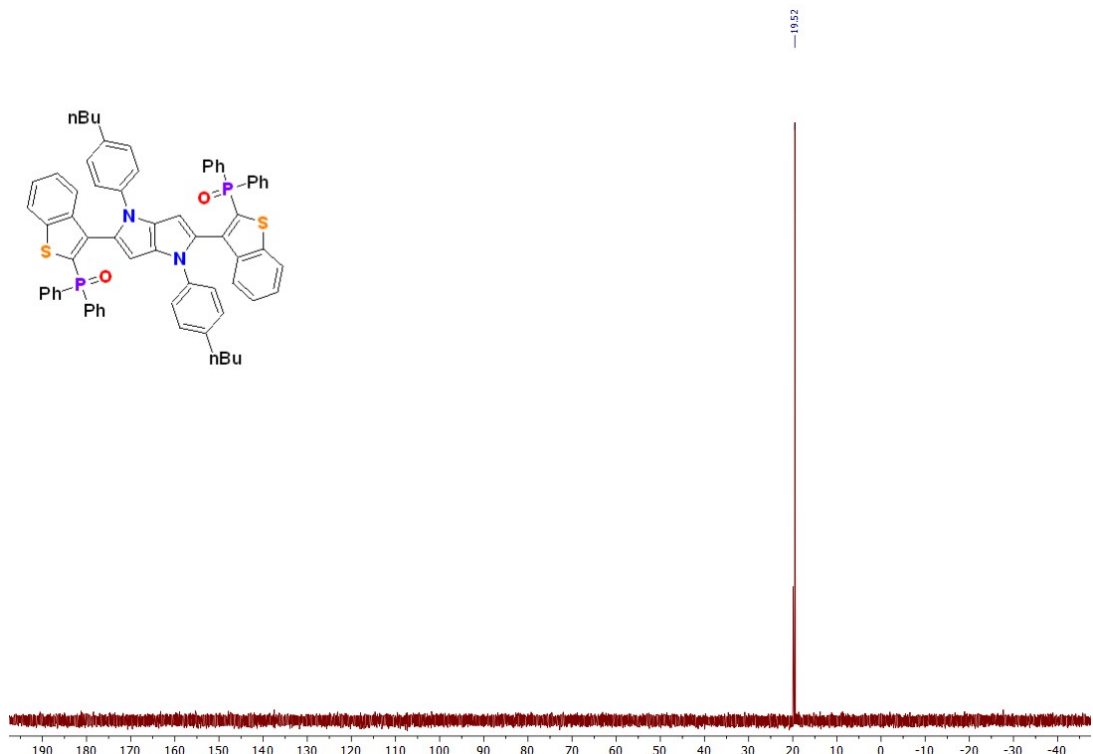


Figure S28: 243 MHz ^{31}P NMR spectrum of 1j in CD_2Cl_2

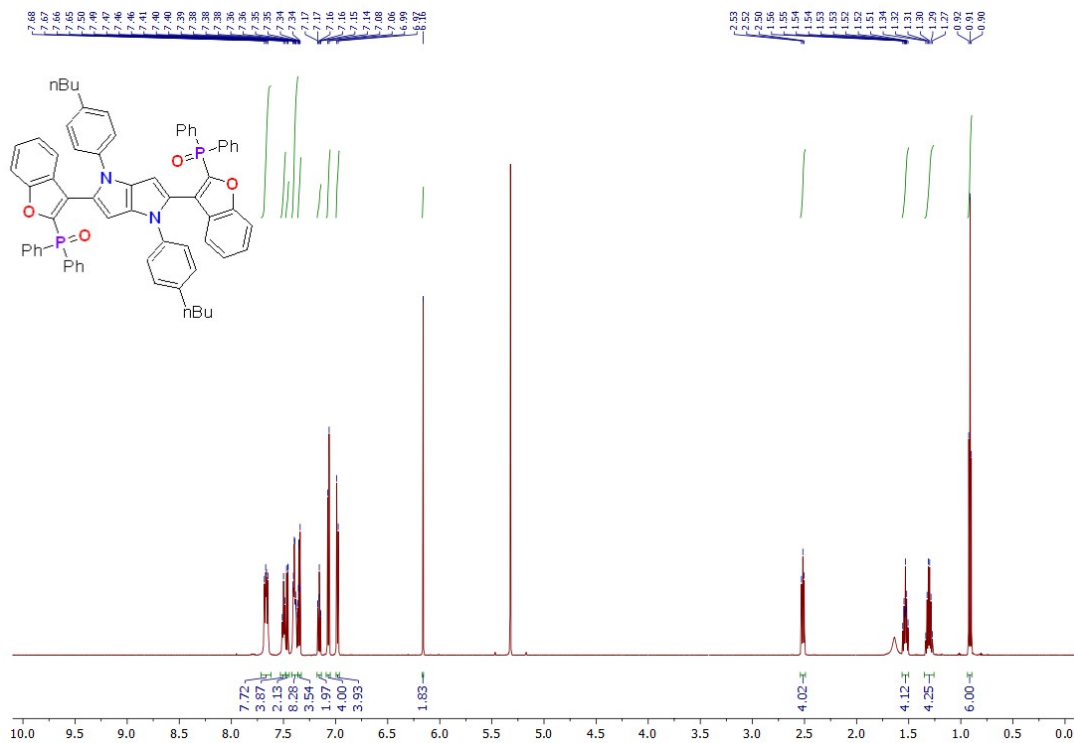


Figure S29: 600 MHz ^1H NMR spectrum of 1k in CD_2Cl_2

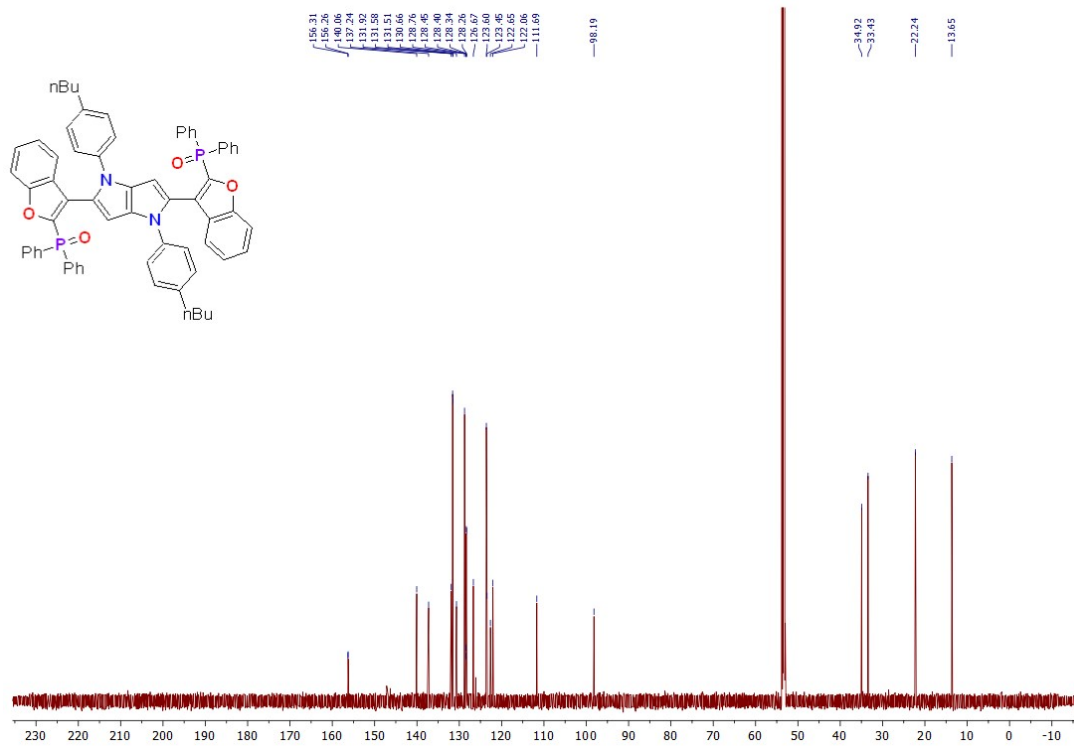


Figure S30: 151 MHz ^{13}C { ^1H } NMR spectrum of 1k in CD_2Cl_2

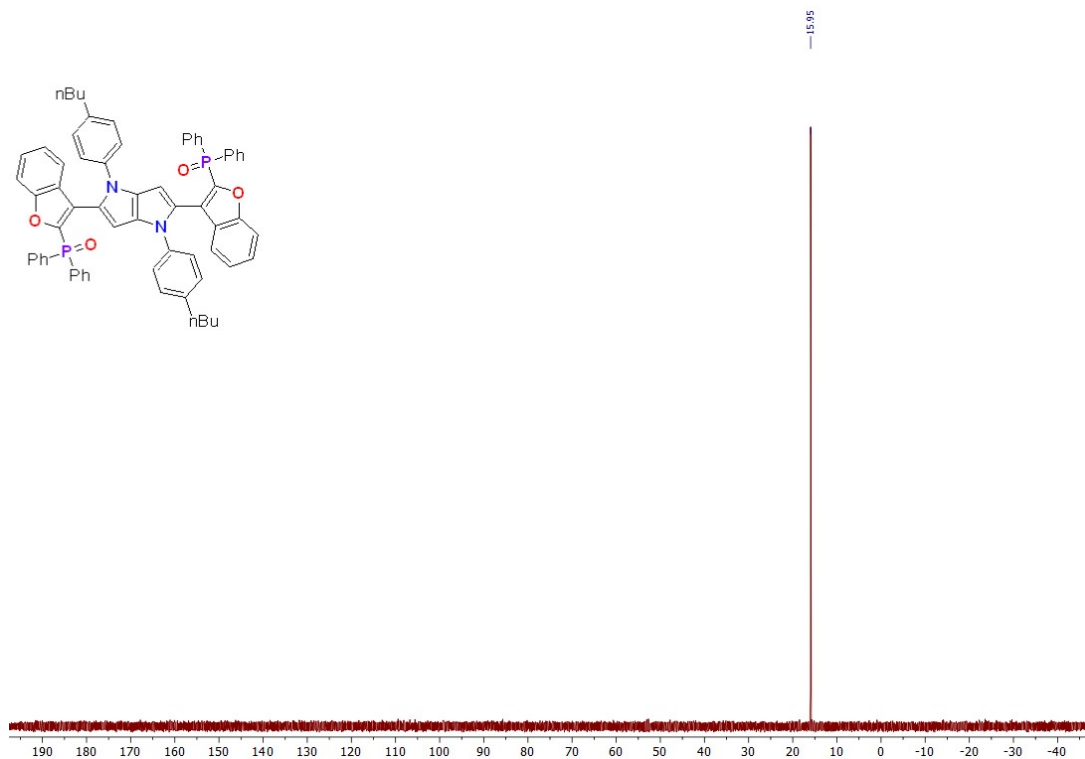


Figure S31: 243 MHz ^{31}P NMR spectrum of **1k** in CD_2Cl_2

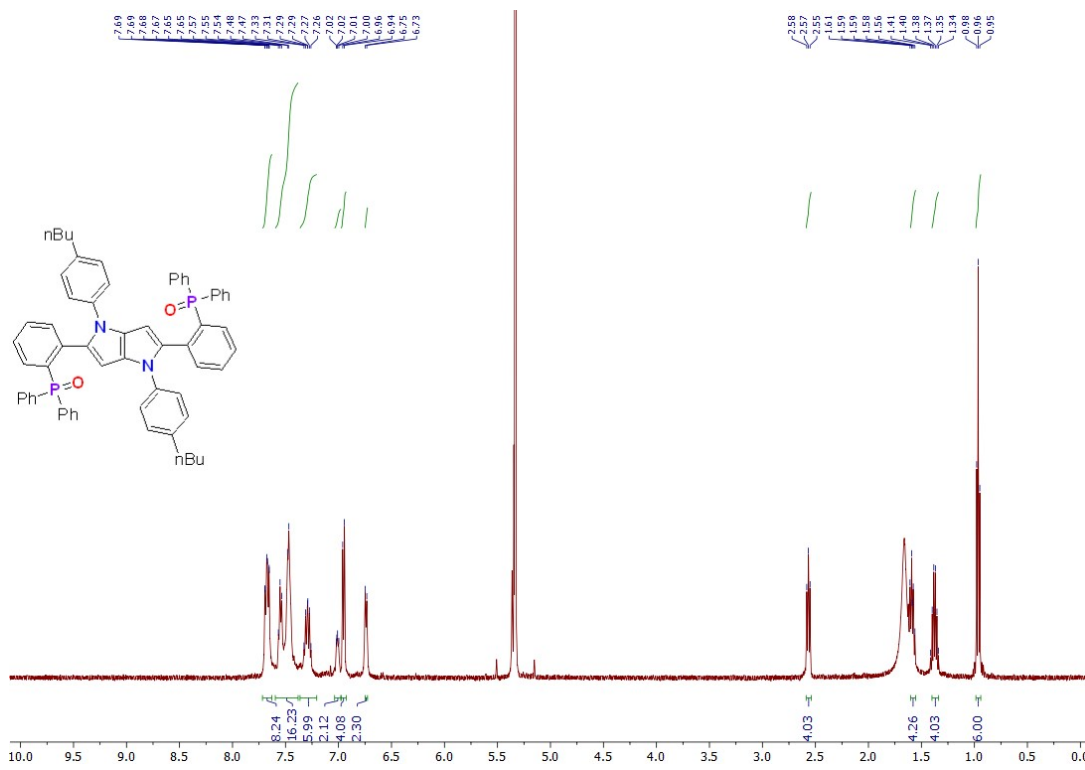


Figure S32: 500 MHz ^1H NMR spectrum of **1l** in CD_2Cl_2

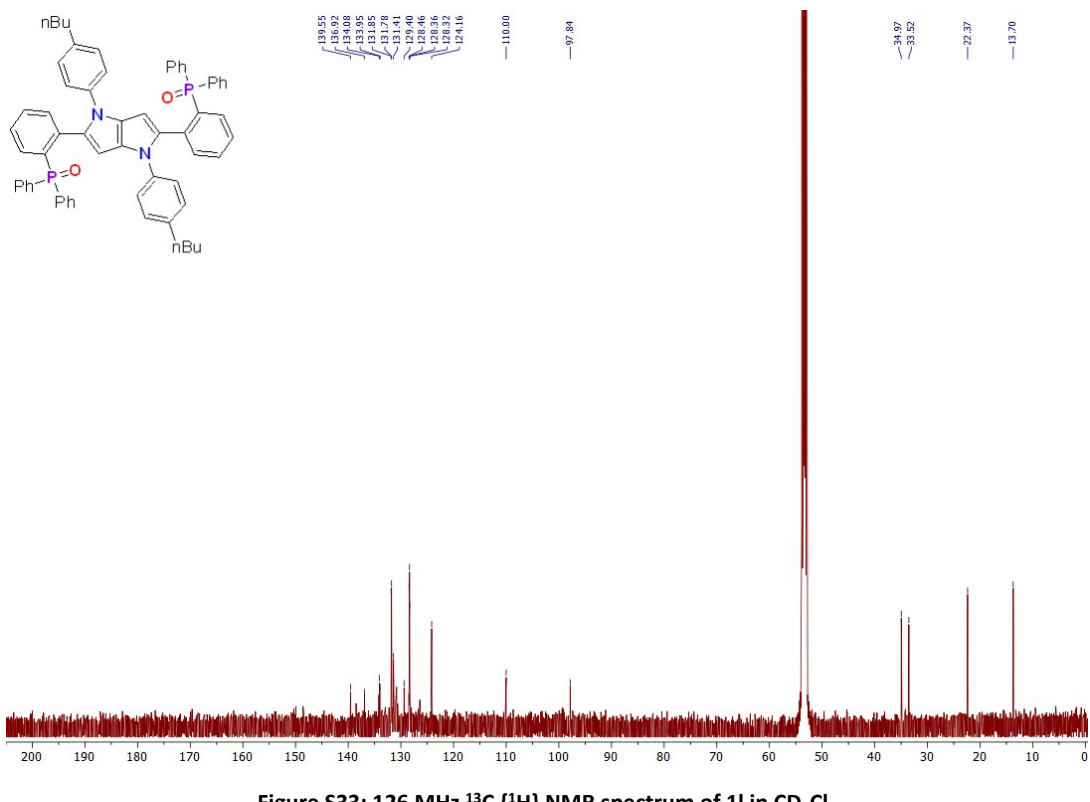


Figure S33: 126 MHz ^{13}C { ^1H } NMR spectrum of **1l** in CD_2Cl_2

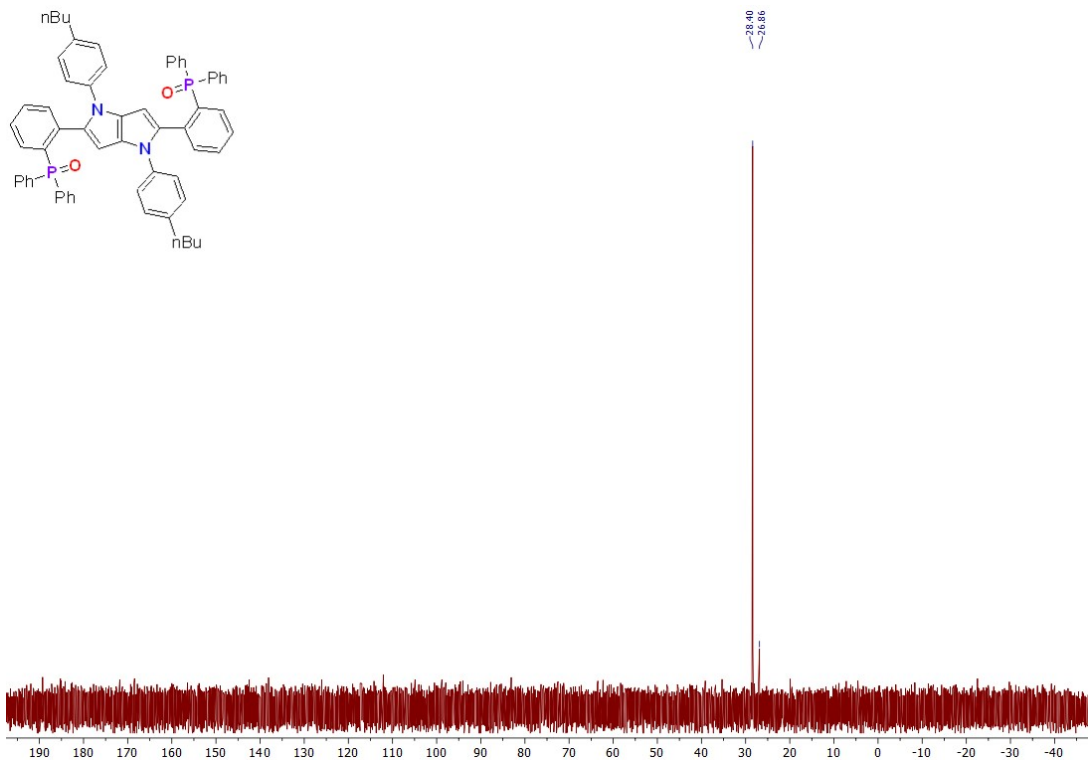


Figure S34: 202 MHz ^{31}P NMR spectrum of **1l** in CD_2Cl_2

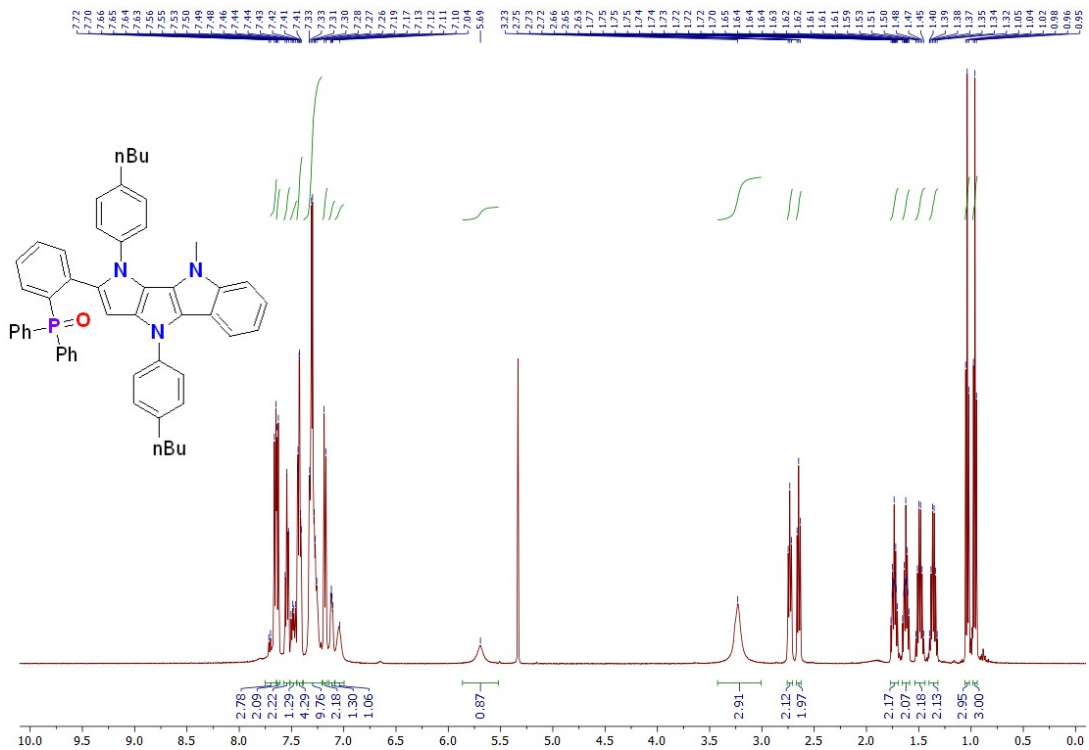


Figure S35: 500 MHz ^1H NMR spectrum of 1m in CD_2Cl_2

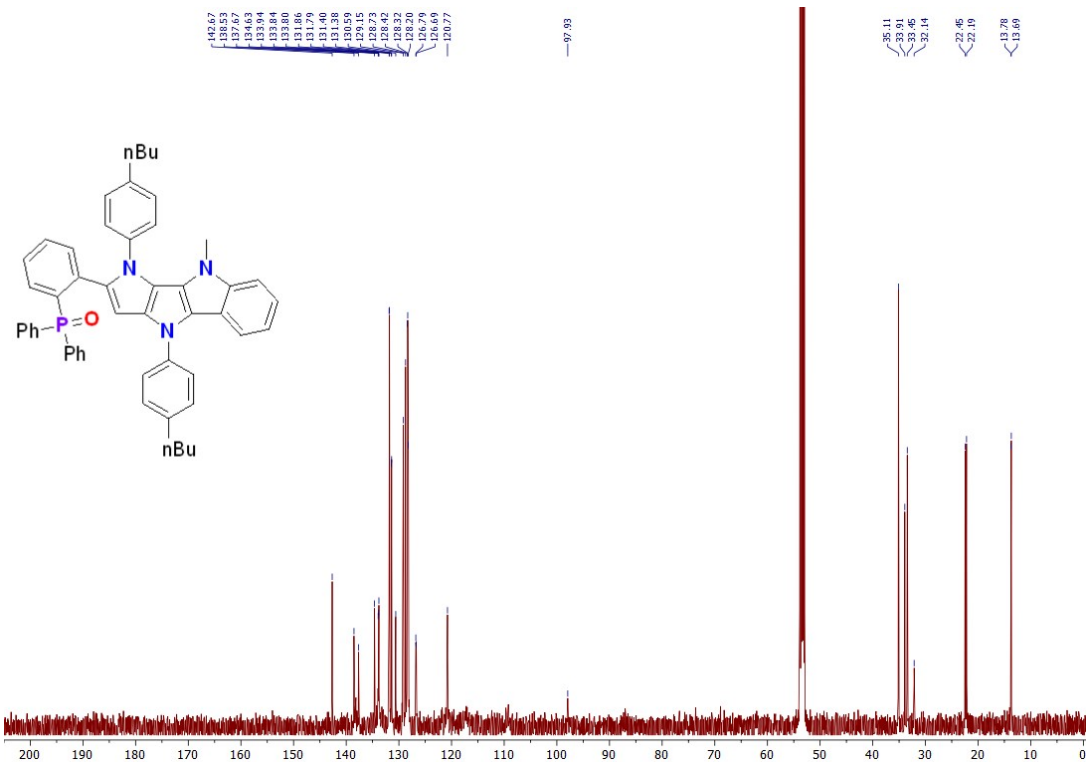


Figure S36: 126 MHz ^{13}C { ^1H } NMR spectrum of 1m in CD_2Cl_2

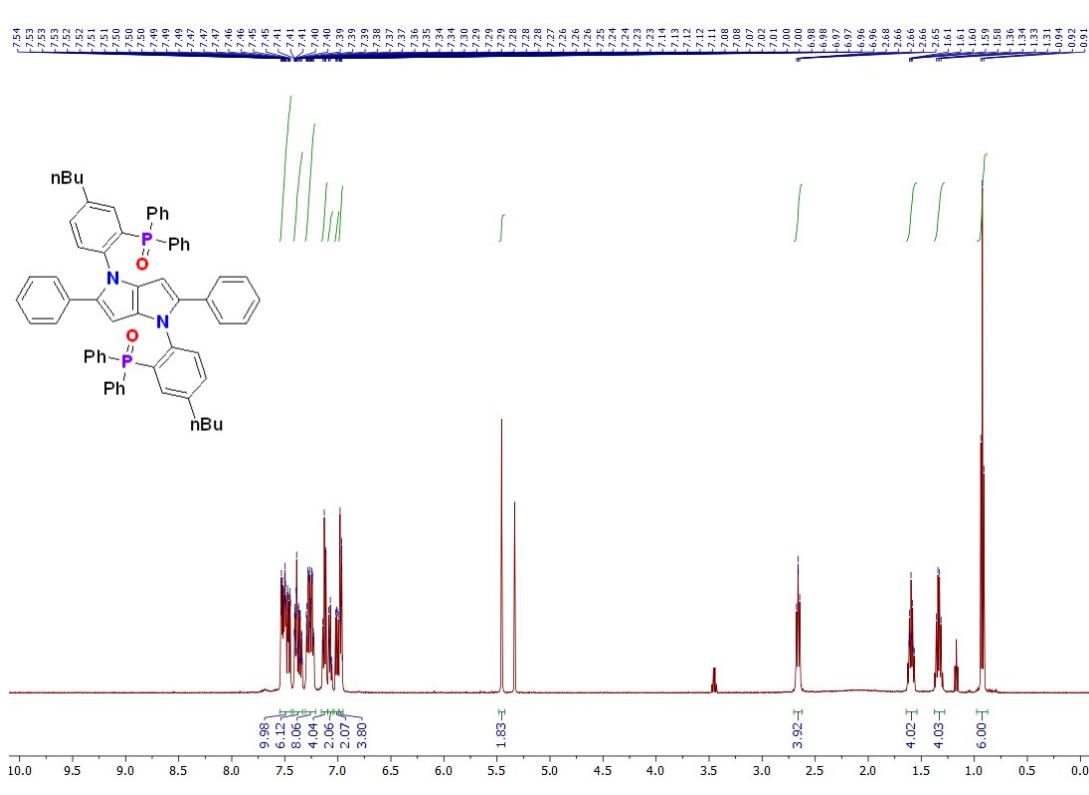
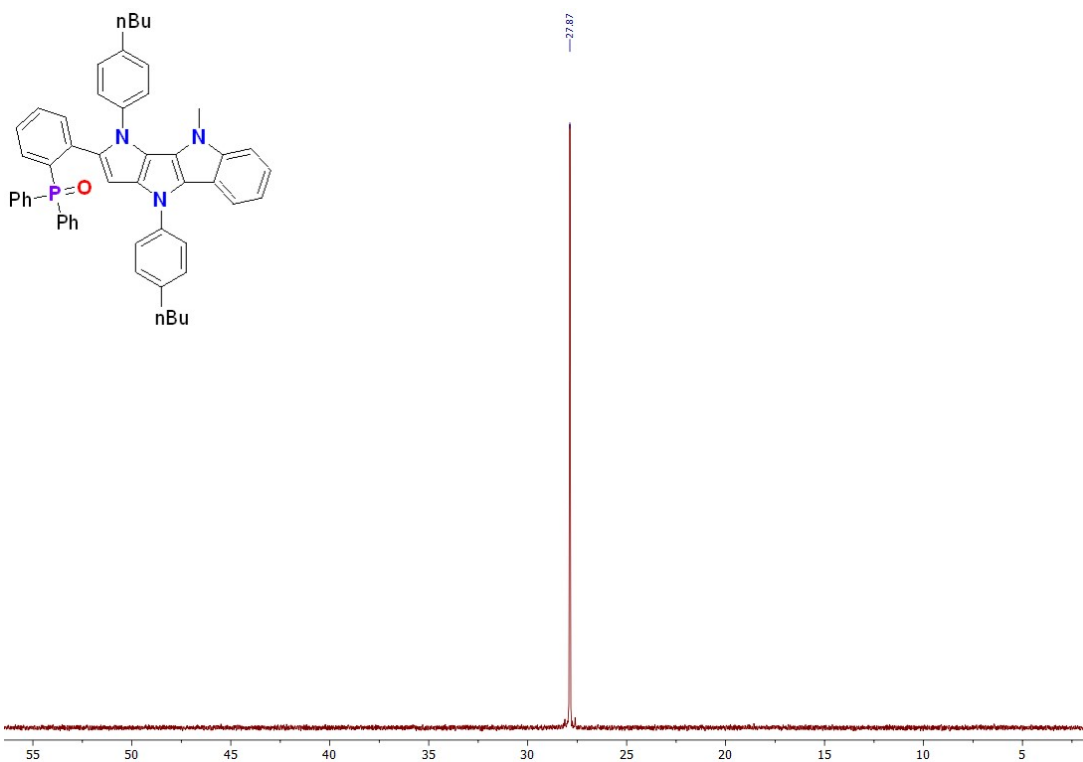


Figure S38: 500 MHz ^1H NMR spectrum of **1n** in CD_2Cl_2

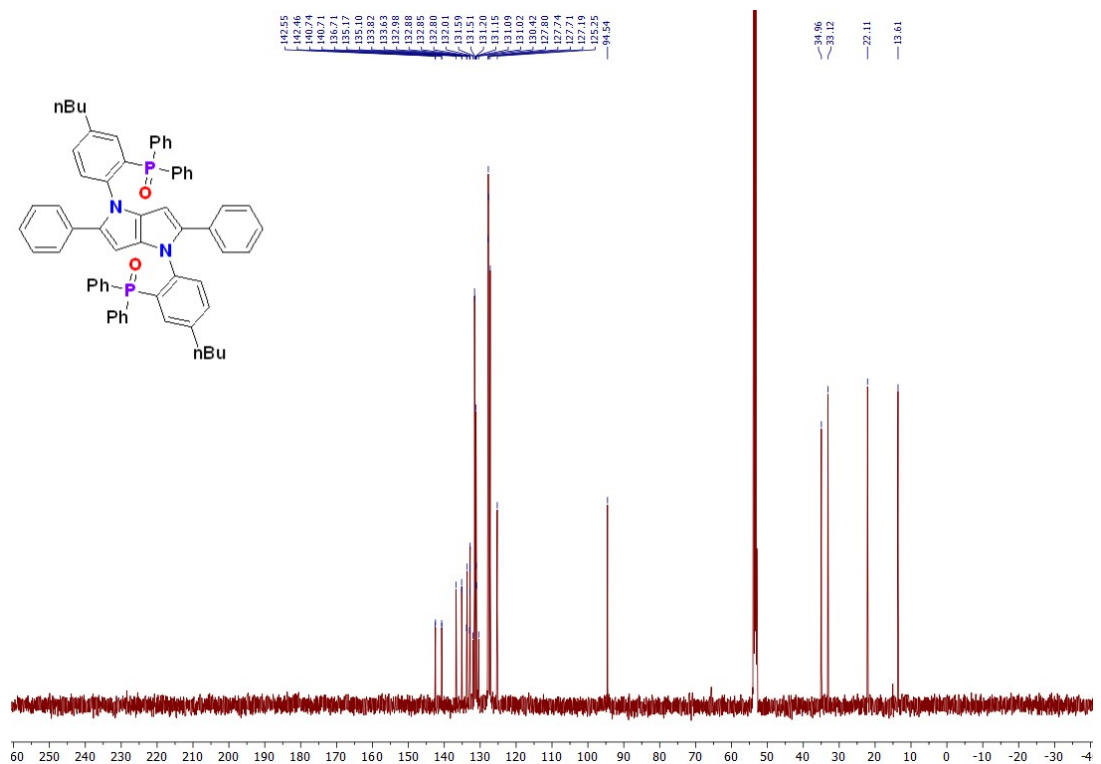


Figure S39: 126 MHz ^{13}C { ^1H } NMR spectrum of 1n in CD_2Cl_2

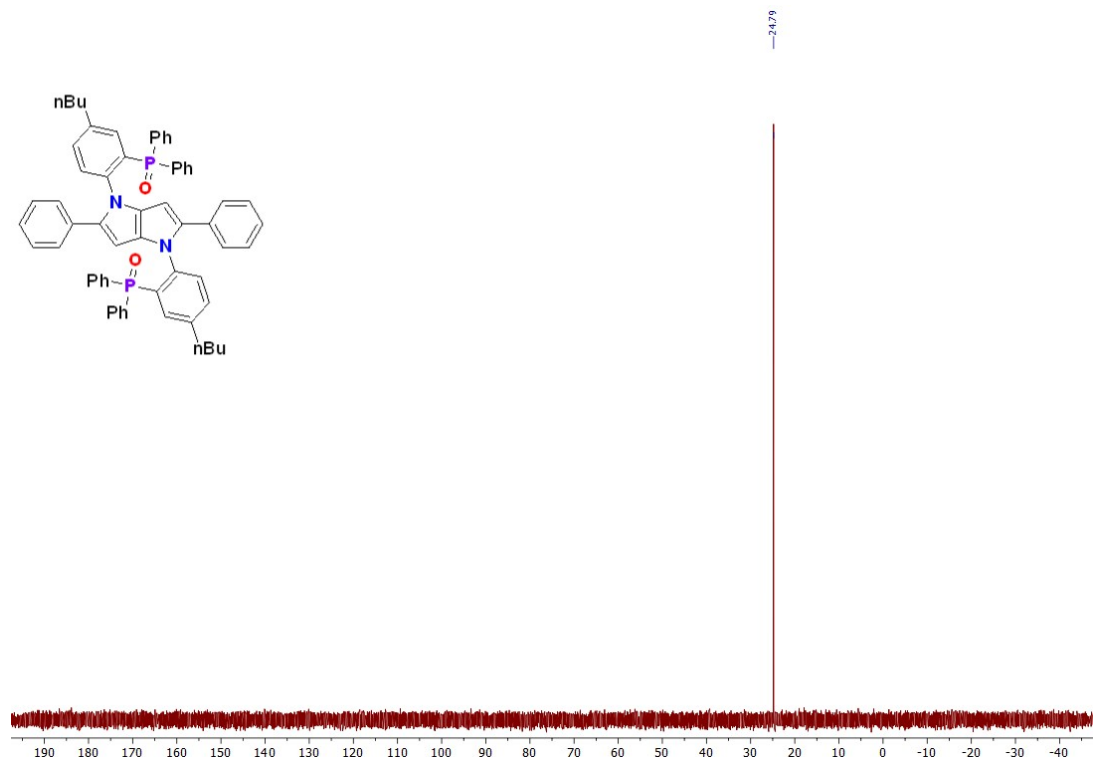
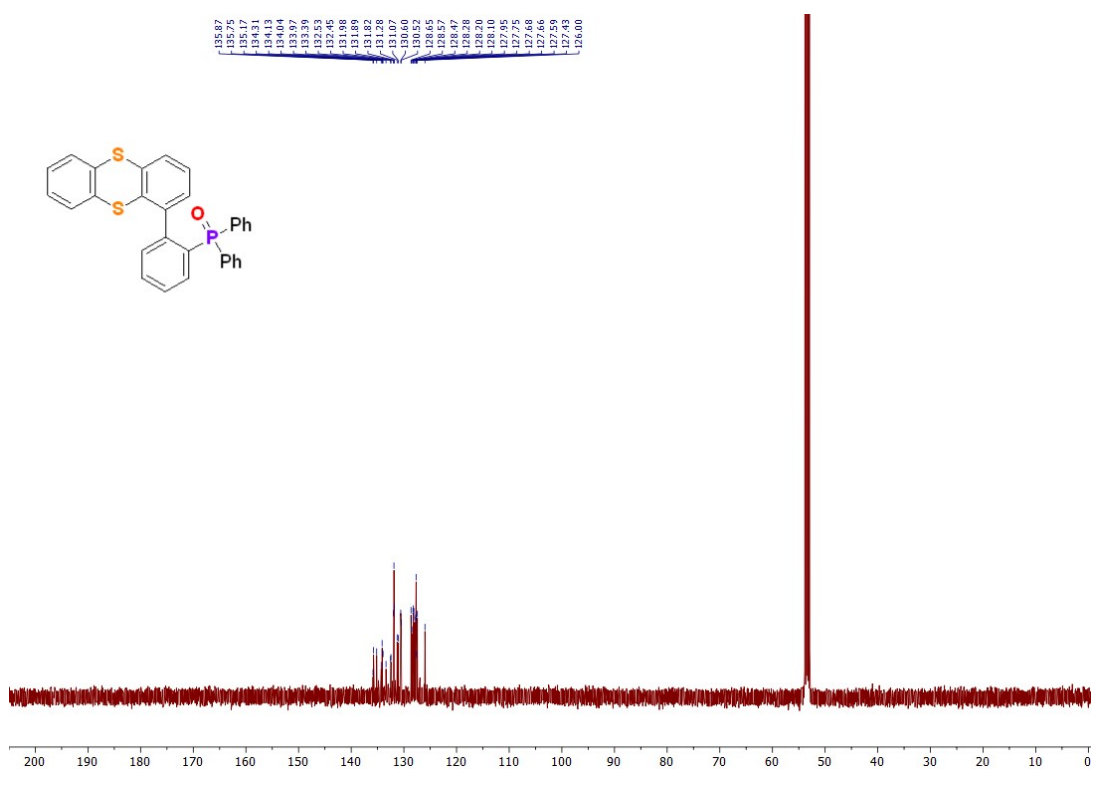
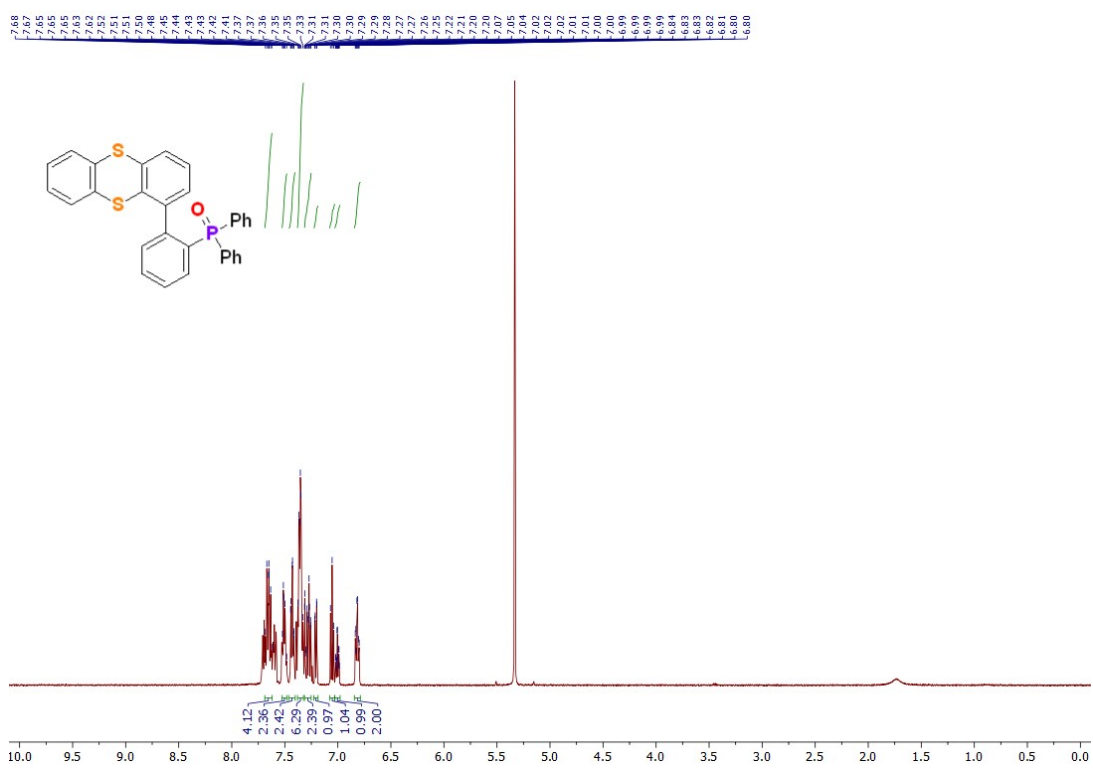


Figure S40: 202 MHz ^{31}P NMR spectrum of 1n in CD_2Cl_2



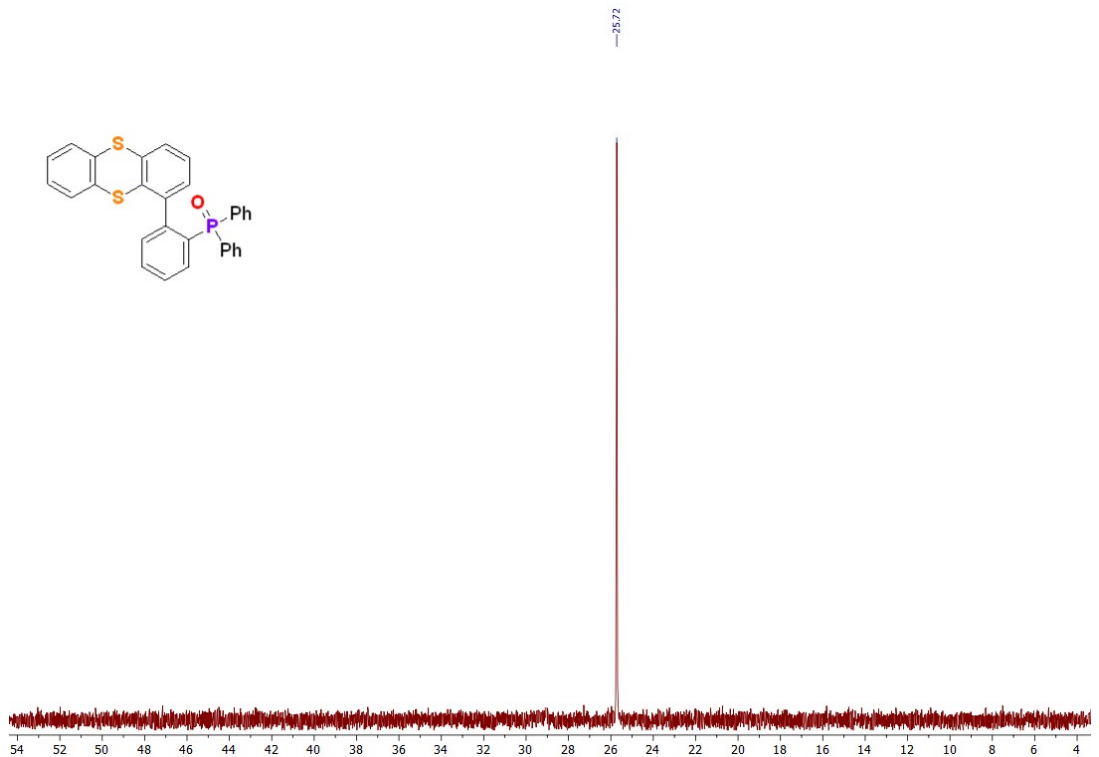


Figure S43: 202 MHz ^{31}P NMR spectrum of **1s** in CD_2Cl_2

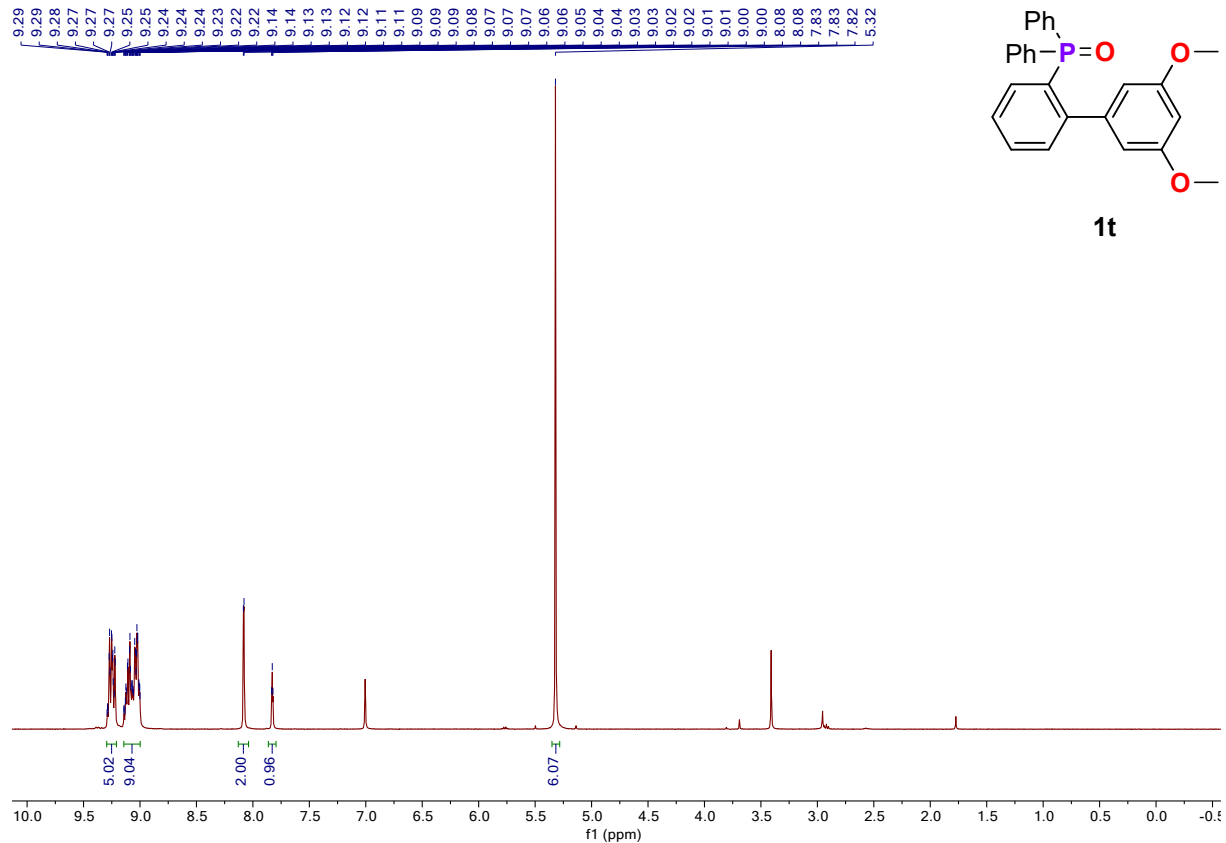


Figure S44: 400 MHz ^1H NMR spectrum of **1t** in CD_2Cl_2

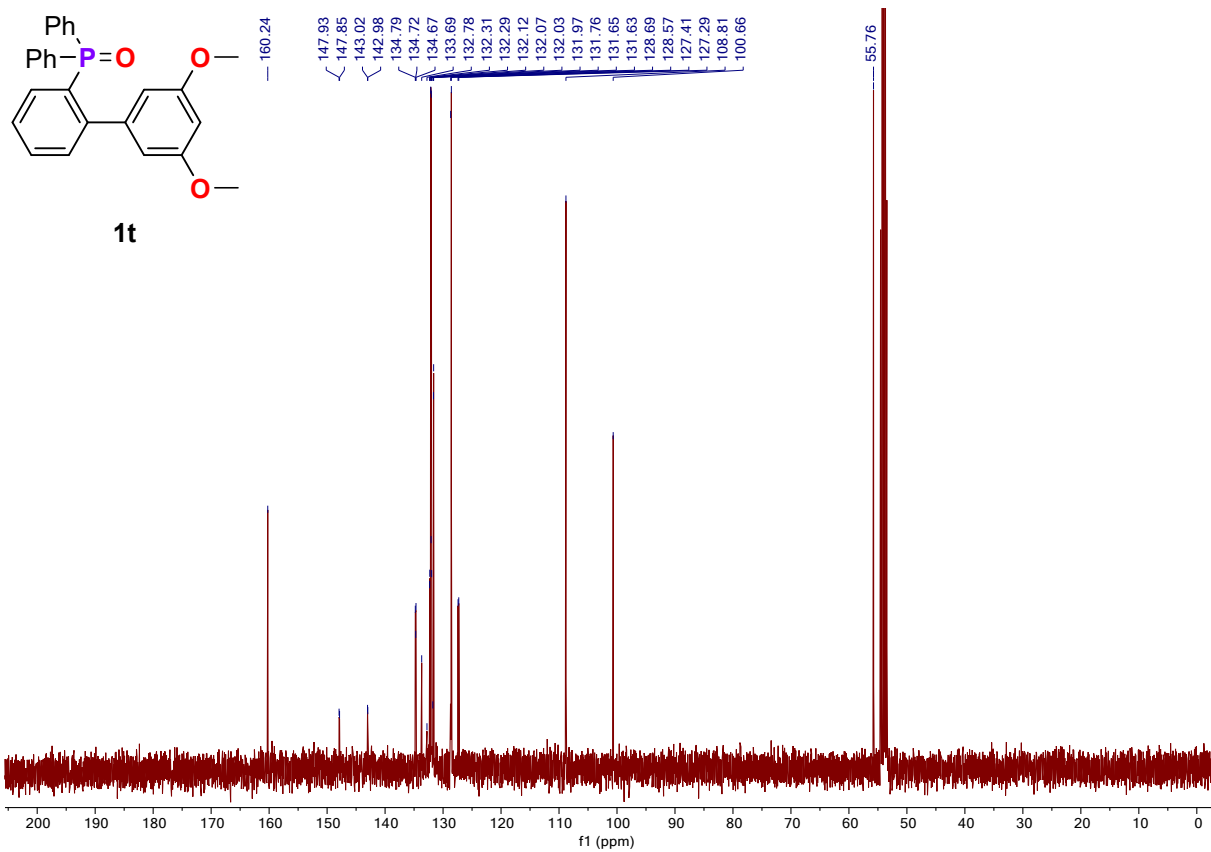


Figure S45: 101 MHz ^{13}C { ^1H } NMR spectrum of 1t in CD_2Cl_2

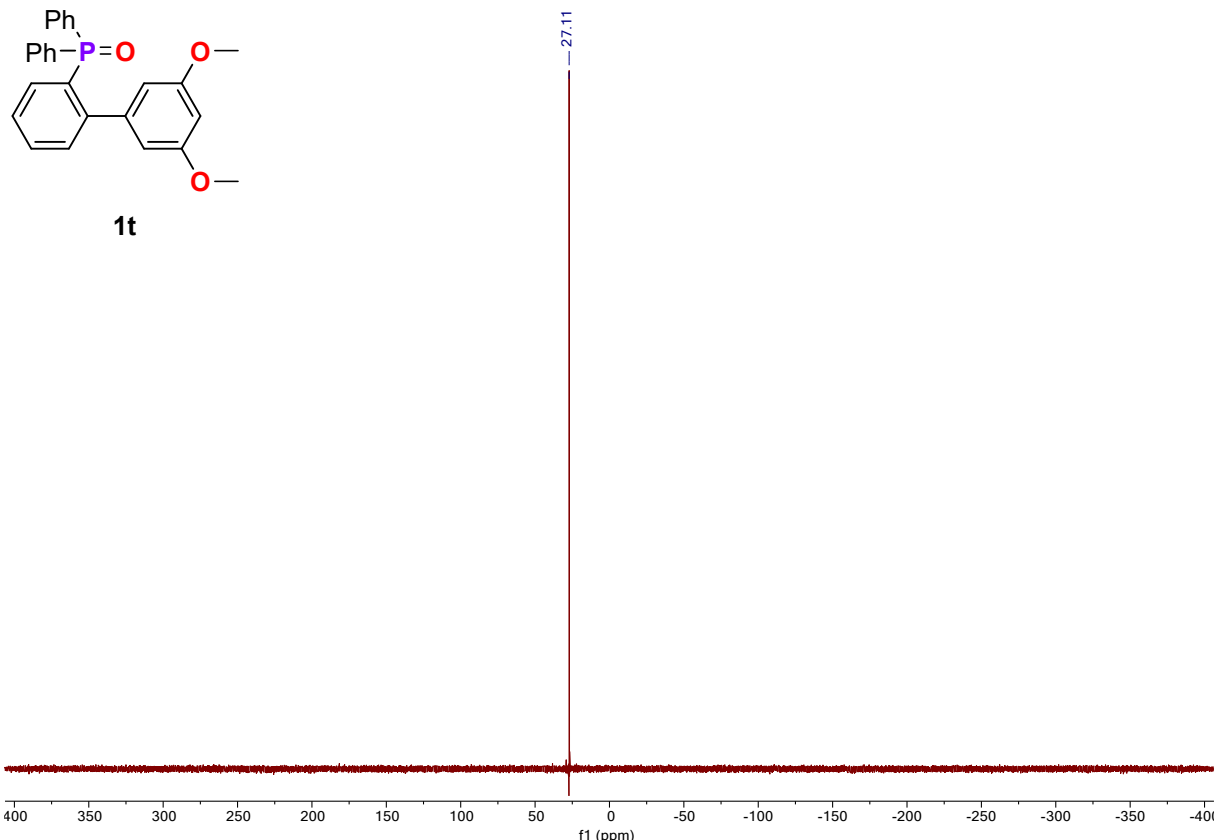


Figure S46: 161 MHz ^{31}P NMR spectrum of 1t in CD_2Cl_2

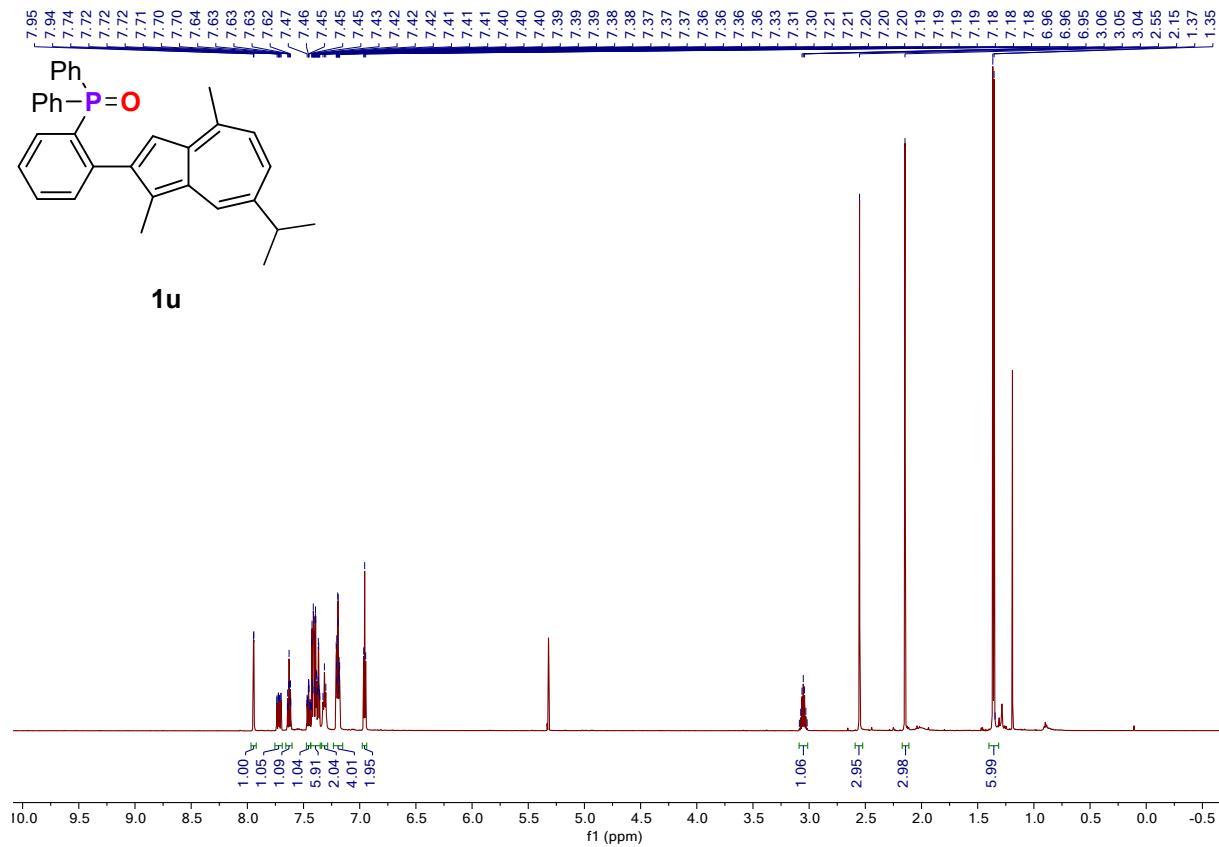


Figure S47: 600 MHz ^1H NMR spectrum of **1u** in CD_2Cl_2

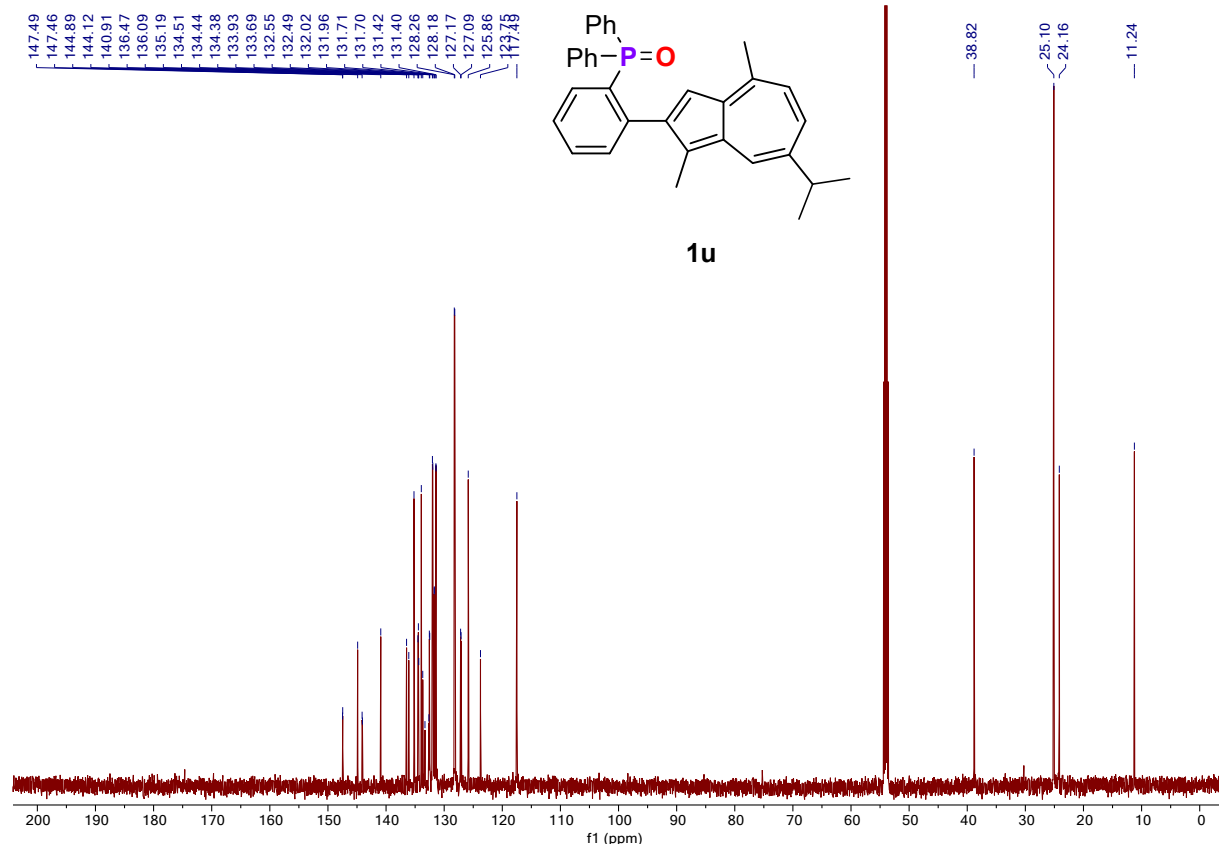


Figure S48: 151 MHz ^{13}C $\{{}^1\text{H}\}$ NMR spectrum of **1u** in CD_2Cl_2

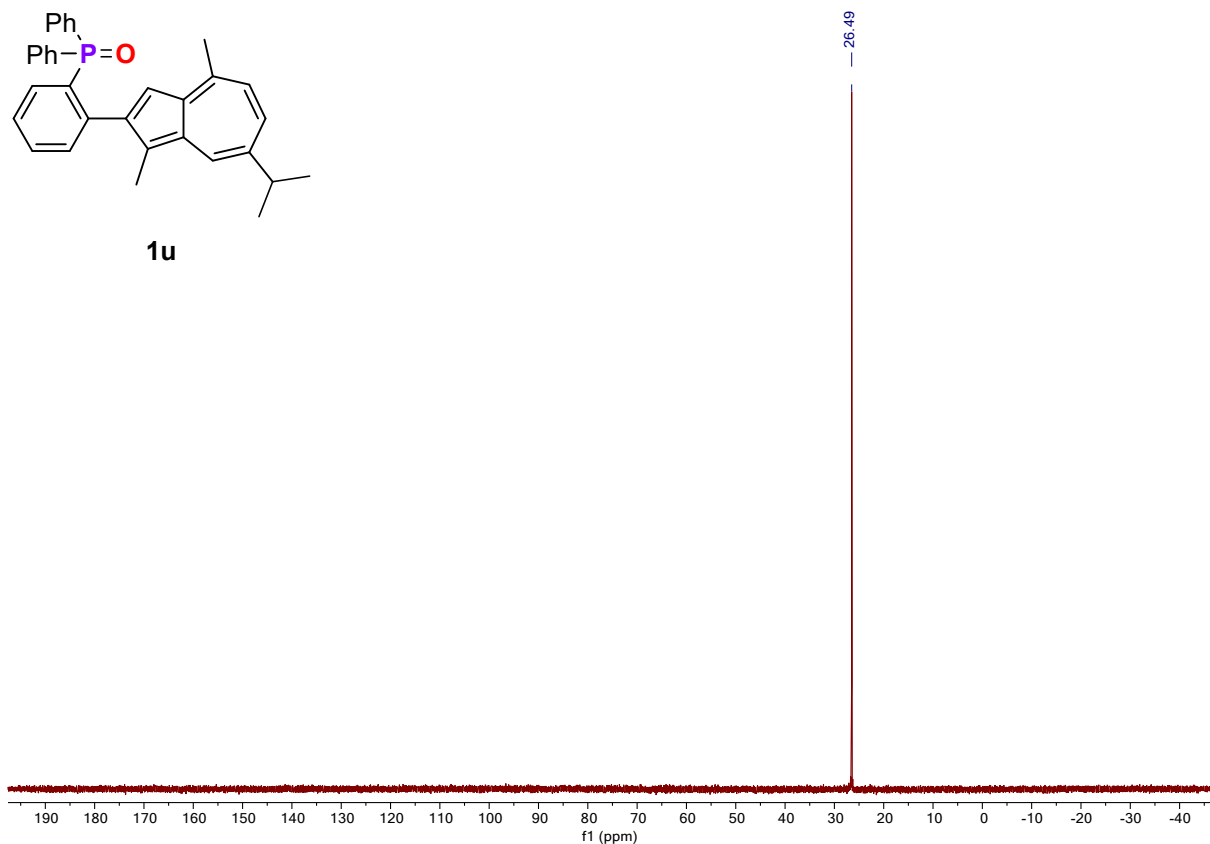
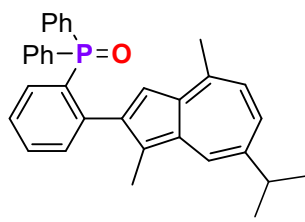


Figure S49: 243 MHz ^{31}P NMR spectrum of **1u** in CD_2Cl_2

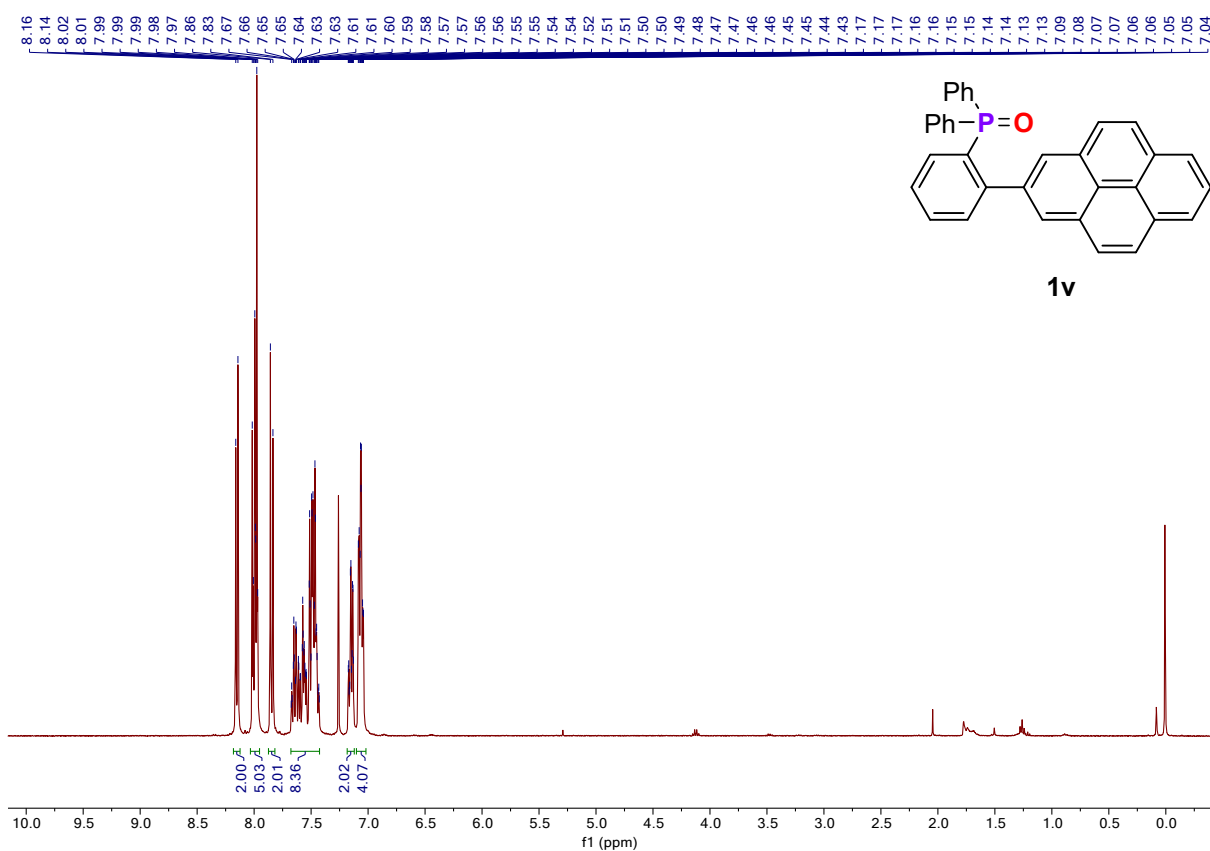
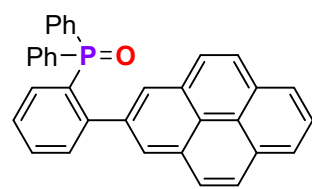


Figure S50: 400 MHz ^1H NMR spectrum of **1v** in CDCl_3

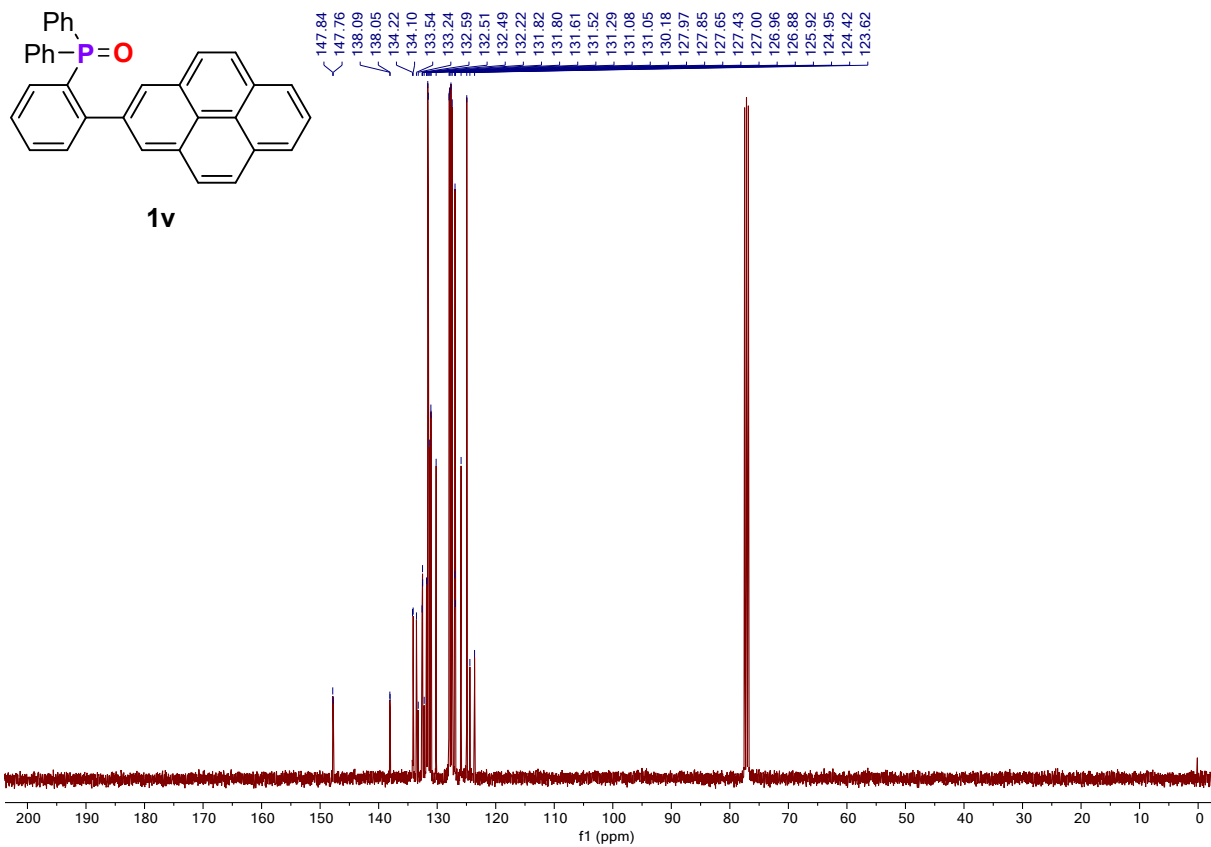


Figure S51: 101 MHz ^{13}C { ^1H } NMR spectrum of **1v** in CDCl_3

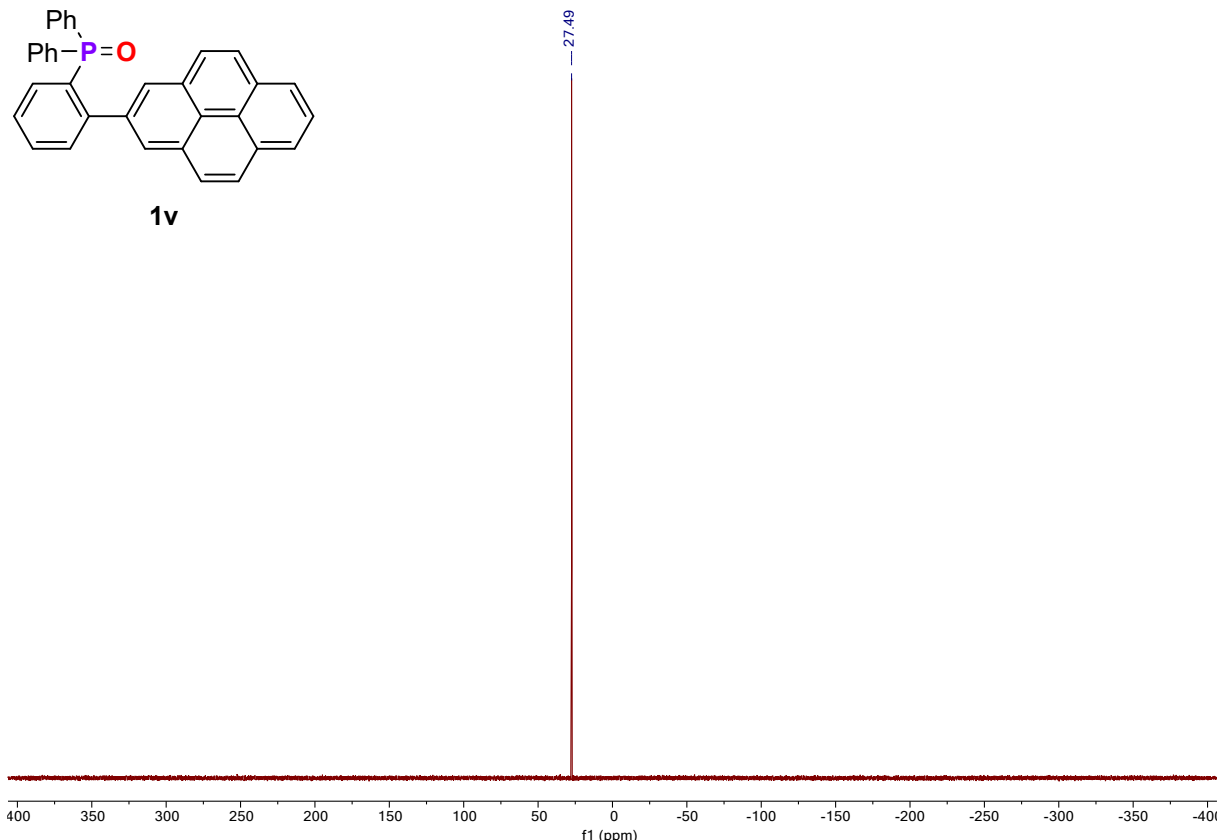


Figure S52: 161 MHz ^{31}P NMR spectrum of **1v** in CDCl_3

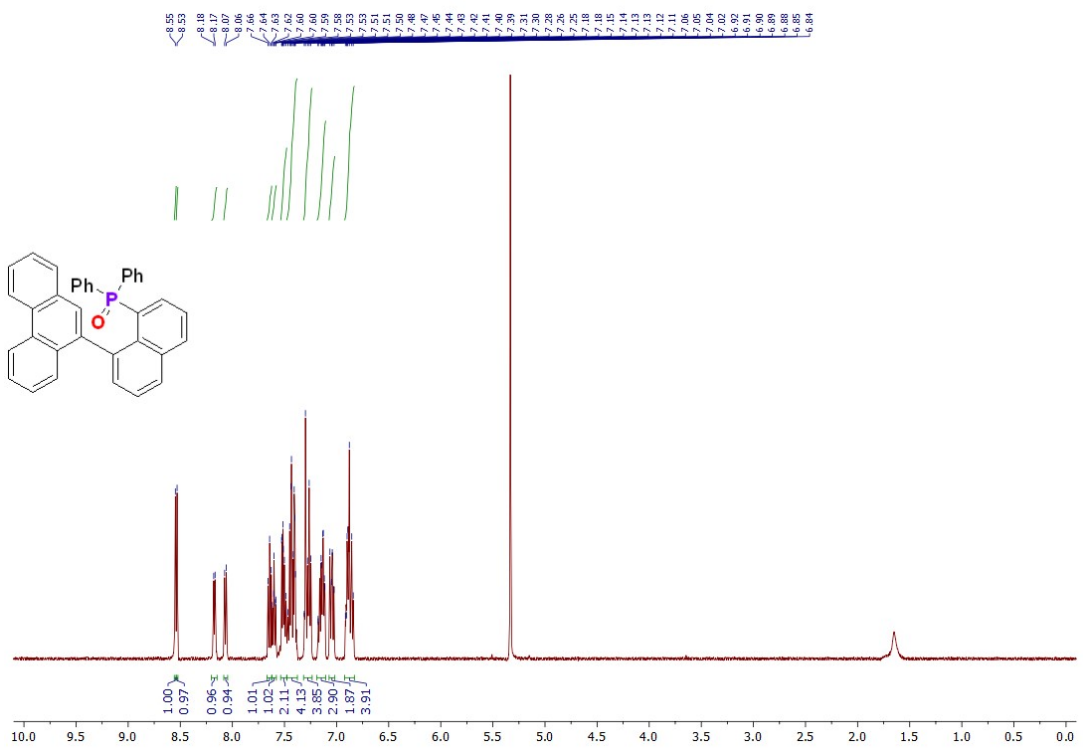


Figure S53: 500 MHz ^1H NMR spectrum of **1w** in CD_2Cl_2

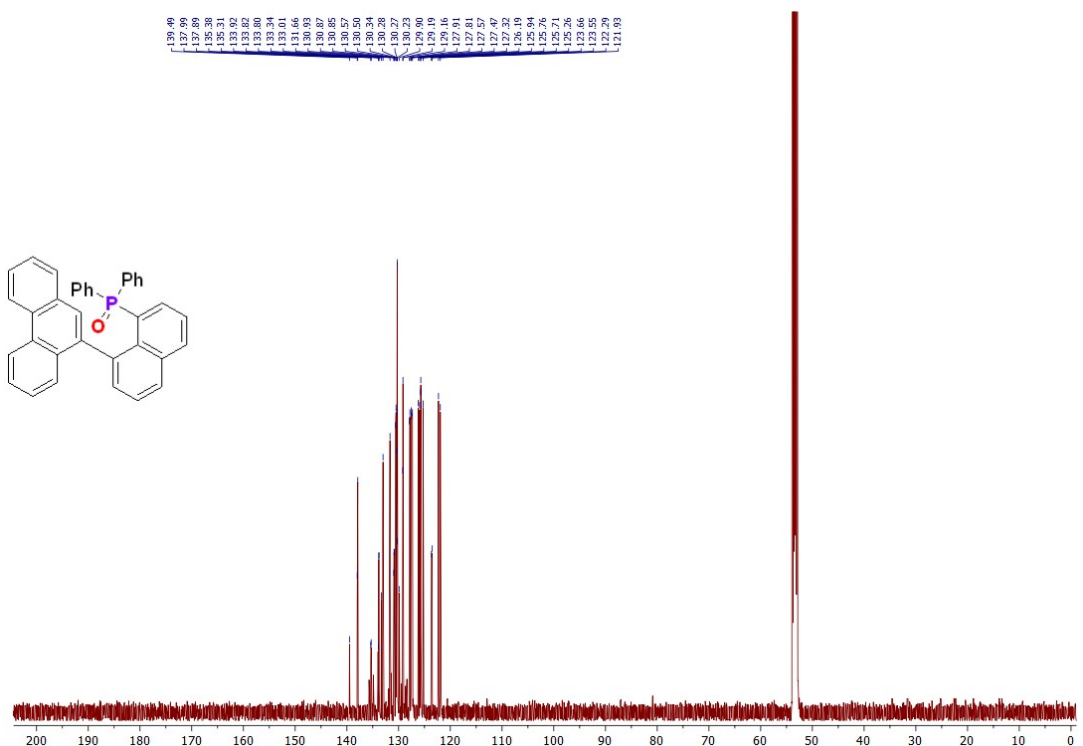


Figure S54: 126 MHz $^{13}\text{C}\{^1\text{H}\}$ NMR spectrum of **1w** in CD_2Cl_2

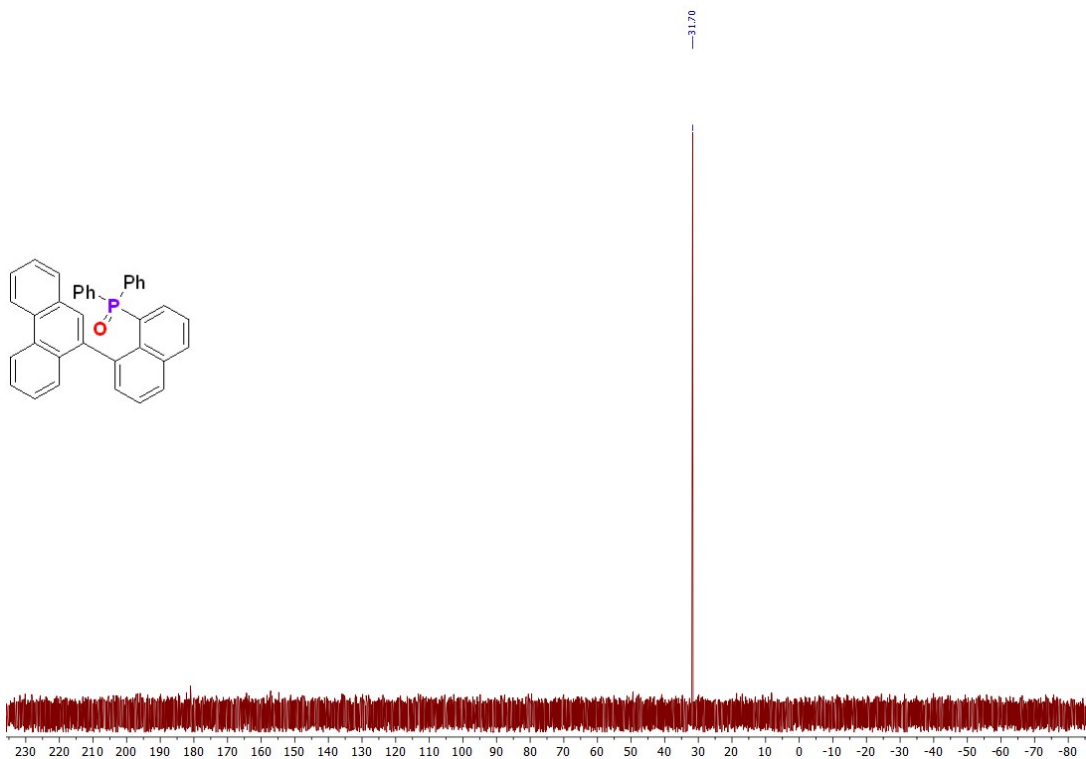


Figure S55: 243 MHz ^{31}P NMR spectrum of **1w** in CD_2Cl_2

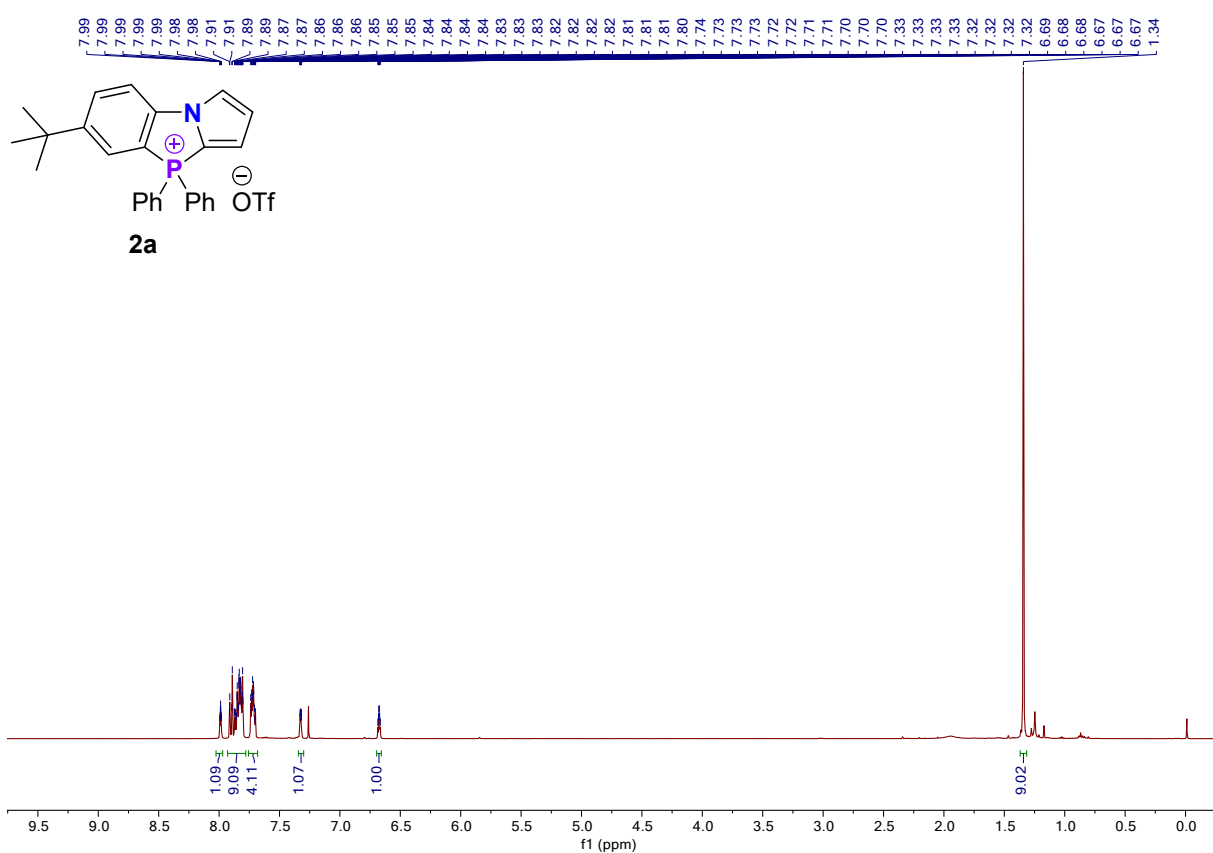


Figure S56: 500 MHz ^1H NMR spectrum of **2a** in CDCl_3

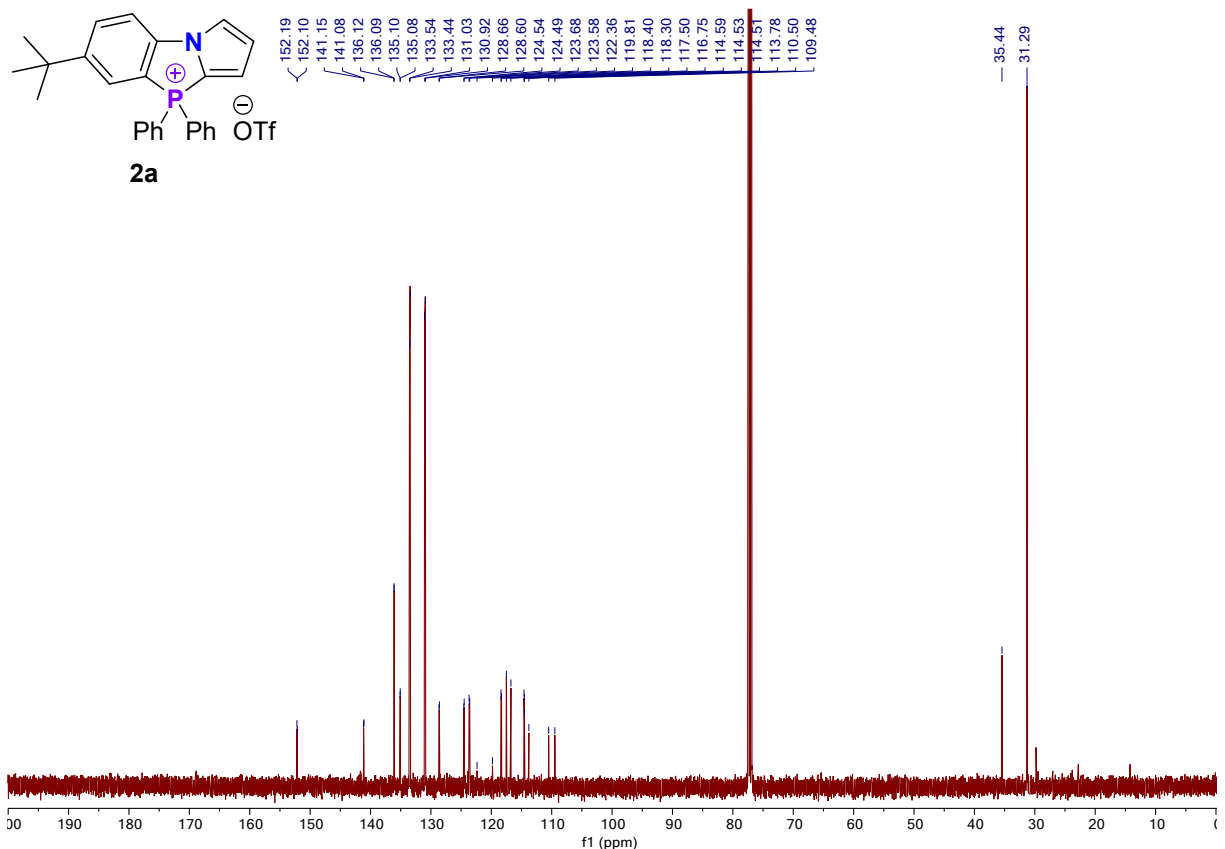


Figure S57: 126 MHz ^{13}C { ^1H } NMR spectrum of **2a** in CDCl_3

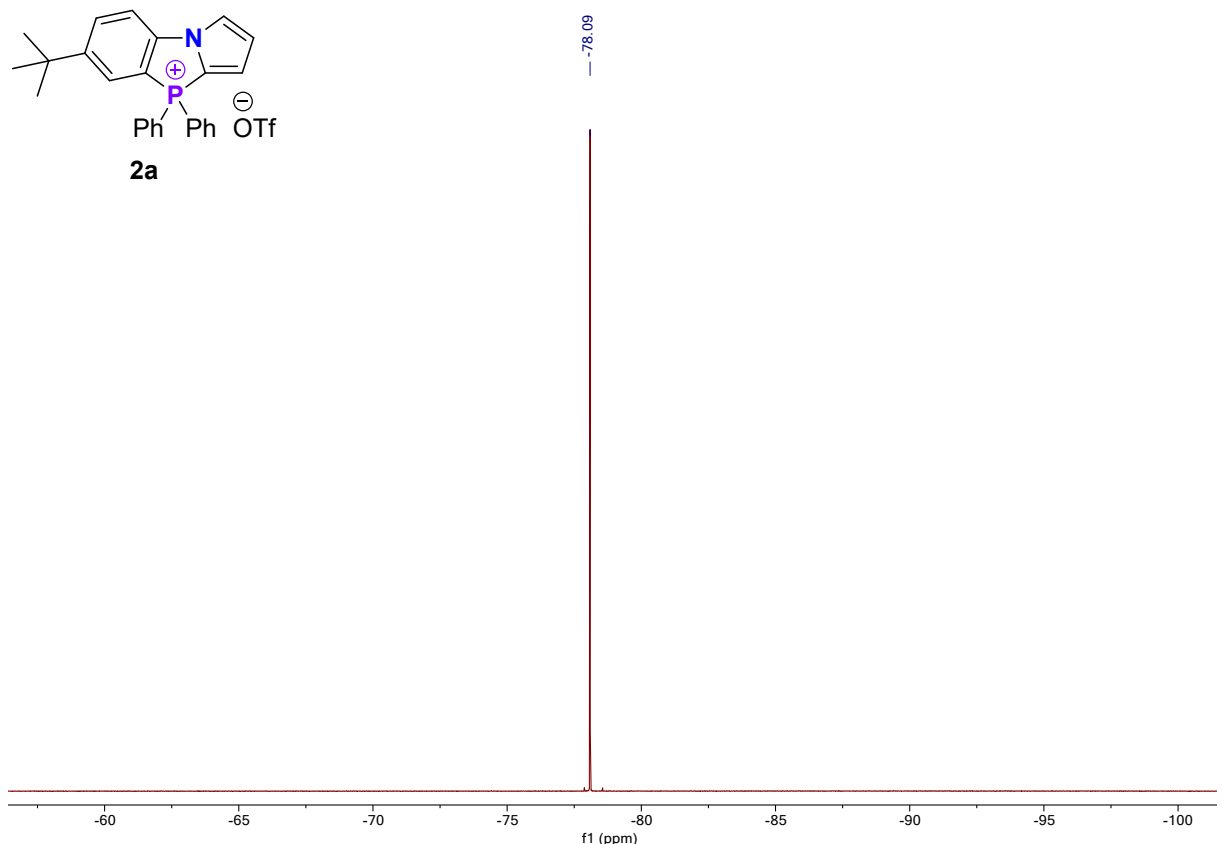


Figure S58: 470 MHz ^{19}F NMR spectrum of **2a** in CDCl_3

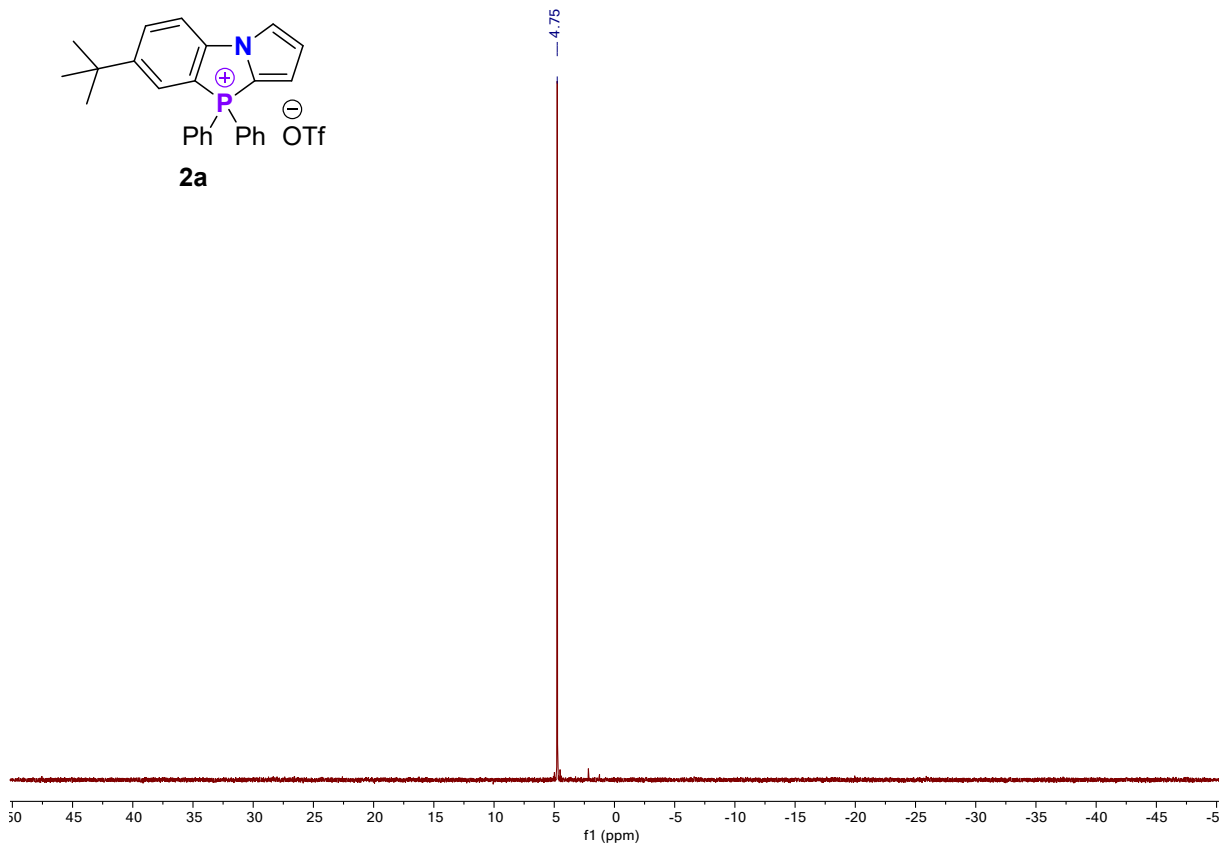


Figure S59: 202 MHz ^{31}P NMR spectrum of **2a** in CDCl_3

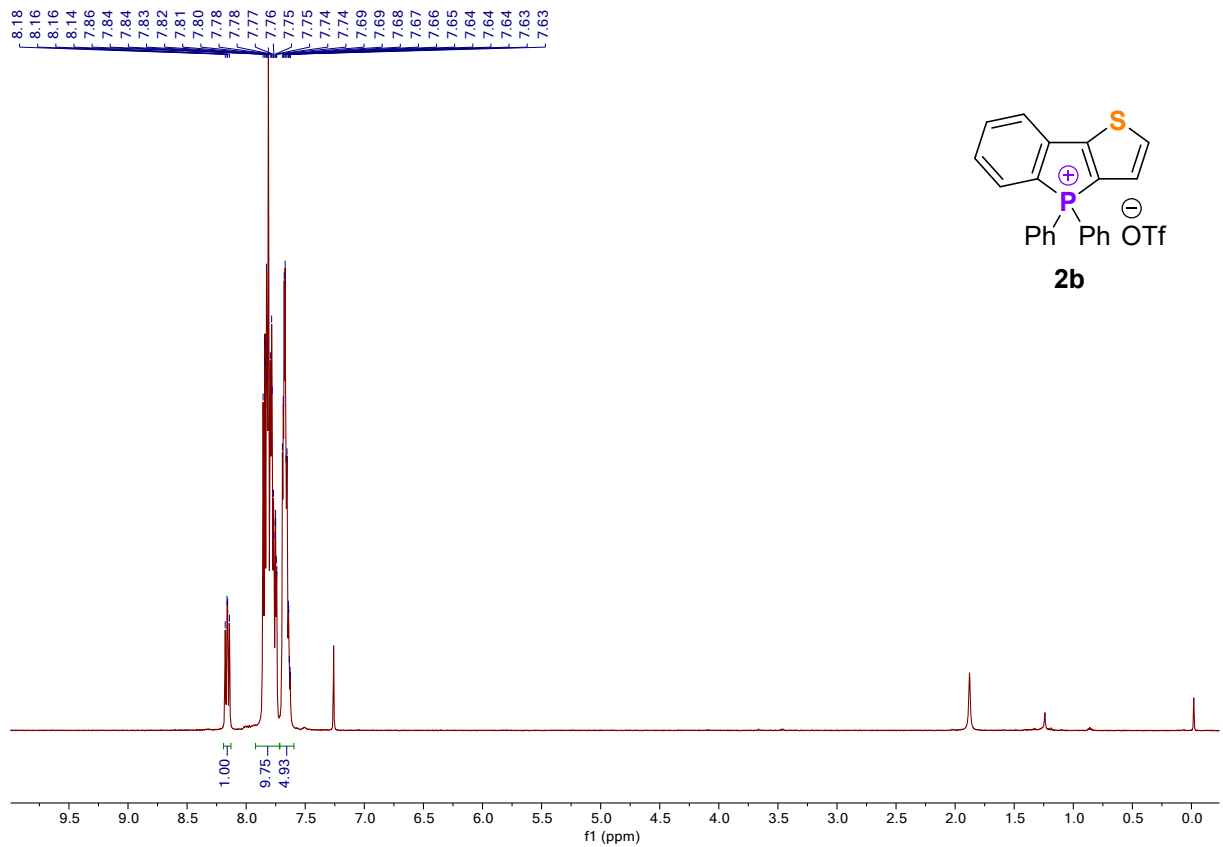


Figure S60: 500 MHz ^1H NMR spectrum of **2b** in CDCl_3

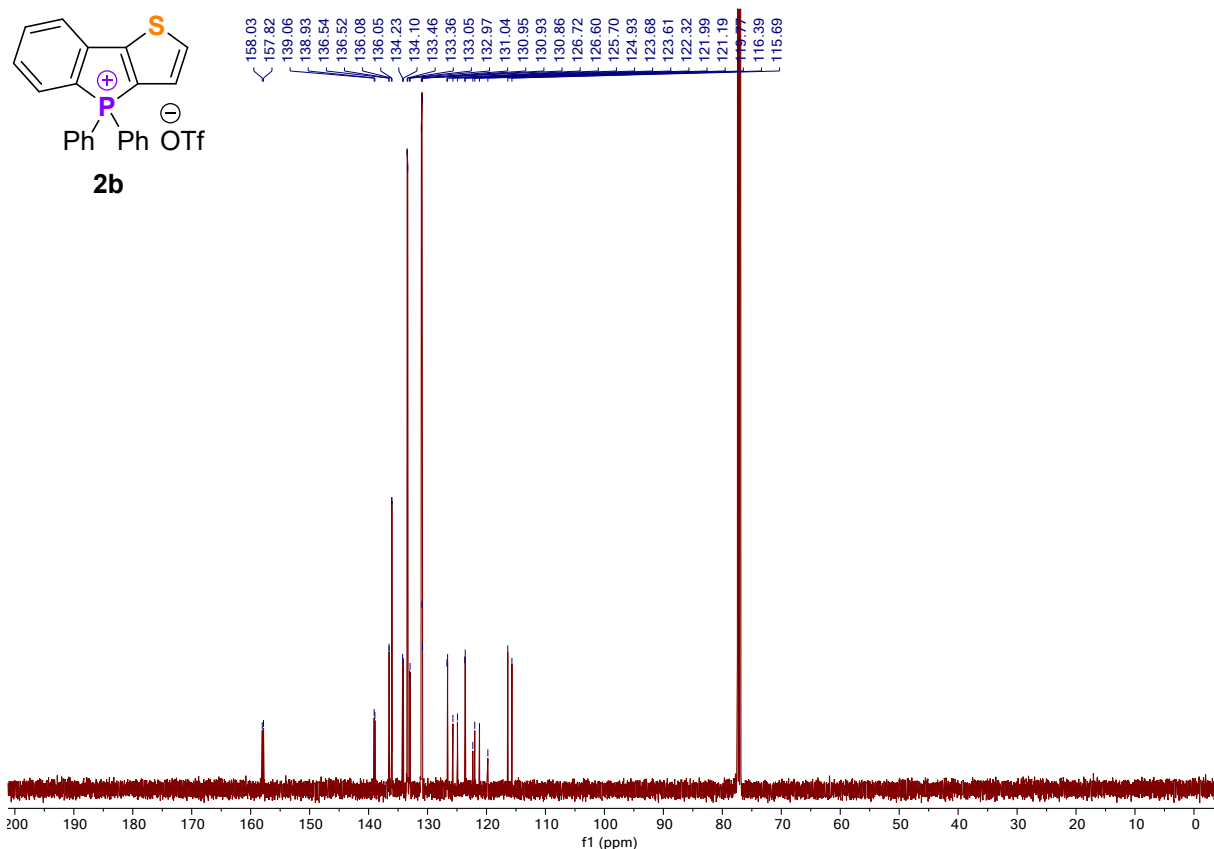


Figure S61: 126 MHz ^{13}C { ^1H } NMR spectrum of **2b** in CDCl_3

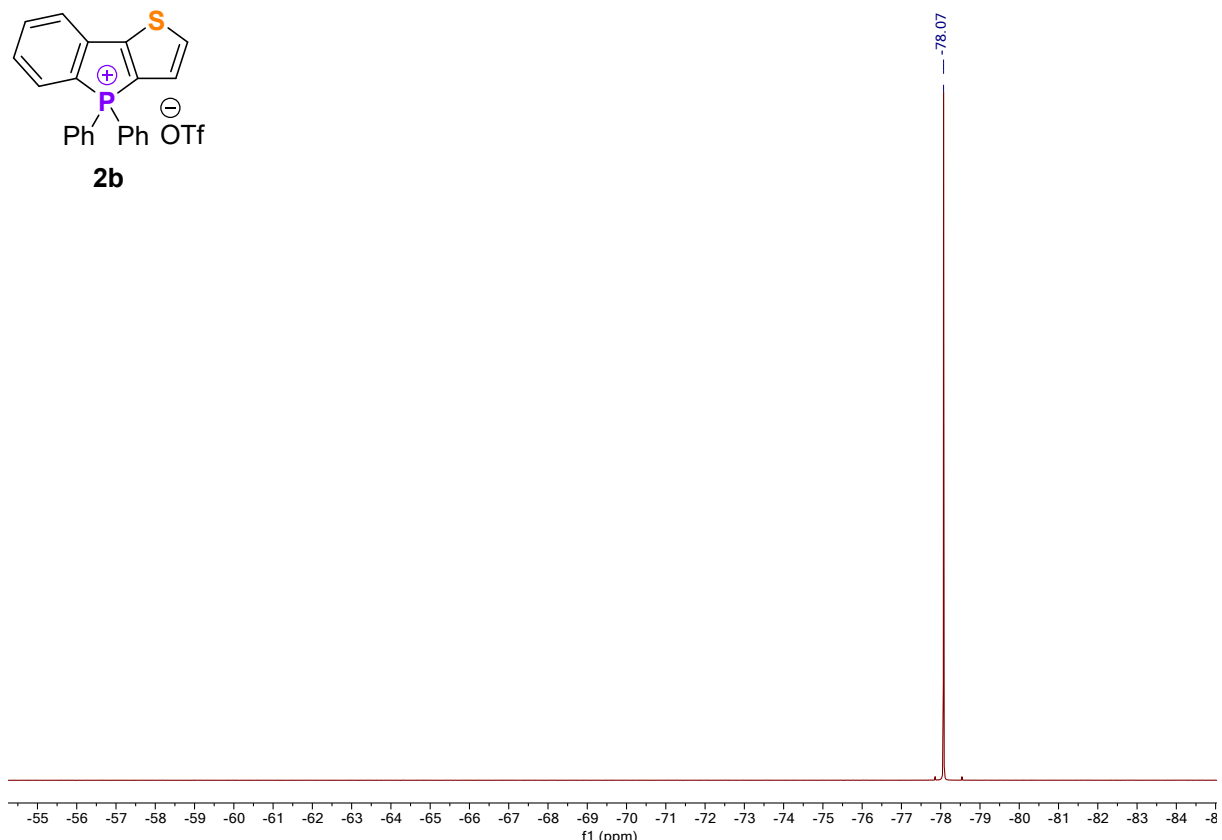


Figure S62: 470 MHz ^{19}F NMR spectrum of **2b** in CDCl_3

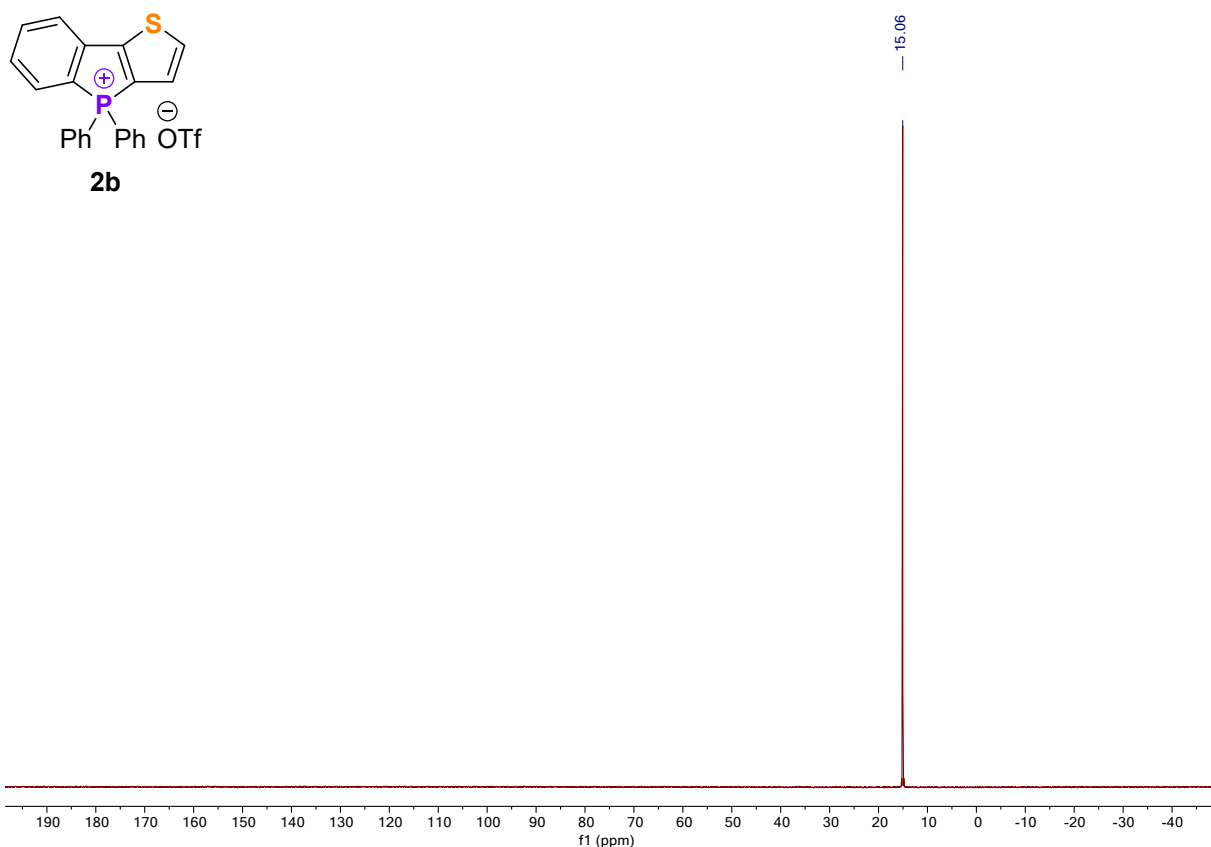


Figure S63: 202 MHz ^{31}P NMR spectrum of **2b** in CDCl_3

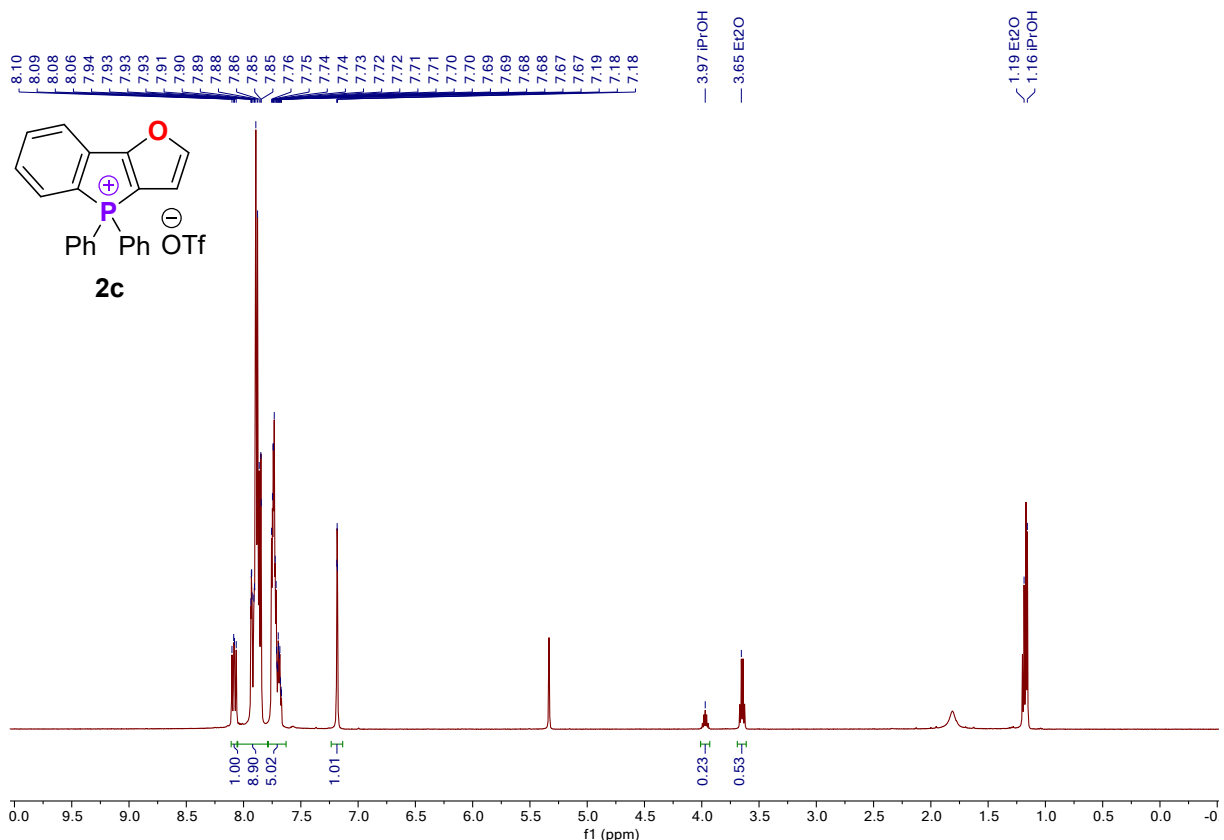


Figure S64: 500 MHz ^1H NMR spectrum of **2c** in CD_2Cl_2

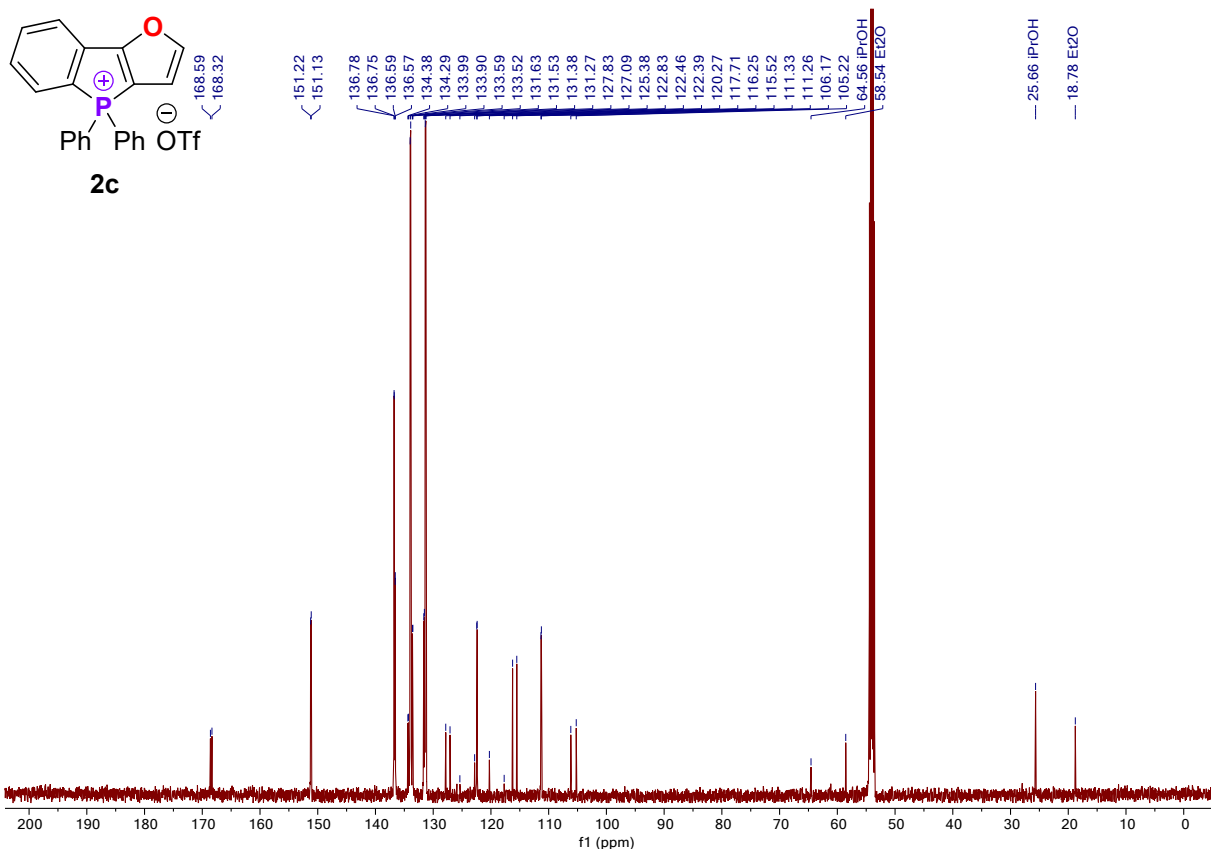


Figure S65: 126 MHz ^{13}C { ^1H } NMR spectrum of **2c** in CD_2Cl_2

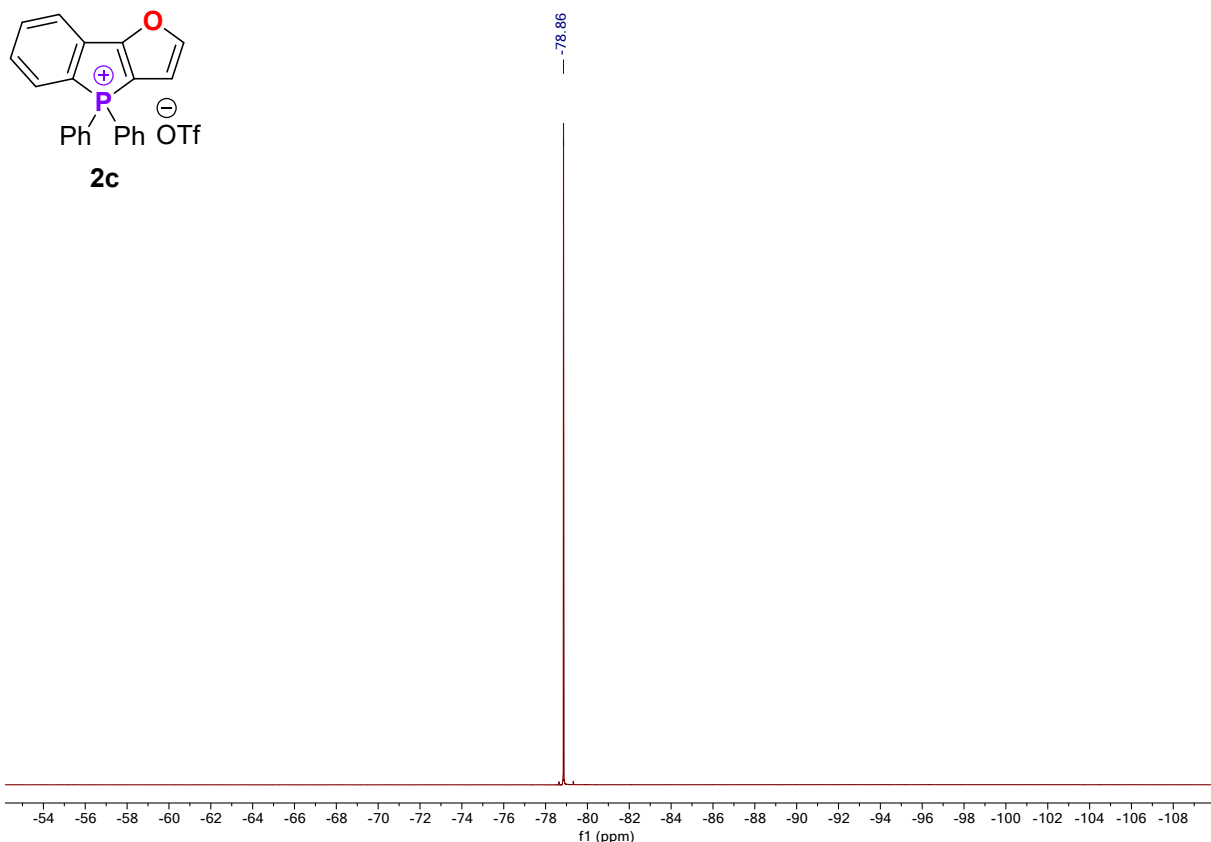


Figure S66: 470 MHz ^{19}F NMR spectrum of **2c** in CD_2Cl_2

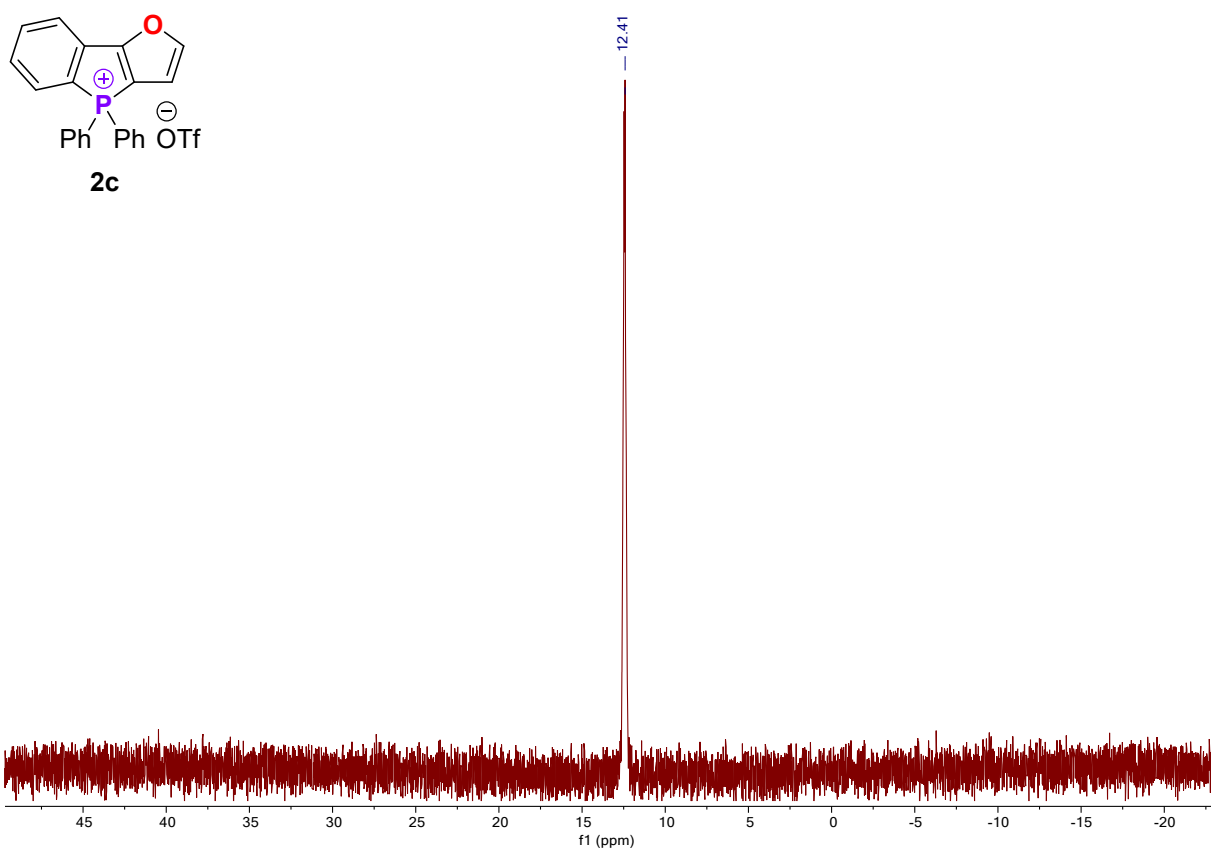


Figure S67: 202 MHz ^{31}P NMR spectrum of **2c** in CD_2Cl_2

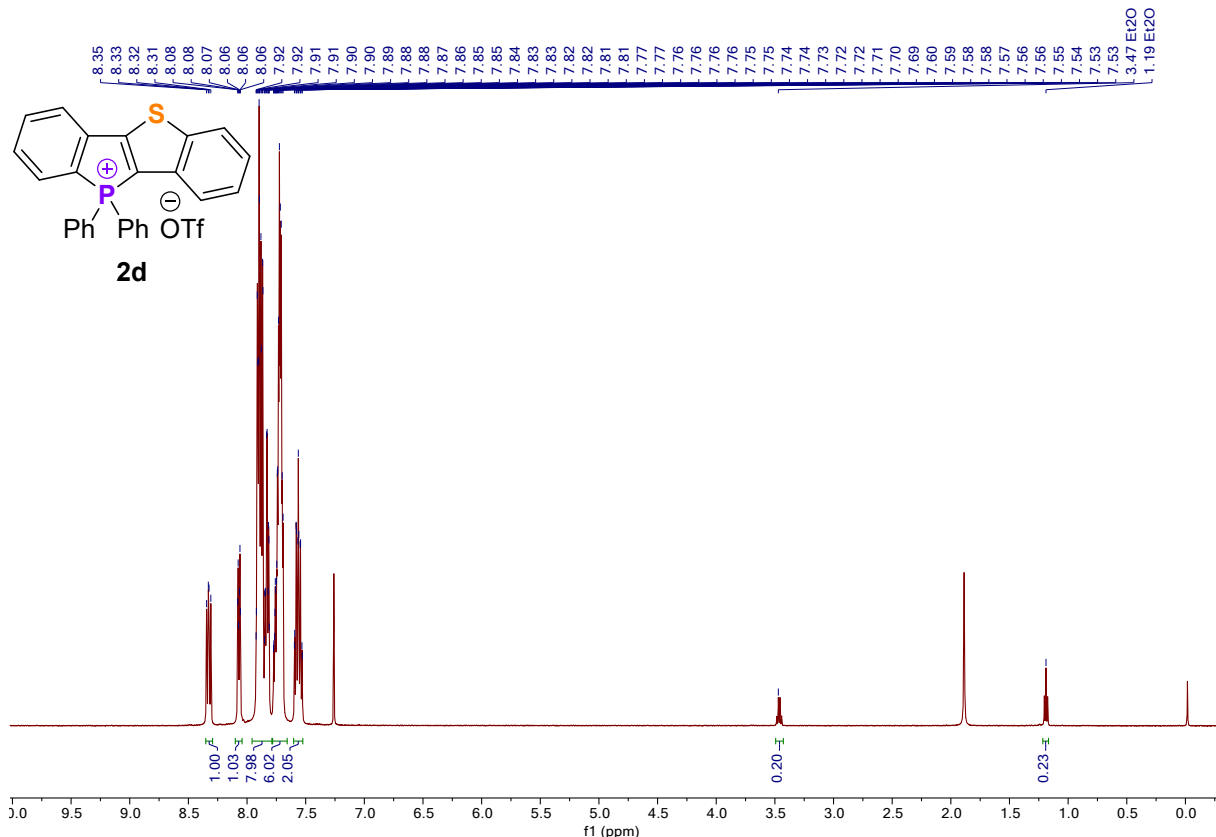


Figure S68: 500 MHz ^1H NMR spectrum of **2d** in CDCl_3

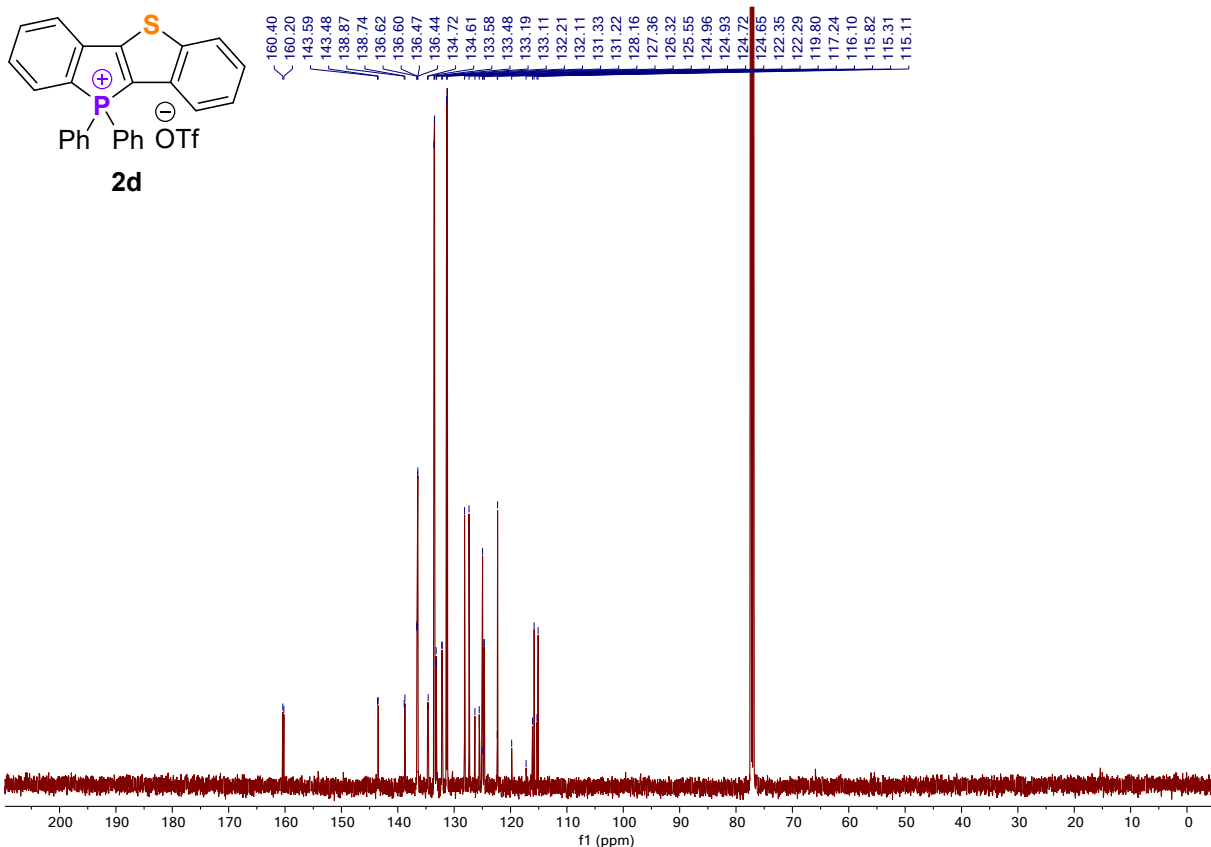


Figure S69: 126 MHz ^{13}C { ^1H } NMR spectrum of **2d** in CDCl_3

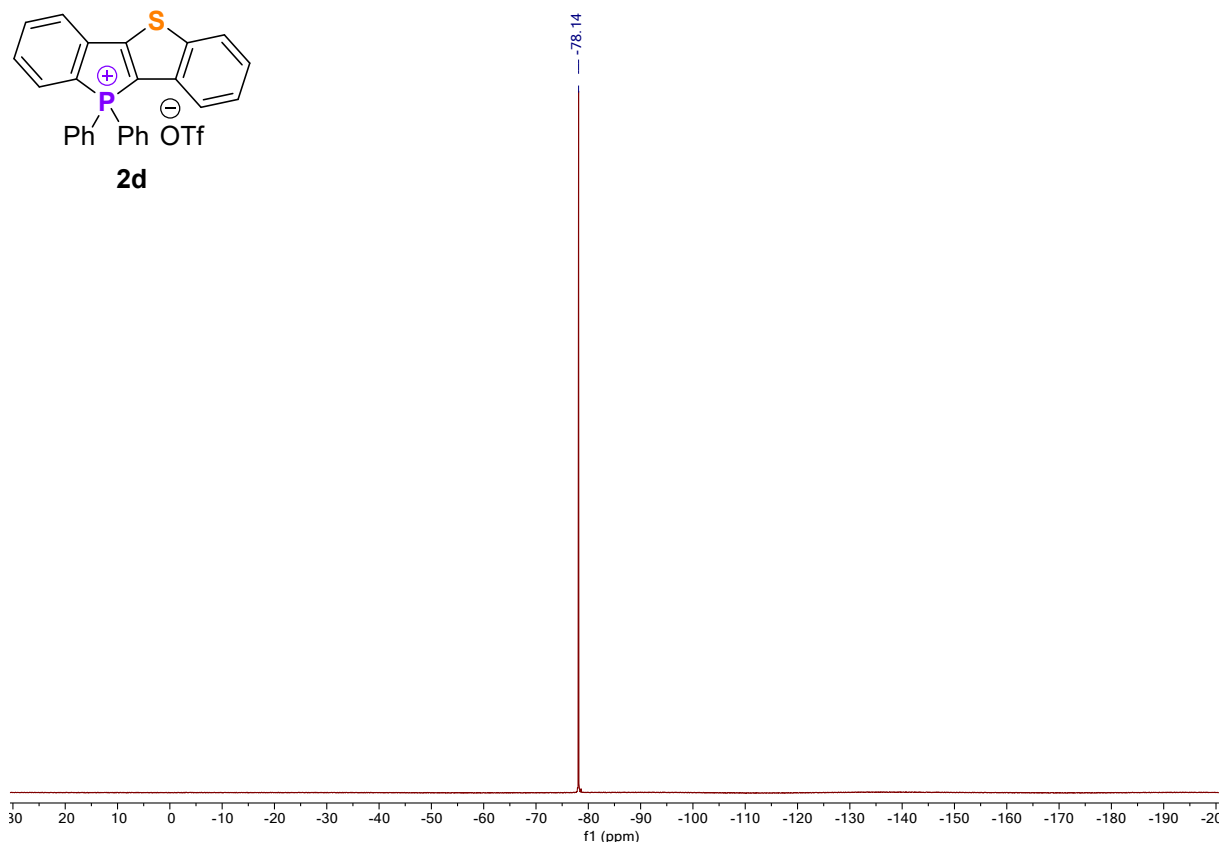


Figure S70: 470 MHz ^{19}F NMR spectrum of **2d** in CDCl_3

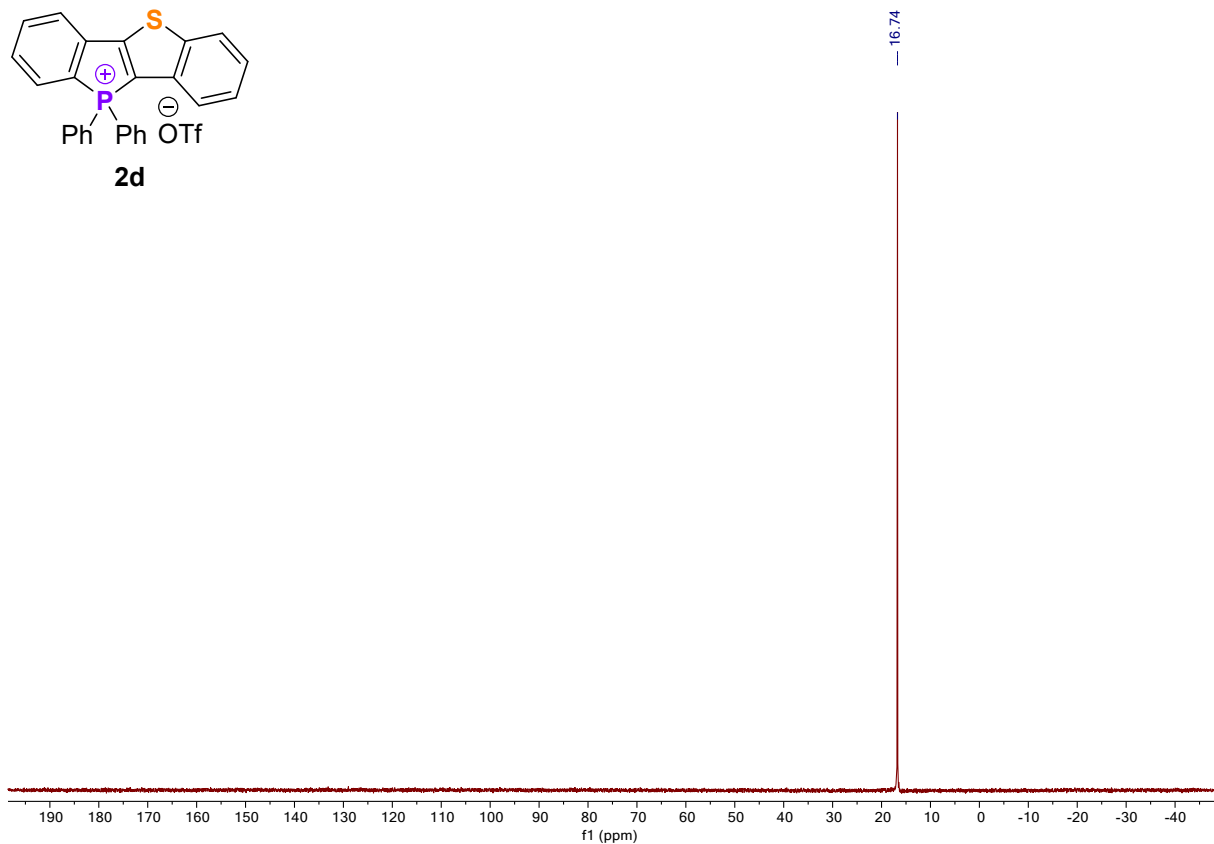


Figure S71: 202 MHz ^{31}P NMR spectrum of **2d** in CDCl_3

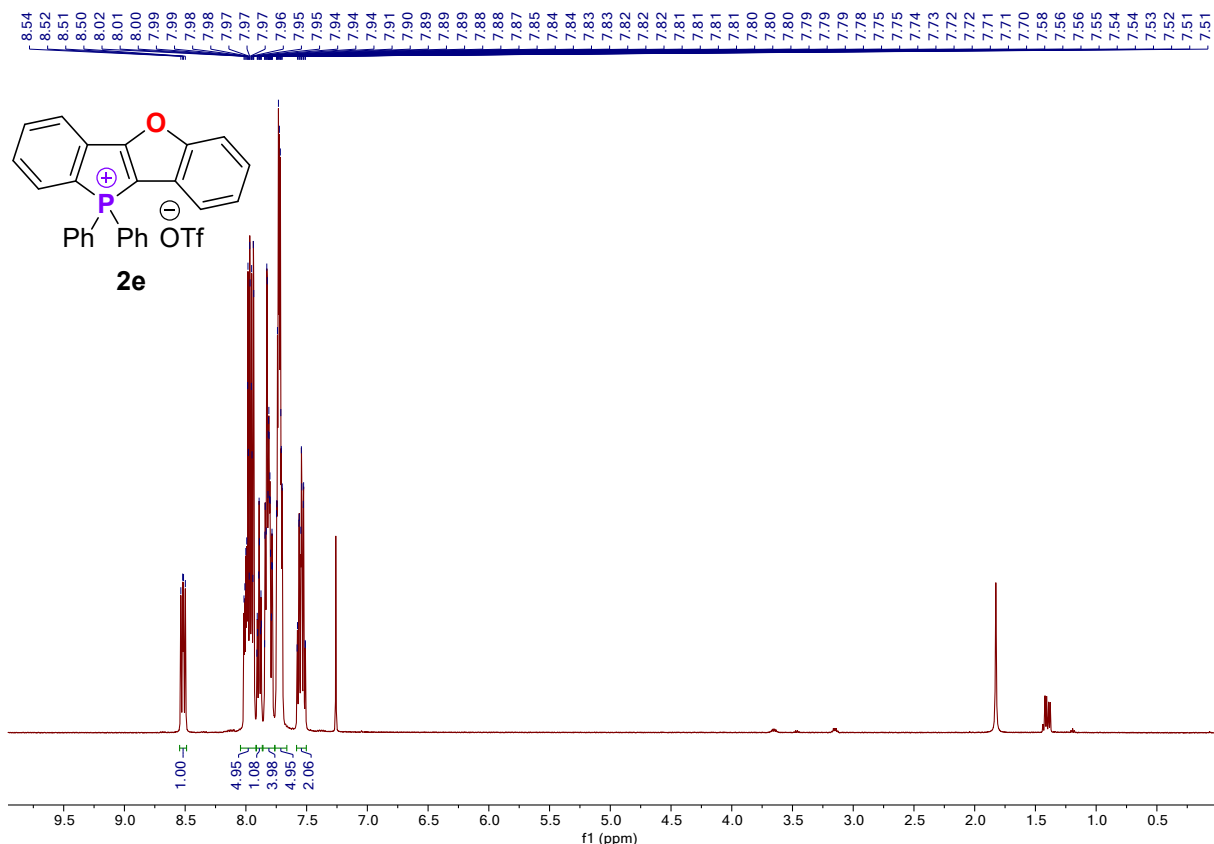


Figure S72: 500 MHz ^1H NMR spectrum of **2e** in CDCl_3

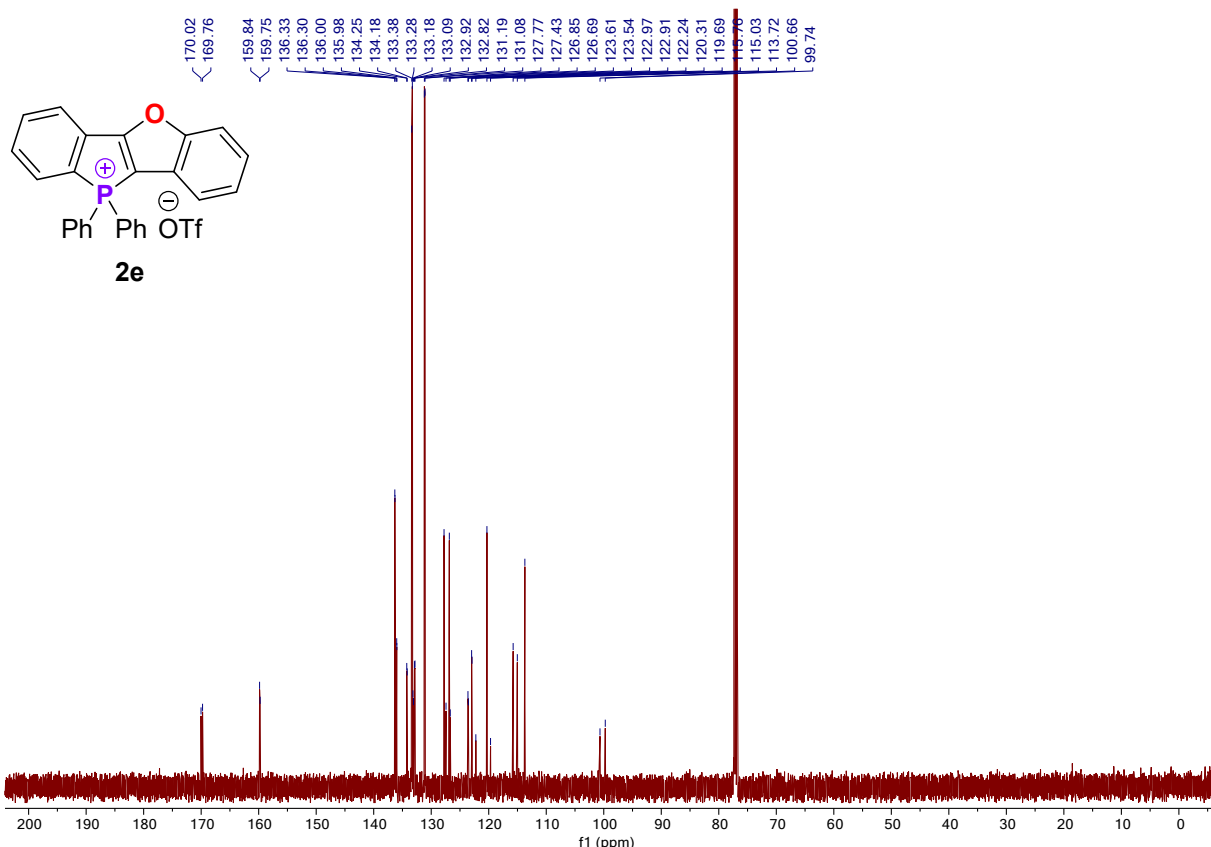


Figure S73: 126 MHz ^{13}C { ^1H } NMR spectrum of **2e** in CDCl_3

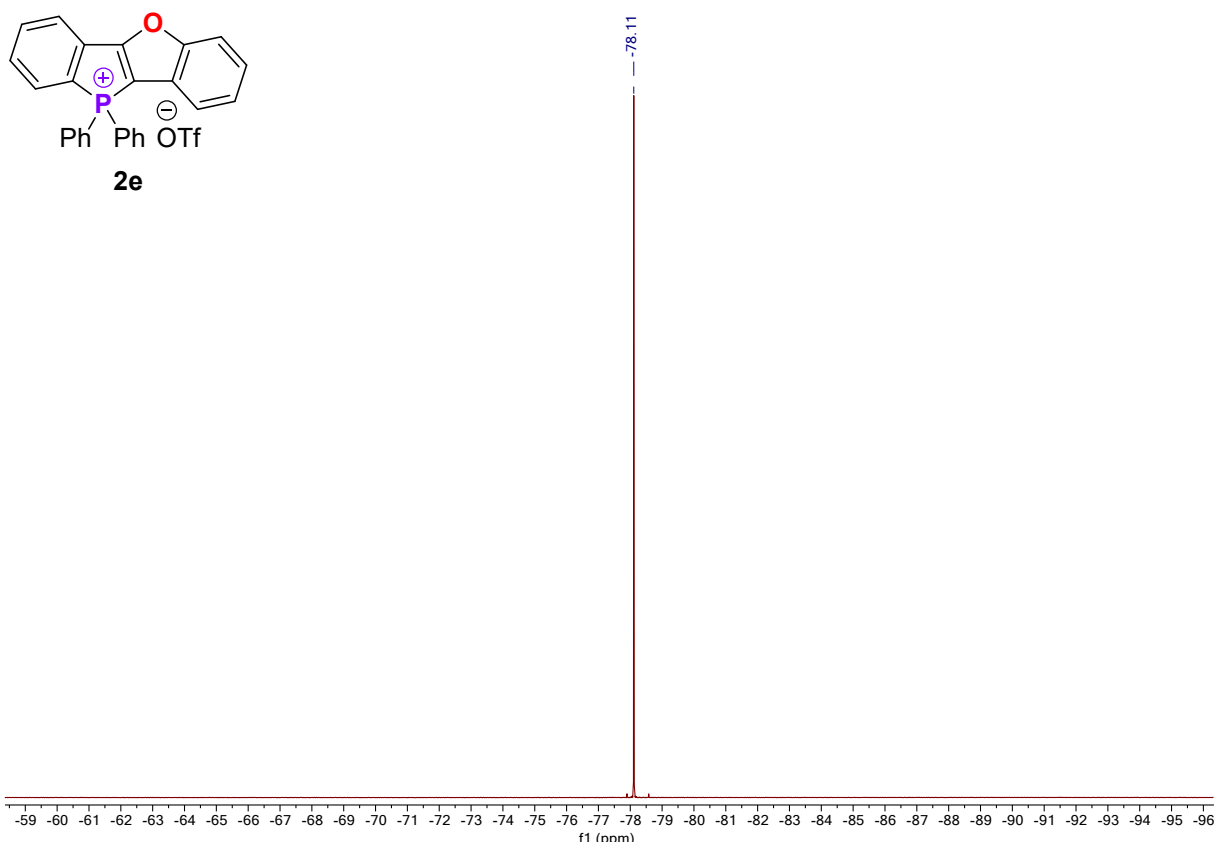


Figure S74: 470 MHz ^{19}F NMR spectrum of **2e** in CDCl_3

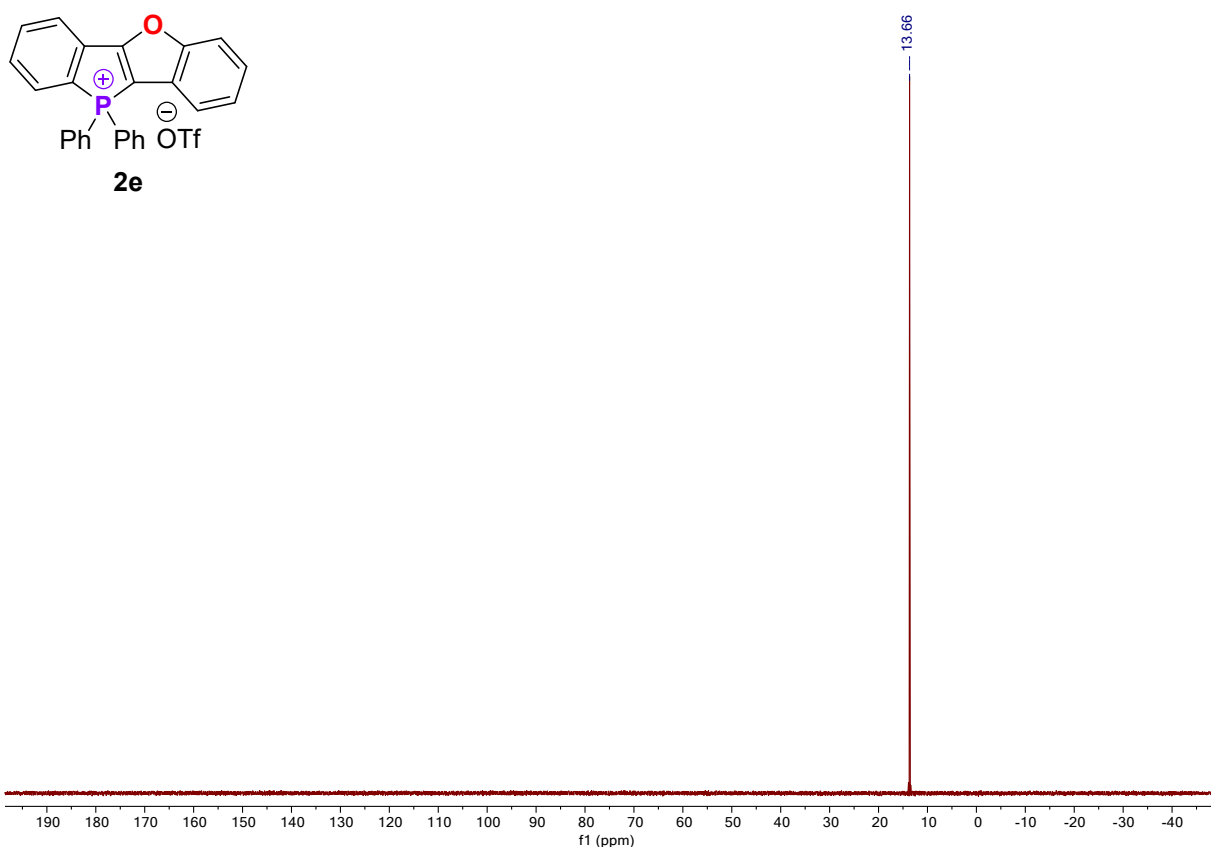


Figure S75: 202 MHz ^{31}P NMR spectrum of **2e** in CDCl_3

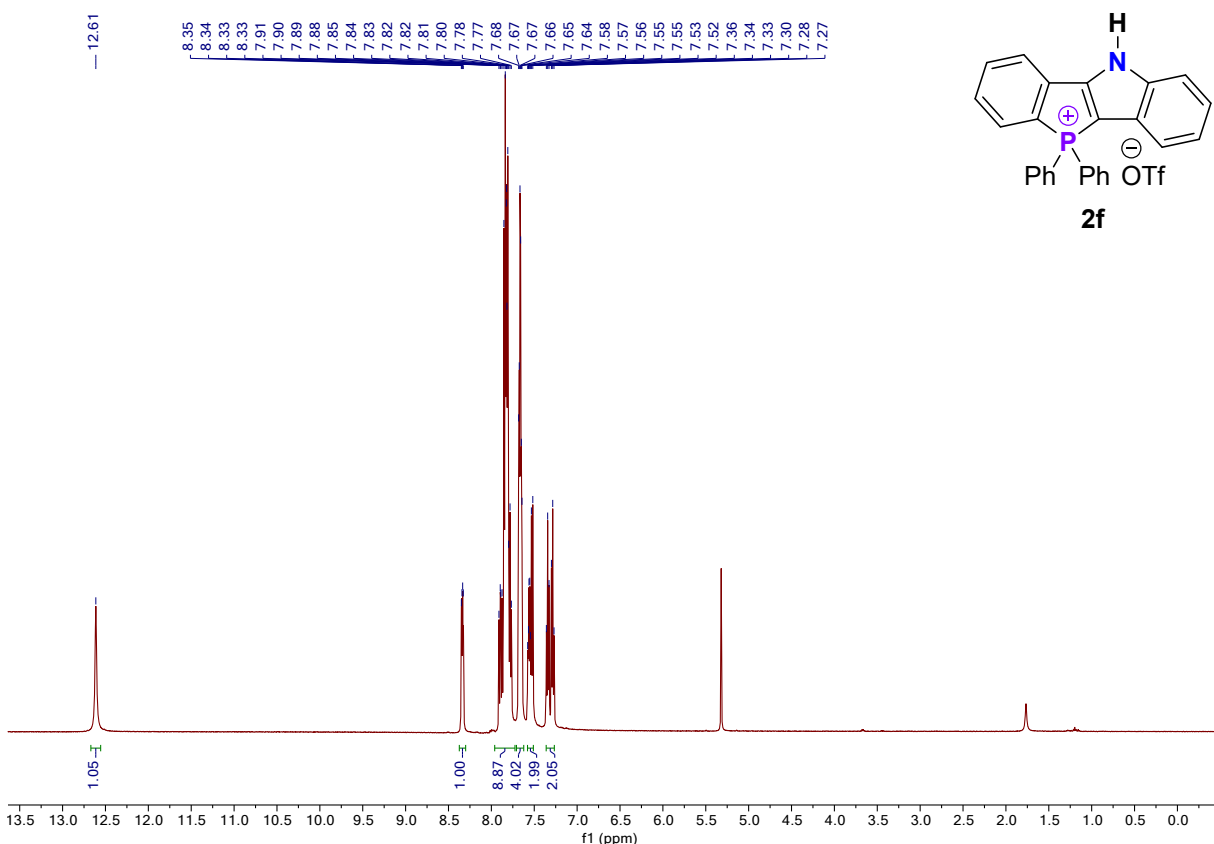


Figure S76: 500 MHz ^1H NMR spectrum of **2f** in CD_2Cl_2

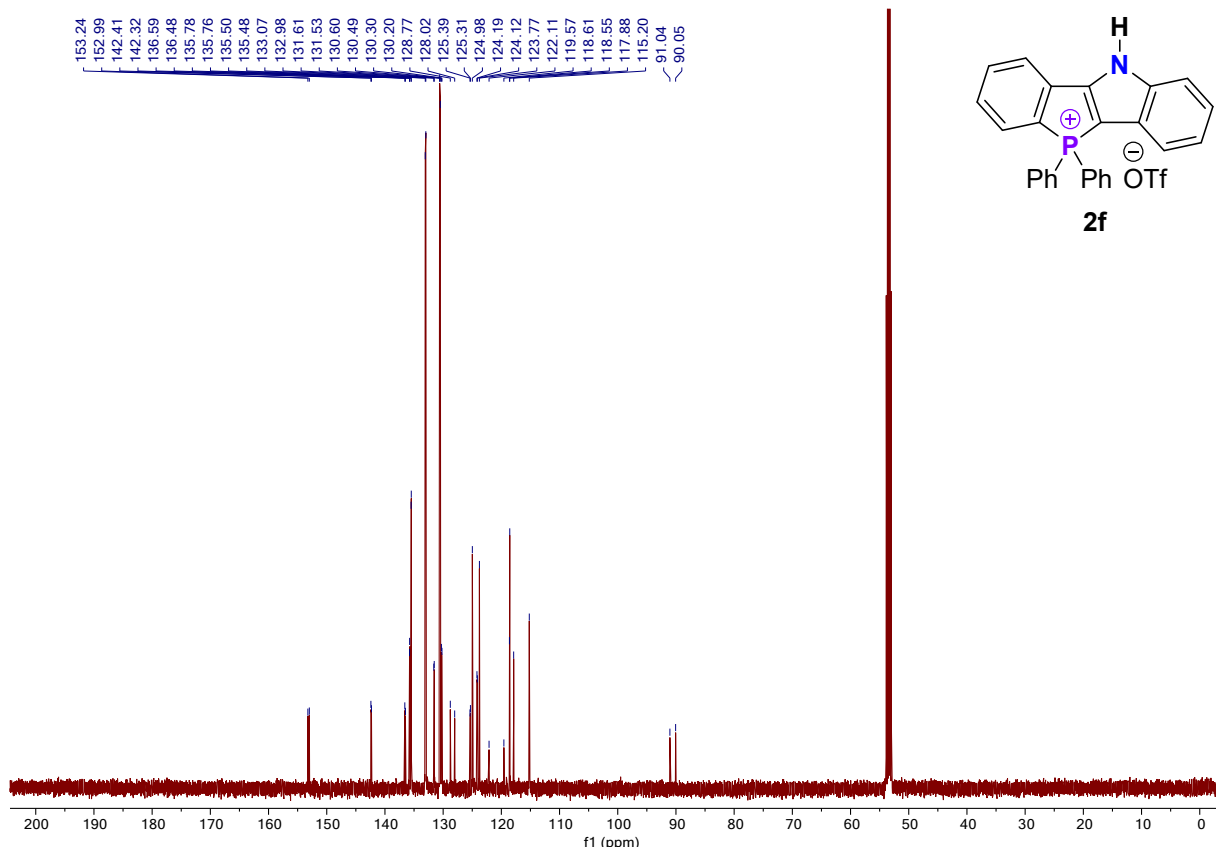


Figure S77: 126 MHz ^{13}C { ^1H } NMR spectrum of **2f** in CD_2Cl_2

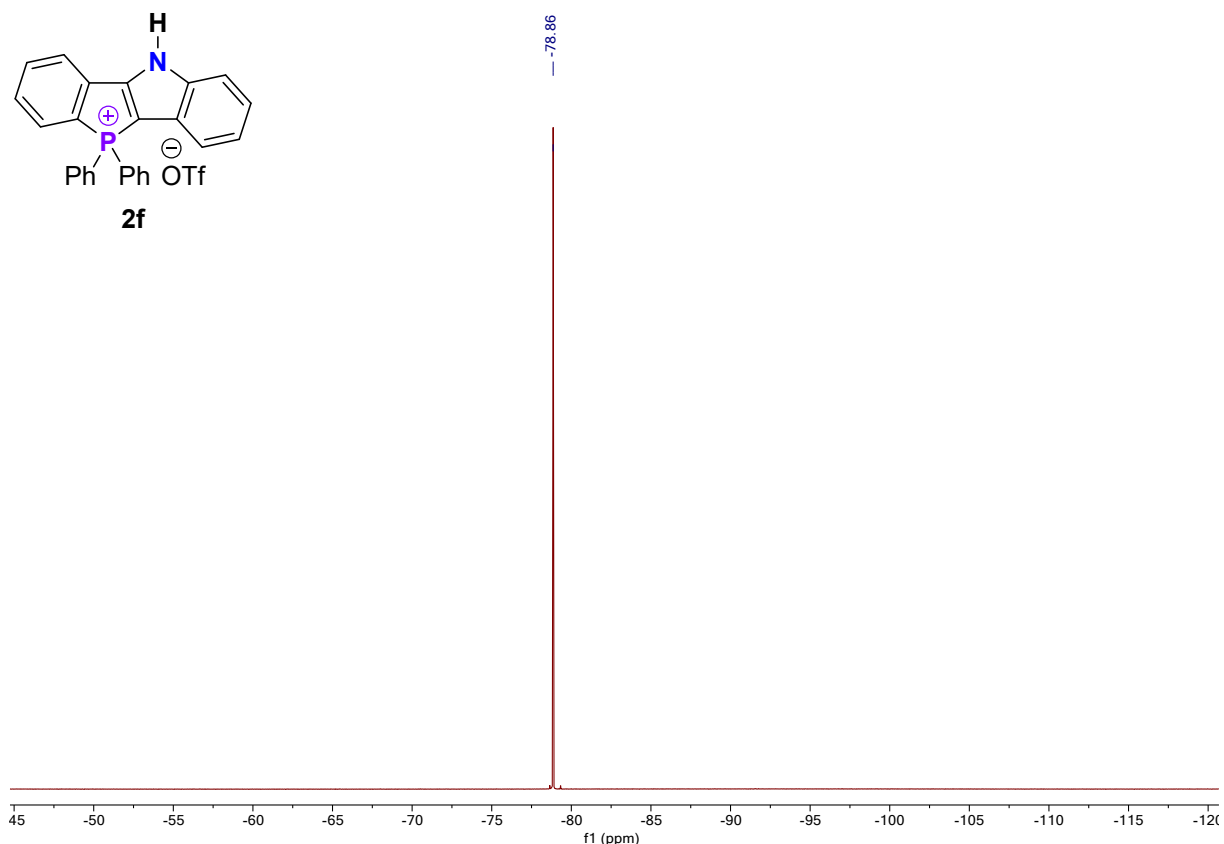


Figure S78: 470 MHz ^{19}F NMR spectrum of **2f** in CD_2Cl_2

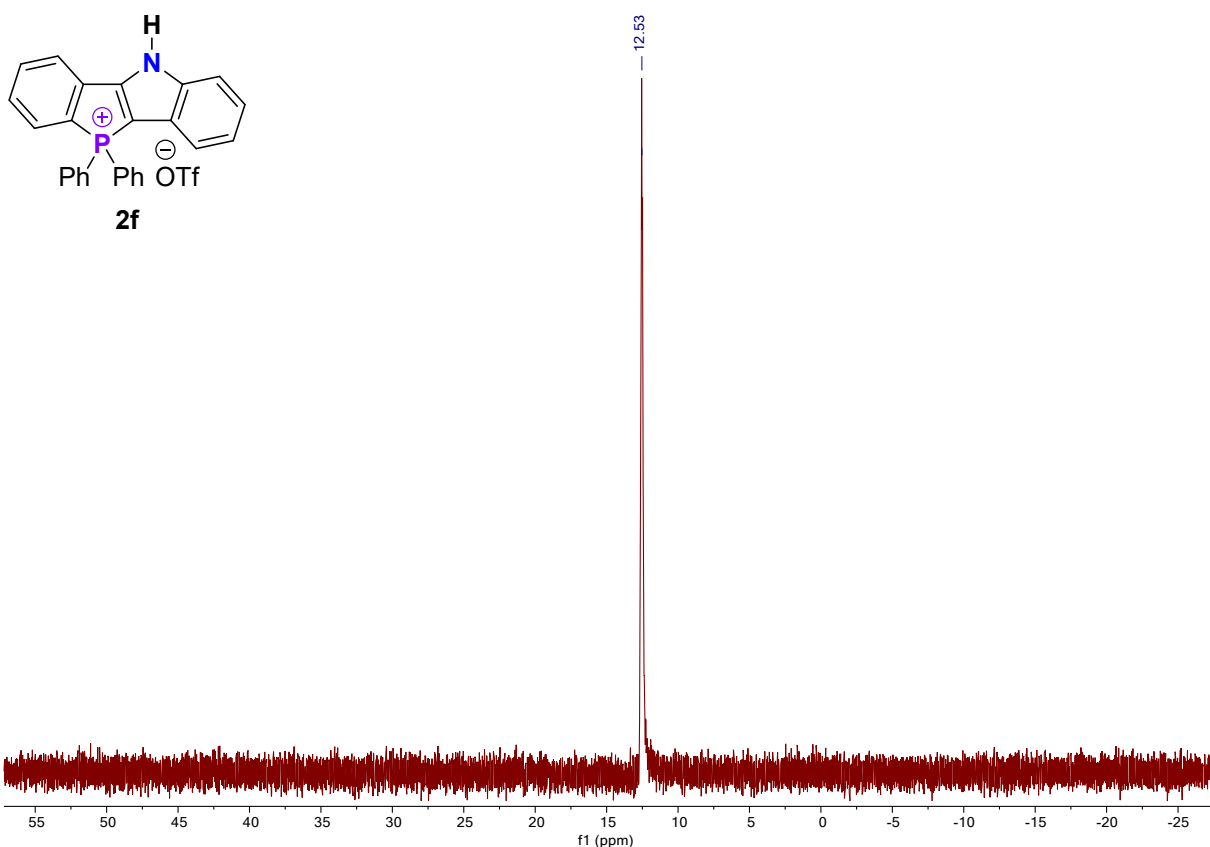


Figure S79: 202 MHz ^{31}P NMR spectrum of **2f** in CD_2Cl_2

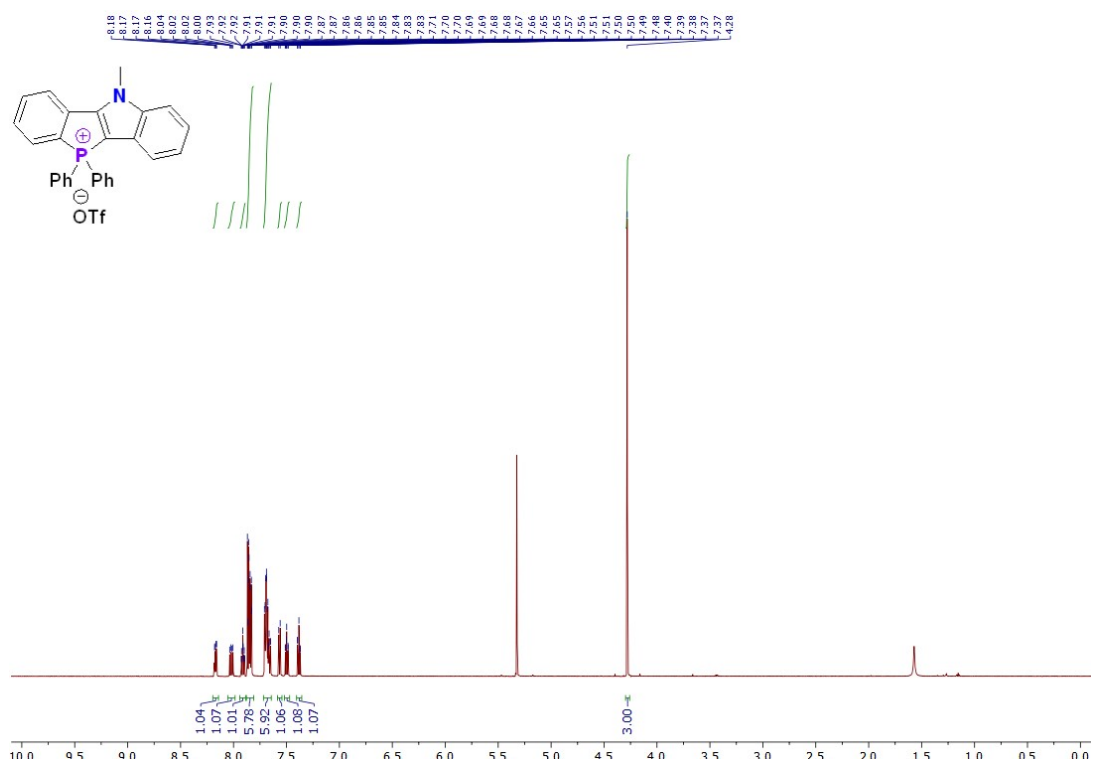


Figure S80: 600 MHz ^1H NMR spectrum of **2g** in CD_2Cl_2

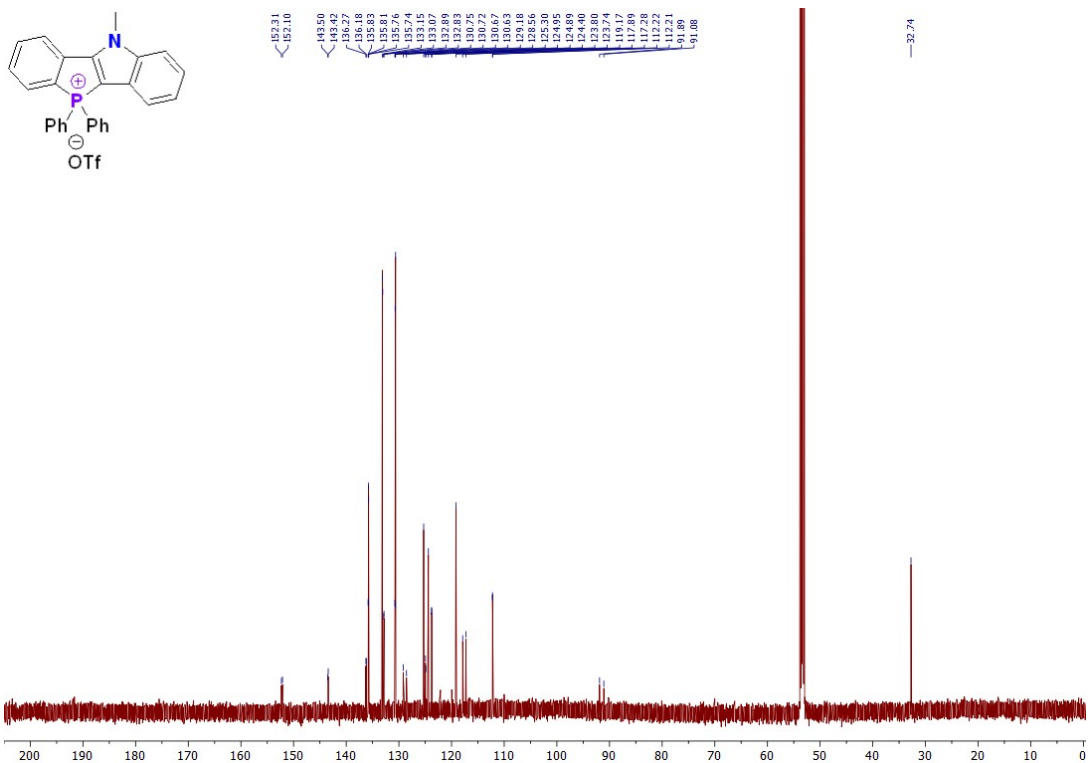


Figure S81: 151 MHz ^{13}C { ^1H } NMR spectrum of **2g** in CD_2Cl_2

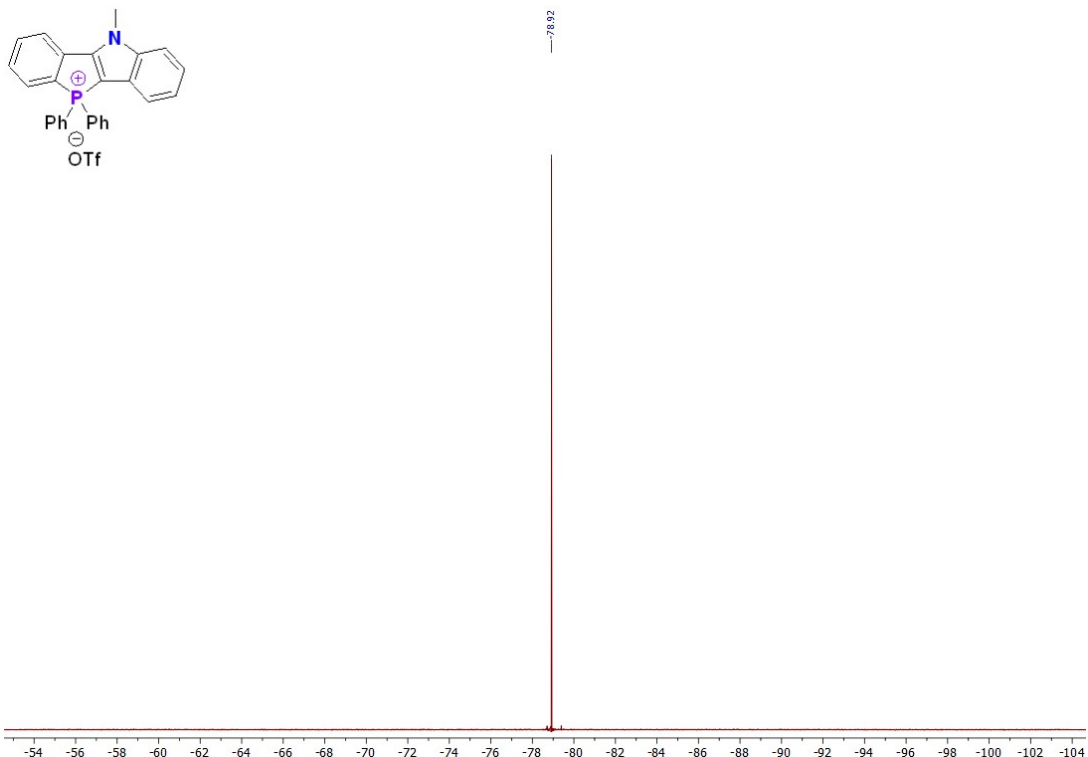


Figure S82: 470 MHz ^{19}F NMR spectrum of **2g** in CD_2Cl_2

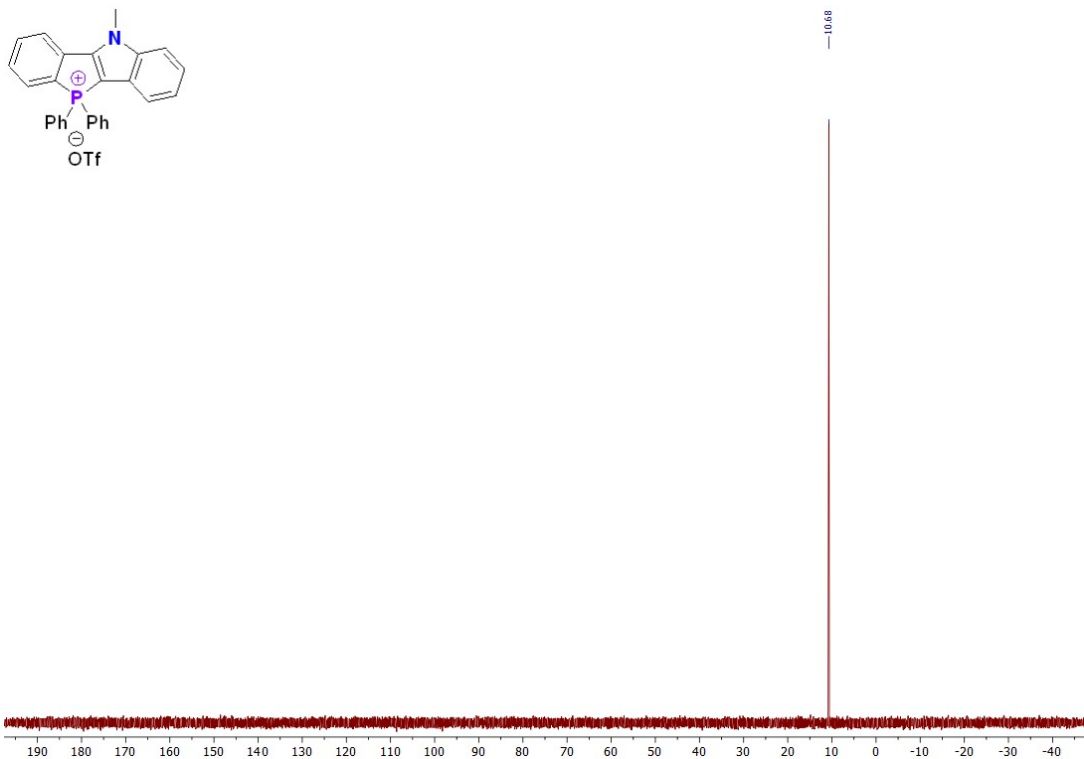


Figure S83: 243 MHz ^{31}P NMR spectrum of 2g in CD_2Cl_2

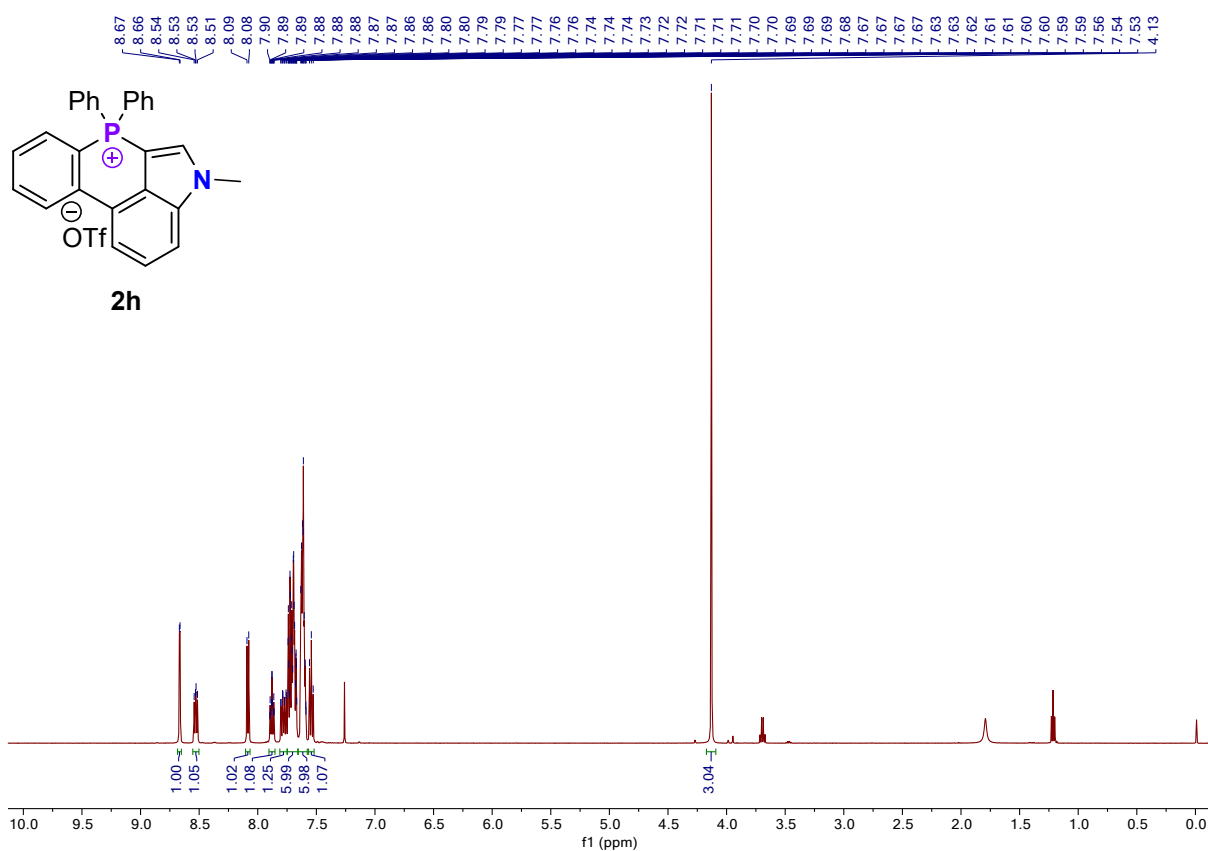


Figure S84: 500 MHz ^1H NMR spectrum of 2h in CDCl_3

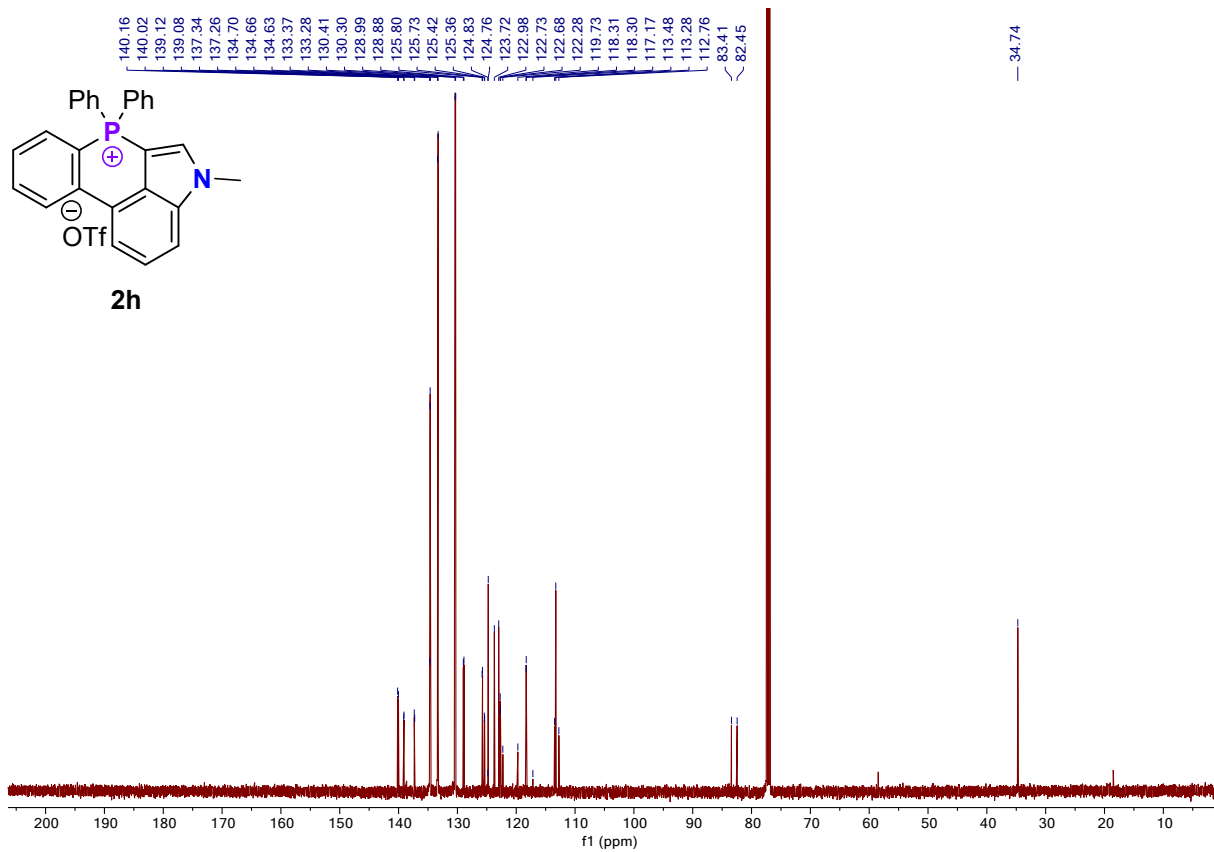


Figure S85: 126 MHz ^{13}C { ^1H } NMR spectrum of 2h in CDCl_3

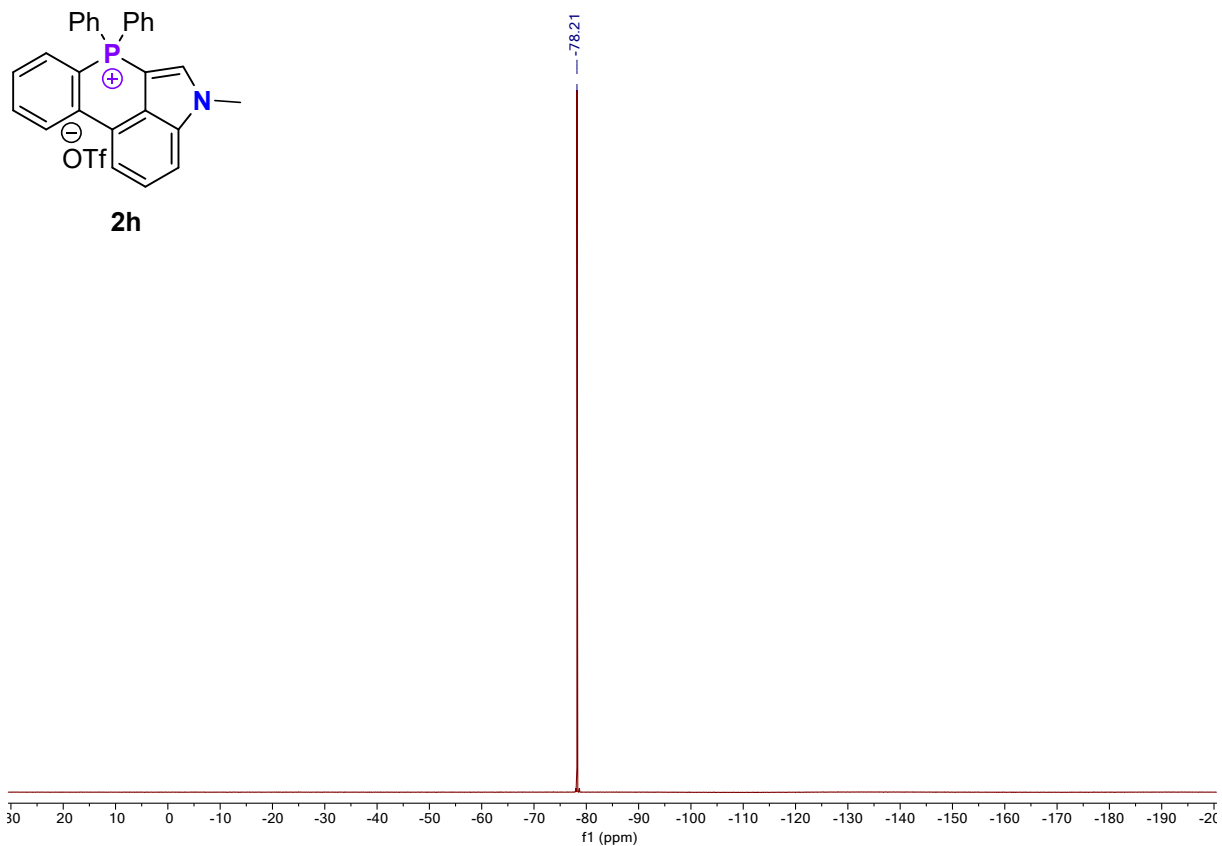


Figure S86: 470 MHz ^{19}F NMR spectrum of 2h in CDCl_3

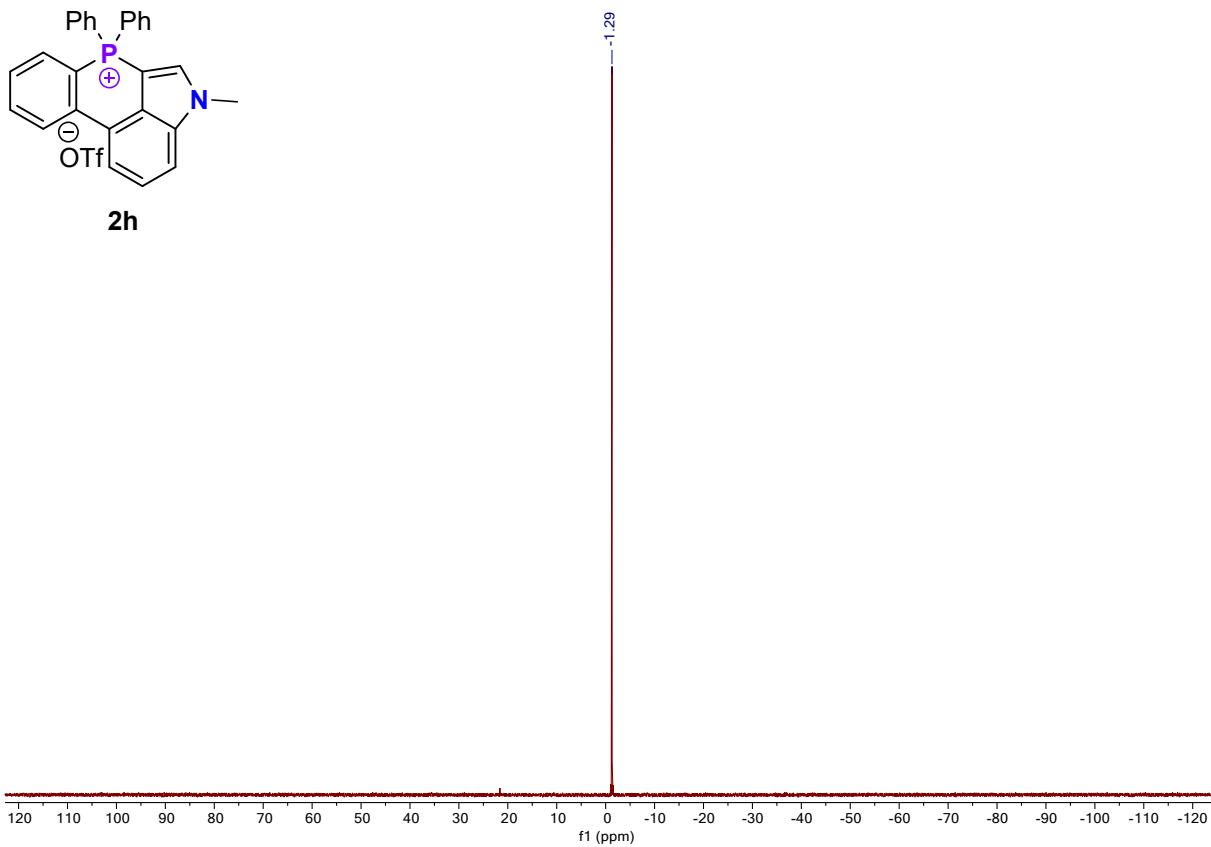


Figure S87: 202 MHz ^{31}P NMR spectrum of **2h** in CDCl_3

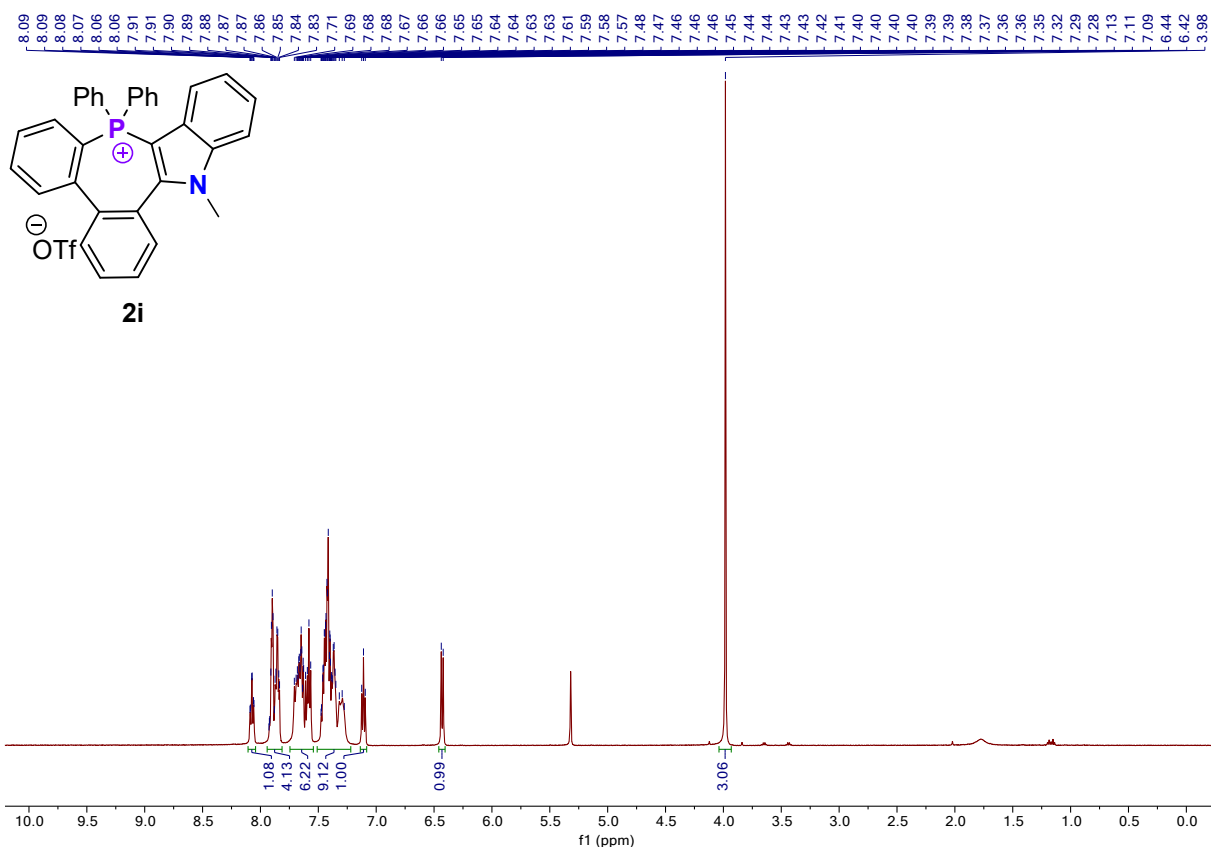


Figure S88: 500 MHz ^1H NMR spectrum of **2i** in CD_2Cl_2

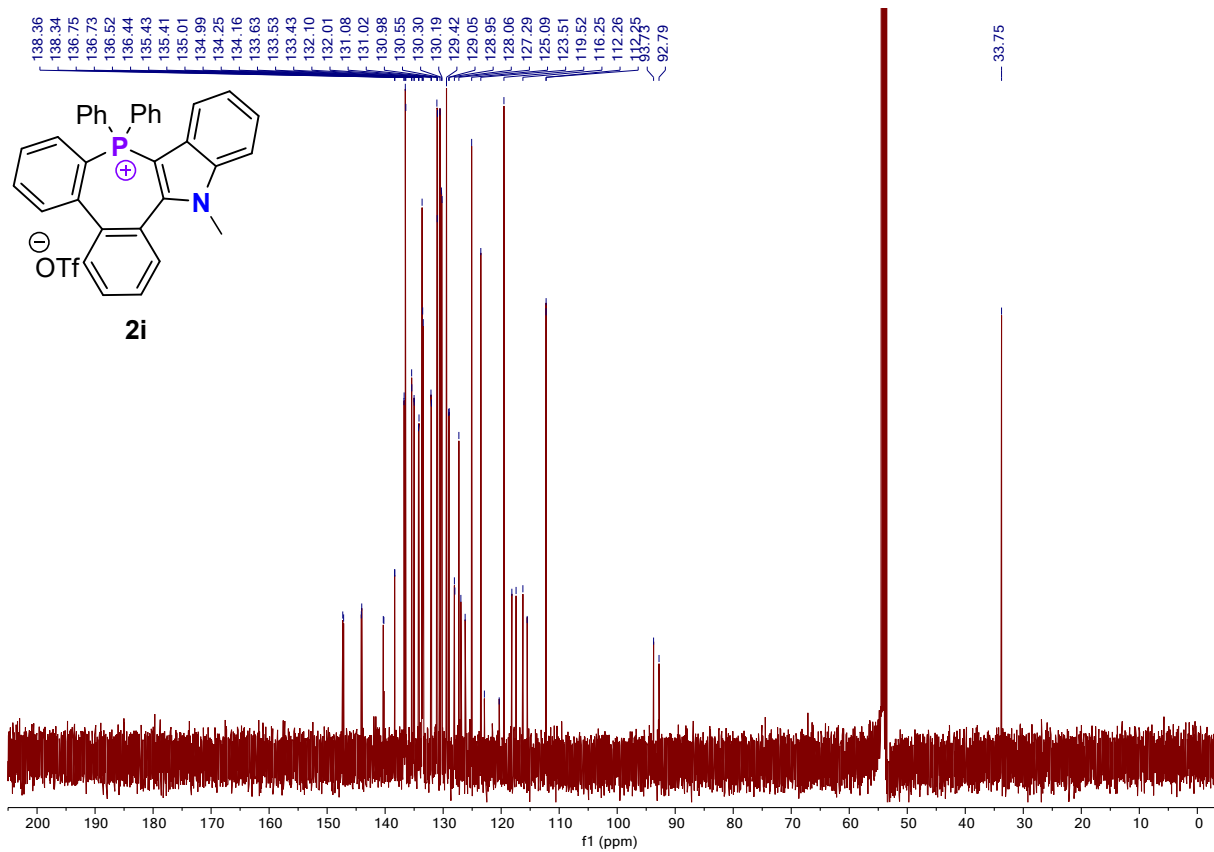


Figure S89: 126 MHz ^{13}C $\{^1\text{H}\}$ NMR spectrum of **2i** in CD_2Cl_2

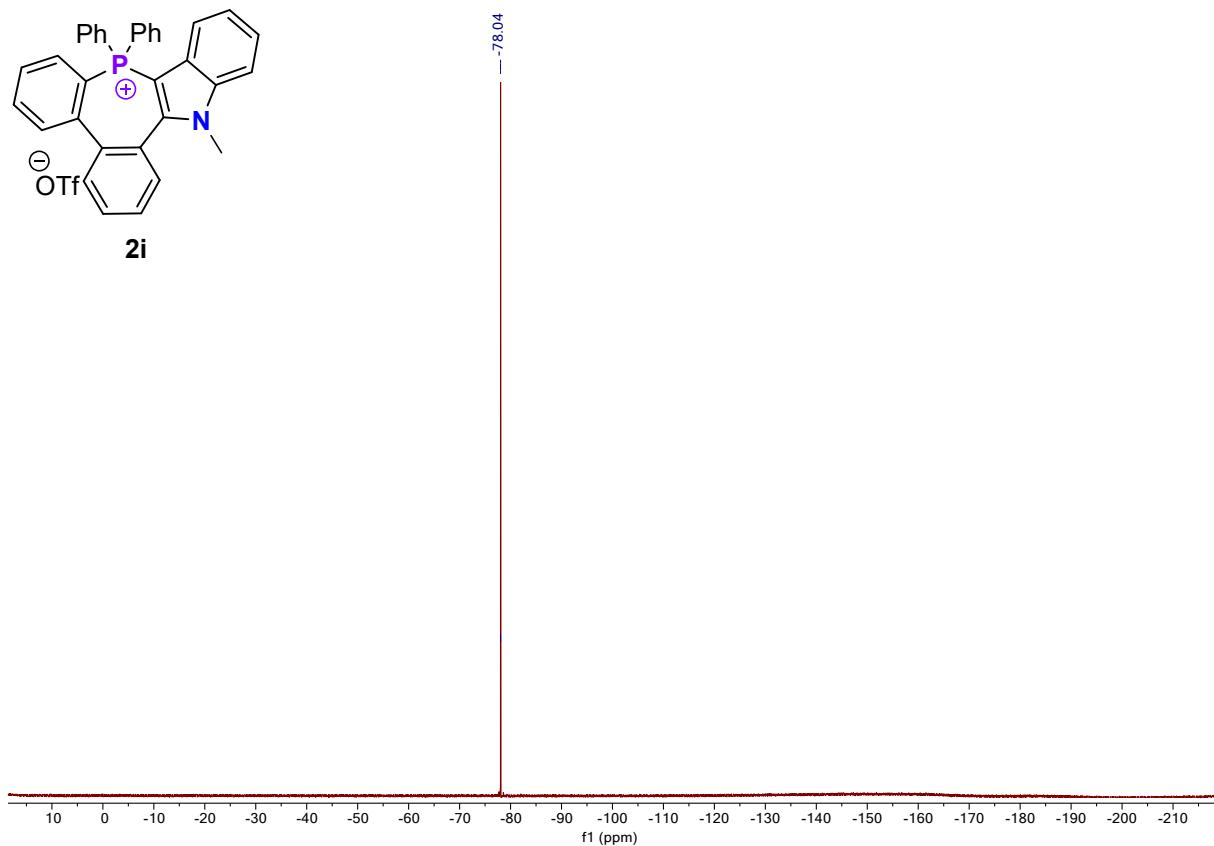


Figure S90: 470 MHz ^{19}F NMR spectrum of **2i** in CD_2Cl_2

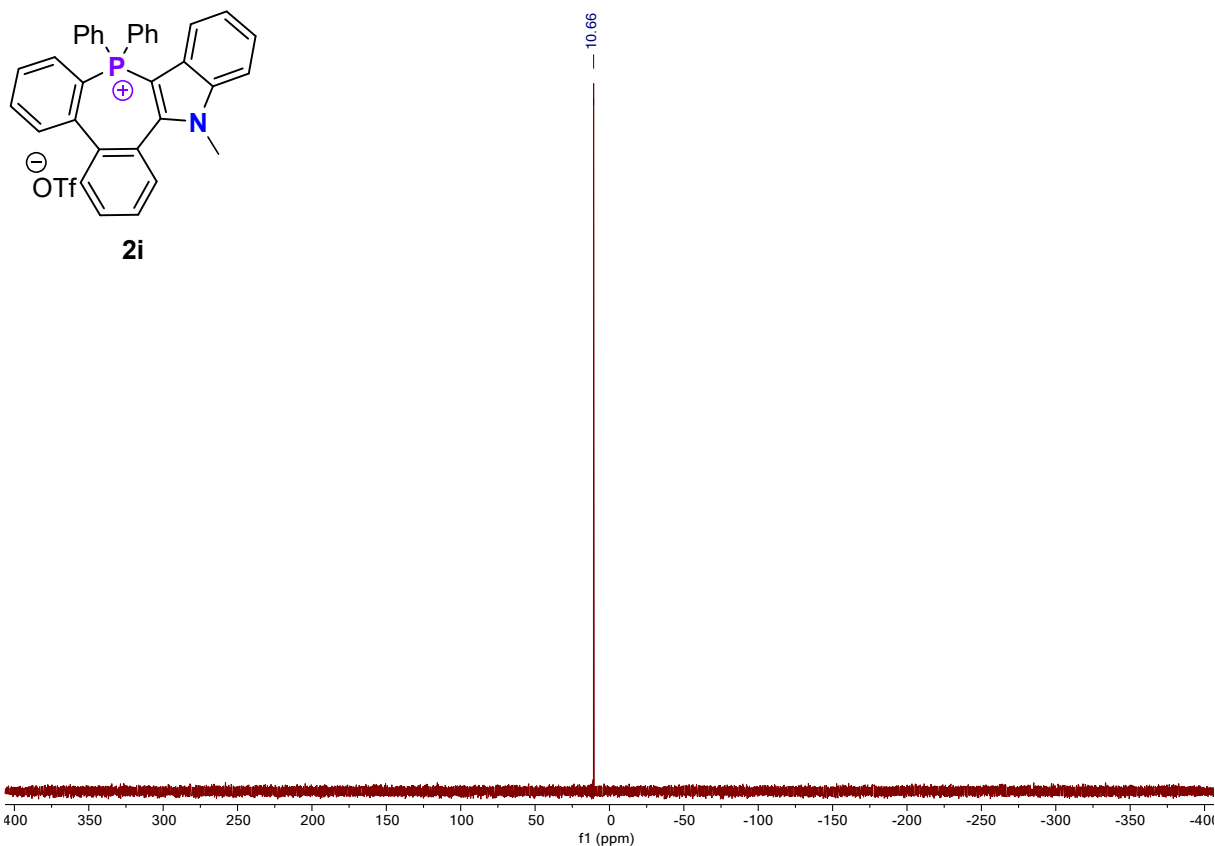


Figure S91: 202 MHz ^{31}P NMR spectrum of **2i** in CD_2Cl_2

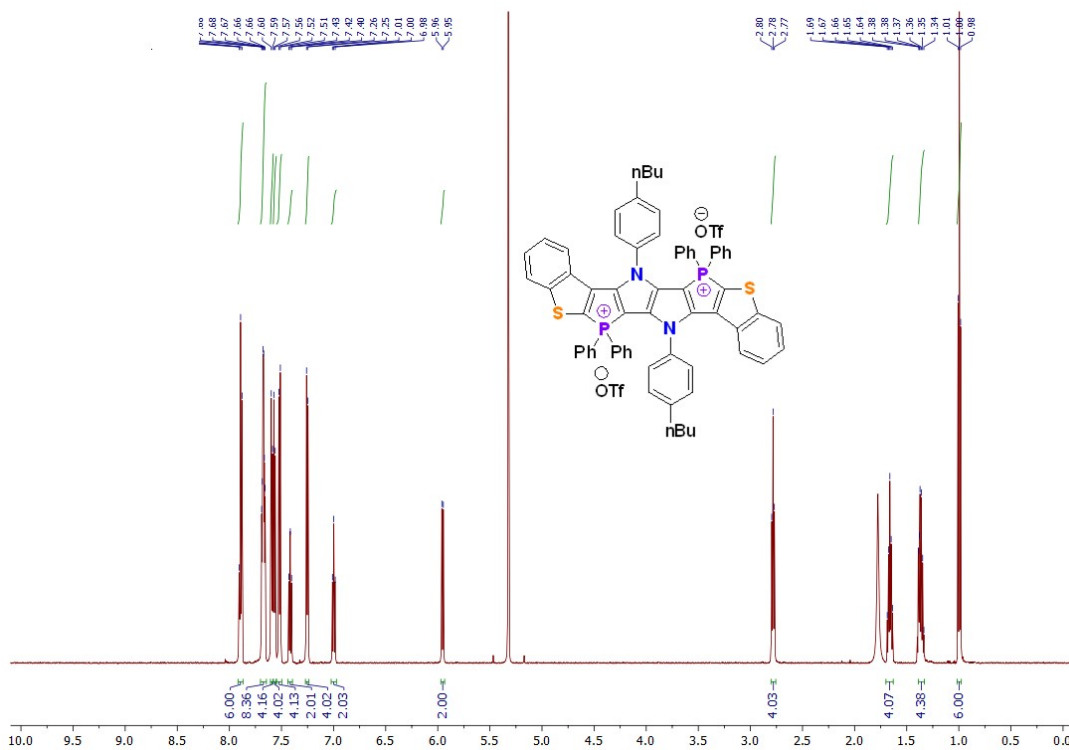


Figure S92: 600 MHz ^1H NMR spectrum of **2j** in CD_2Cl_2

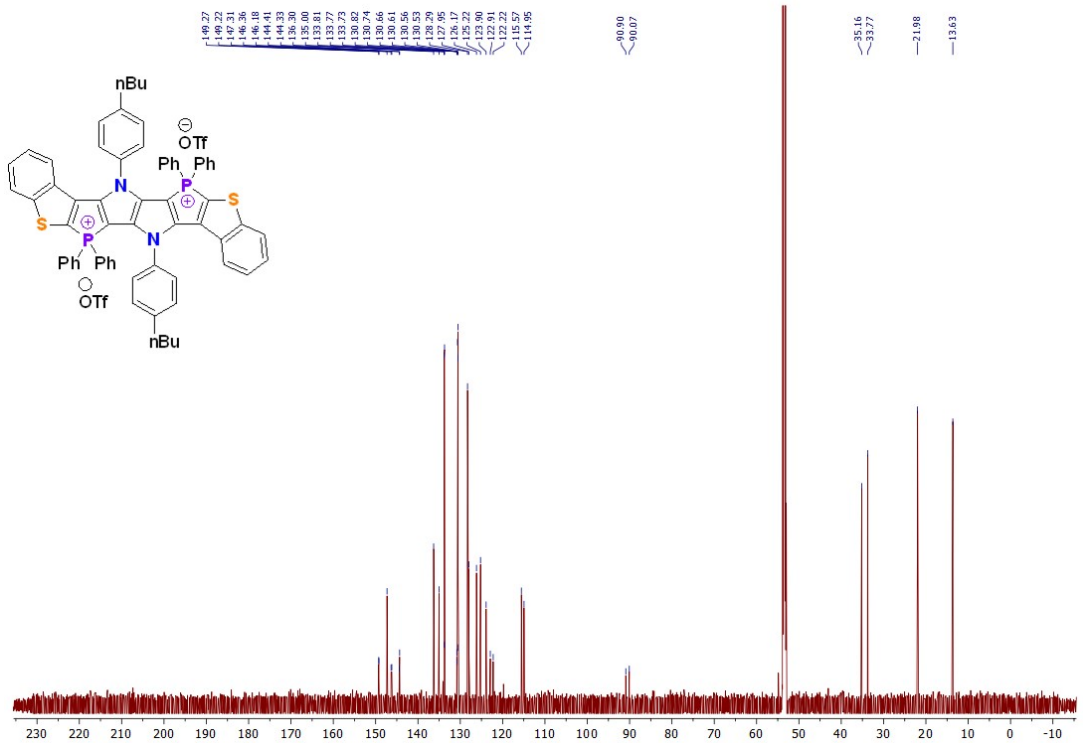


Figure S93: 151 MHz ^{13}C { ^1H } NMR spectrum of 2j in CD_2Cl_2

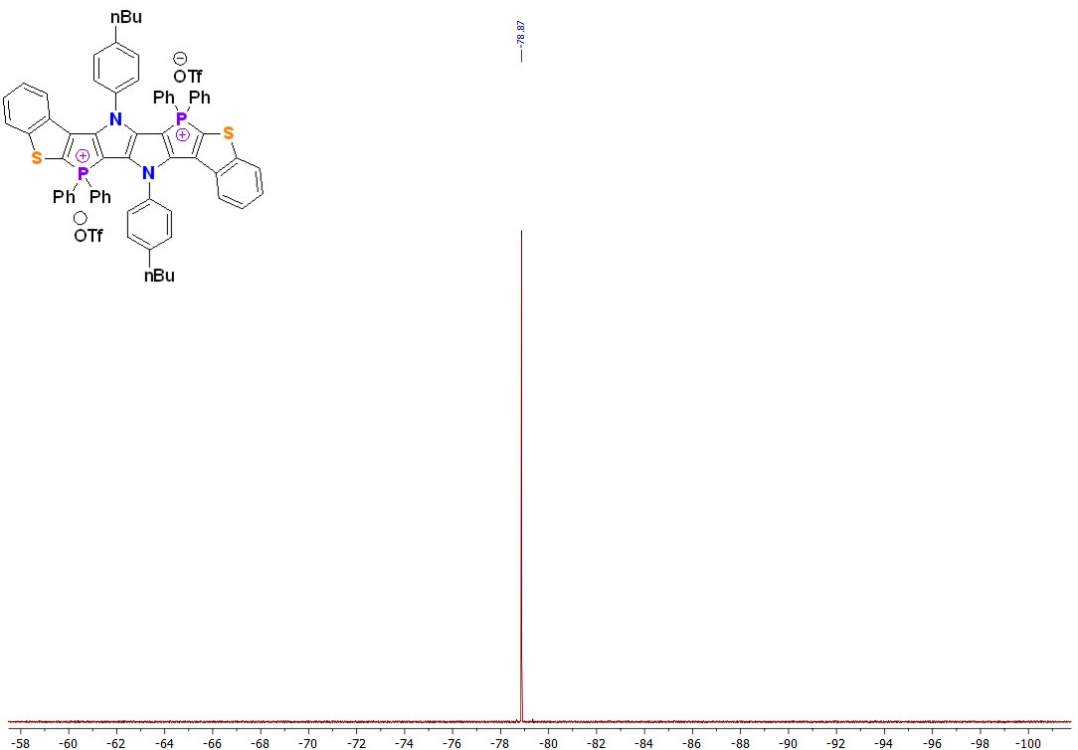


Figure S94: 470 MHz ^{19}F NMR spectrum of 2j in CD_2Cl_2

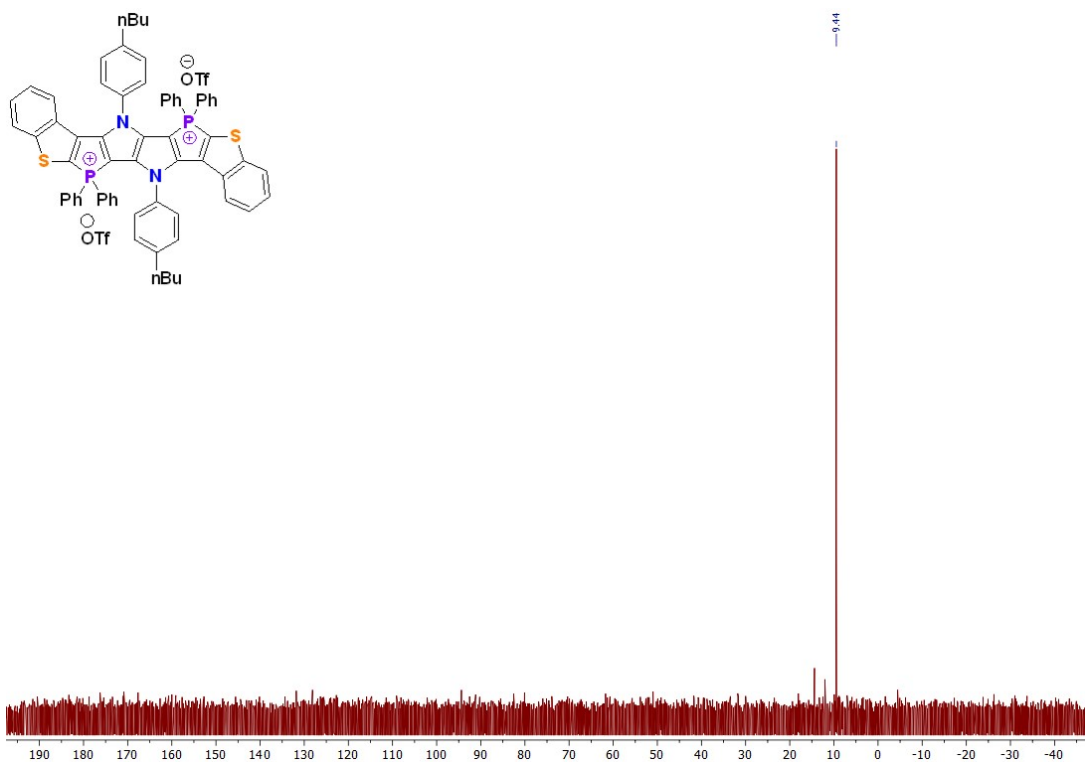


Figure S95: 243 MHz ^{31}P NMR spectrum of 2j in CD_2Cl_2

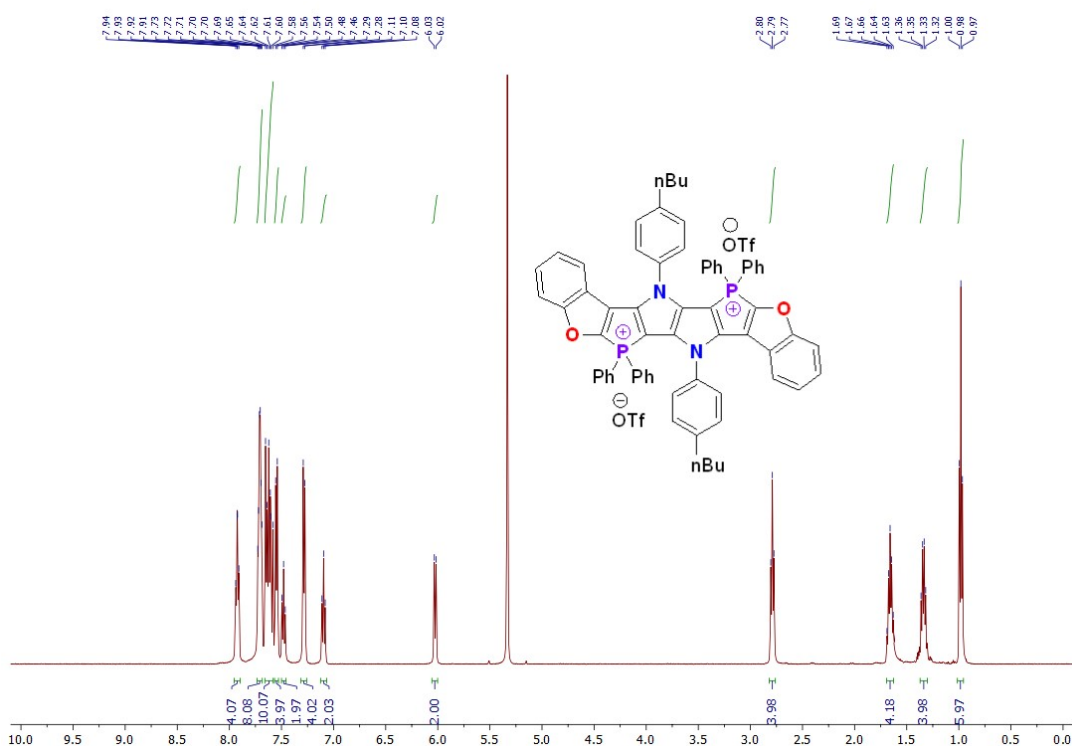


Figure S96: 500 MHz ^1H NMR spectrum of 2k in CD_2Cl_2

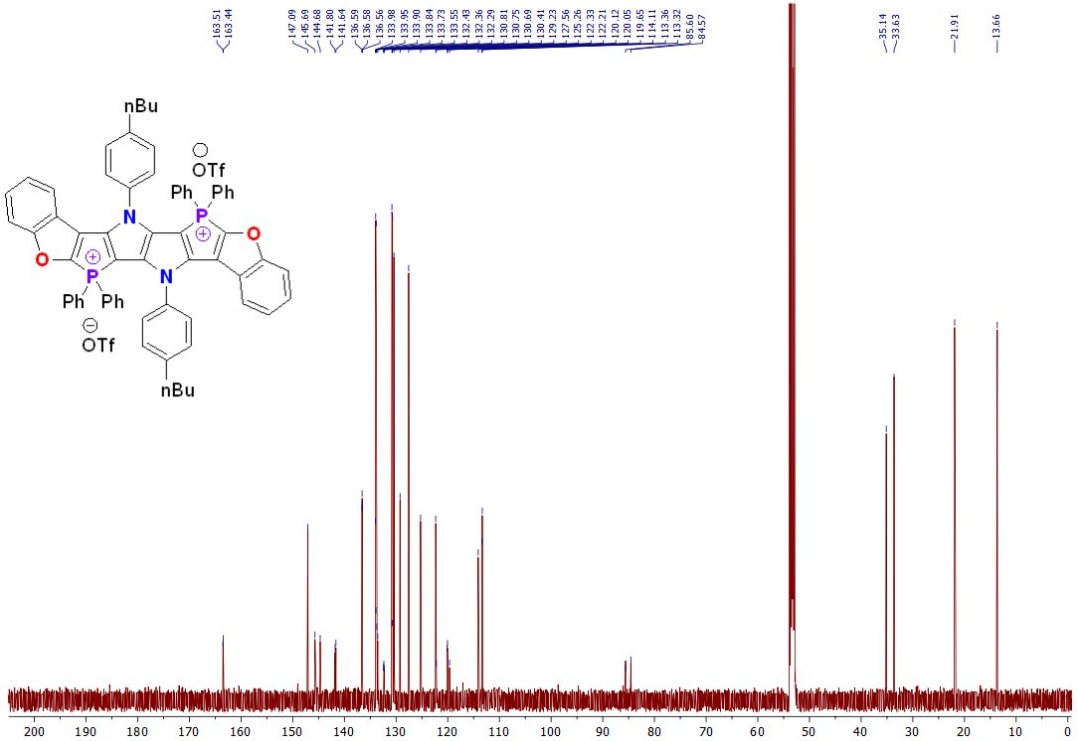


Figure S97: 126 MHz ^{13}C { ^1H } NMR spectrum of 2k in CD_2Cl_2

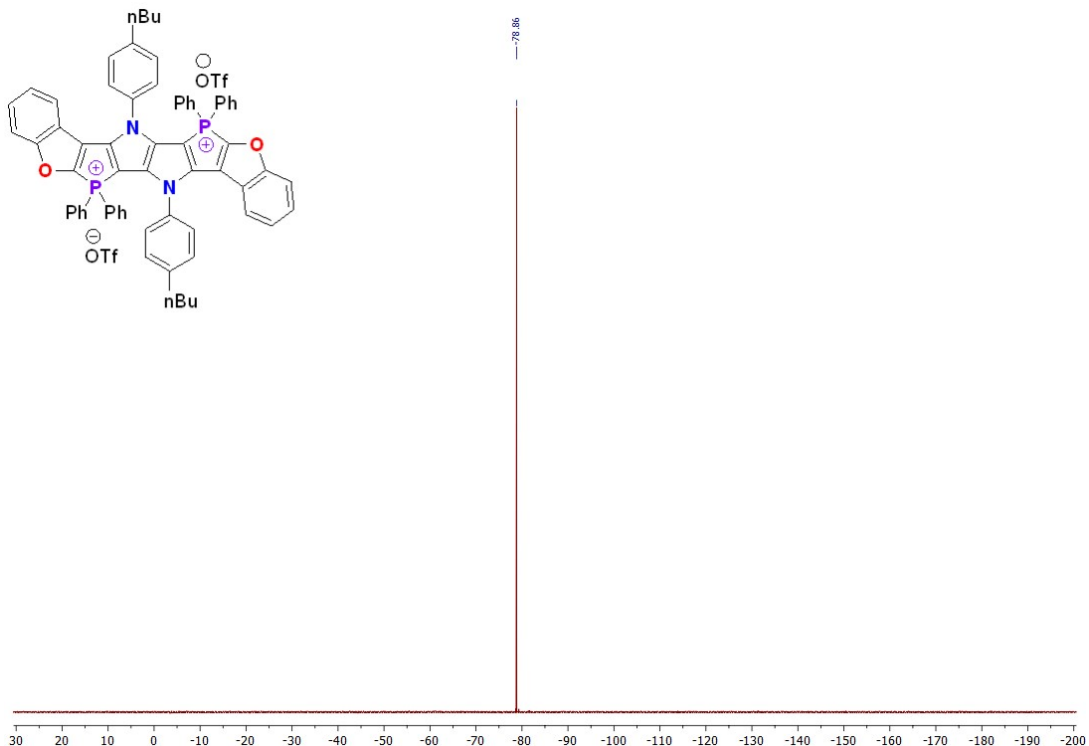


Figure S98: 470 MHz ^{19}F NMR spectrum of 2k in CD_2Cl_2

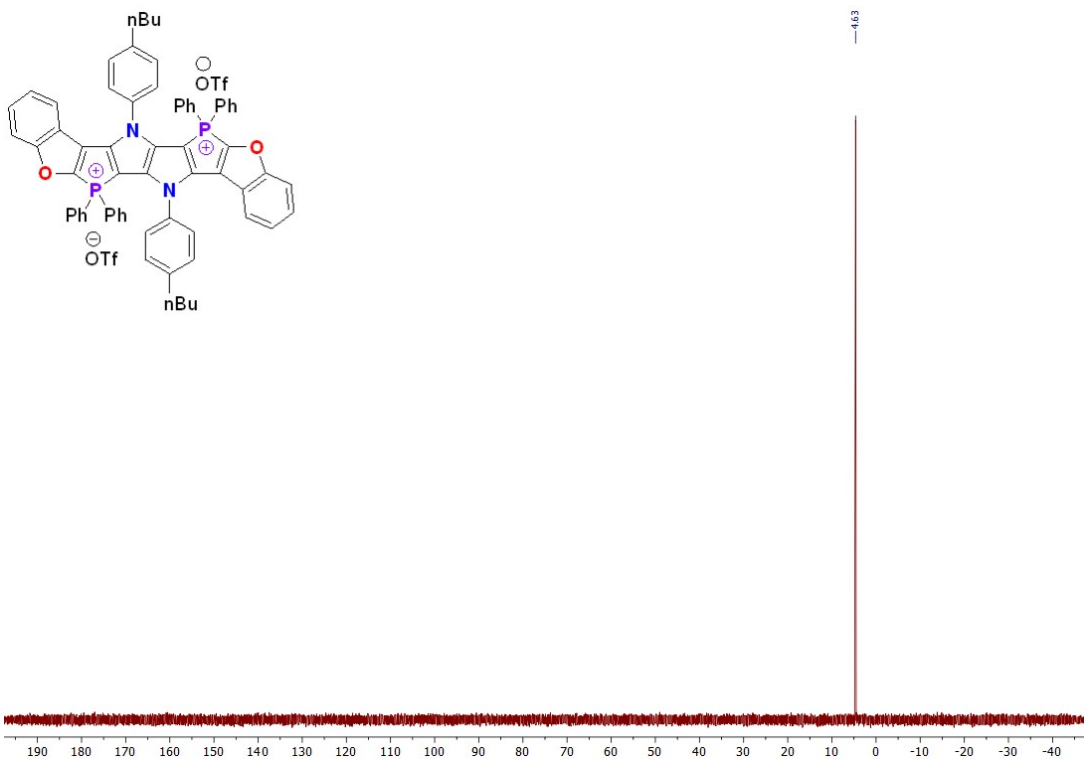


Figure S99: 243 MHz ^{31}P NMR spectrum of **2k** in CD_2Cl_2

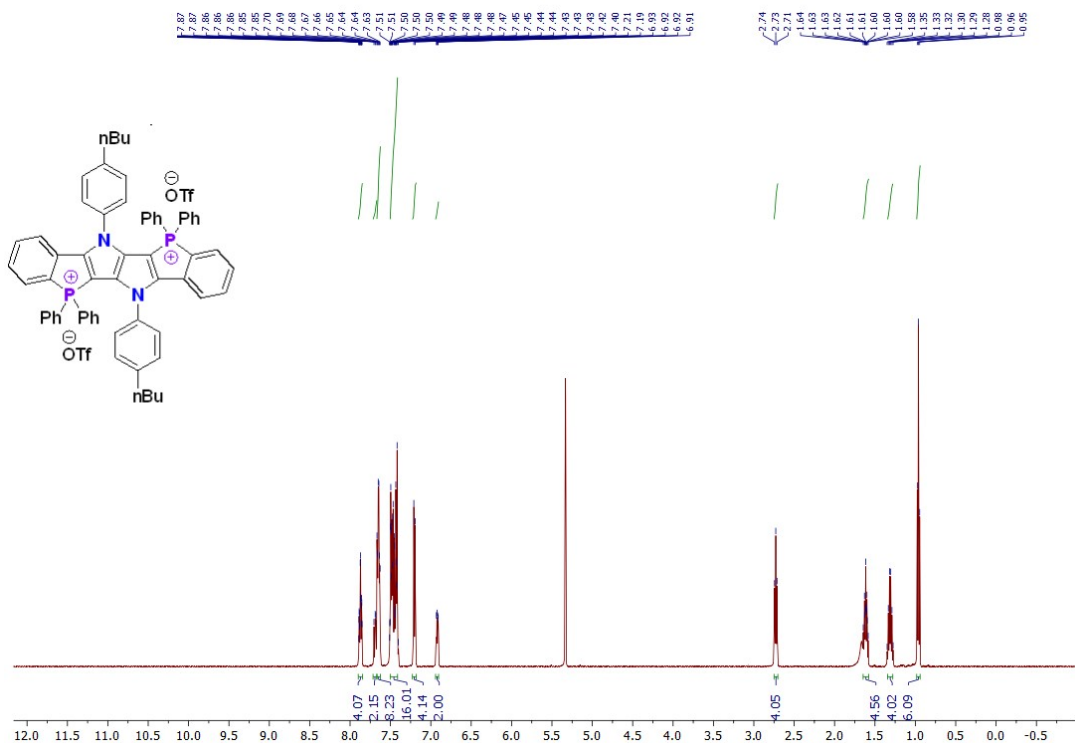


Figure S100: 500 MHz ^1H NMR spectrum of **2l** in CD_2Cl_2

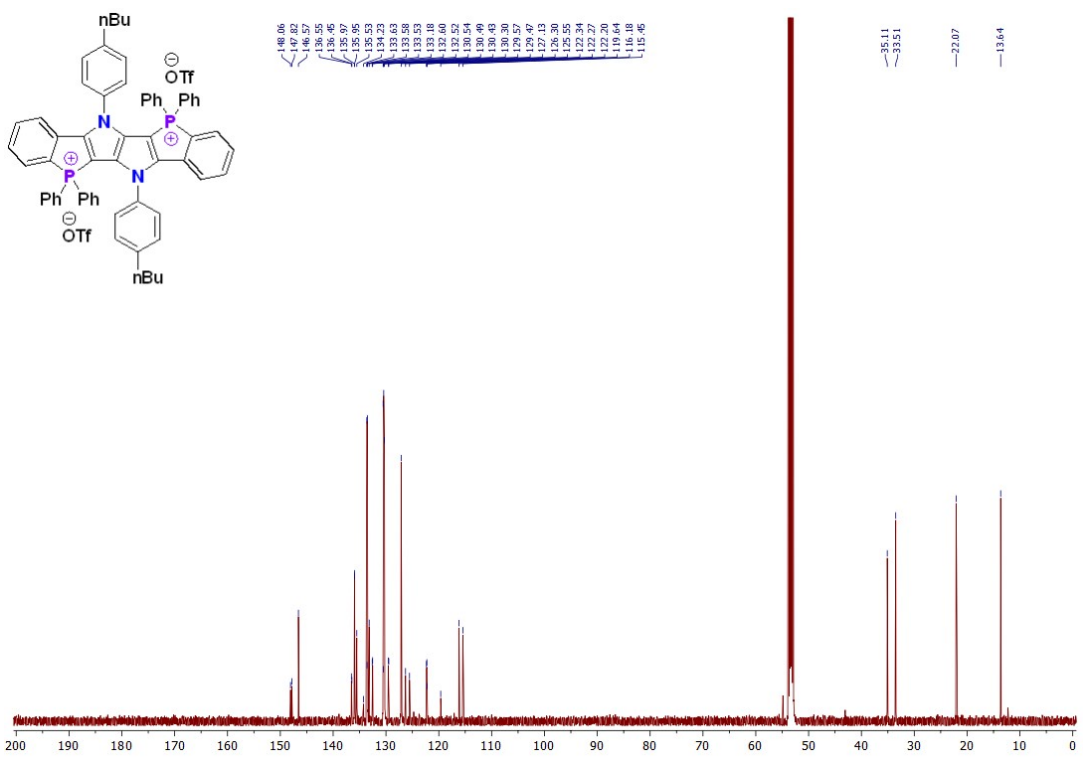


Figure S101: 126 MHz ^{13}C NMR spectrum of 2l in CD_2Cl_2

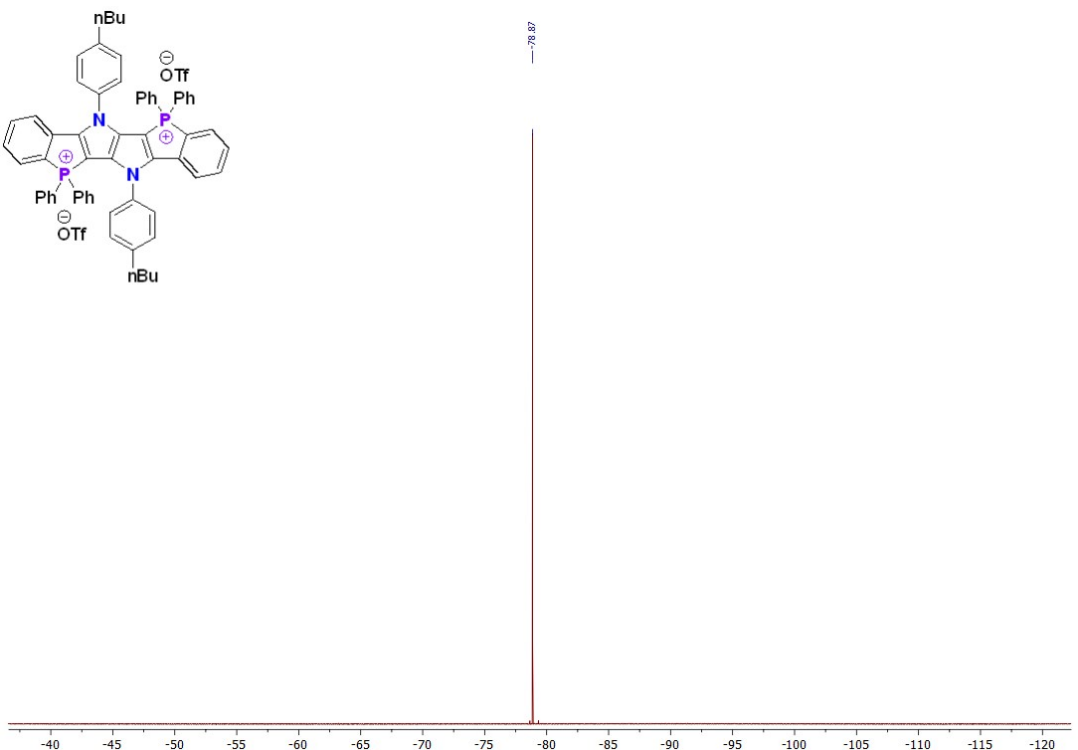
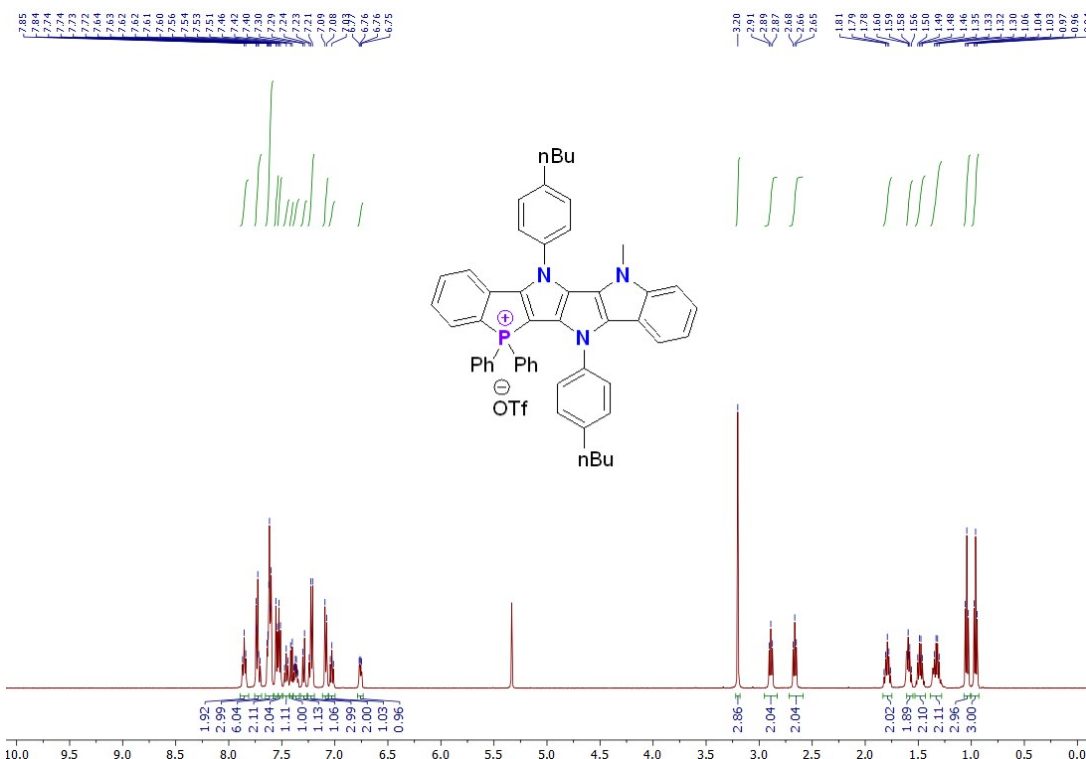
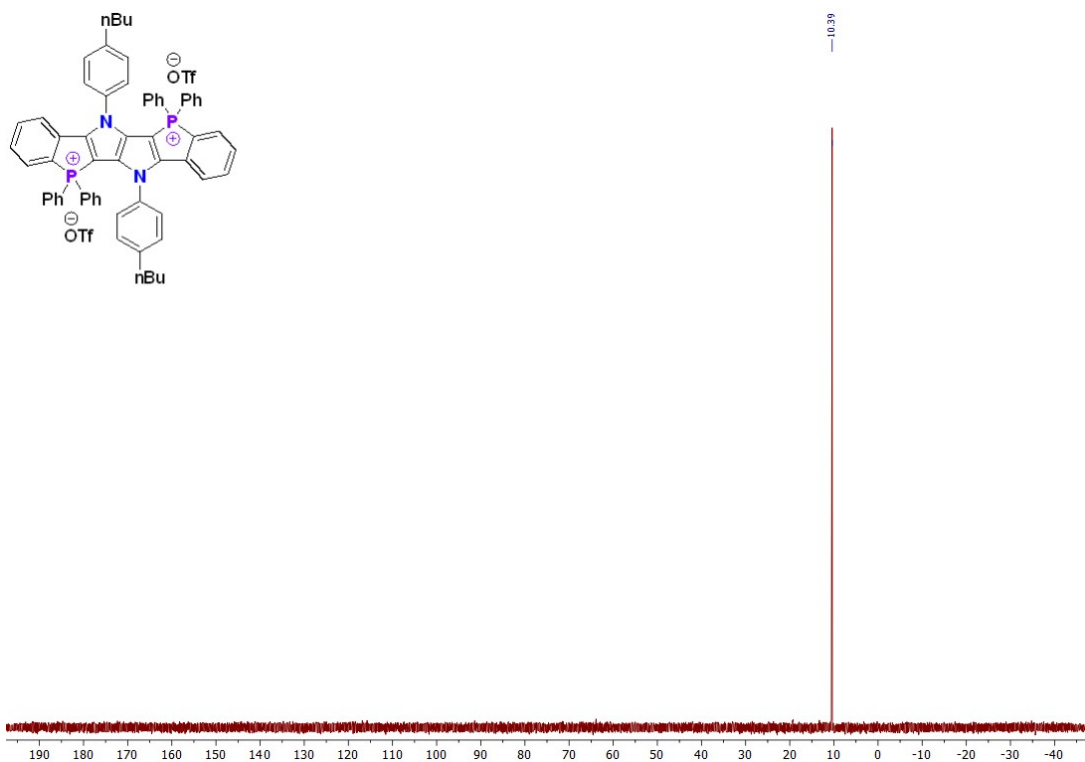


Figure S102: 470 MHz ^{19}F NMR spectrum of 2l in CD_2Cl_2



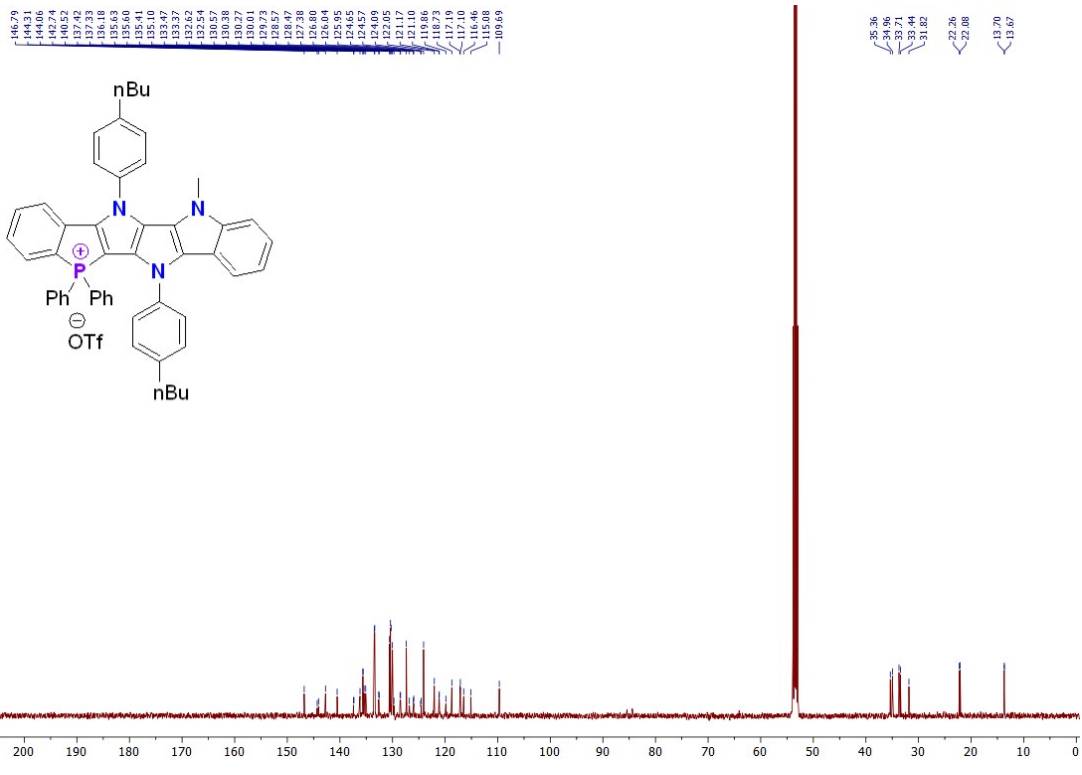


Figure S105: 126 MHz ^{13}C { ^1H } NMR spectrum of **2m** in CD_2Cl_2

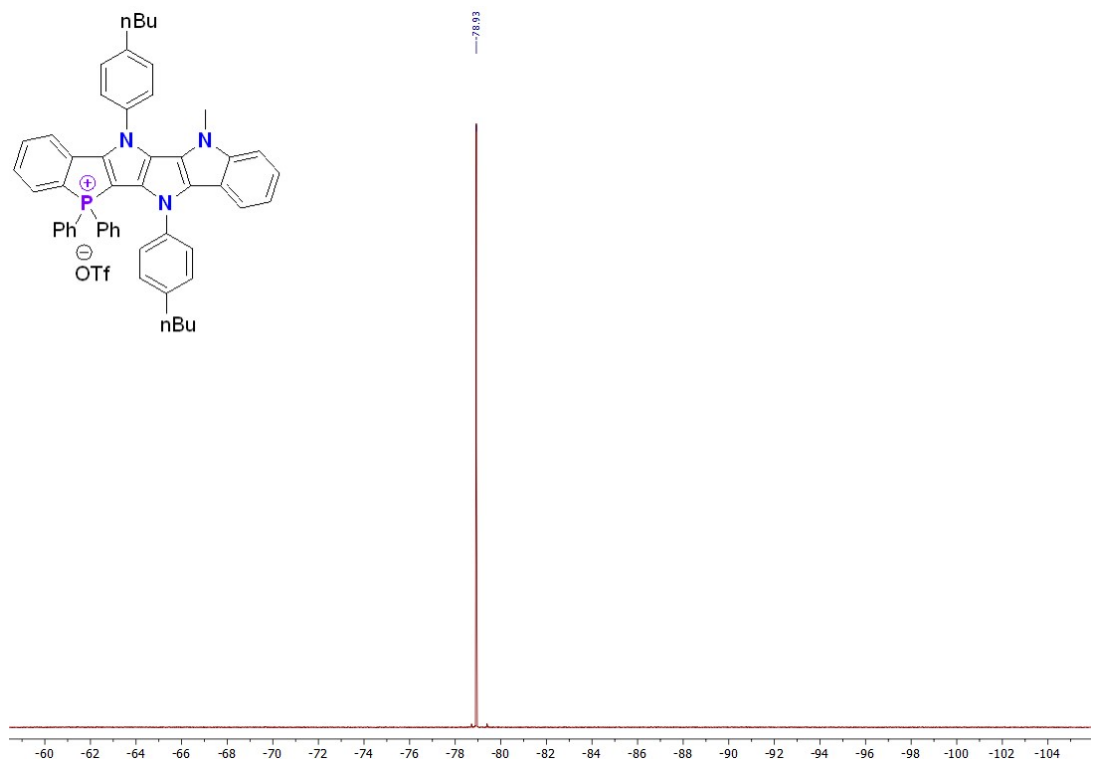


Figure S106: 470 MHz ^{19}F NMR spectrum of **2m** in CD_2Cl_2

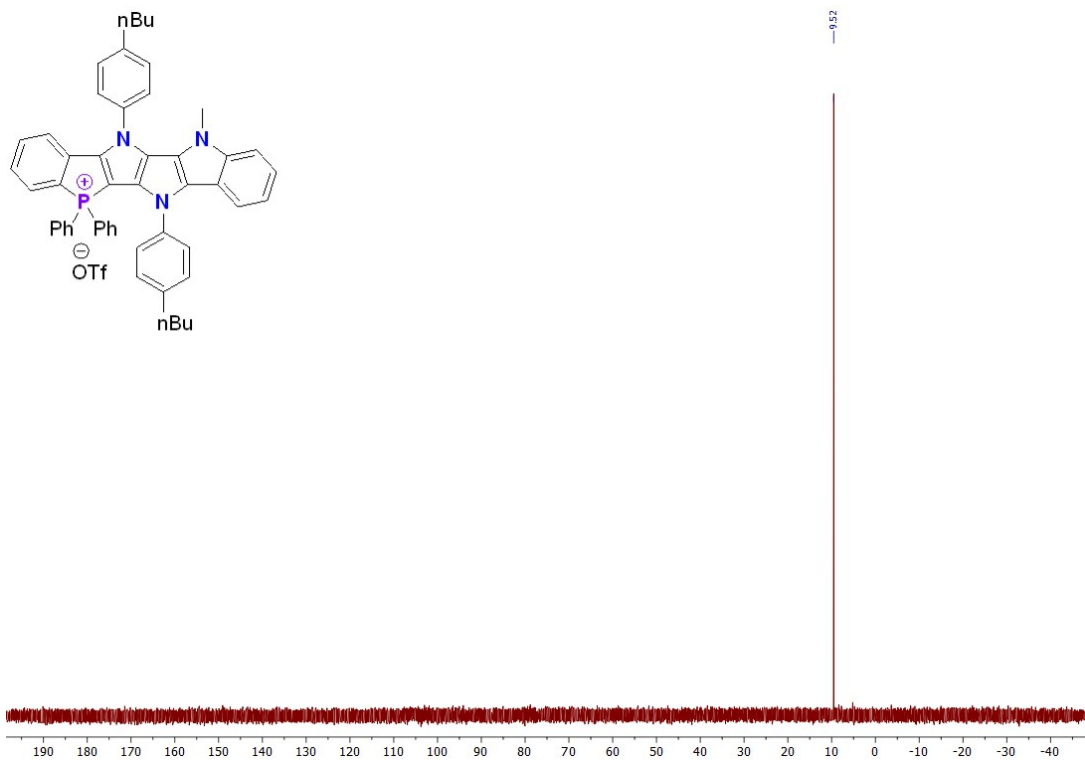


Figure S107: 202 MHz ³¹P NMR spectrum of **2m** in CD_2Cl_2

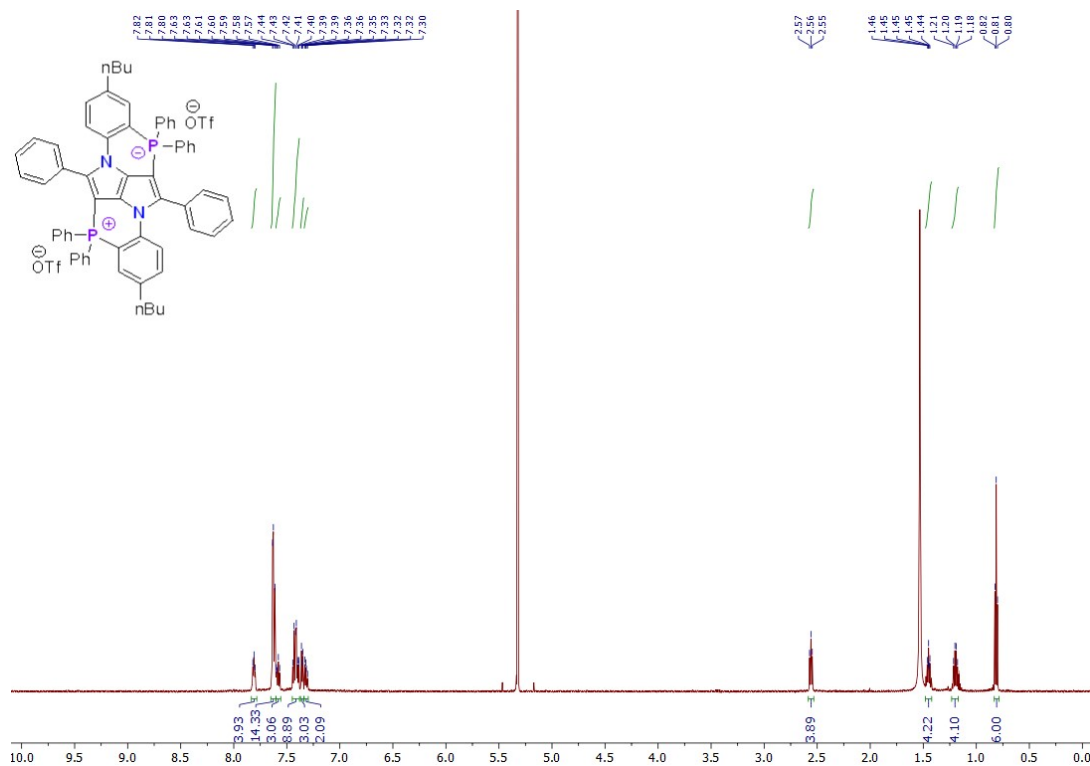


Figure S108: 600 MHz ¹H NMR spectrum of **2n** in CD_2Cl_2

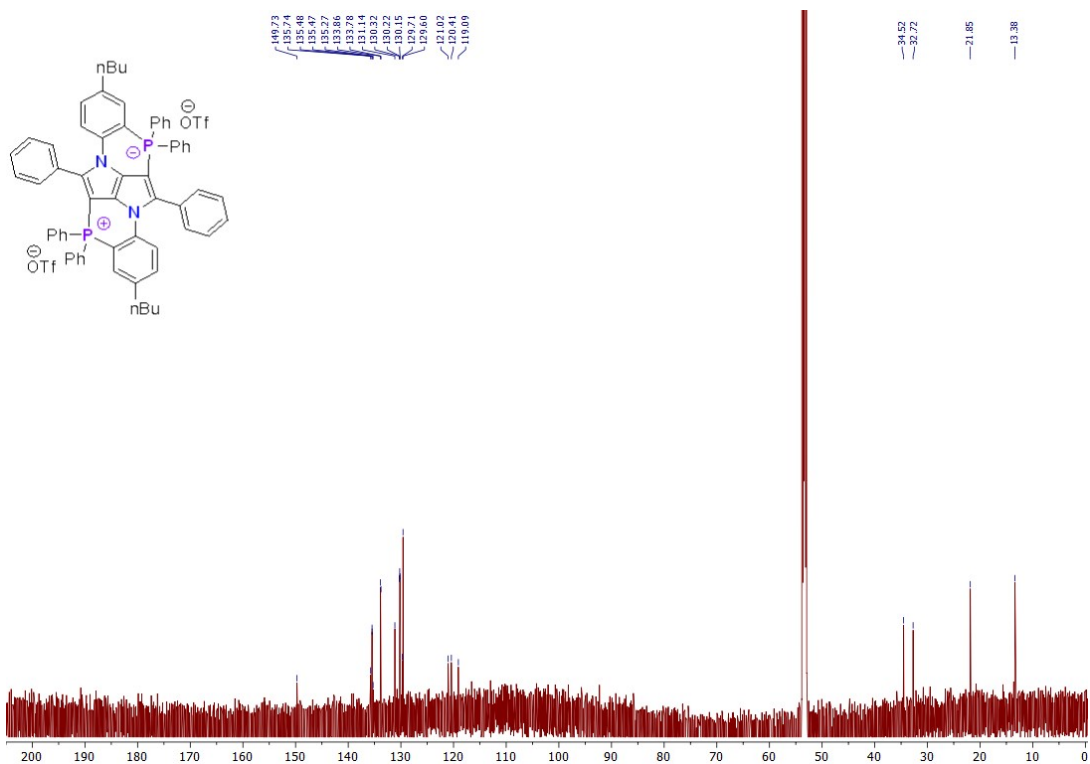


Figure S109: 151 MHz ¹³C {¹H} NMR spectrum of **2n** in CD₂Cl₂

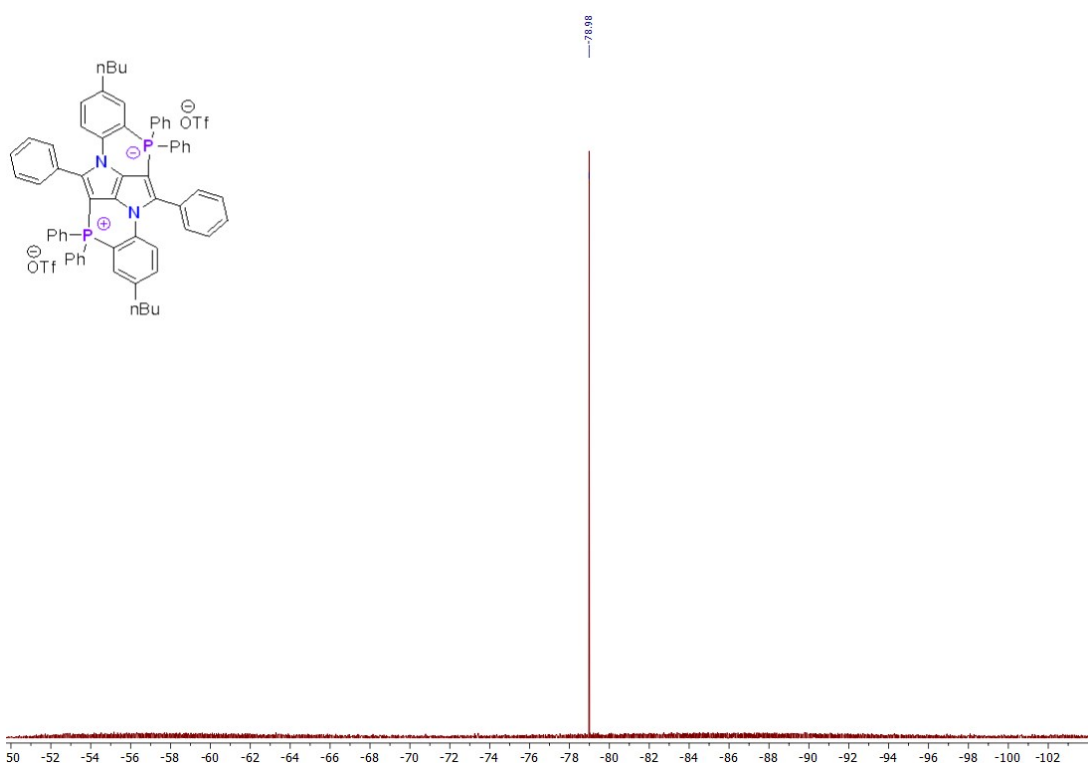


Figure S110: 470 MHz ¹⁹F NMR spectrum of **2n** in CD₂Cl₂

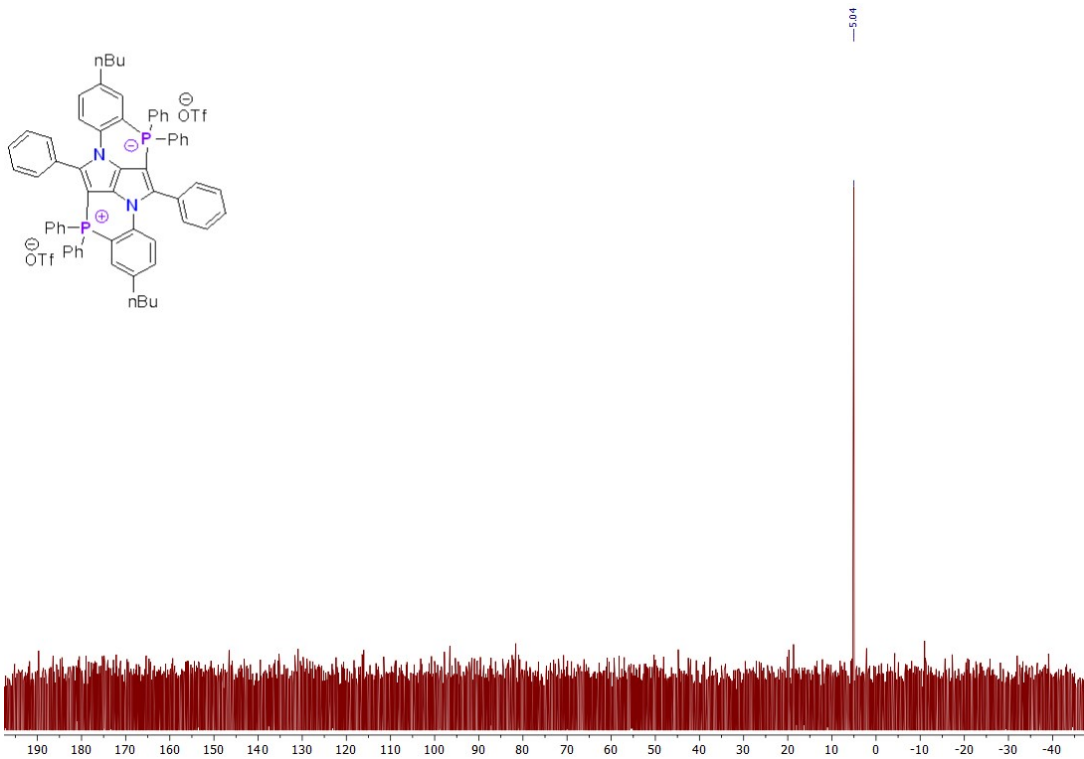


Figure S111: 243 MHz ³¹P NMR spectrum of **2n** in CD₂Cl₂

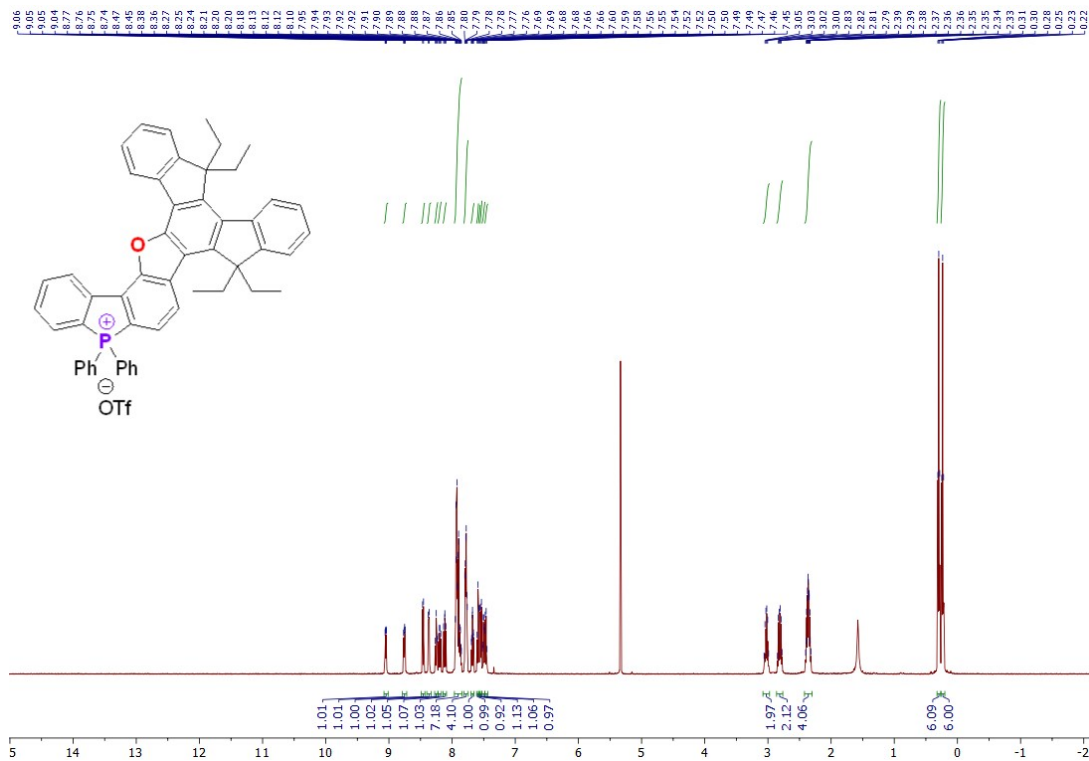


Figure S112: 500 MHz ¹H NMR spectrum of **2o** in CD₂Cl₂

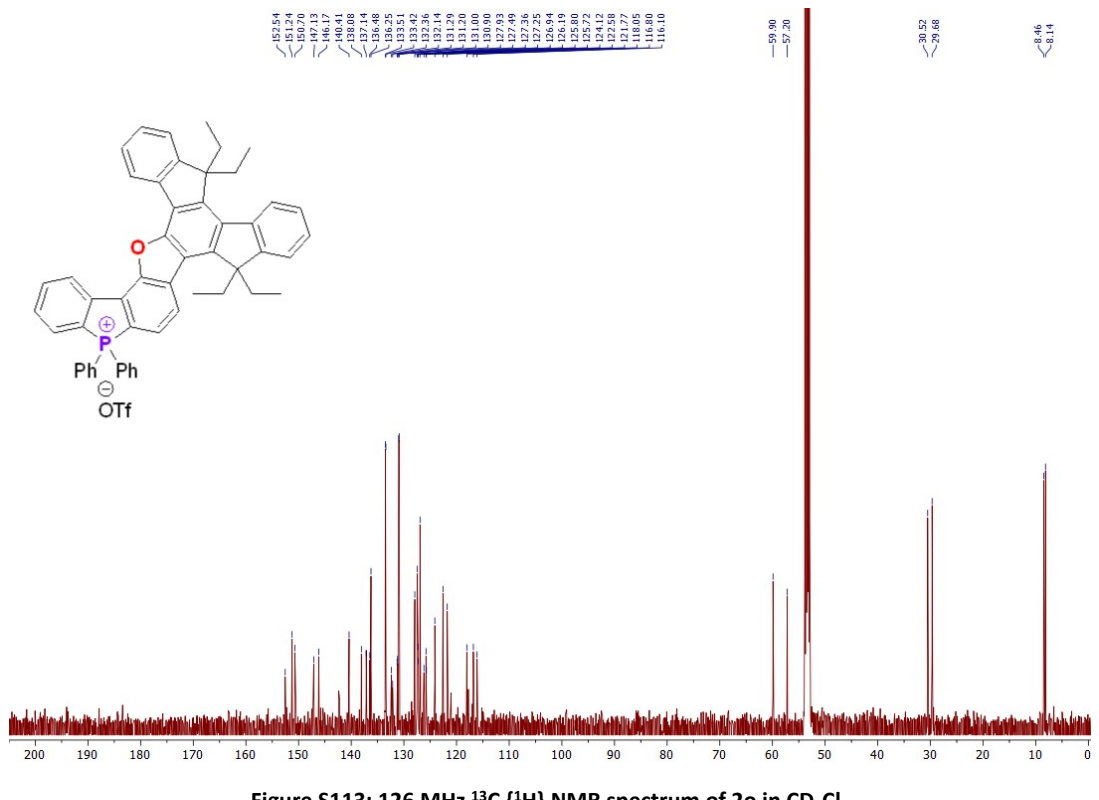


Figure S113: 126 MHz ^{13}C { ^1H } NMR spectrum of 2o in CD_2Cl_2

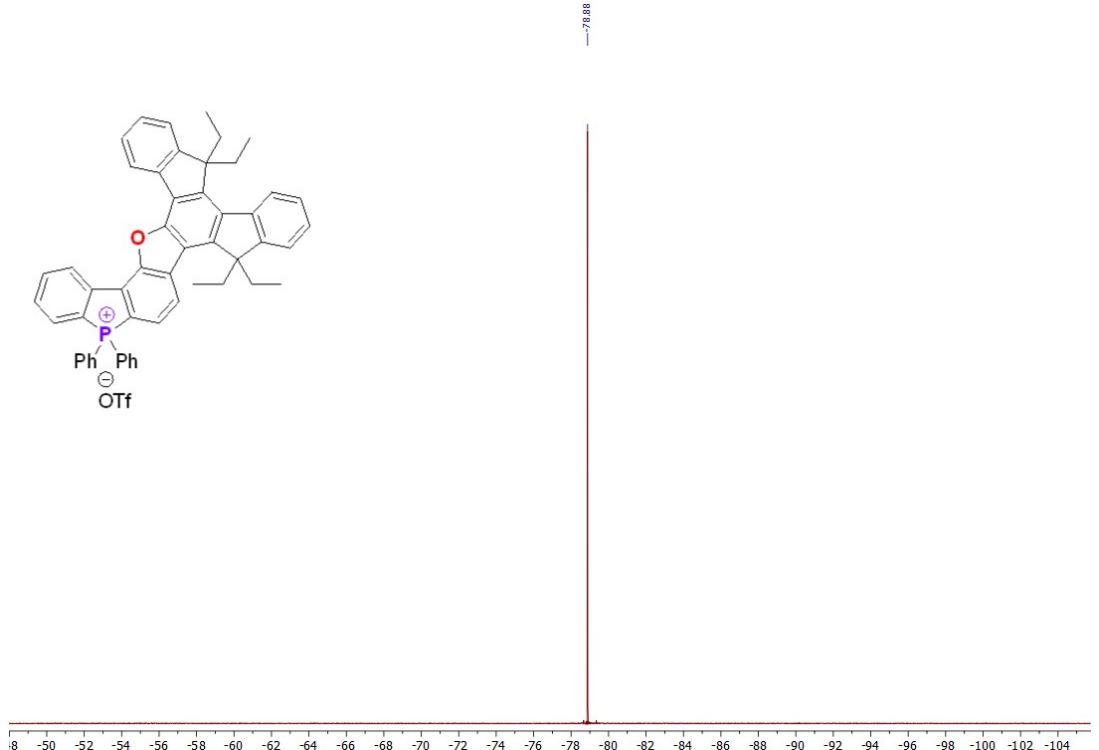


Figure S114: 470 MHz ^{19}F NMR spectrum of 2o in CD_2Cl_2

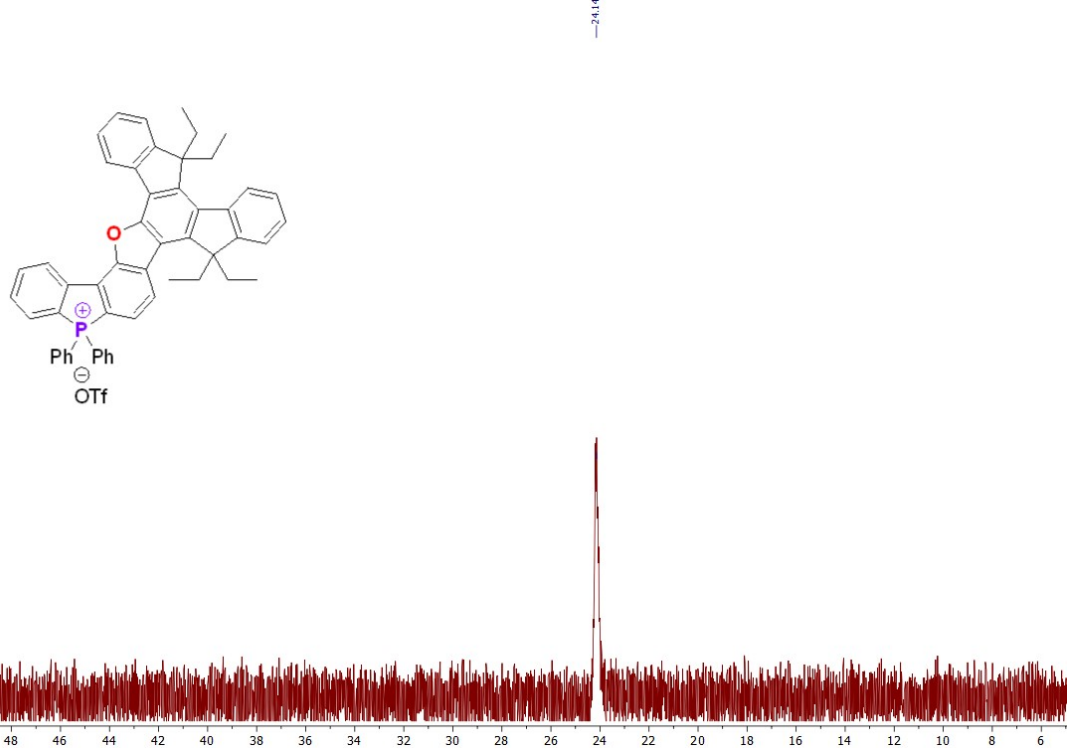


Figure S115: 202 MHz ^{31}P NMR spectrum of **2o** in CD_2Cl_2

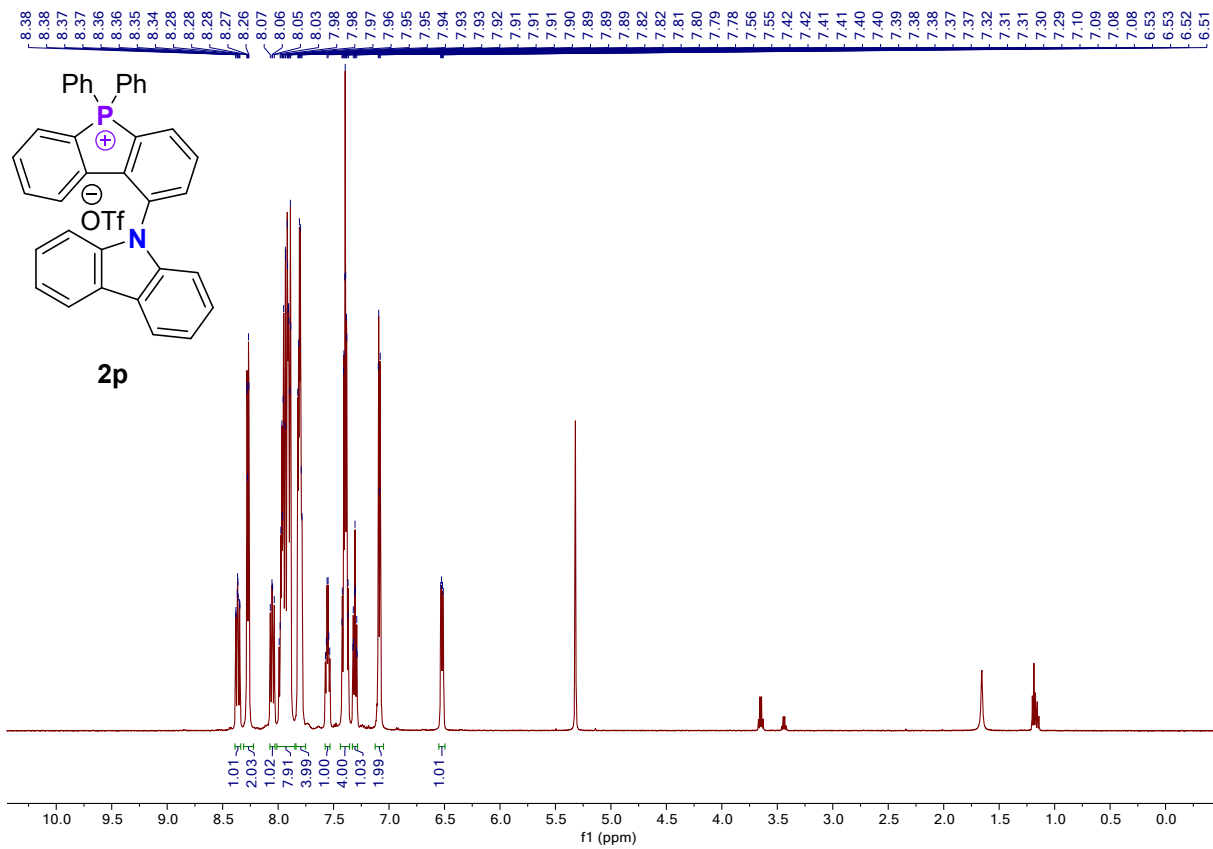


Figure S116: 500 MHz ^1H NMR spectrum of **2p** in CD_2Cl_2

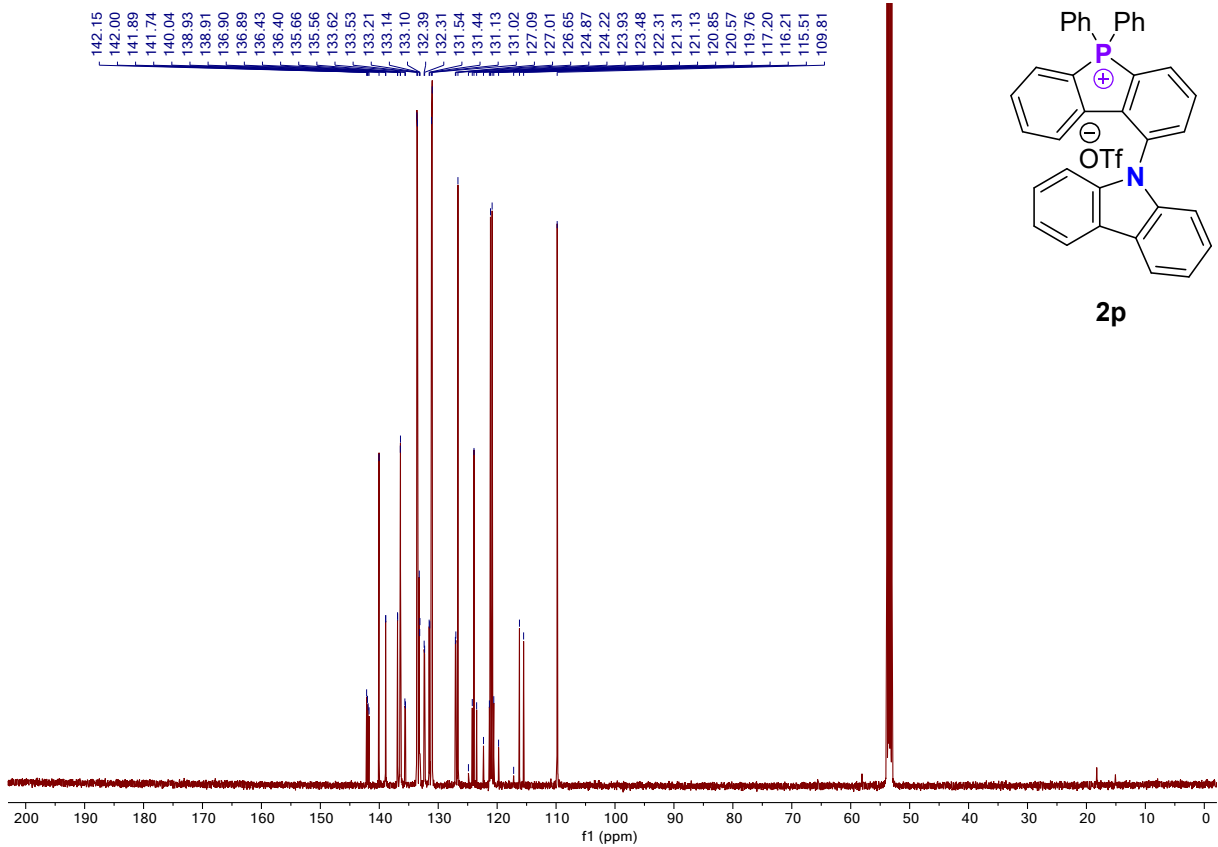


Figure S117: 126 MHz ^{13}C { ^1H } NMR spectrum of **2p** in CD_2Cl_2

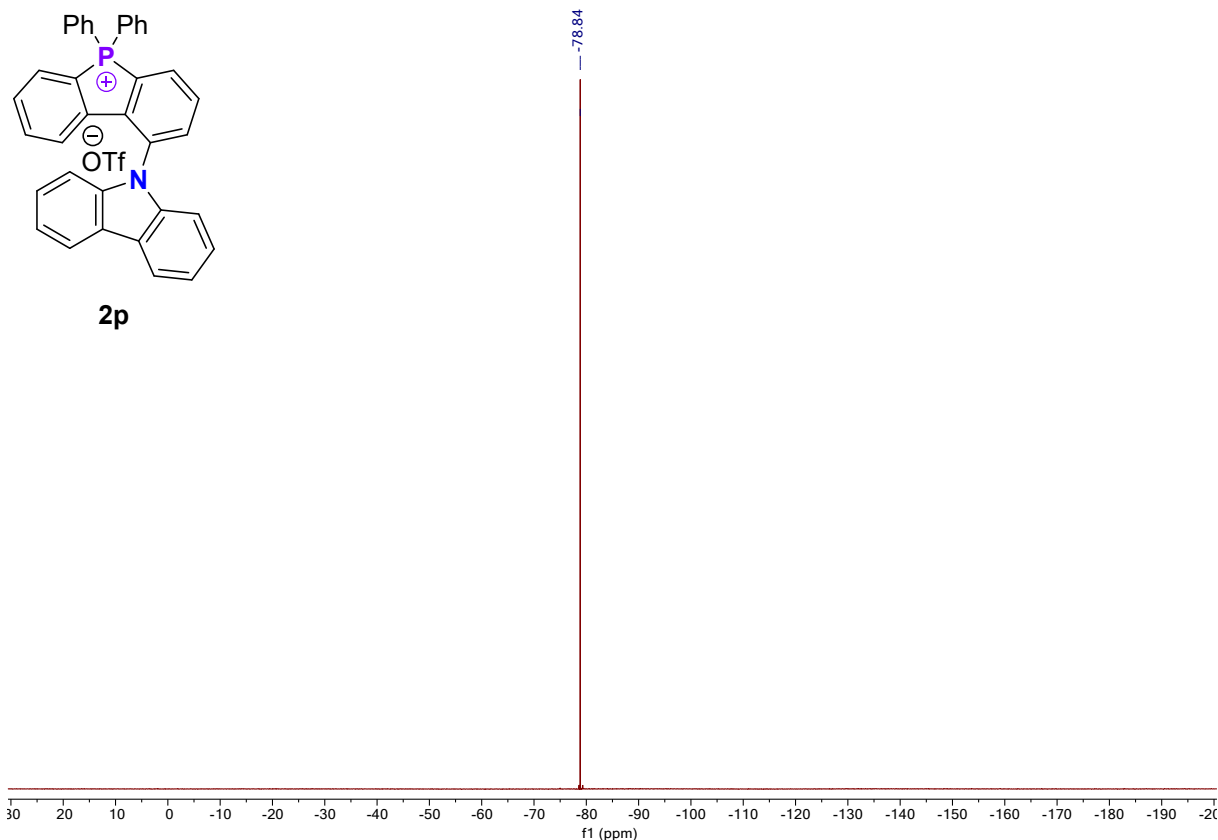


Figure S118: 470 MHz ^{19}F NMR spectrum of **2p** in CD_2Cl_2

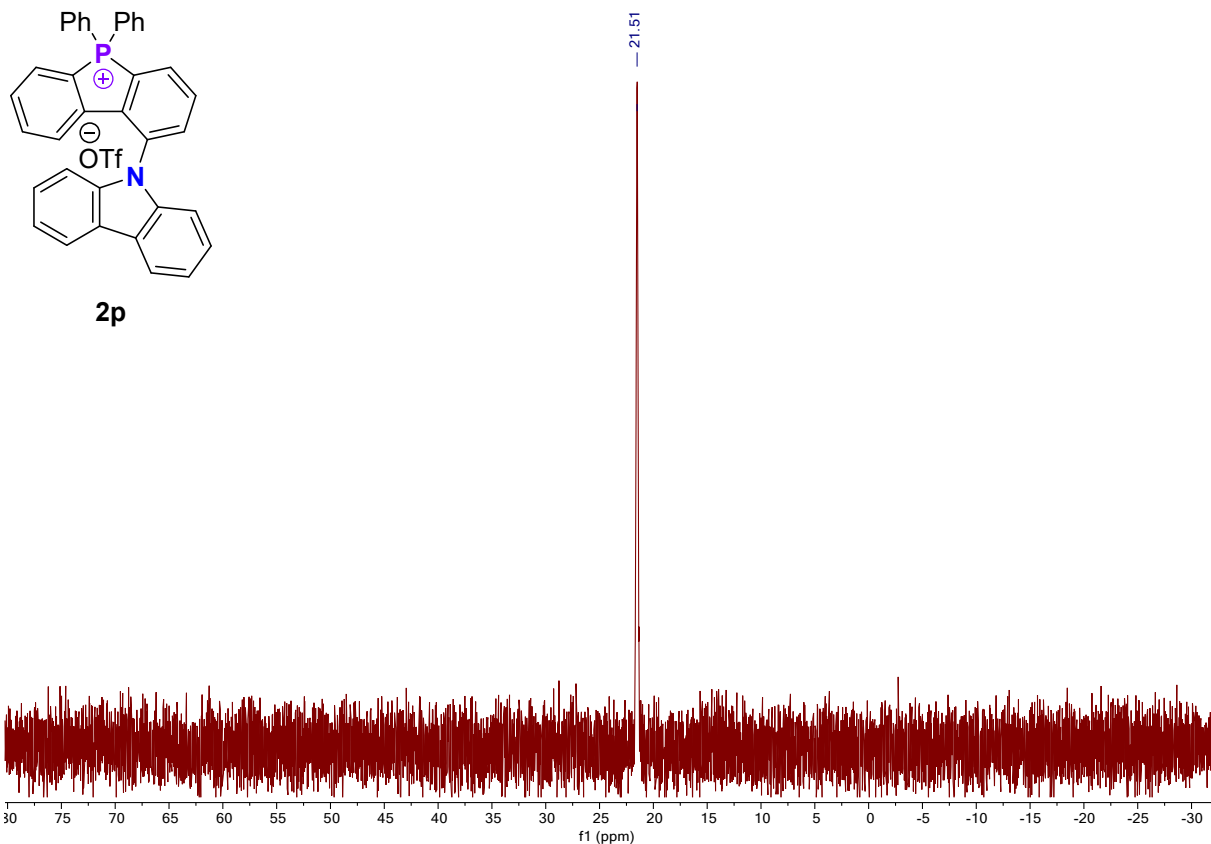


Figure S119: 202 MHz ^{31}P NMR spectrum of **2p** in CD_2Cl_2

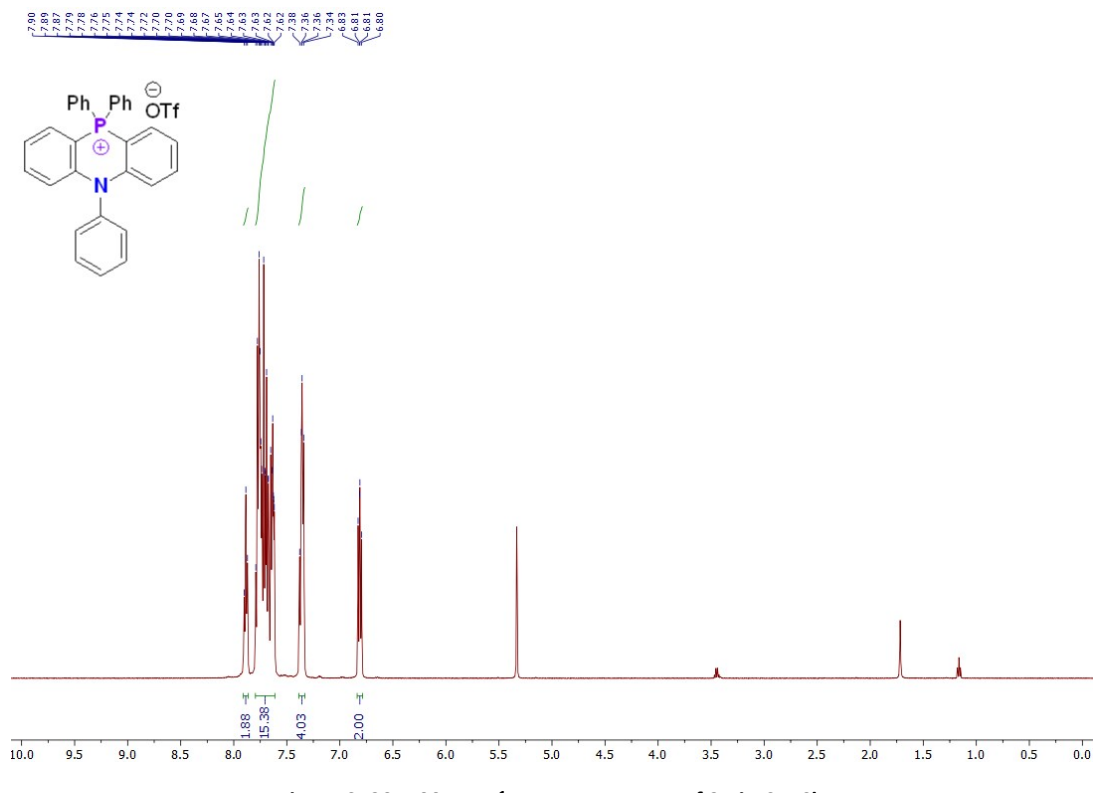


Figure S120: 500 MHz ^1H NMR spectrum of **2q** in CD_2Cl_2

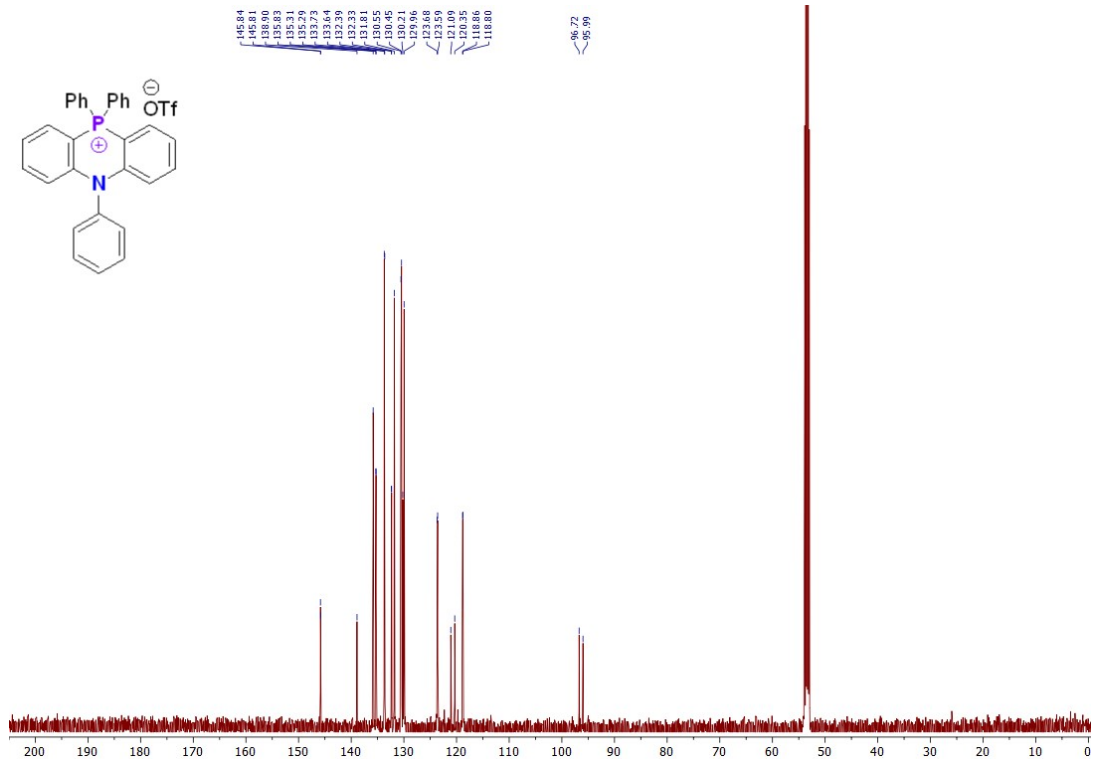


Figure S121: 126 MHz ^{13}C { ^1H } NMR spectrum of 2q in CD_2Cl_2

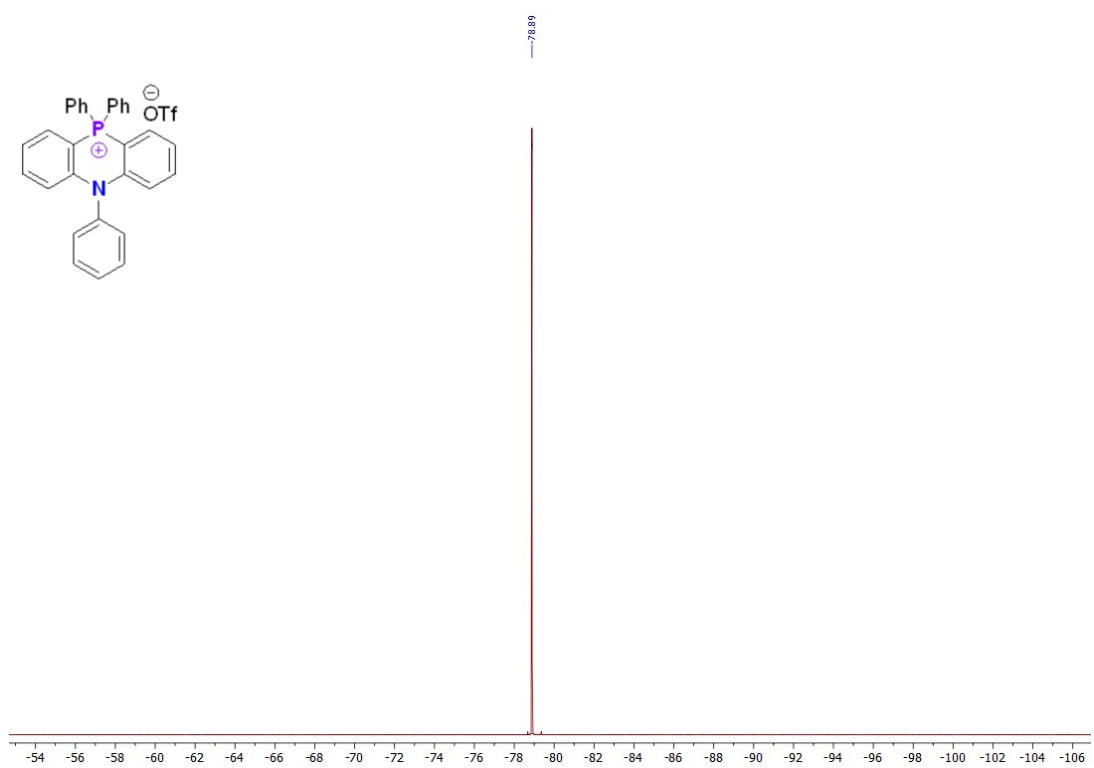
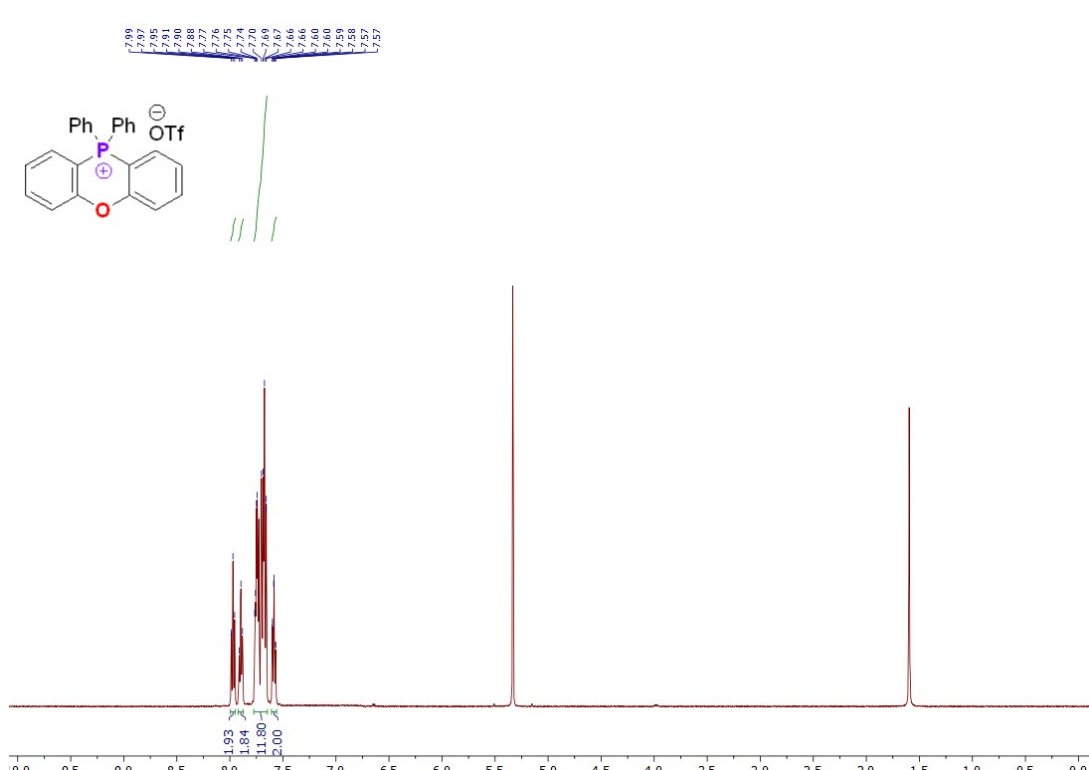
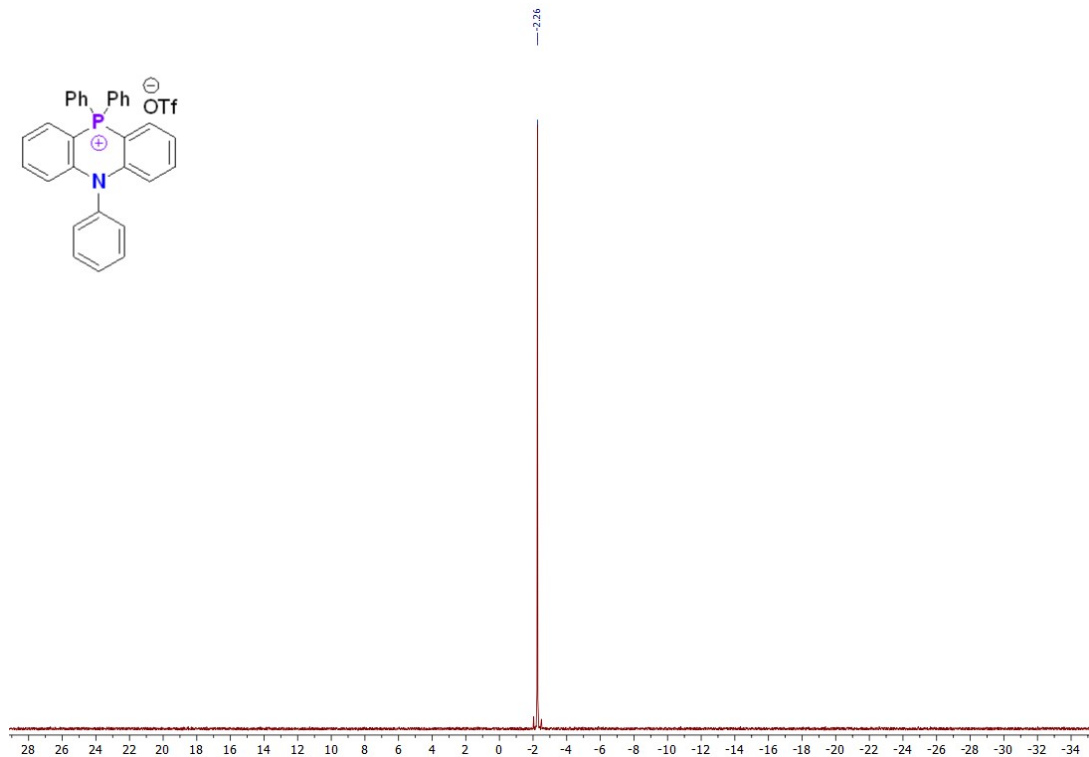


Figure S122: 470 MHz ^{19}F NMR spectrum of 2q in CD_2Cl_2



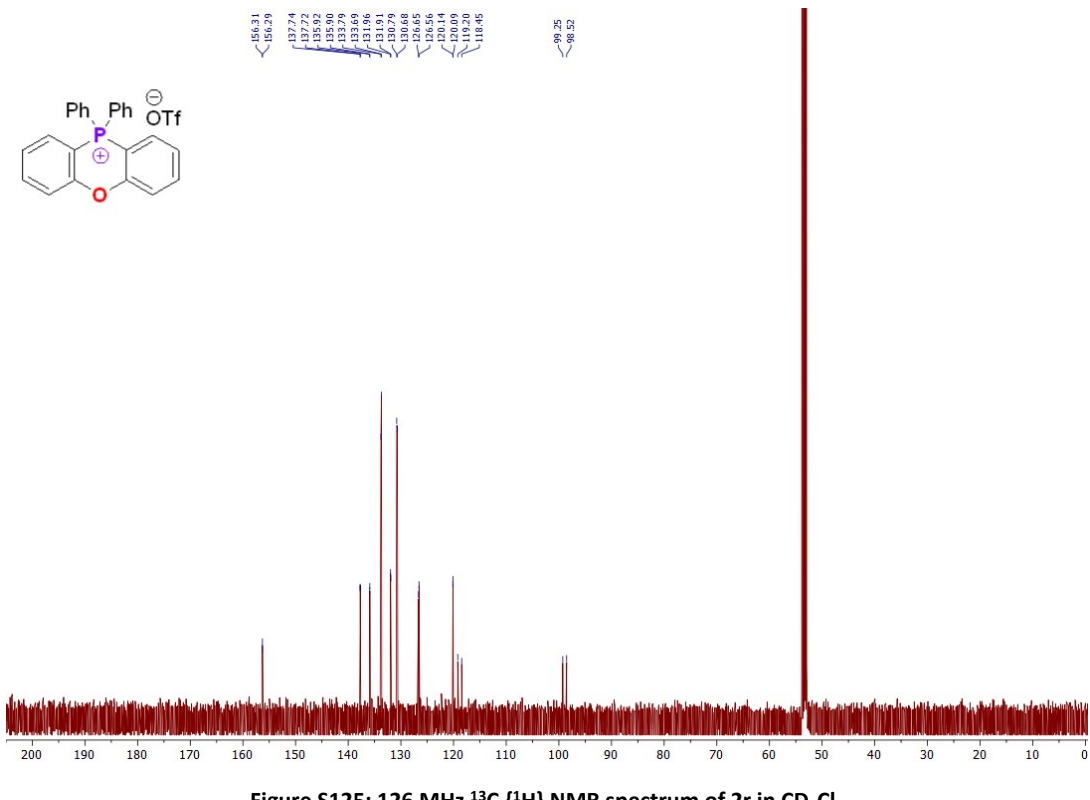


Figure S125: 126 MHz ^{13}C { ^1H } NMR spectrum of 2r in CD_2Cl_2

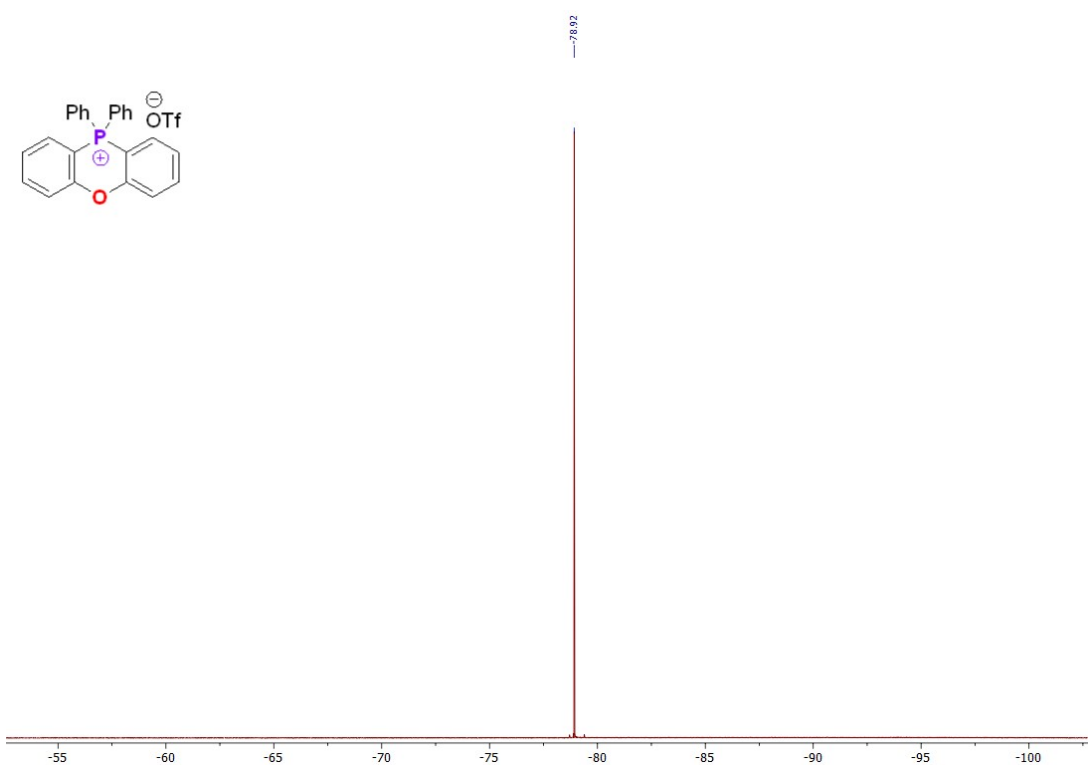


Figure S126: 470 MHz ^{19}F NMR spectrum of 2r in CD_2Cl_2

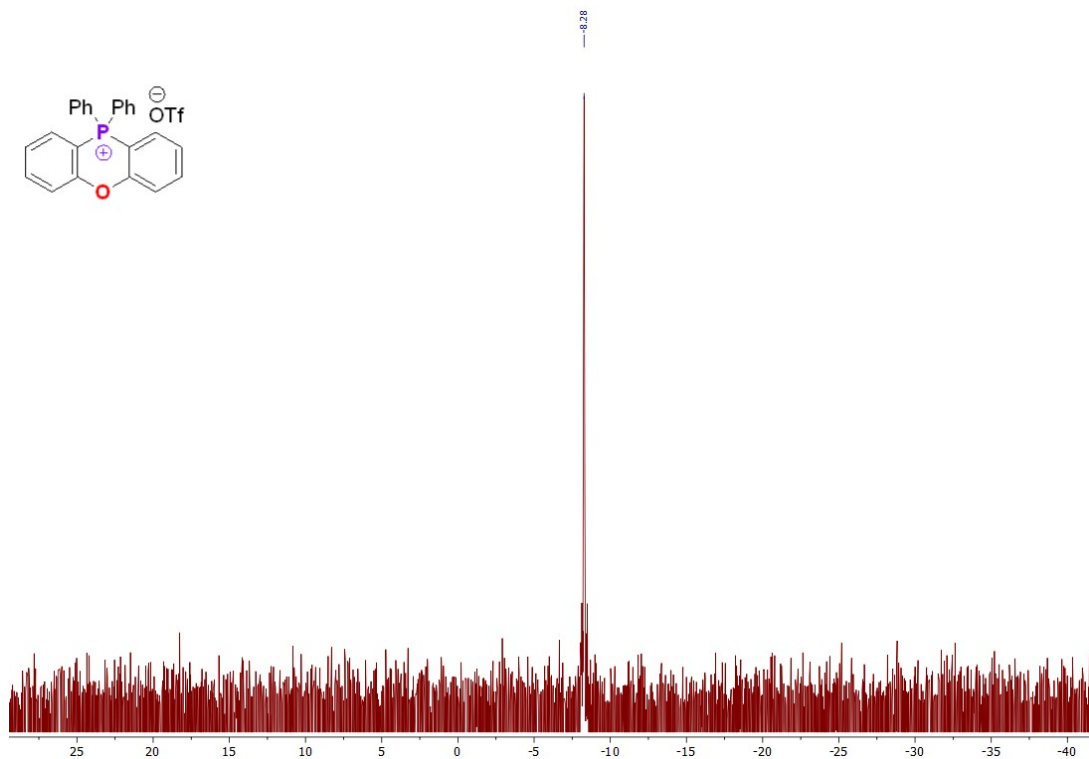


Figure S127: 202 MHz ³¹P NMR spectrum of **2r** in CD₂Cl₂

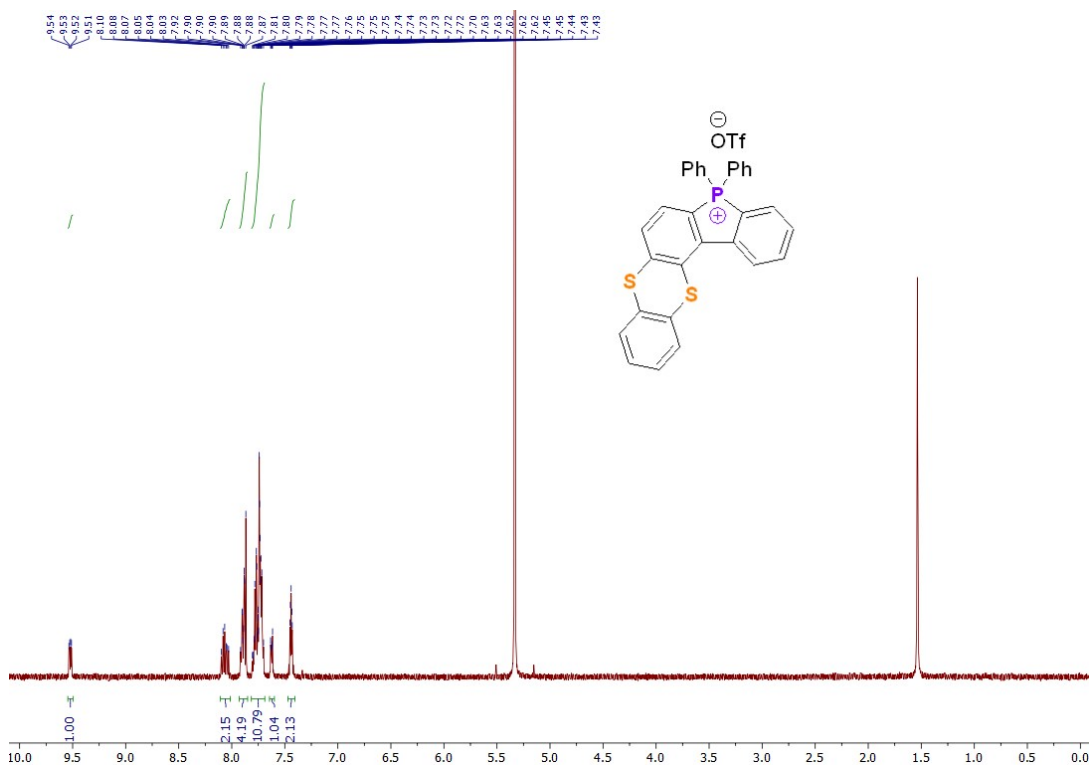


Figure S128: 500 MHz ¹H NMR spectrum of **2s** in CD₂Cl₂

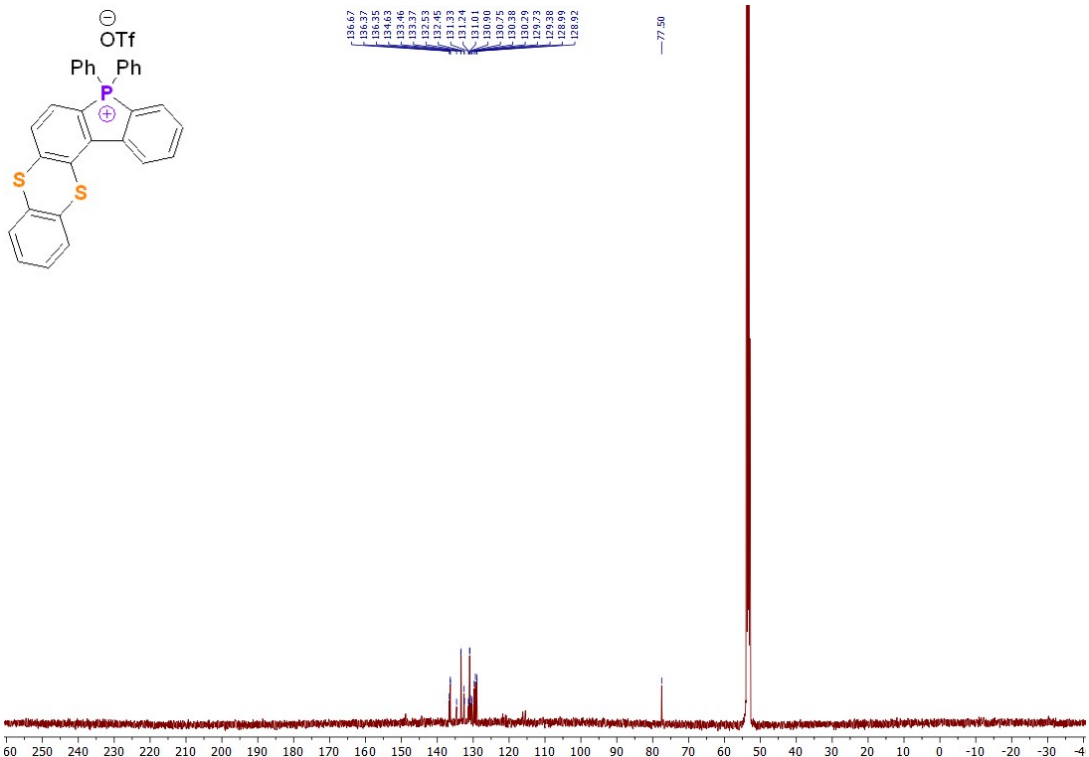


Figure S129: 126 MHz ^{13}C { ^1H } NMR spectrum of 2s in CD_2Cl_2

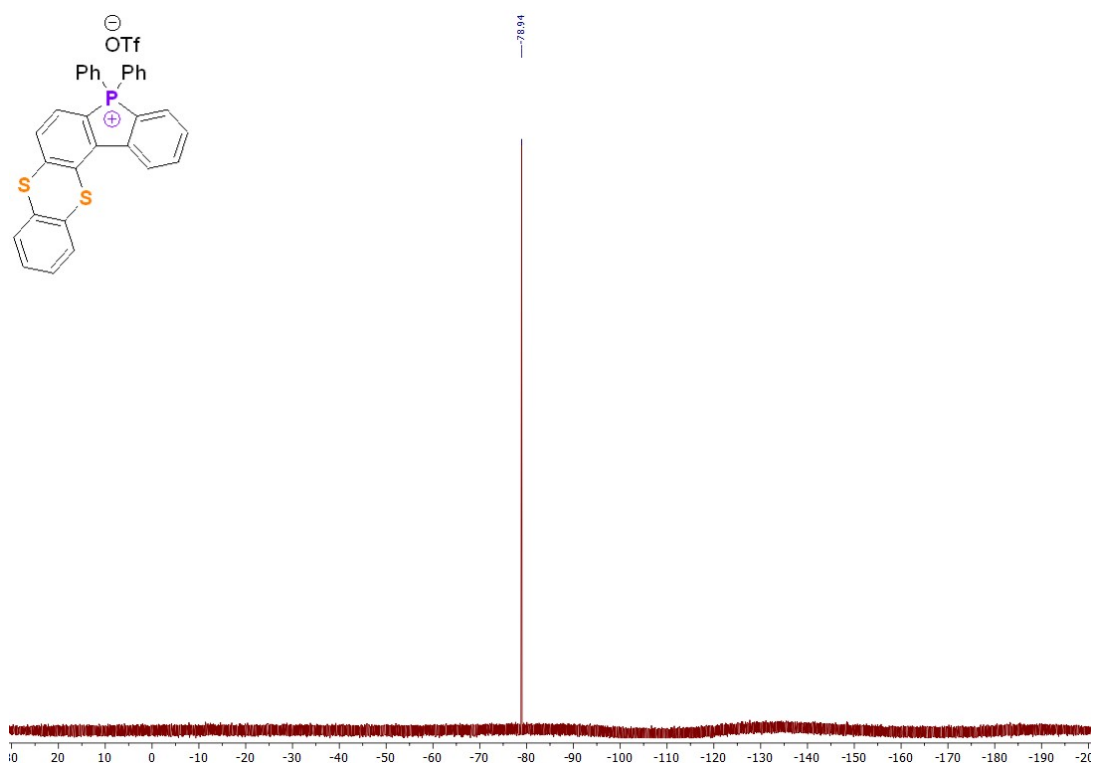
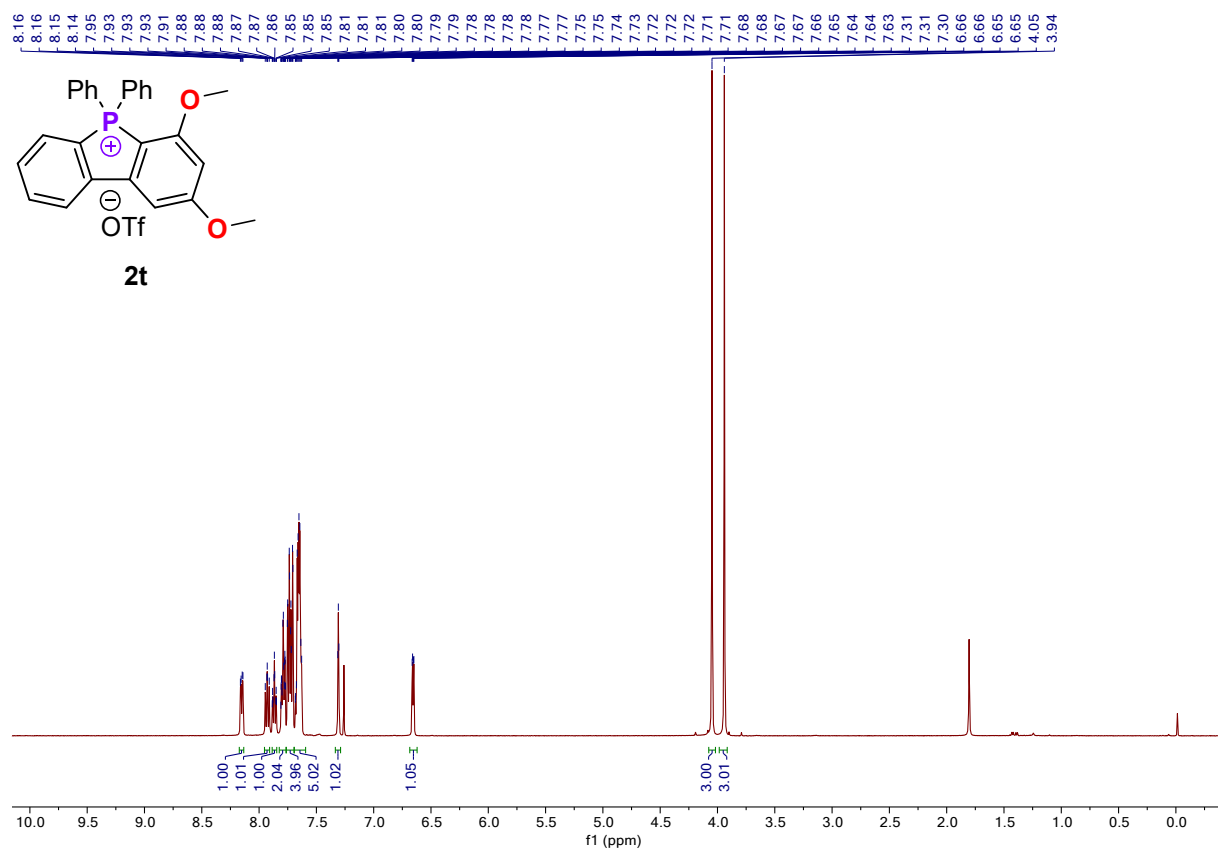
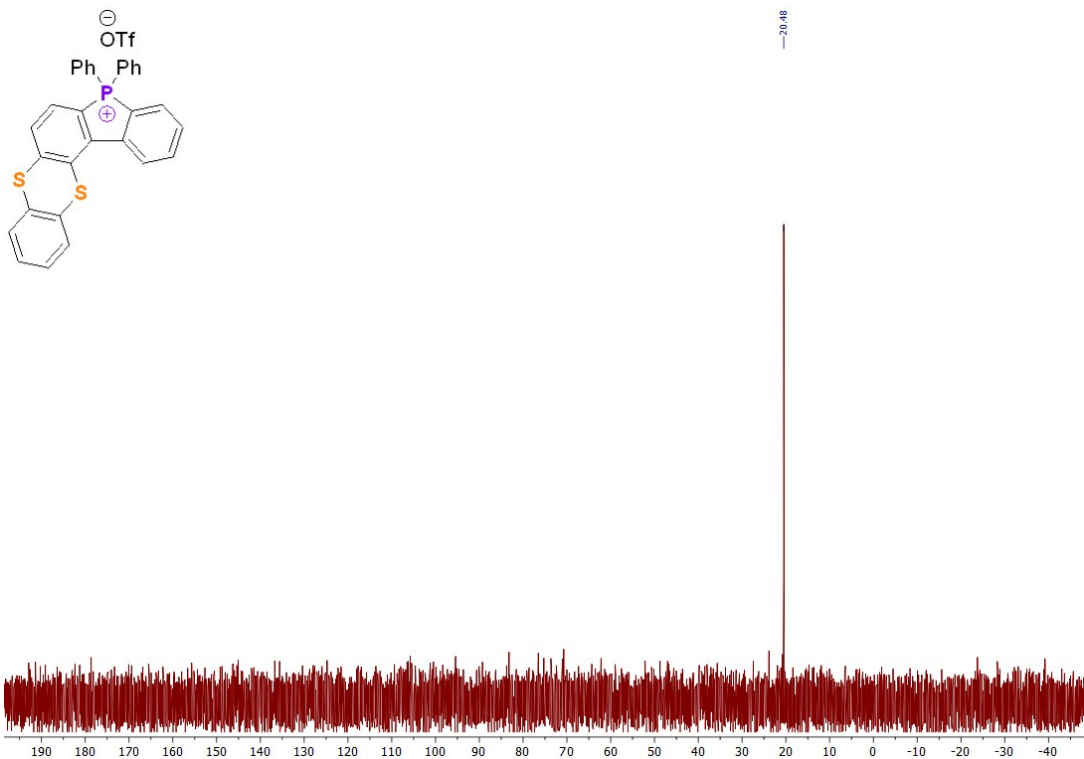


Figure S130: 470 MHz ^{19}F NMR spectrum of **2s** in CD_2Cl_2



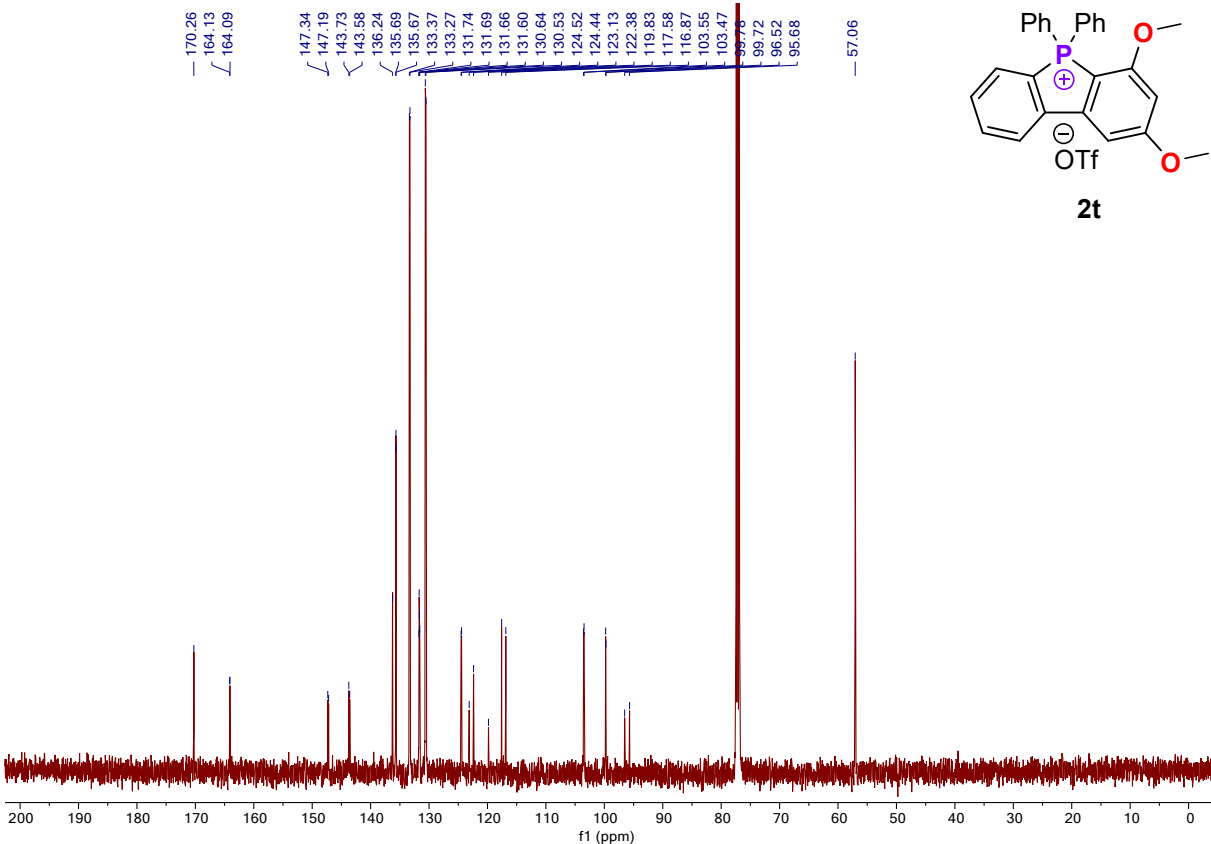


Figure S133: 126 MHz ^{13}C { ^1H } NMR spectrum of 2t in CDCl_3

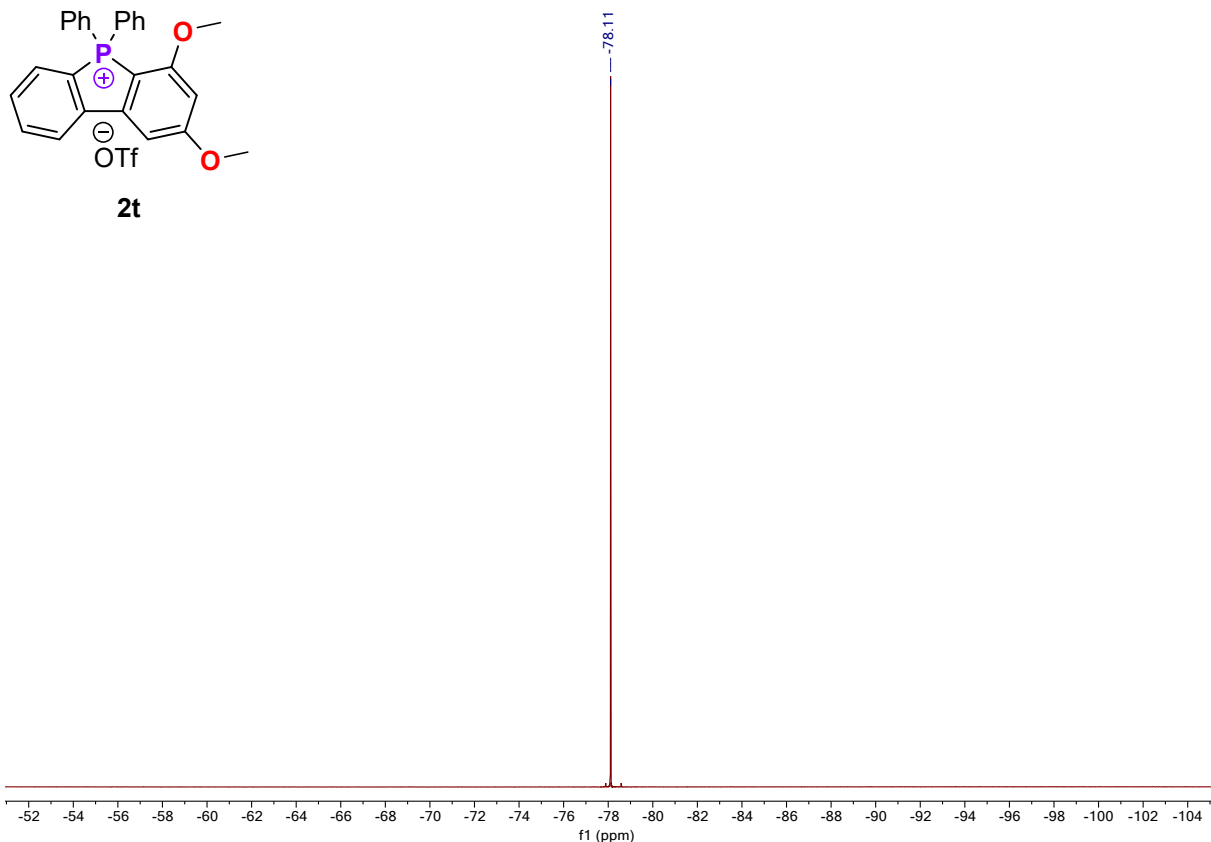


Figure S134: 470 MHz ^{19}F NMR spectrum of 2t in CDCl_3

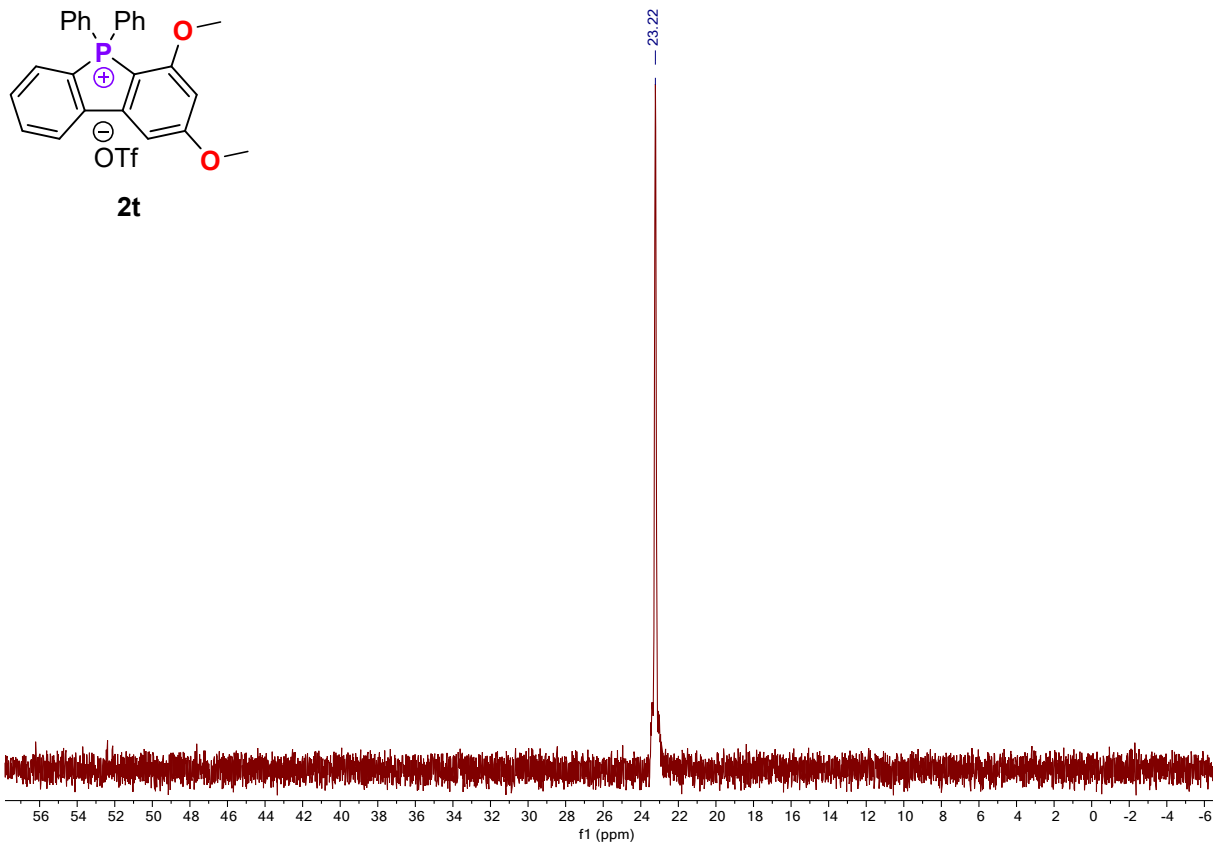
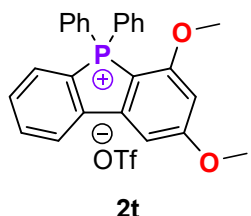


Figure S135: 202 MHz ^{31}P NMR spectrum of 2t in CDCl_3

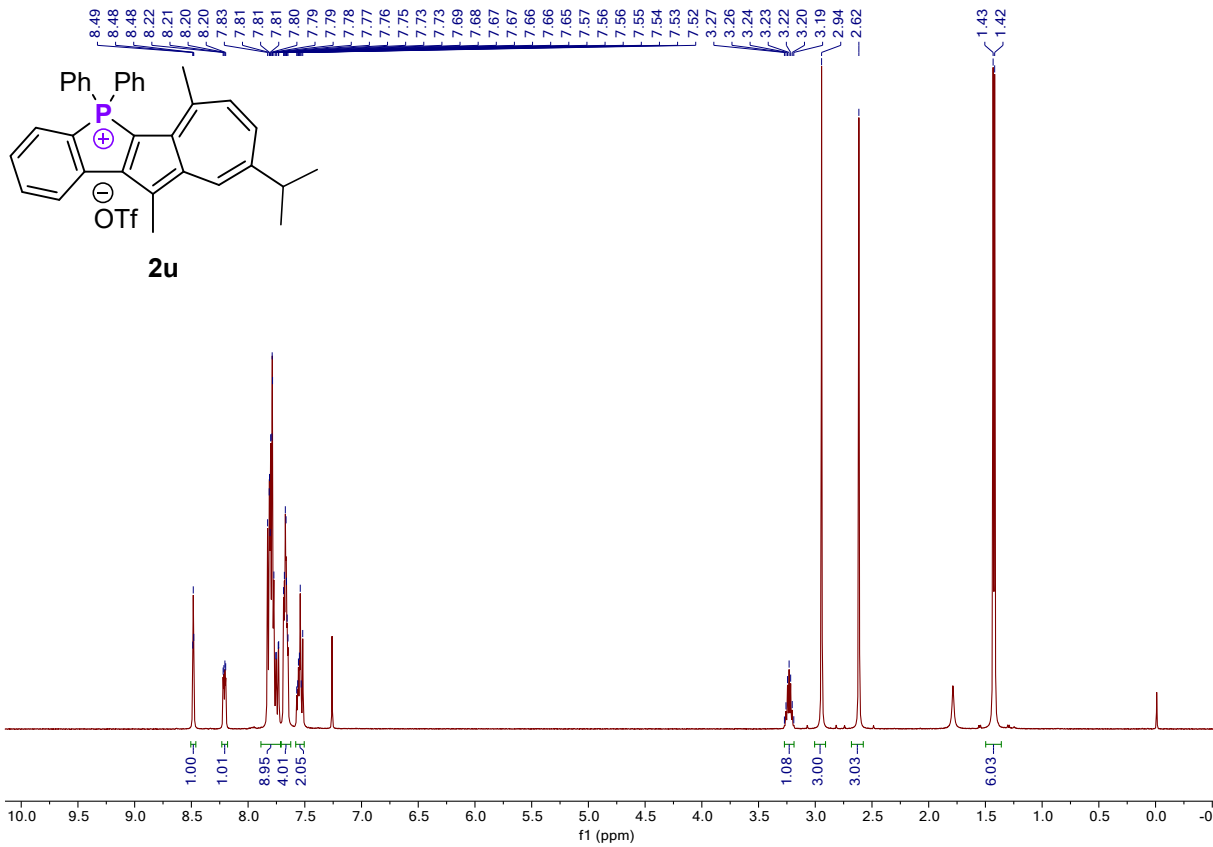
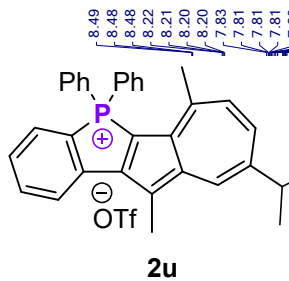


Figure S136: 500 MHz ^1H NMR spectrum of 2u in CDCl_3

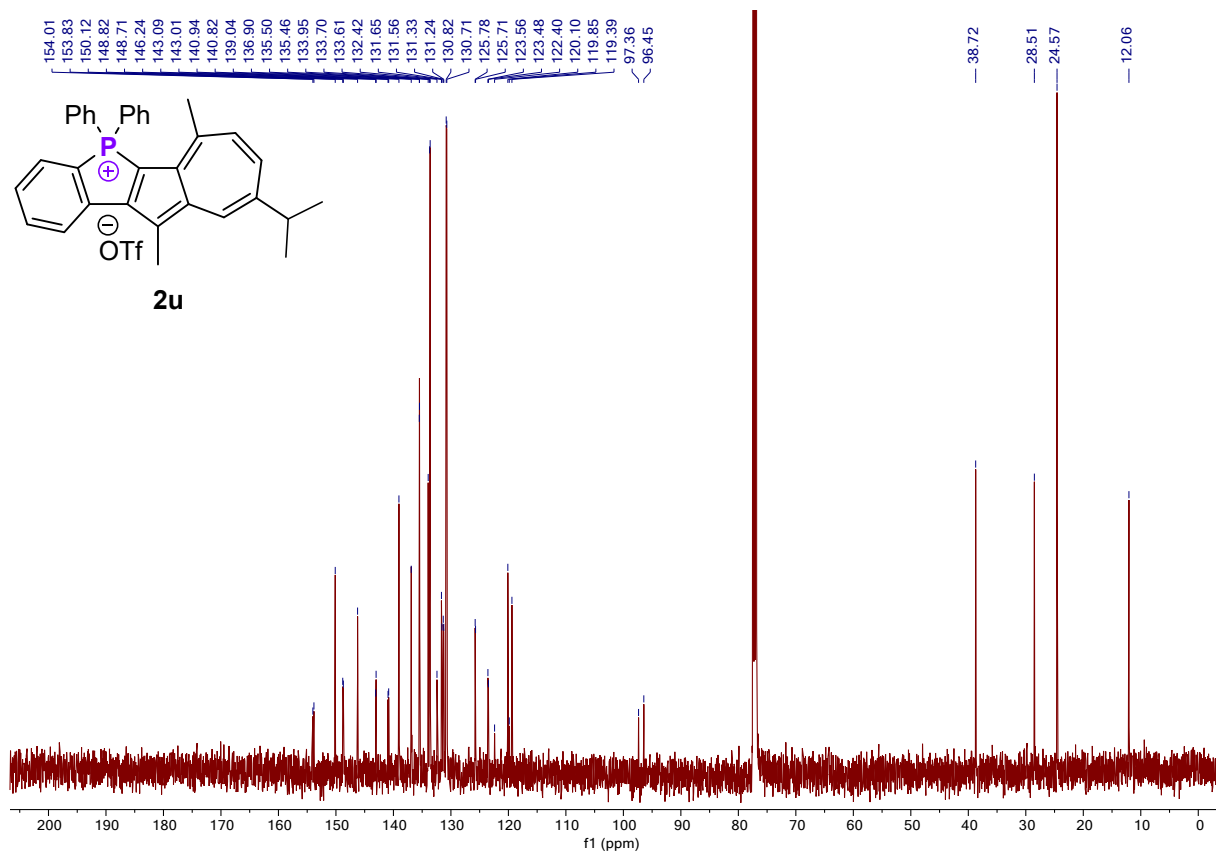


Figure S137: 126 MHz ^{13}C { ^1H } NMR spectrum of **2u** in CDCl_3

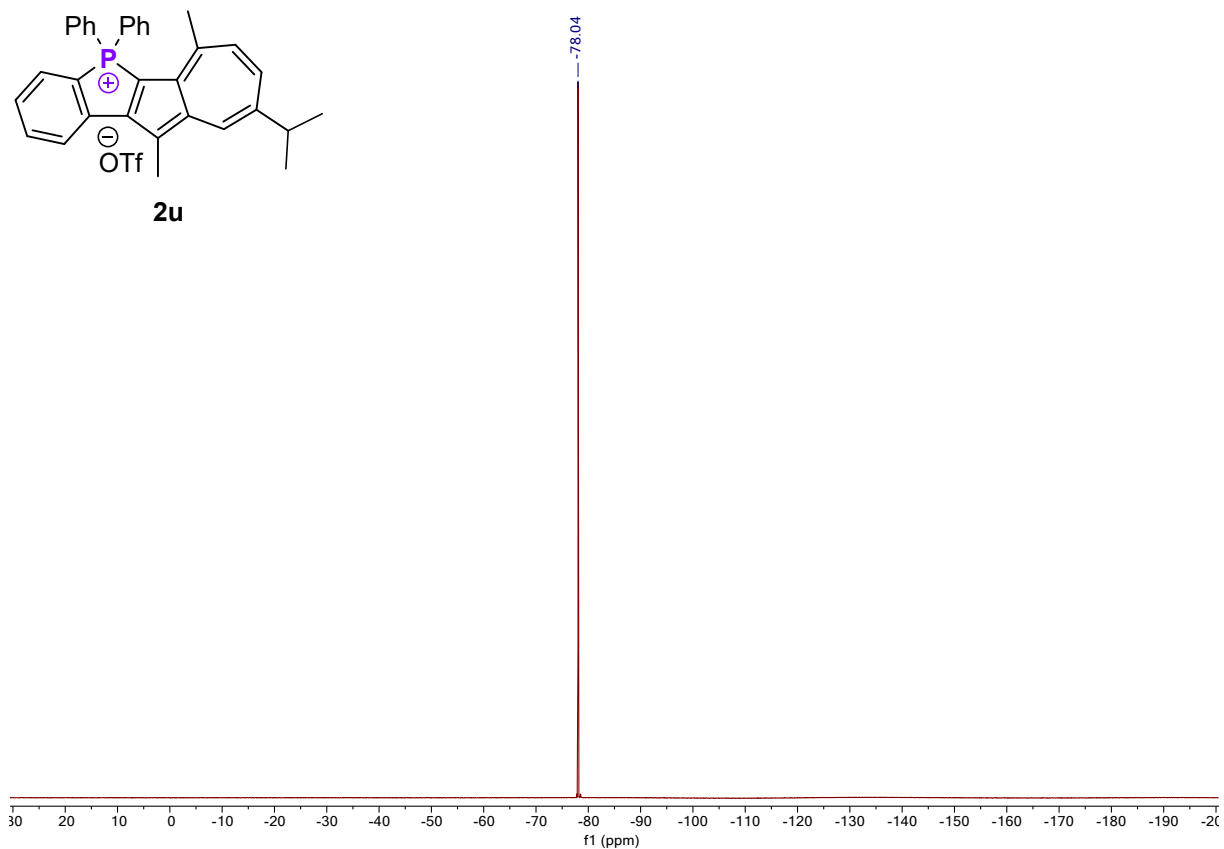


Figure S138: 470 MHz ^{19}F NMR spectrum of **2u** in CDCl_3

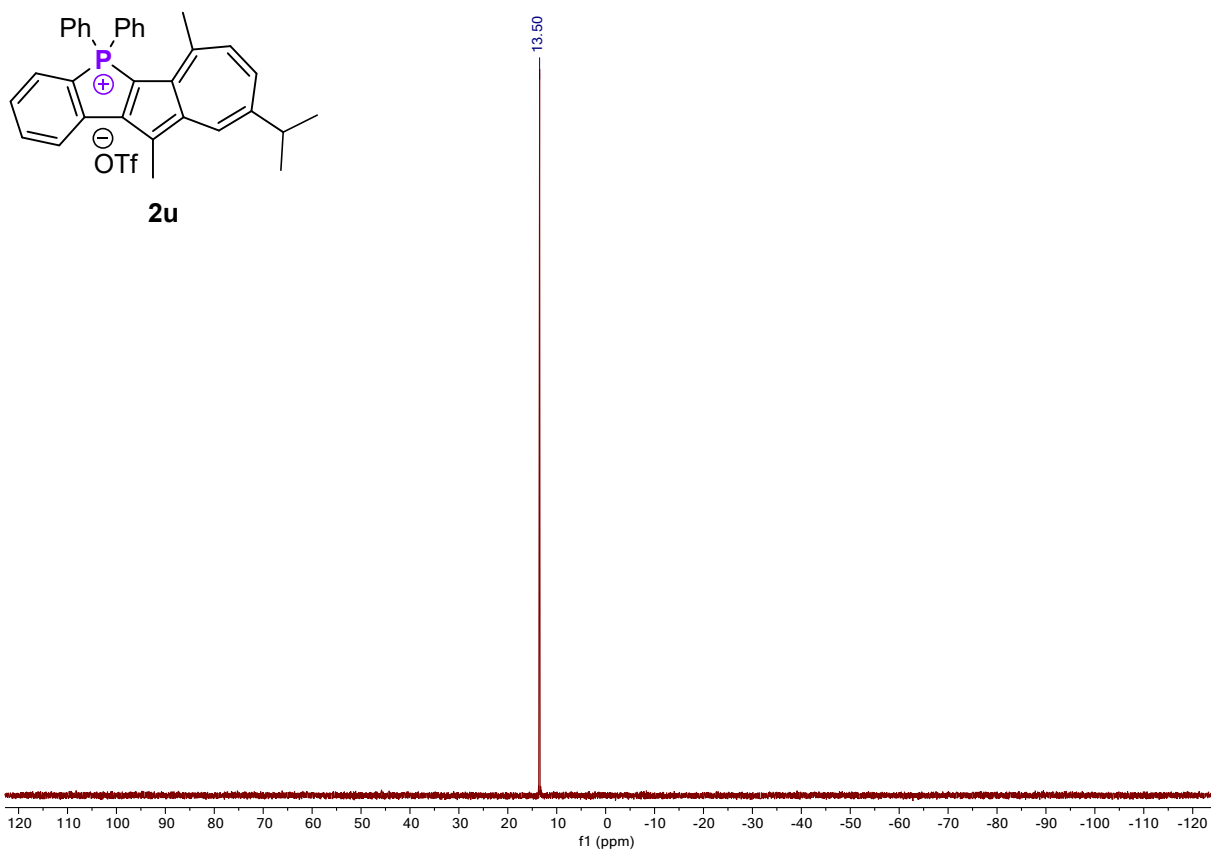


Figure S139: 202 MHz ^{31}P NMR spectrum of **2u** in CDCl_3

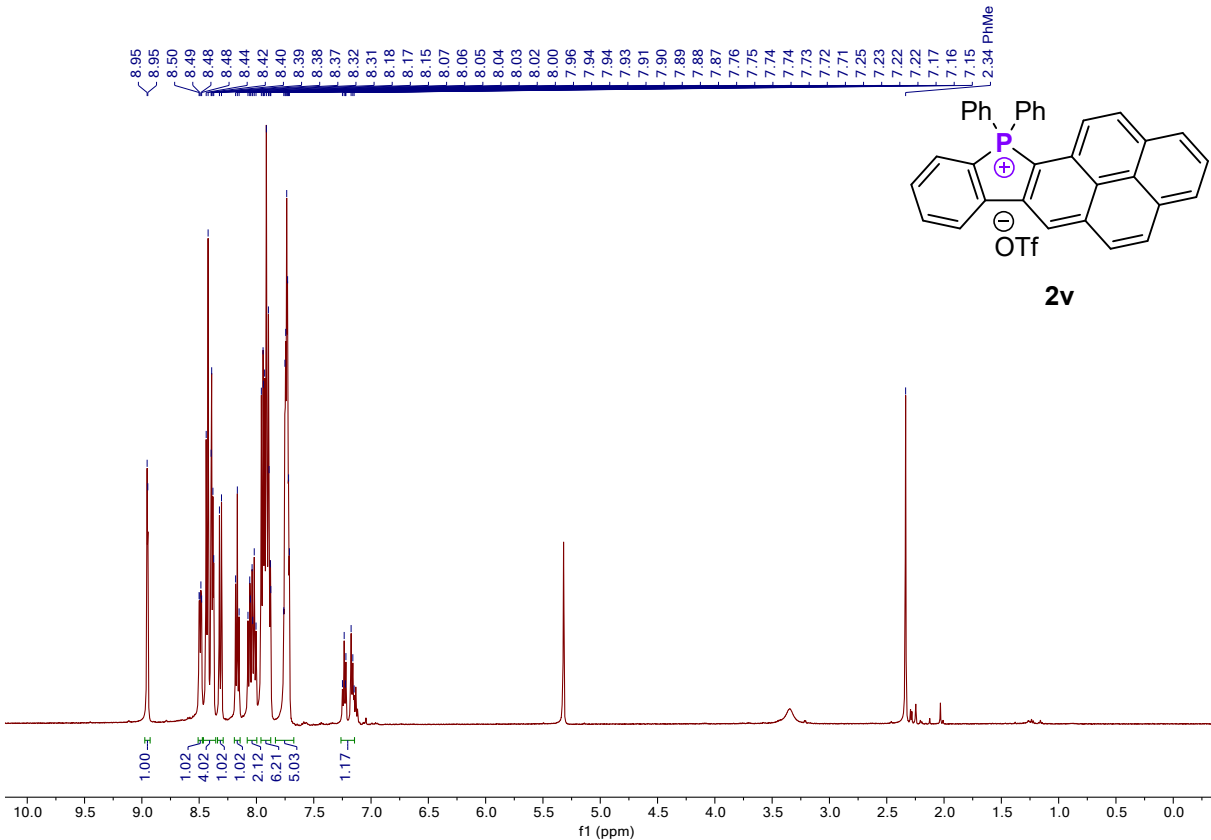


Figure S140: 500 MHz ^1H NMR spectrum of **2v** in CD_2Cl_2

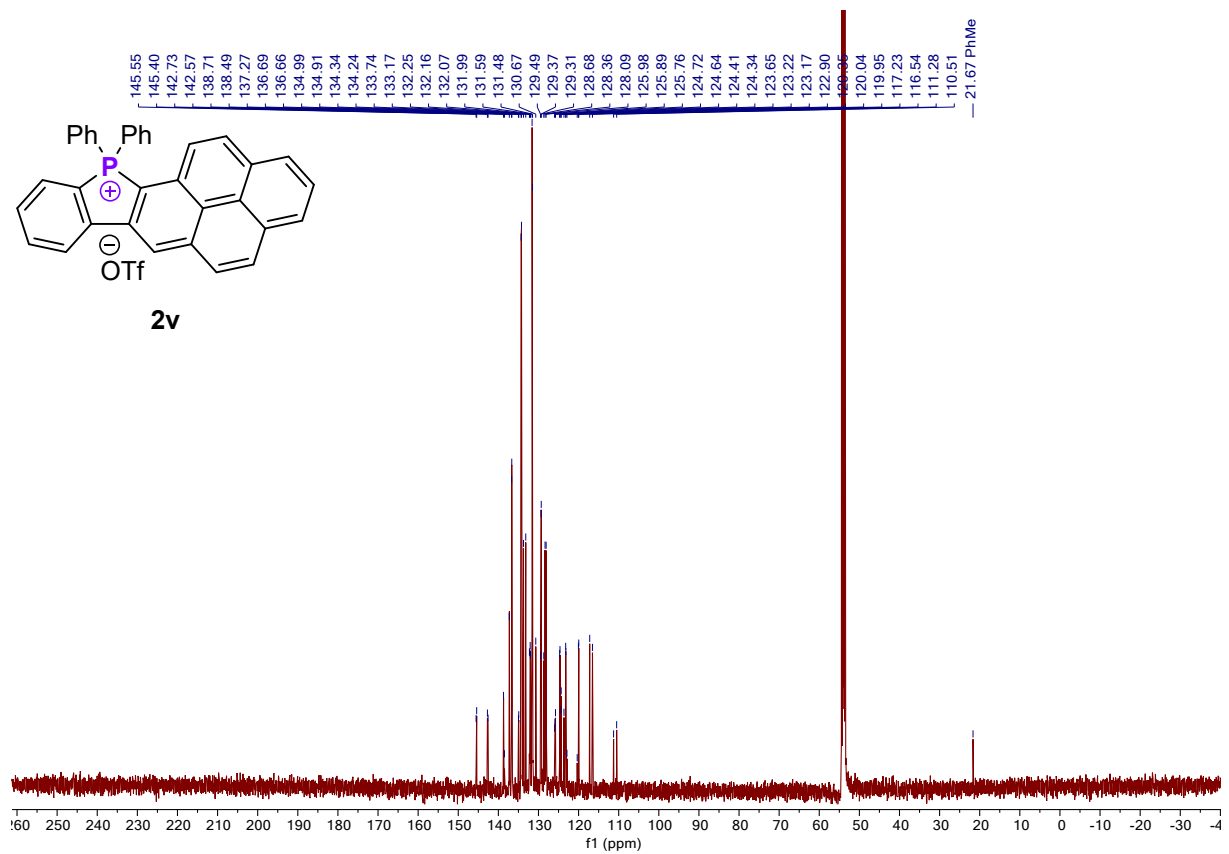


Figure S141: 126 MHz ^{13}C { ^1H } NMR spectrum of **2v** in CD_2Cl_2

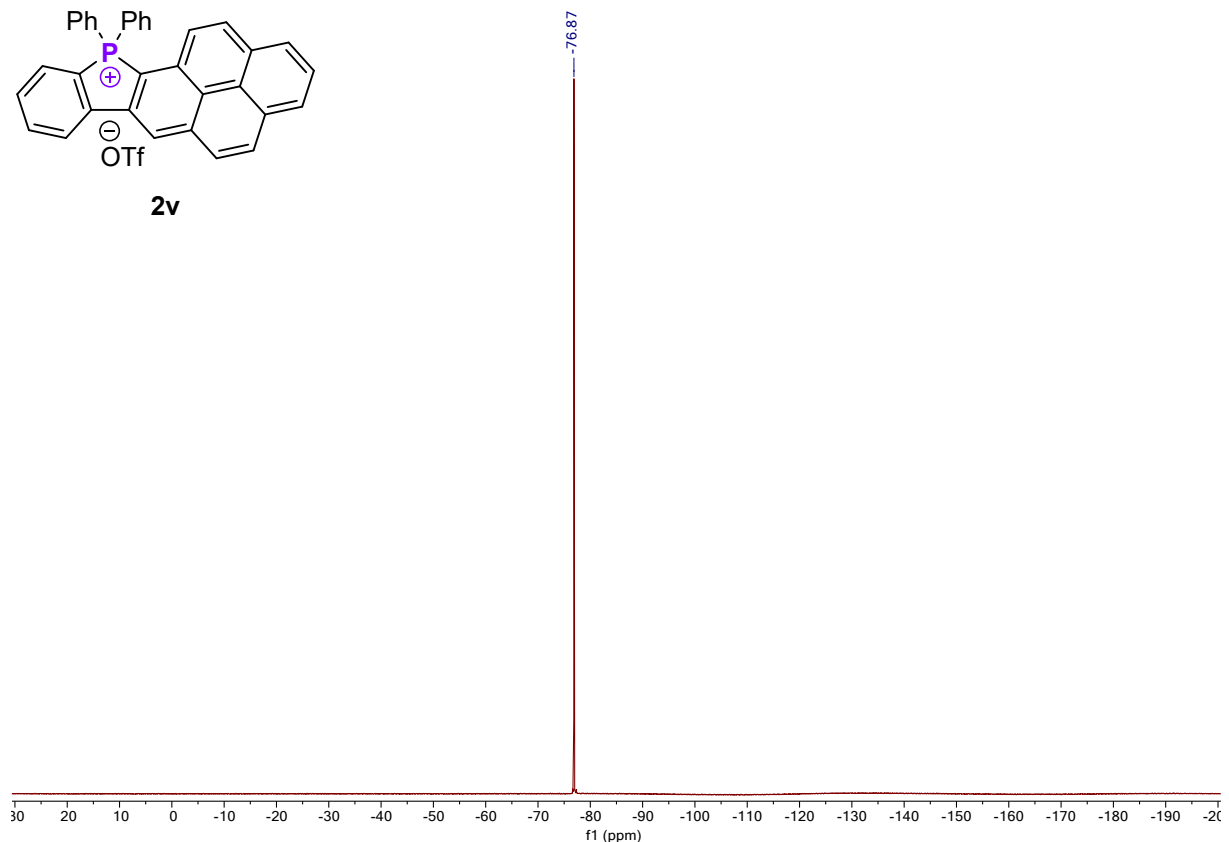


Figure S142: 470 MHz ^{19}F NMR spectrum of **2v** in CD_2Cl_2

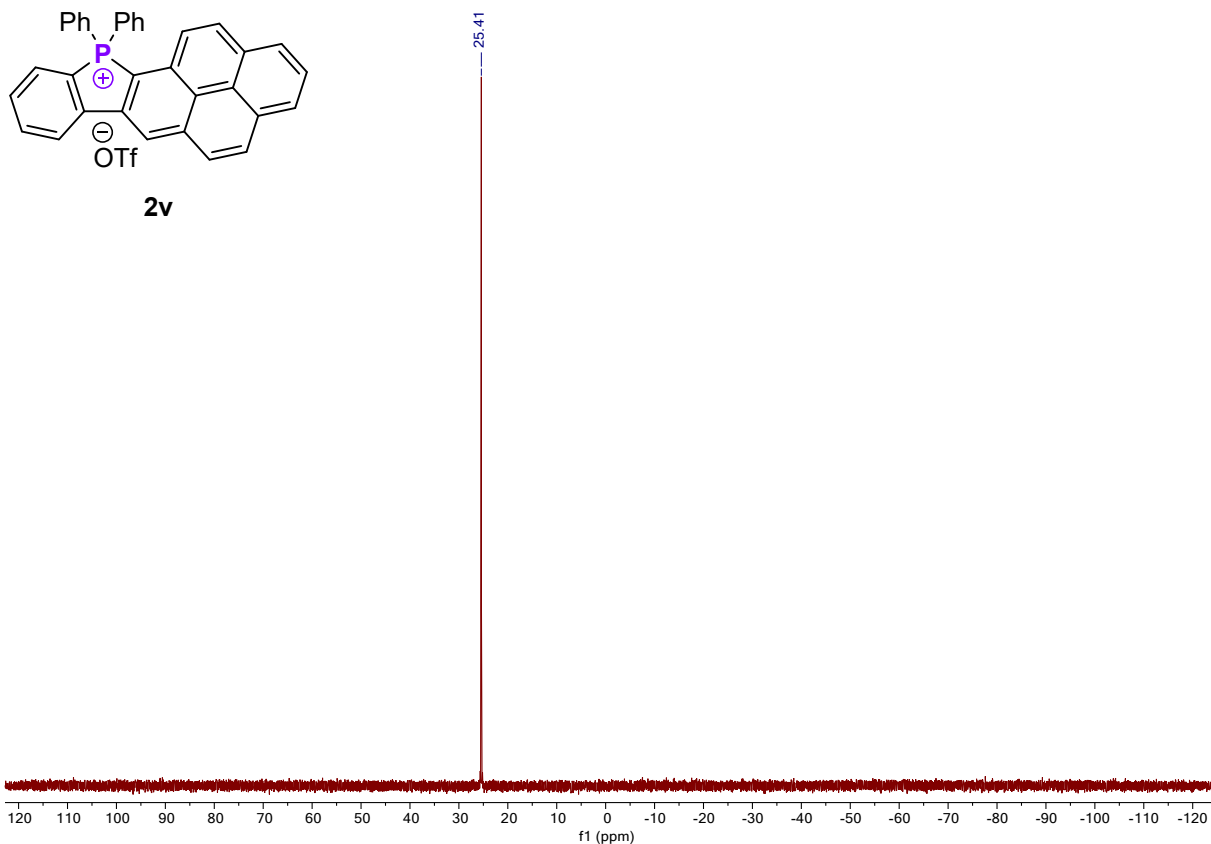


Figure S143: 202 MHz ^{31}P NMR spectrum of **2v** in CD_2Cl_2

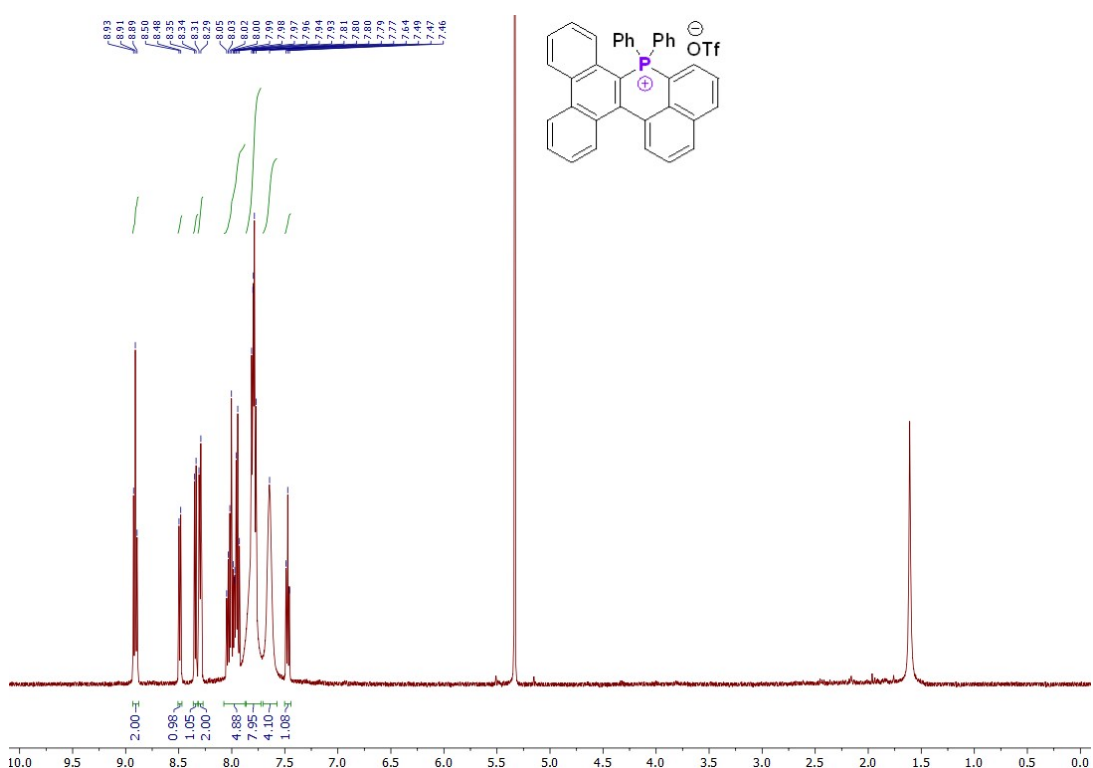


Figure S144: 500 MHz ^1H NMR spectrum of **2w** in CD_2Cl_2

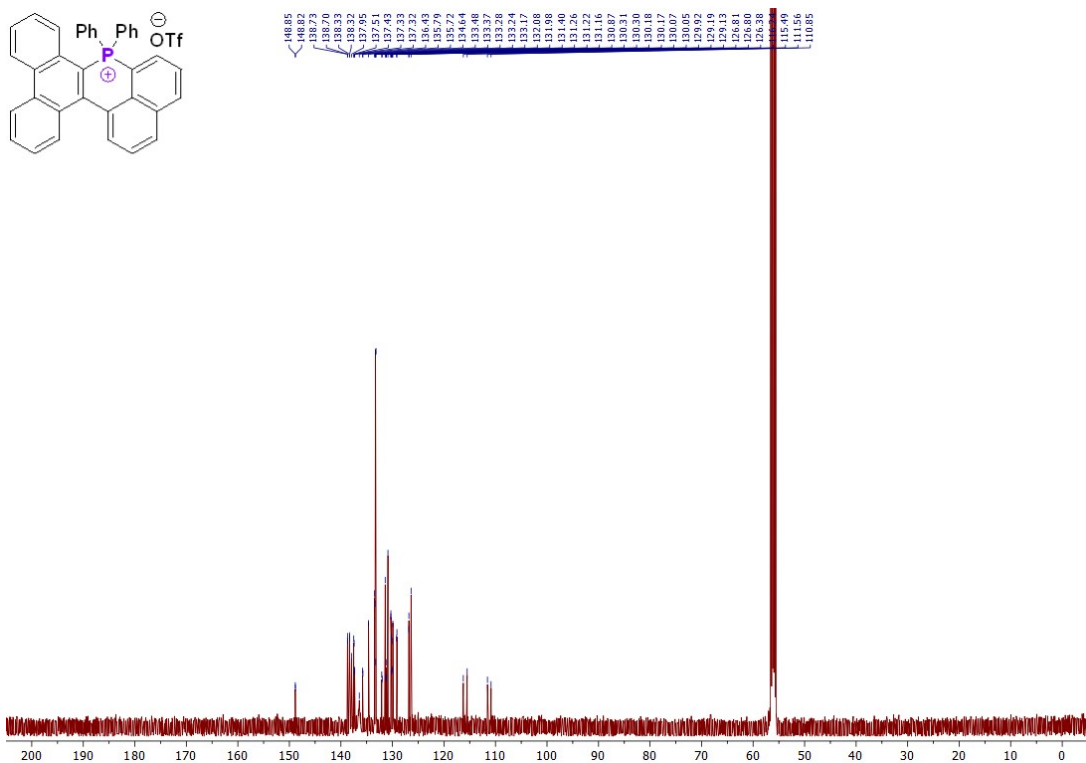
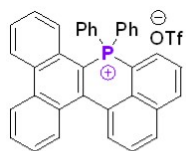


Figure S145: 126 MHz ^{13}C { ^1H } NMR spectrum of 2w in CD_2Cl_2

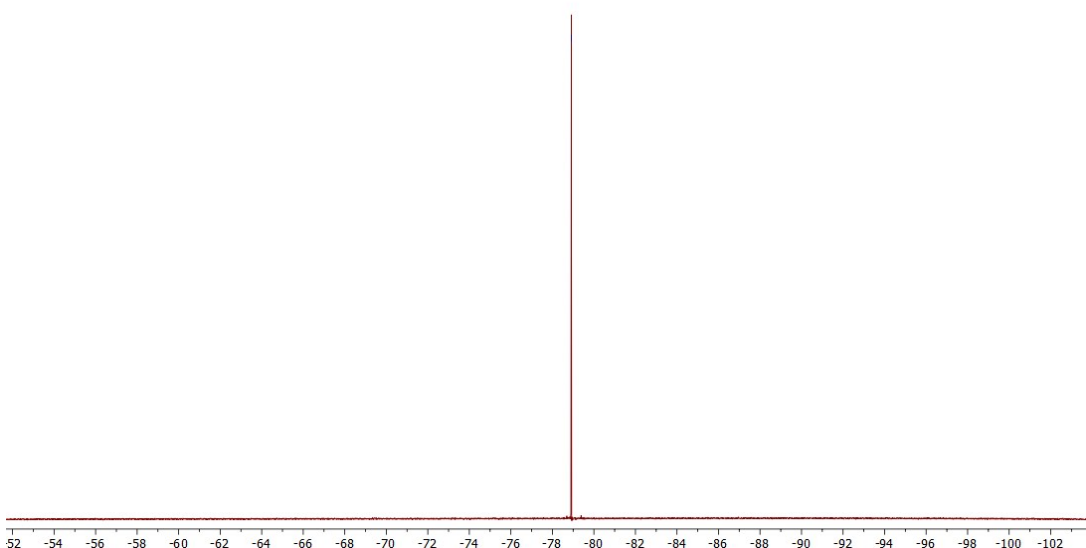
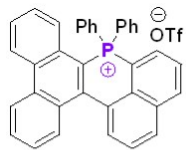


Figure S146: 470 MHz ^{19}F NMR spectrum of 2w in CD_2Cl_2

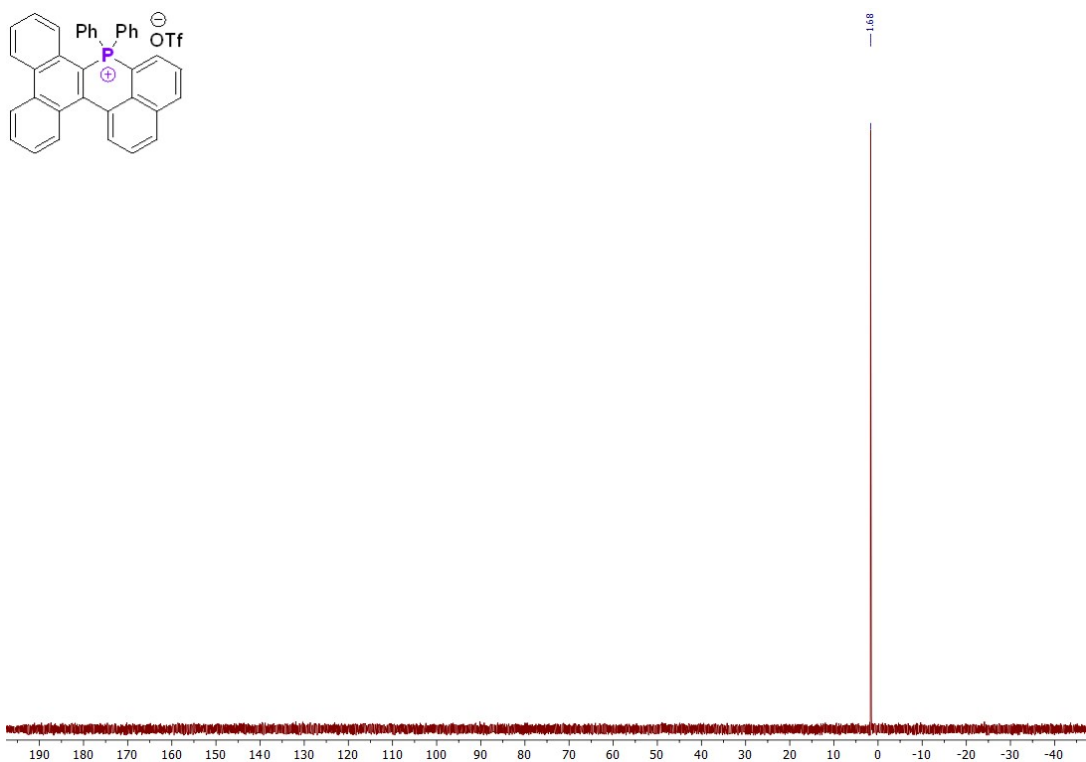


Figure S147: 202 MHz ^{31}P NMR spectrum of **2w** in CD_2Cl_2

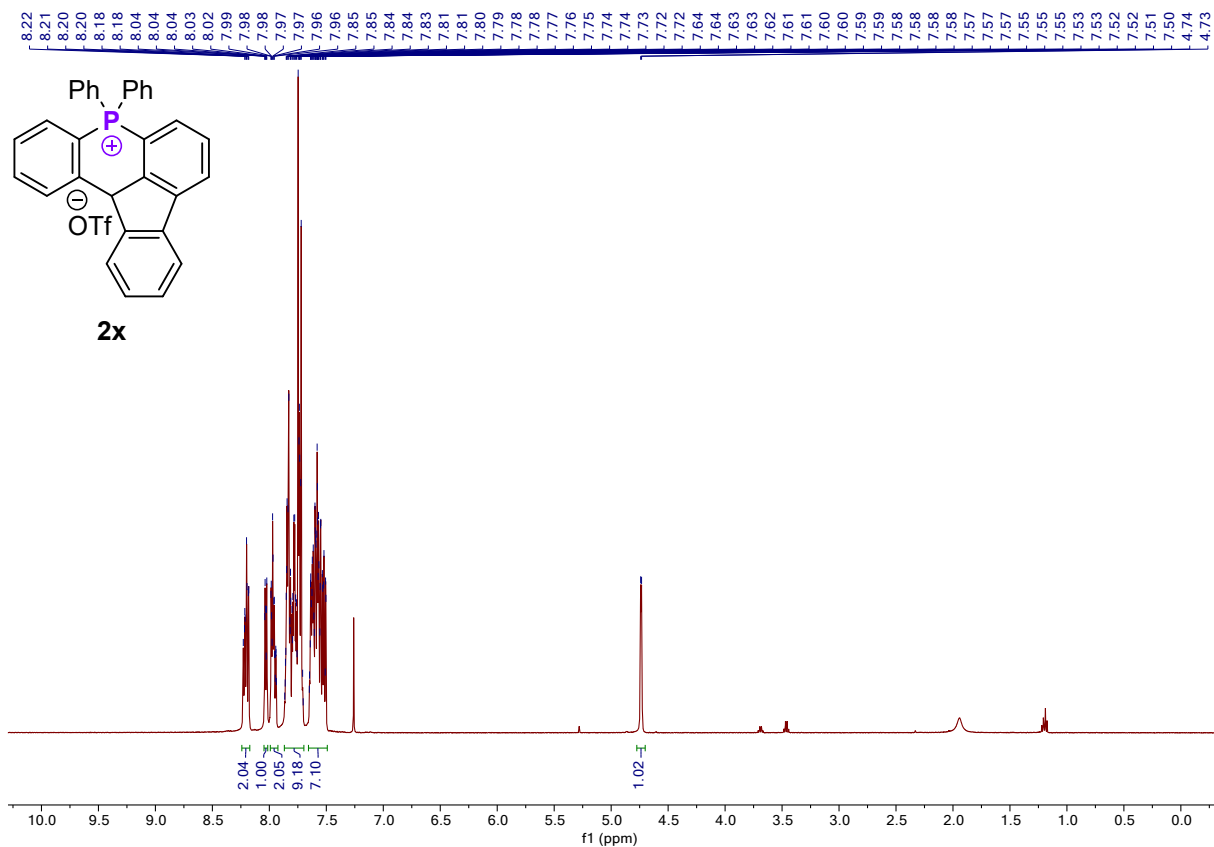


Figure S148: 500 MHz ^1H NMR spectrum of **2x** in CDCl_3

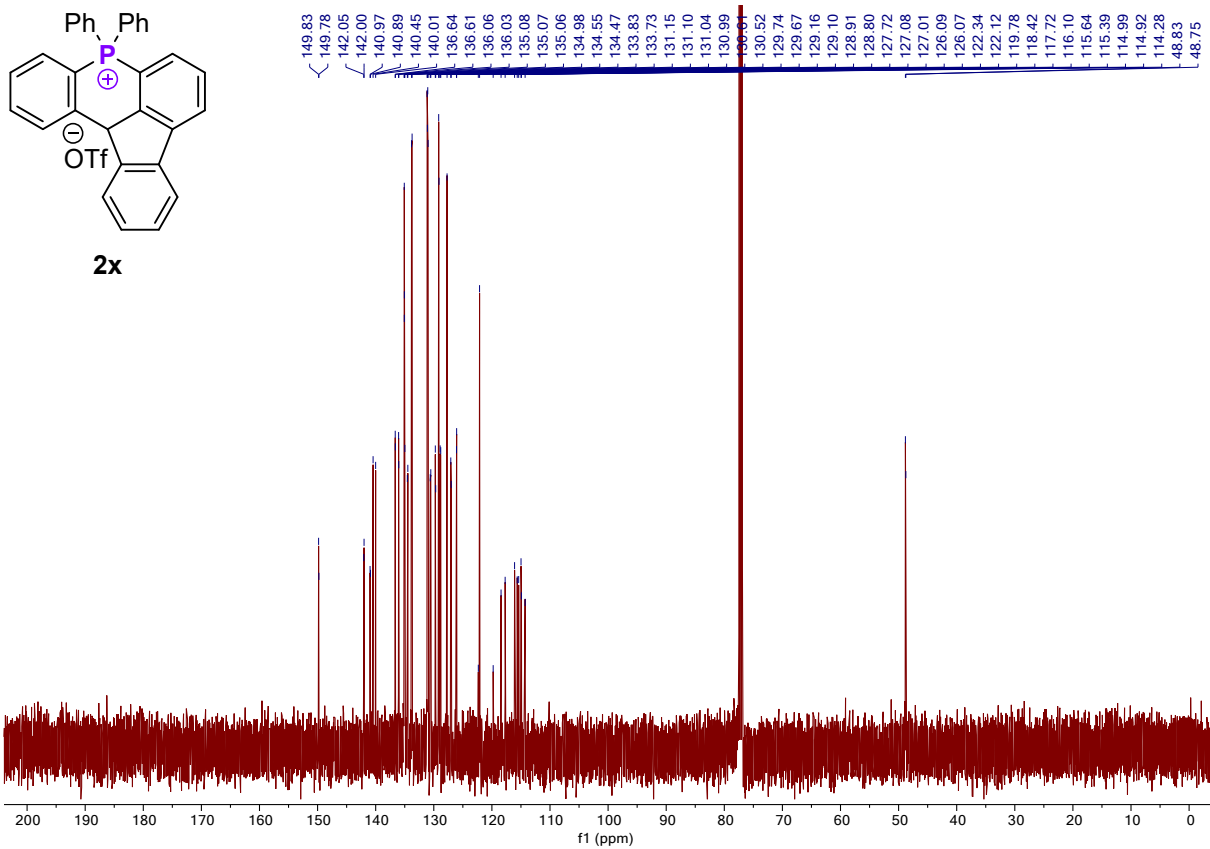


Figure S149: 126 MHz ^{13}C { ^1H } NMR spectrum of **2x** in CDCl_3

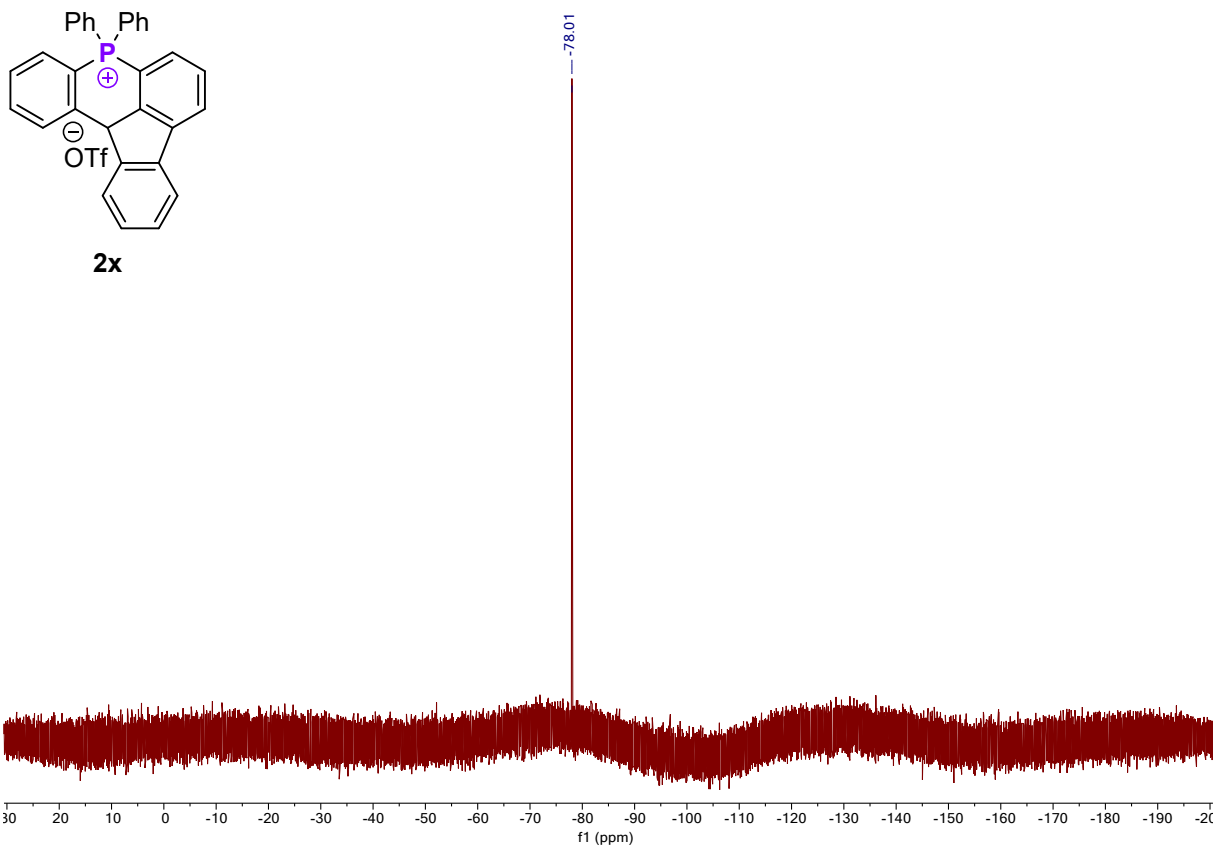


Figure S150: 470 MHz ^{19}F NMR spectrum of **2x** in CDCl_3

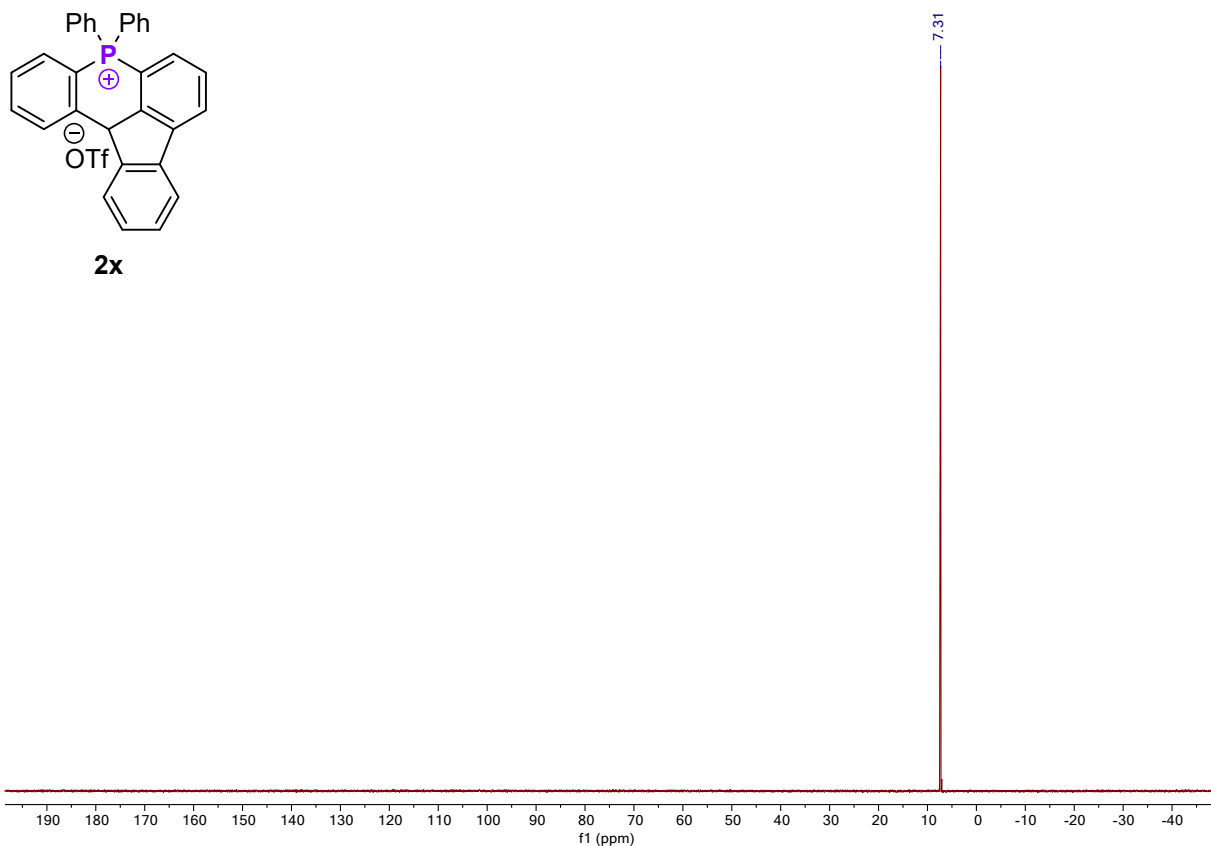


Figure S151: 202 MHz ^{31}P NMR spectrum of **2x** in CDCl_3

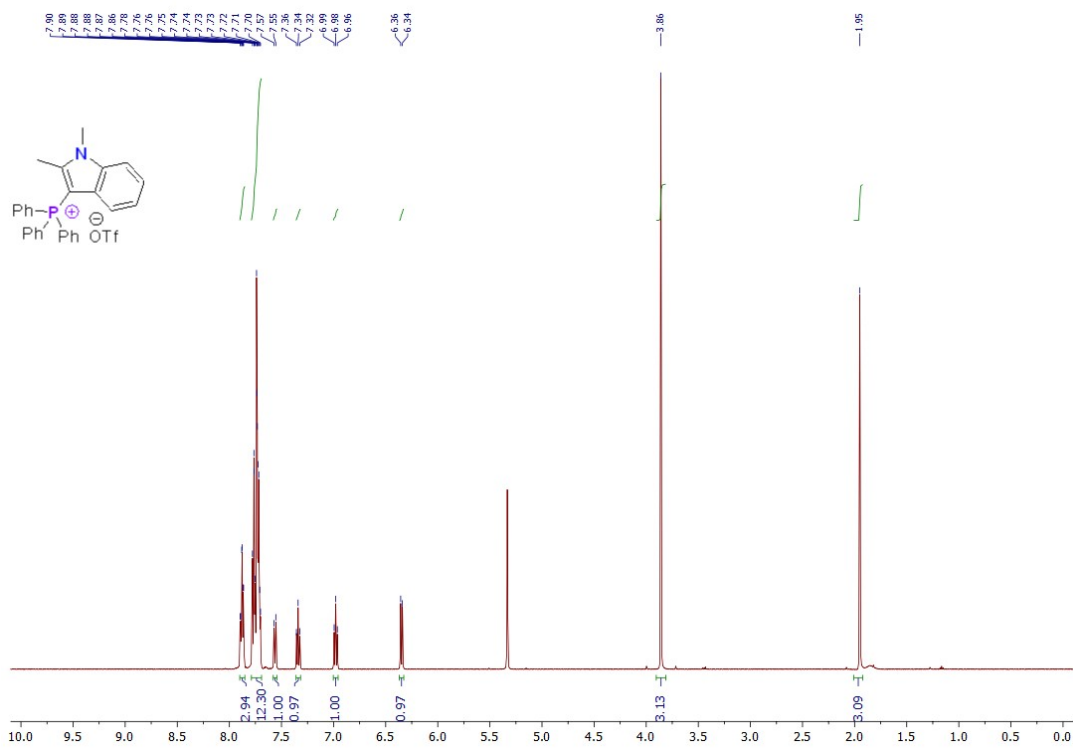


Figure S152: 500 MHz ^1H NMR spectrum of **4a** in CD_2Cl_2

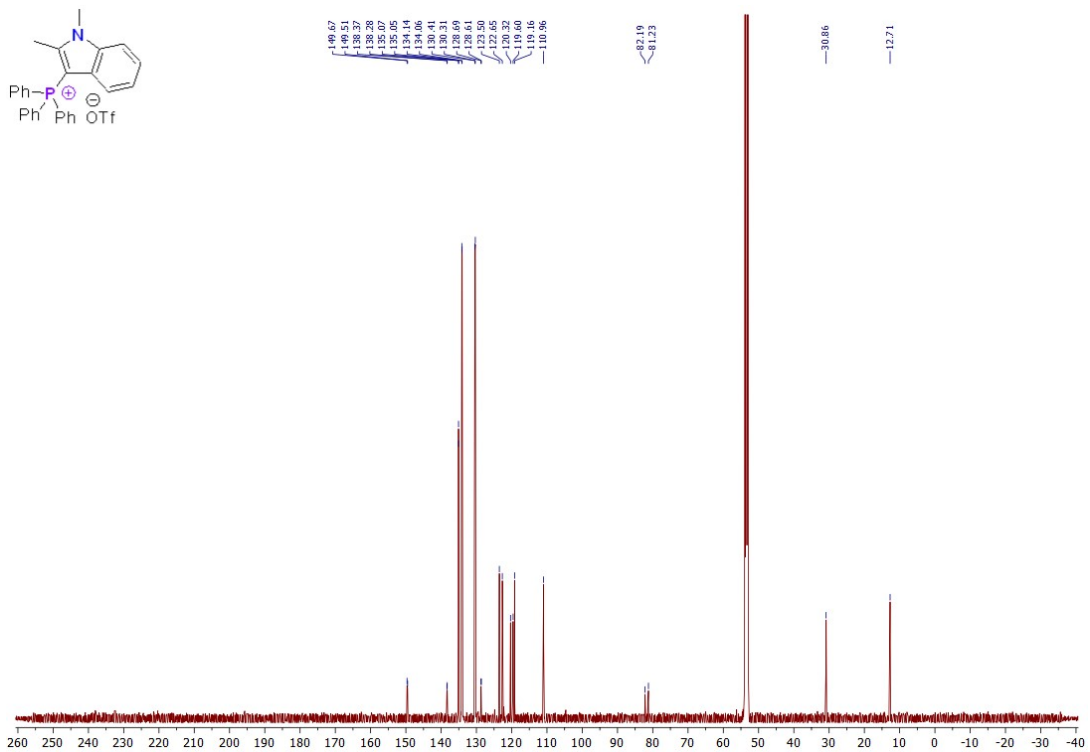


Figure S153: 126 MHz ^{13}C { ^1H } NMR spectrum of 4a in CD_2Cl_2

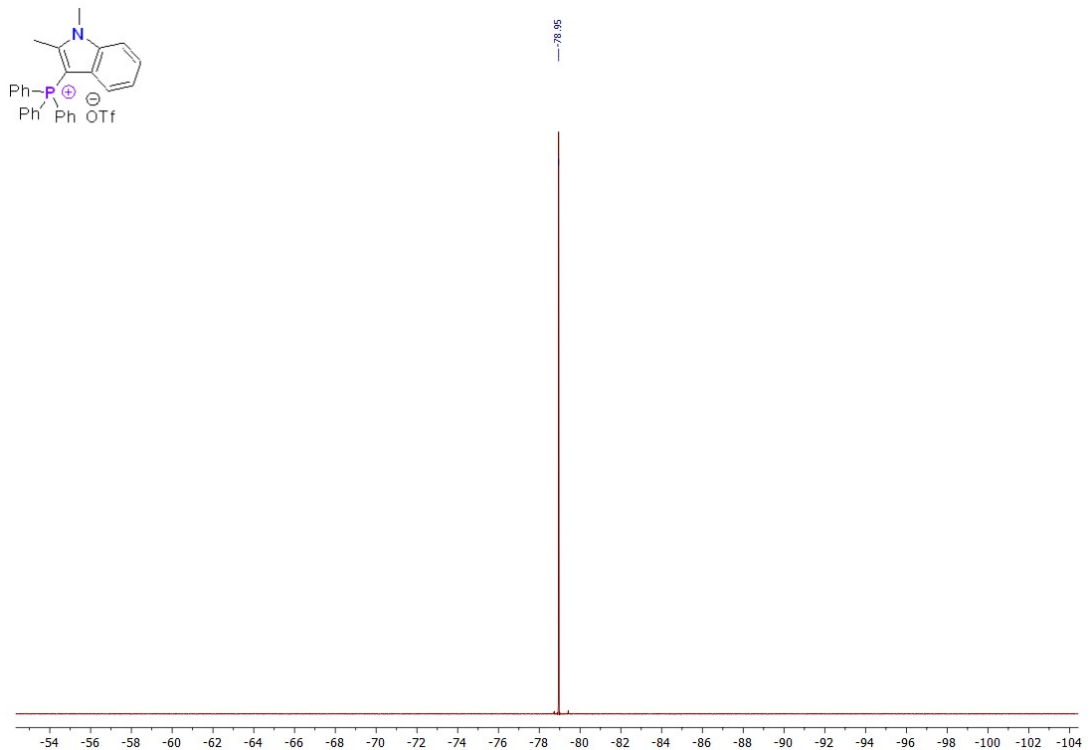


Figure S154: 470 MHz ^{19}F NMR spectrum of 4a in CD_2Cl_2

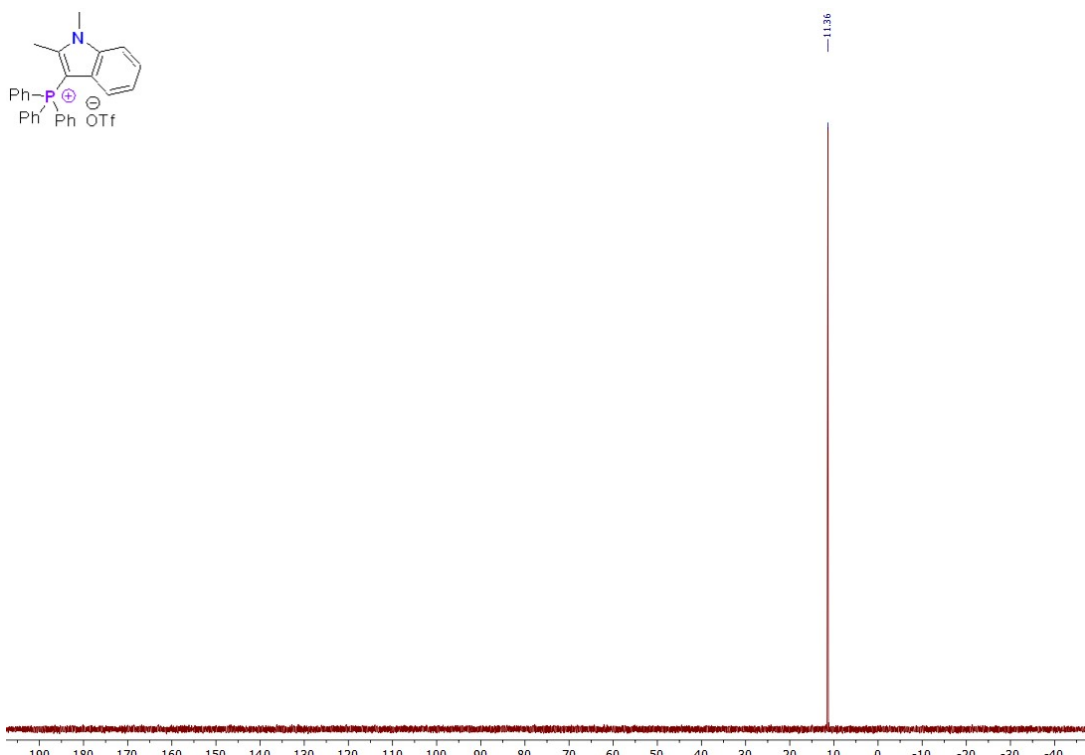


Figure S155: 243 MHz ³¹P NMR spectrum of **4a** in CD₂Cl₂

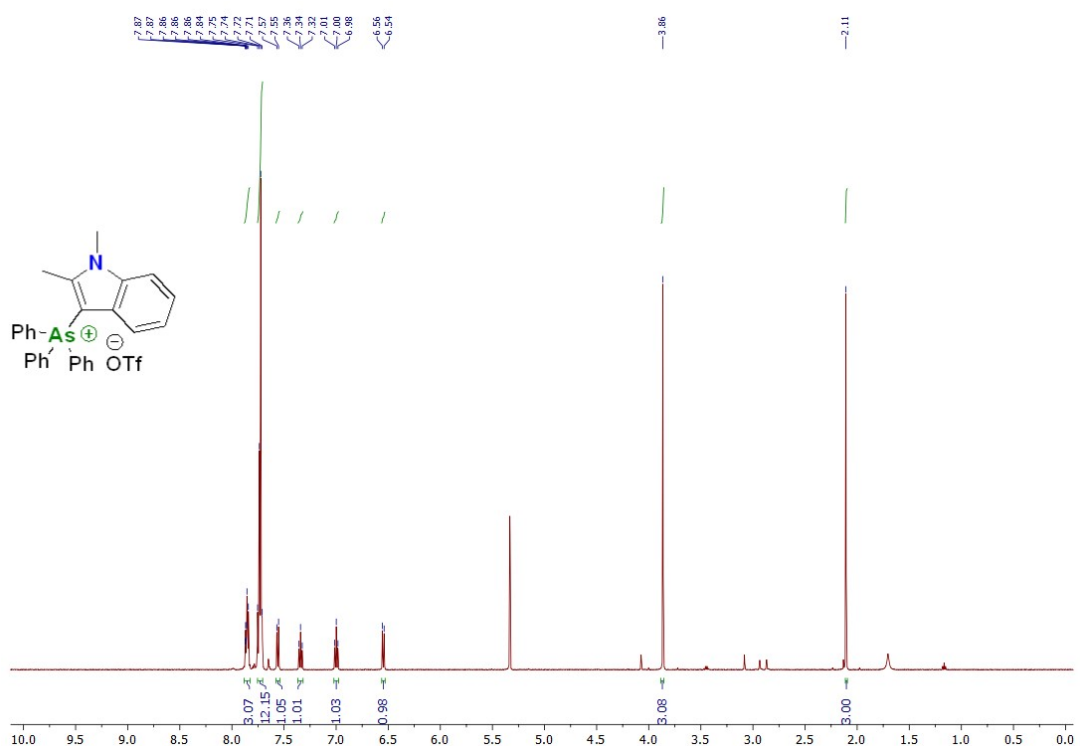


Figure S156: 500 MHz ¹H NMR spectrum of **4b** in CD₂Cl₂

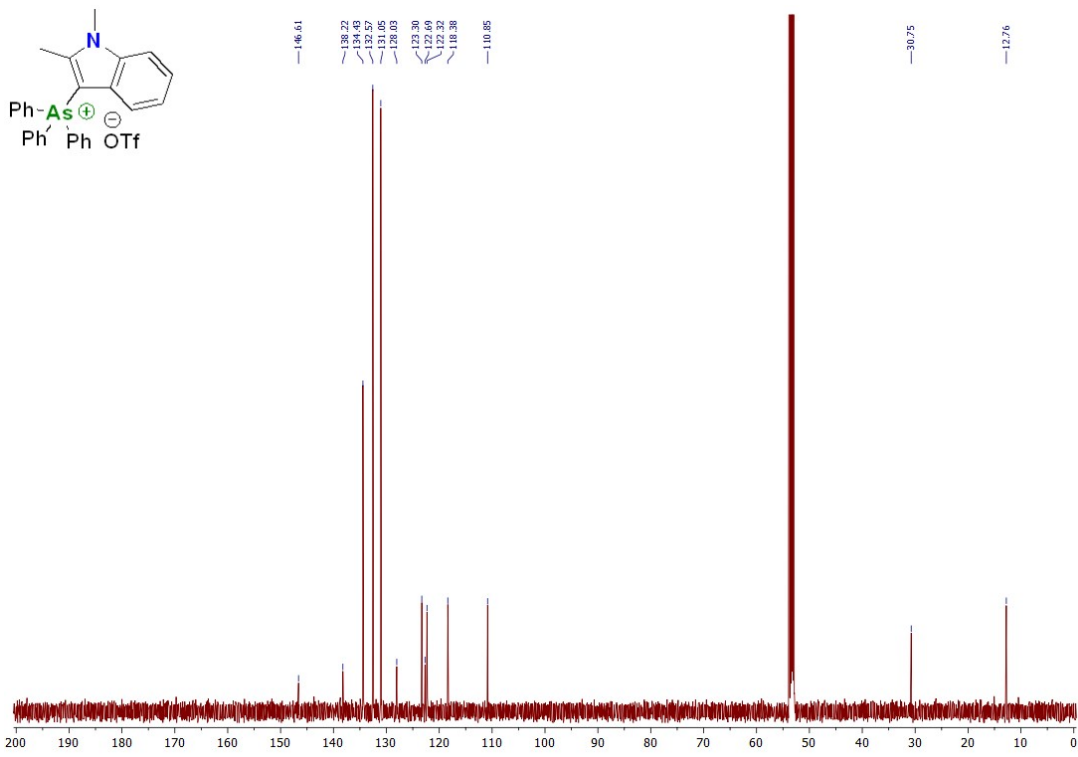


Figure S157: 126 MHz ^{13}C { ^1H } NMR spectrum of 4a in CD_2Cl_2

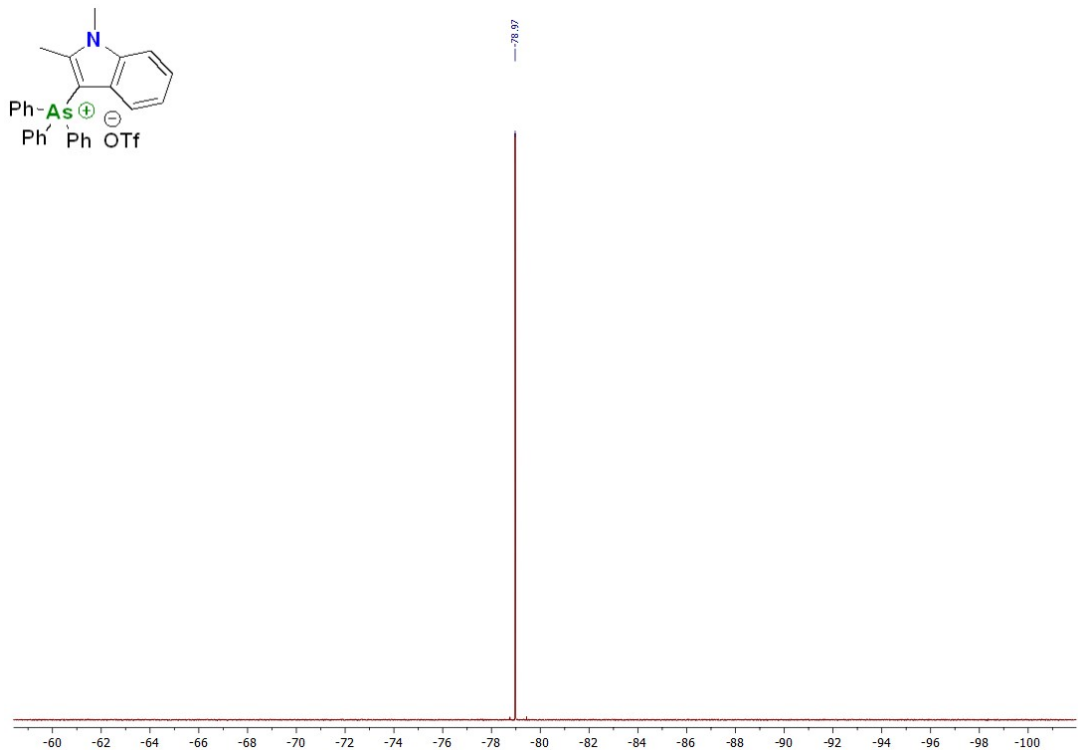


Figure S158: 470 MHz ^{19}F NMR spectrum of 4b in CD_2Cl_2

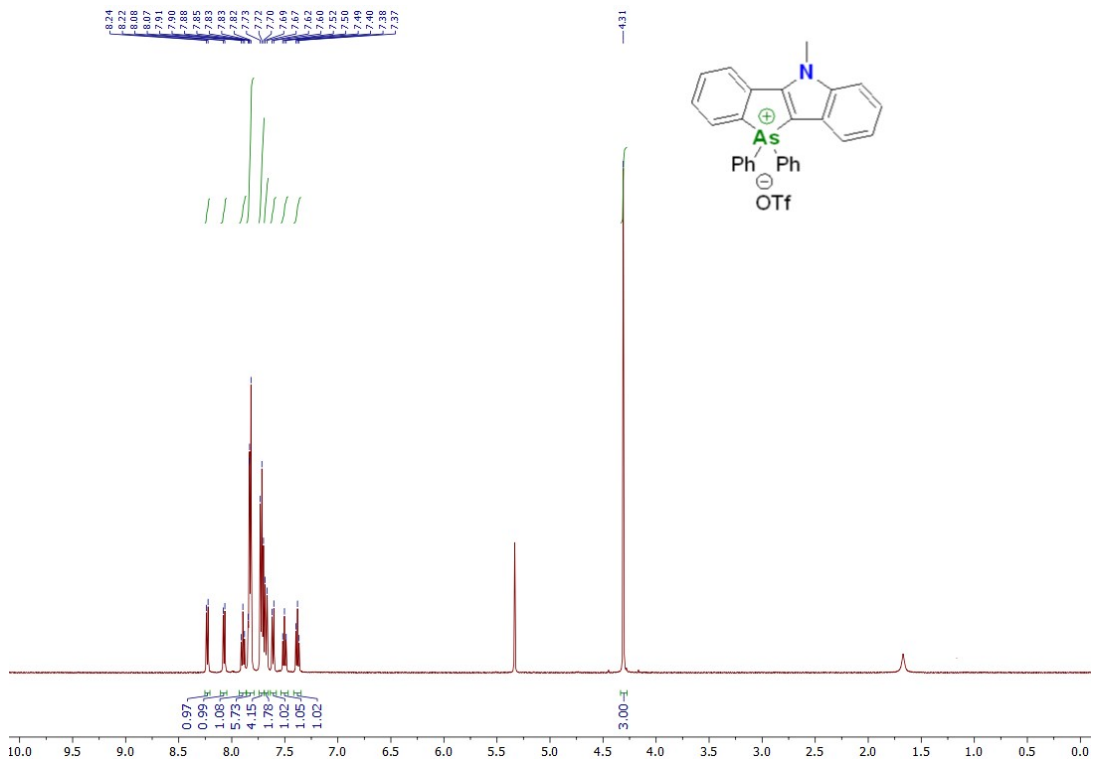


Figure S159: 500 MHz ¹H NMR spectrum of 6 in CD₂Cl₂

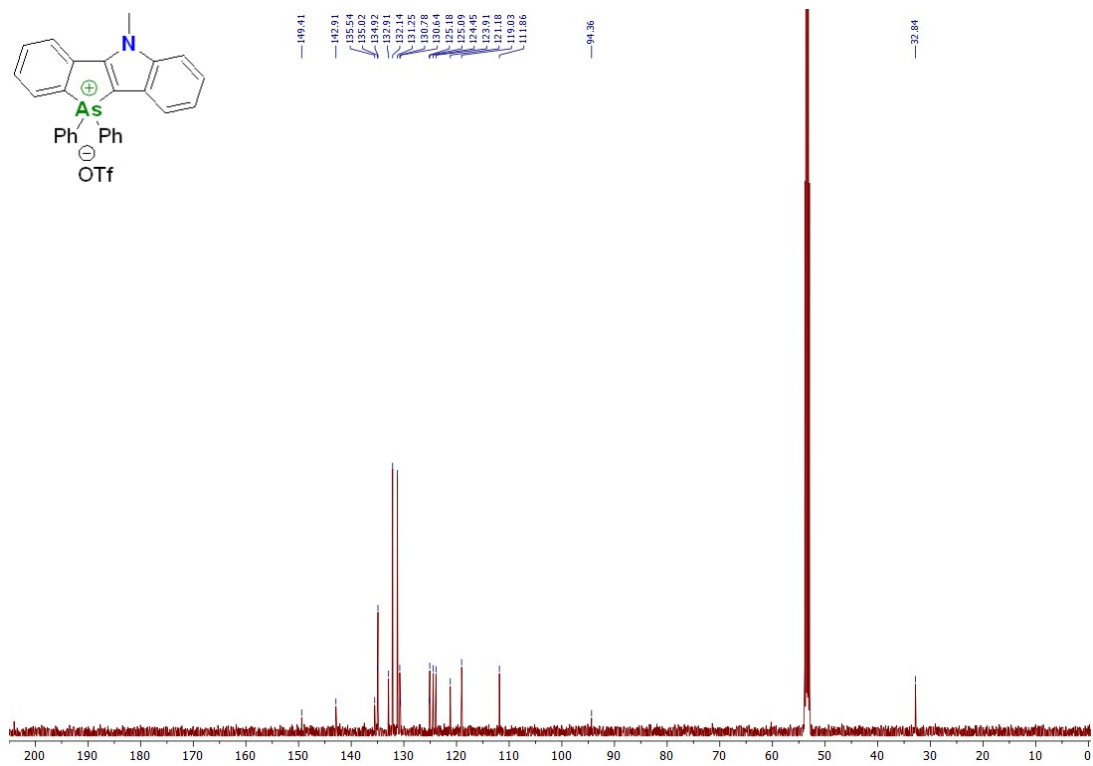


Figure S160: 126 MHz ¹³C {¹H} NMR spectrum of 6 in CD₂Cl₂

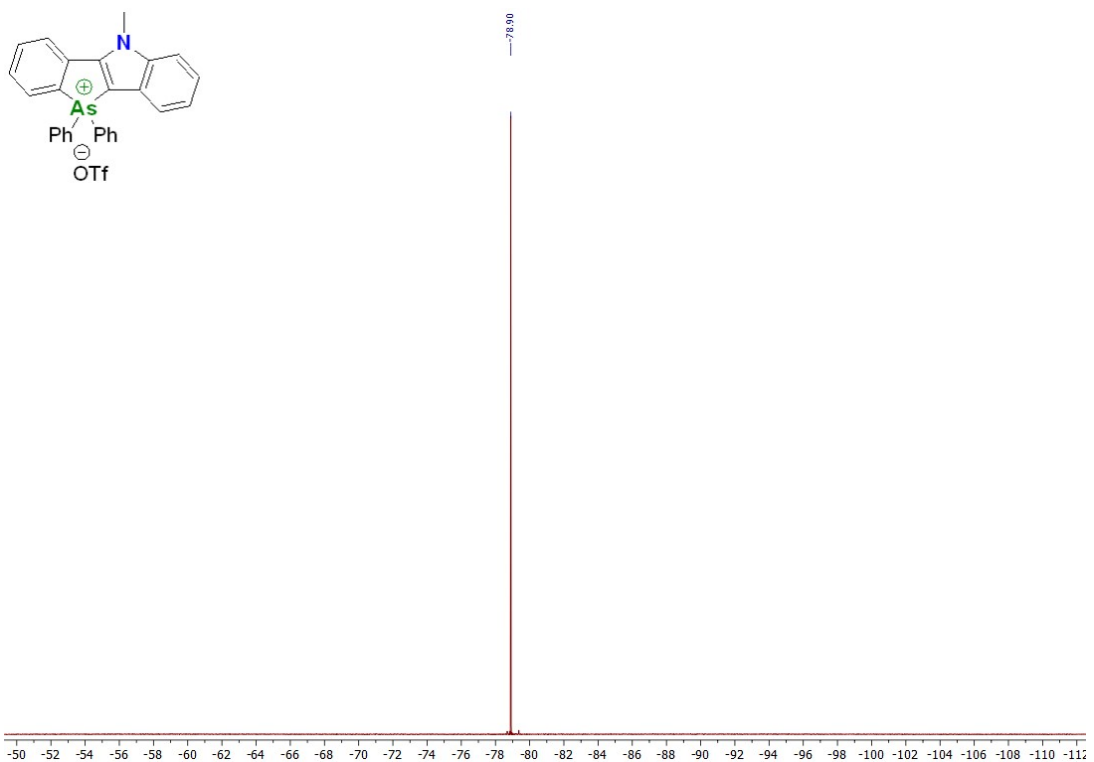


Figure S161: 470 MHz ^{19}F NMR spectrum of 6 in CD_2Cl_2

4. UV-Vis spectra

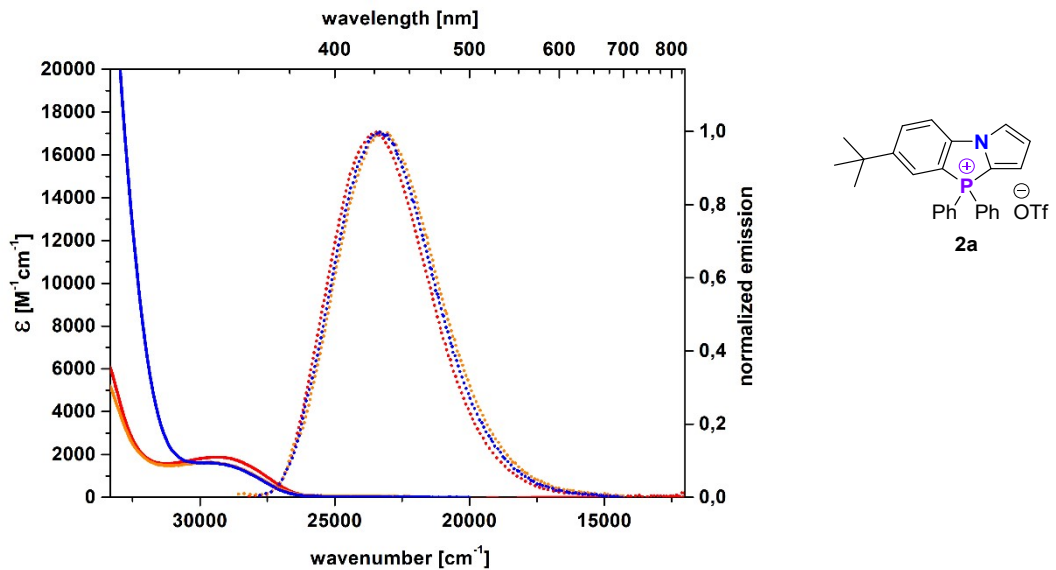


Figure S162: Absorption (solid) and emission (dot) spectra of **2a** in dichloromethane, tetrahydrofuran and acetonitrile

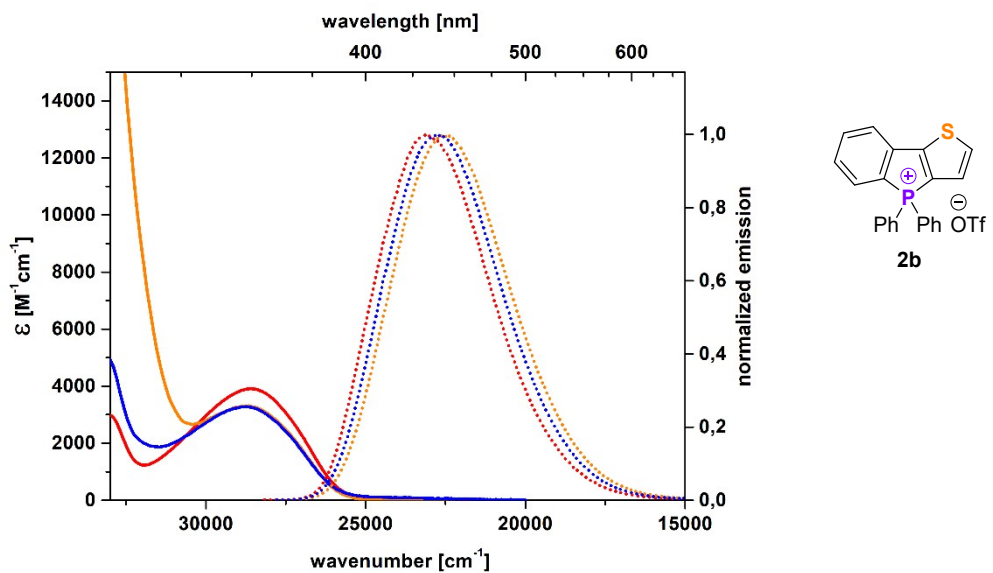


Figure S163: Absorption (solid) and emission (dot) spectra of **2b** in dichloromethane, tetrahydrofuran and acetonitrile

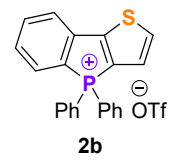
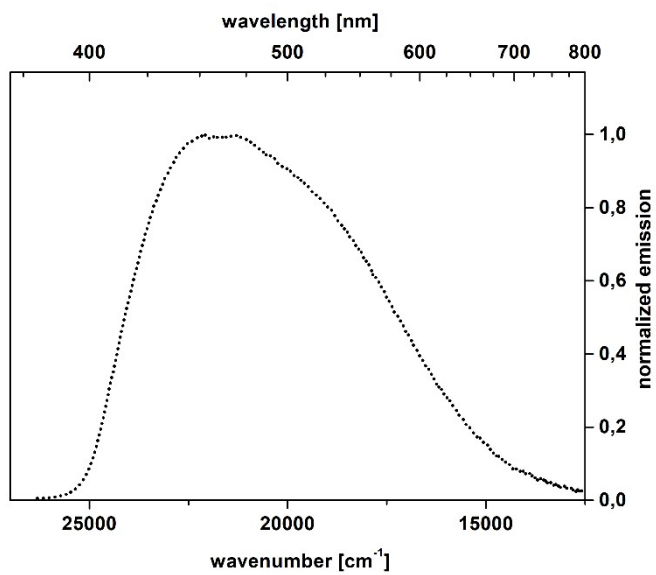


Figure S164: Solid state emission (dot) spectrum of **2b**.

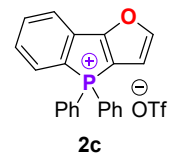
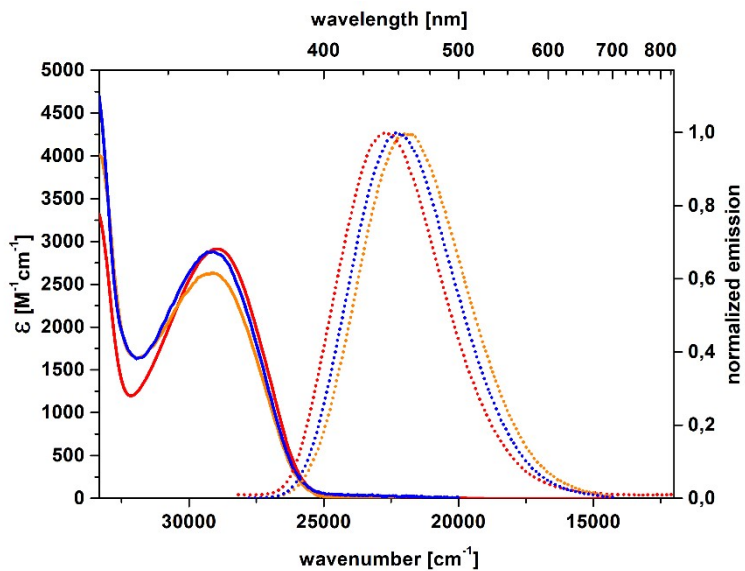


Figure S165: Absorption (solid) and emission (dot) spectra of **2c** in dichloromethane, tetrahydrofuran and acetonitrile

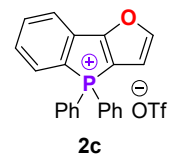
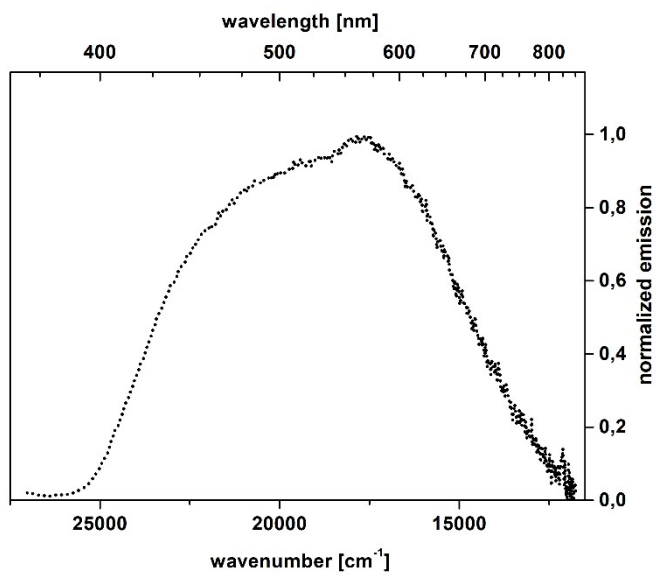


Figure S166: Solid state emission (dot) spectrum of **2c**

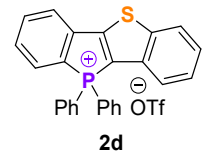
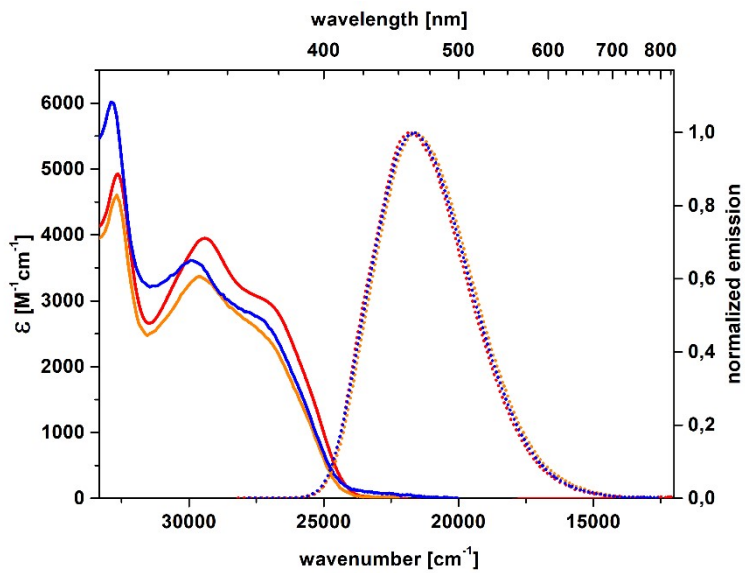


Figure S167: Absorption (solid) and emission (dot) spectra of **2d** in dichloromethane, tetrahydrofuran and acetonitrile

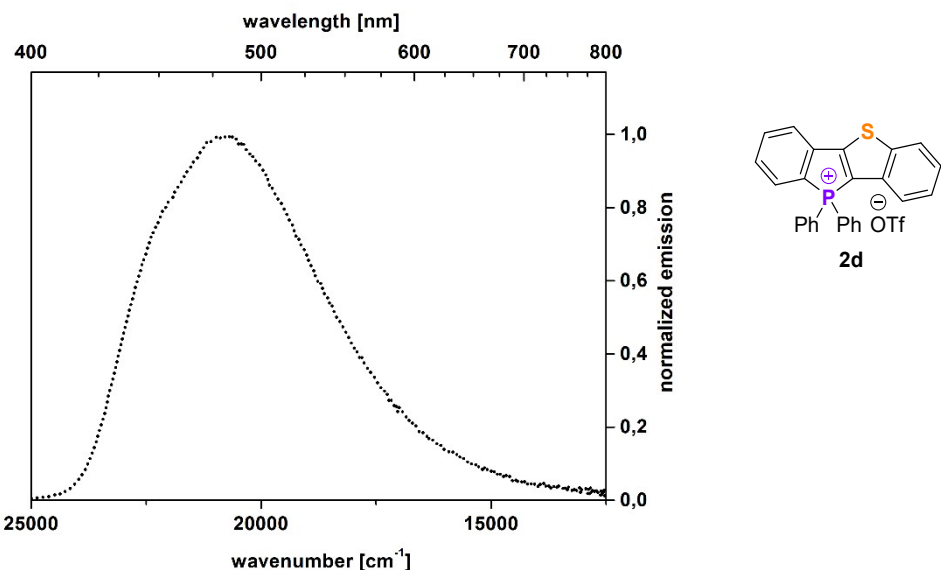


Figure S168: Solid state emission (dot) spectrum of **2d**.

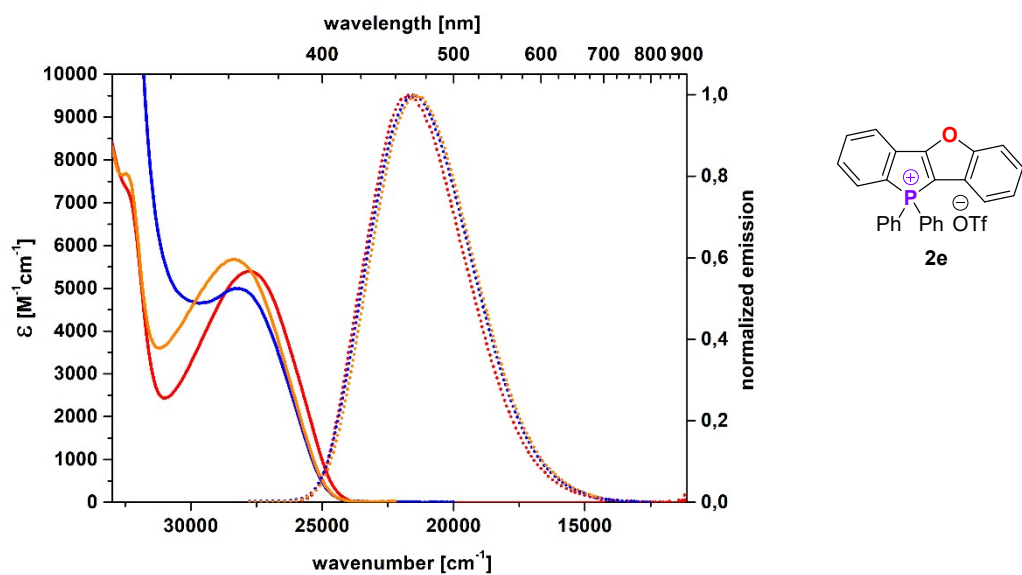


Figure S169: Absorption (solid) and emission (dot) spectra of **2e** in dichloromethane, tetrahydrofuran and acetonitrile

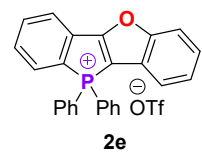
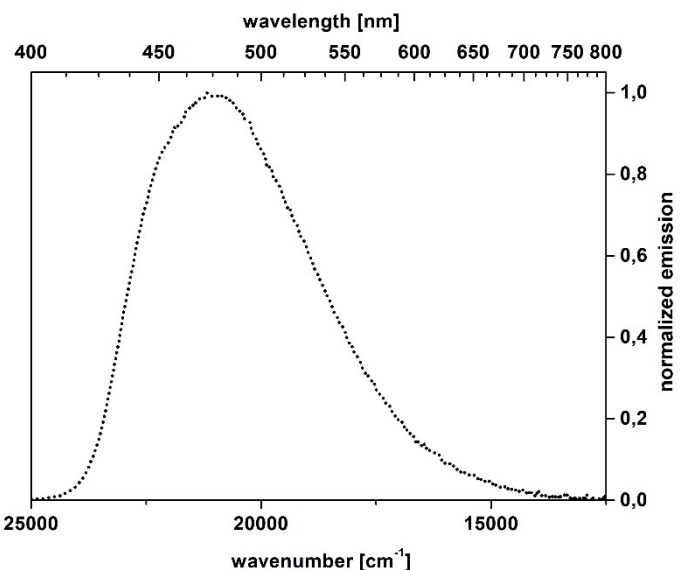


Figure S170: Solid state emission (dot) spectrum of **2e**

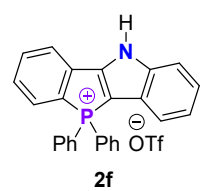
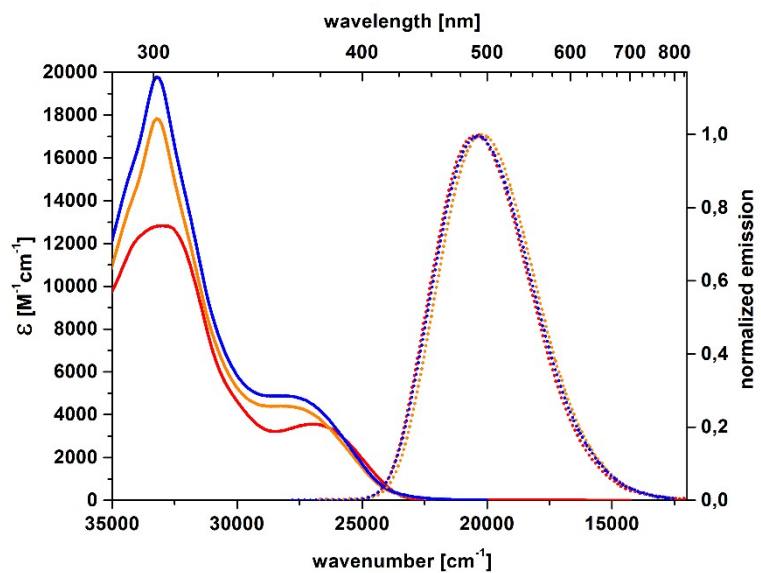


Figure S171: Absorption (solid) and emission (dot) spectra of **2f** in dichloromethane, tetrahydrofuran and acetonitrile

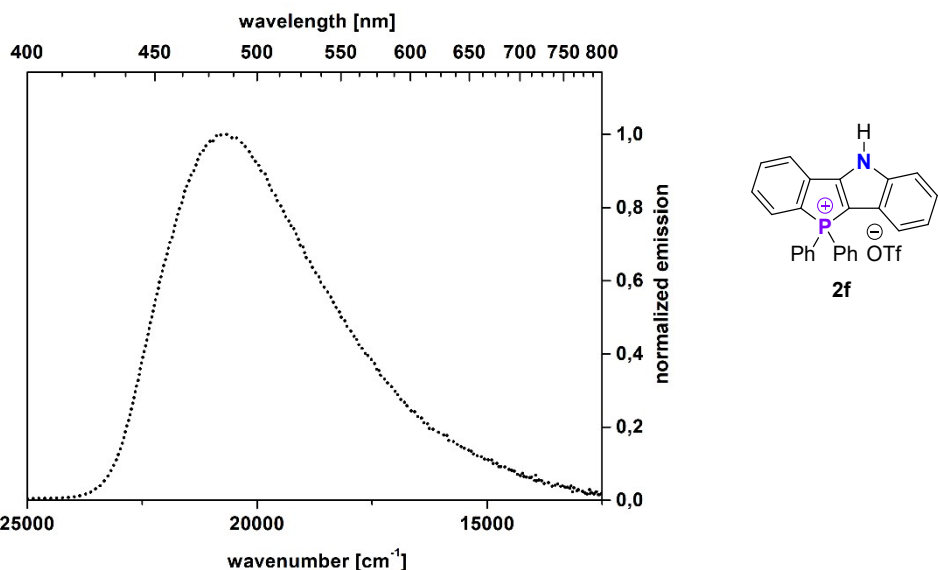


Figure S172: Solid state emission (dot) spectrum of **2f**.

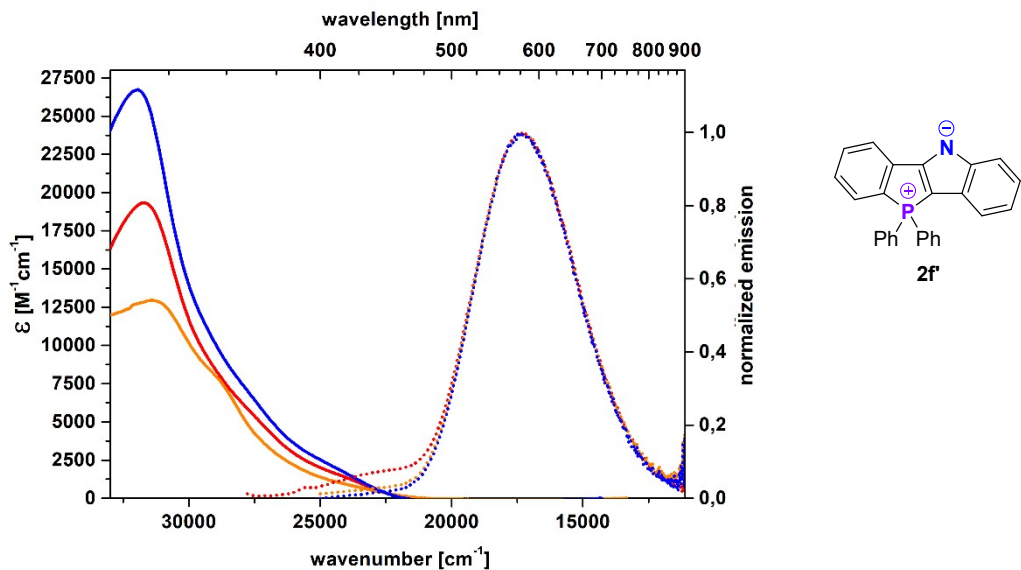


Figure S173: Absorption (solid) and emission (dot) spectra of **2f'** in **dichloromethane**, **tetrahydrofuran** and **acetonitrile** (measured after the addition of 100μl of DBU to **2f** solution)

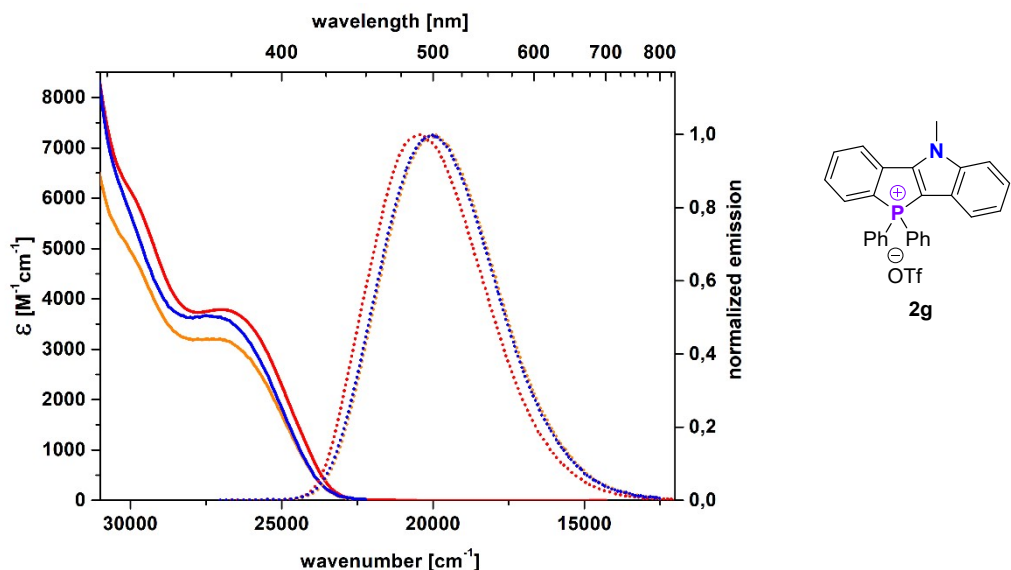


Figure S174: Absorption (solid) and emission (dot) spectra of 2g in dichloromethane, tetrahydrofuran and acetonitrile

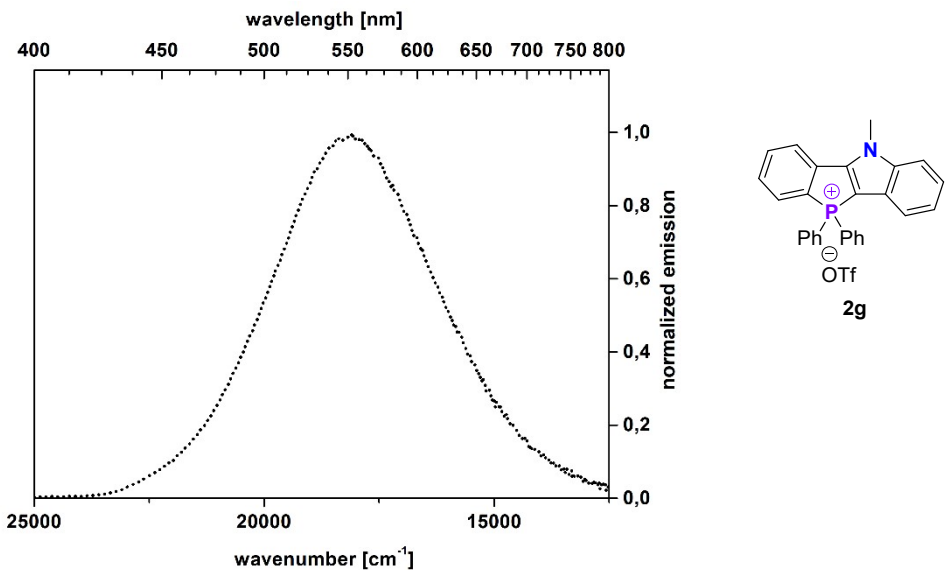


Figure S175: Solid state emission (dot) spectrum of 2g

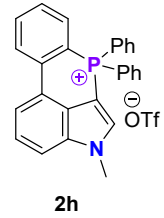
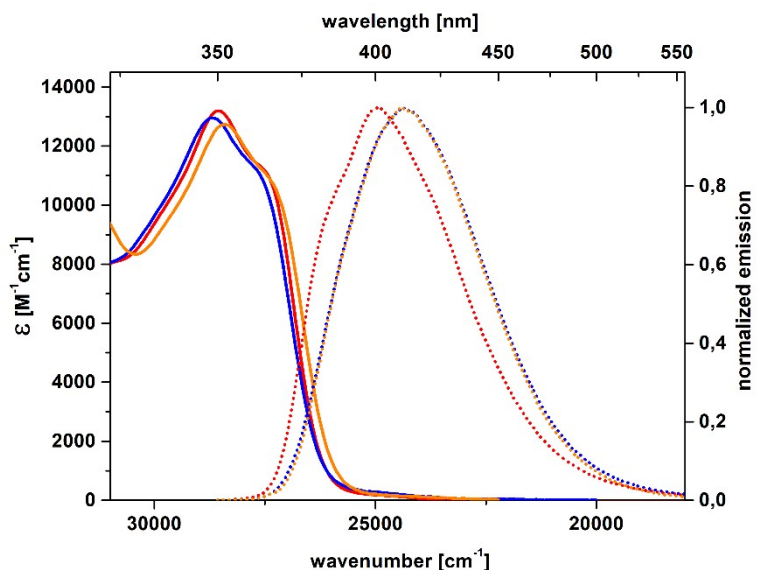


Figure S176: Absorption (solid) and emission (dot) spectra of **2h** in **dichloromethane**, **tetrahydrofuran** and **acetonitrile**

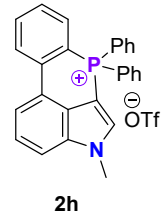
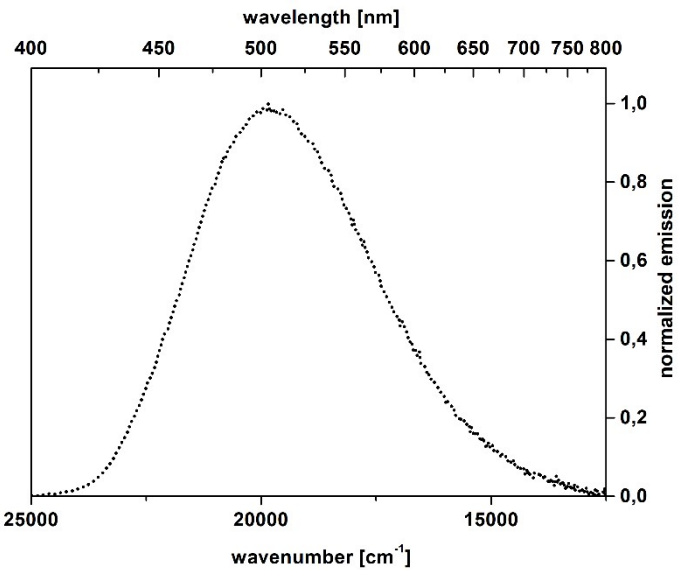


Figure S177: Solid state emission (dot) spectrum of **2h**

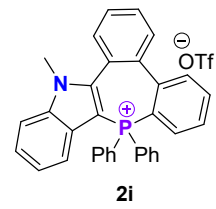
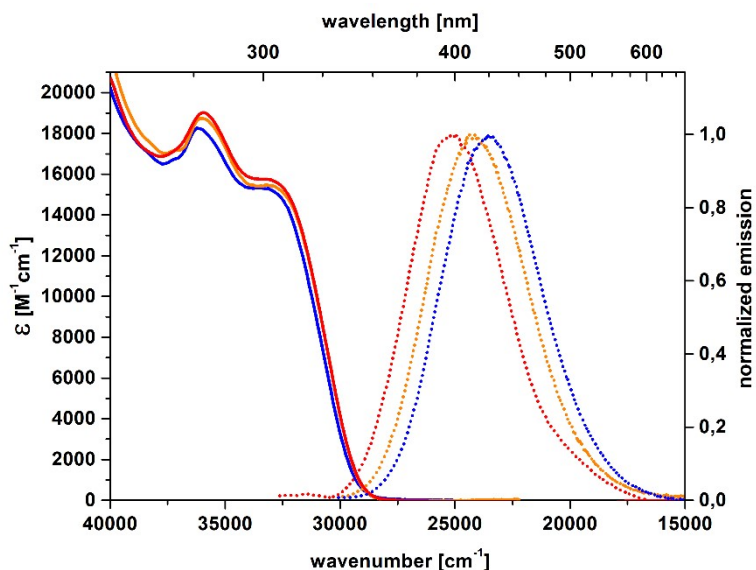


Figure S178: Absorption (solid) and emission (dot) spectra of **2i** in dichloromethane, tetrahydrofuran and acetonitrile

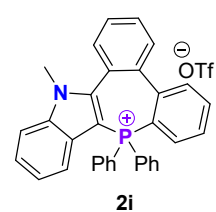
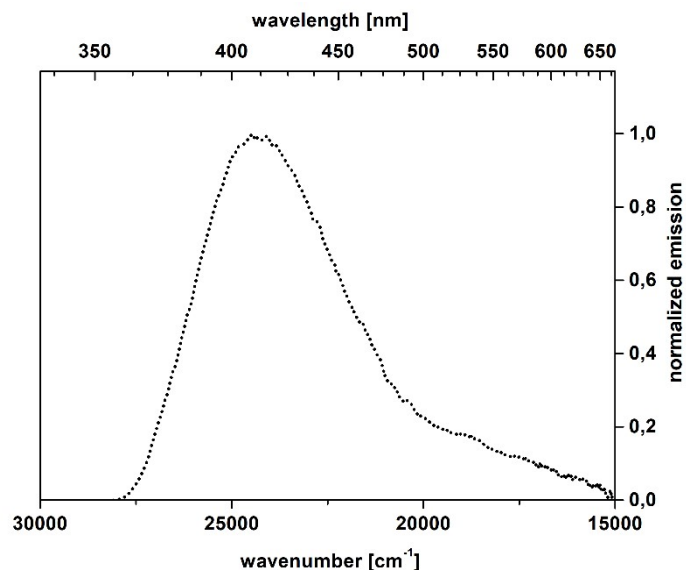


Figure S179: Solid state emission (dot) spectrum of **2i**

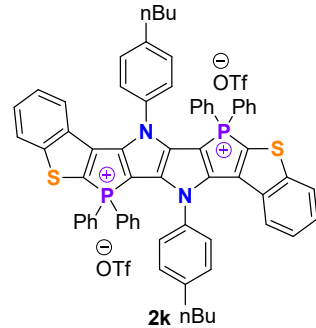
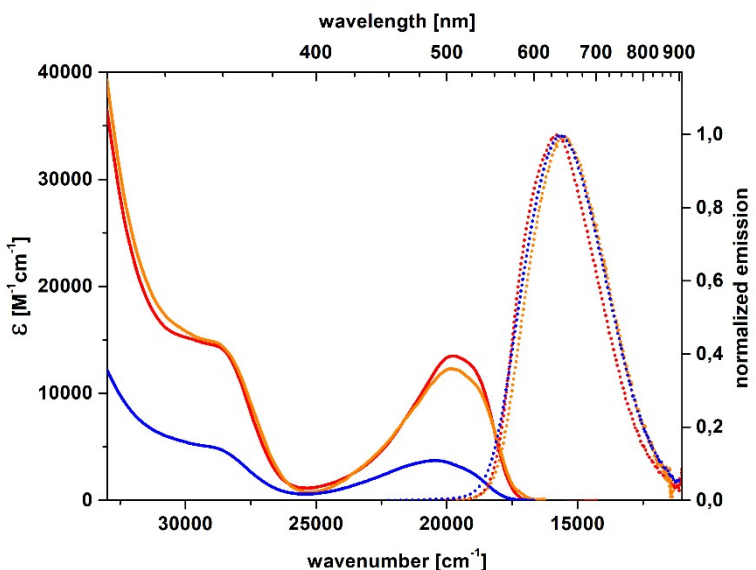


Figure S180: Absorption (solid) and emission (dot) spectra of 2j in dichloromethane, tetrahydrofuran and acetonitrile

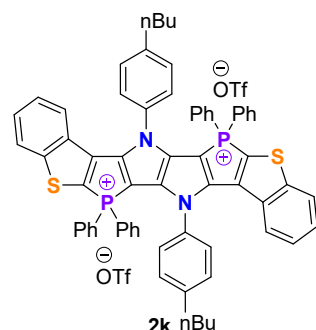
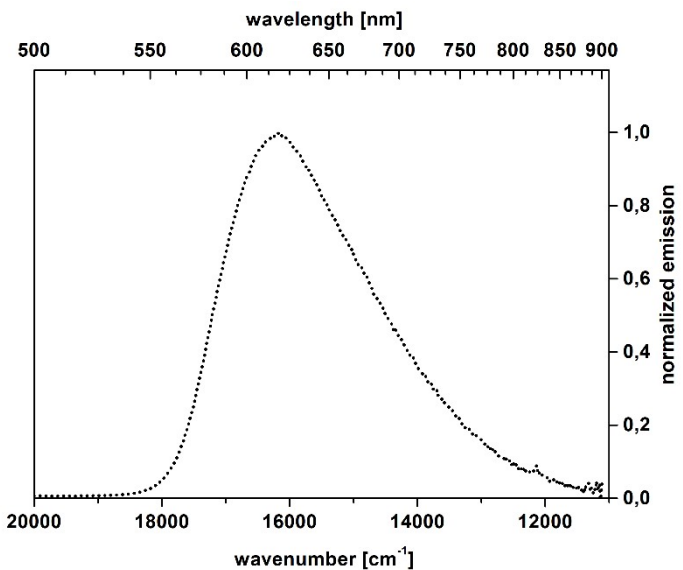


Figure S181: Solid state emission (dot) spectrum of 2j

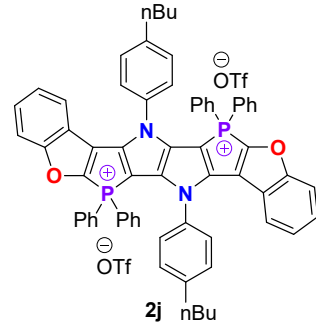
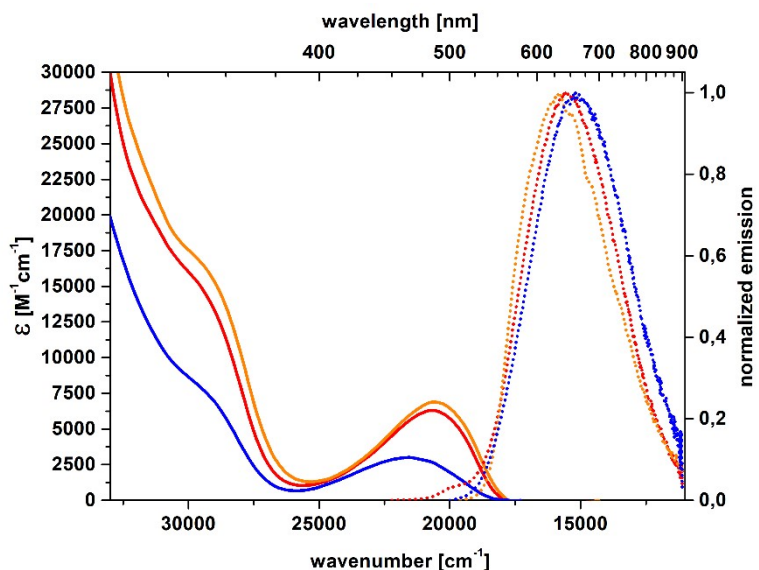


Figure S182: Absorption (solid) and emission (dot) spectra of 2k in dichloromethane, tetrahydrofuran and acetonitrile

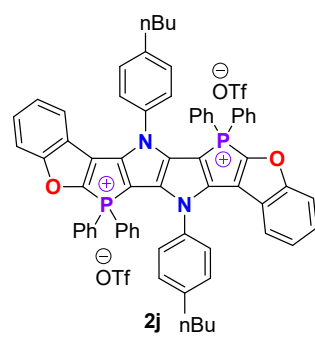
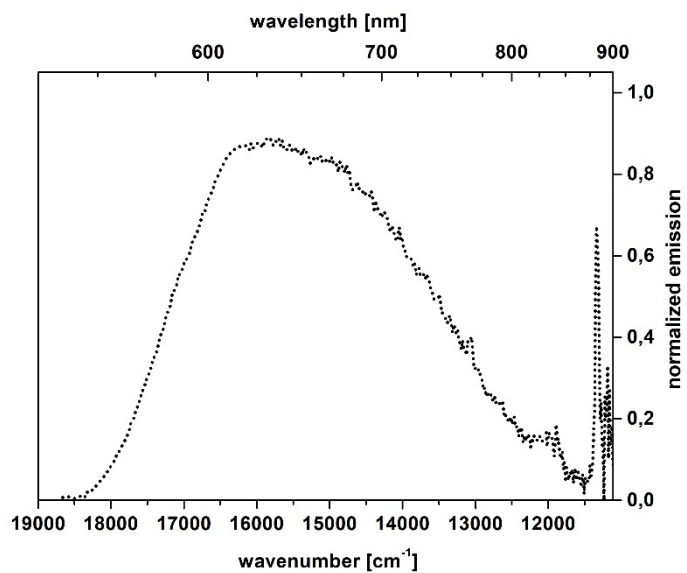


Figure S183: Solid state emission (dot) spectrum of 2k

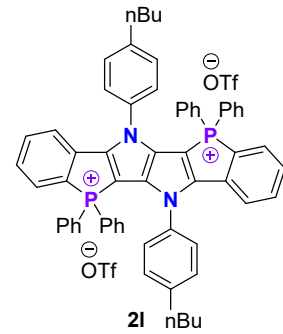
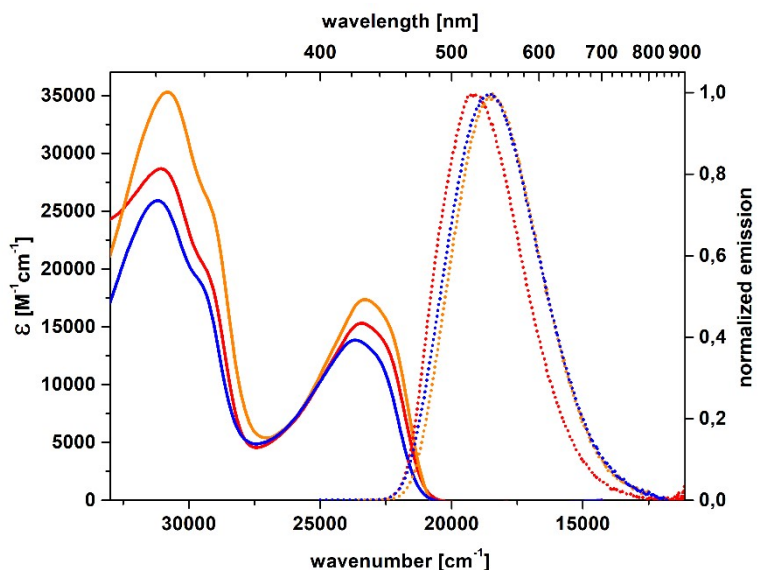


Figure S184: Absorption (solid) and emission (dot) spectra of **2I** in dichloromethane, tetrahydrofuran and acetonitrile

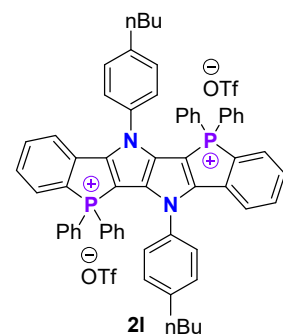
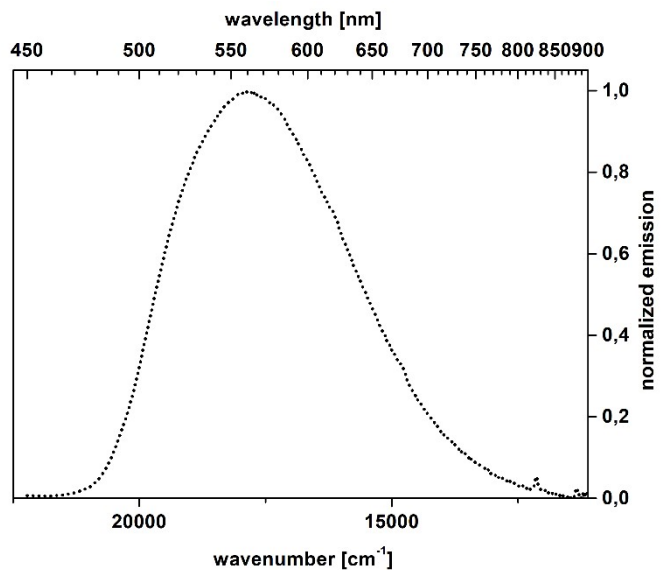


Figure S185: Solid state emission (dot) spectrum of **2I**

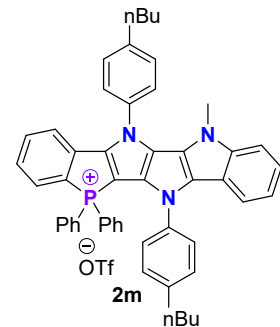
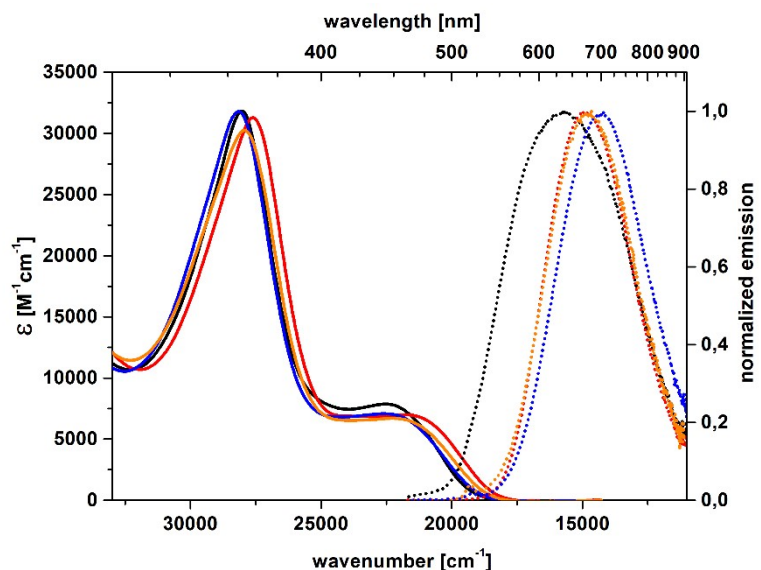


Figure S186: Absorption (solid) and emission (dot) spectra of 2m in toluene in dichloromethane, tetrahydrofuran and acetonitrile

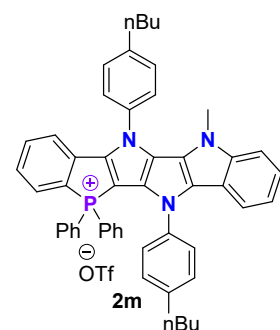
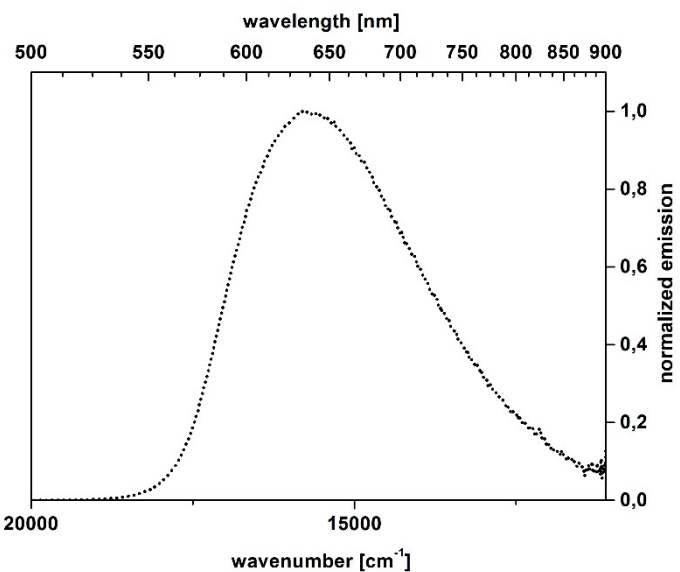


Figure S187: Solid state emission (dot) spectrum of 2m

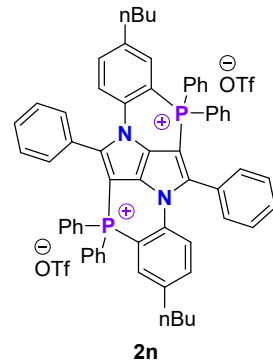
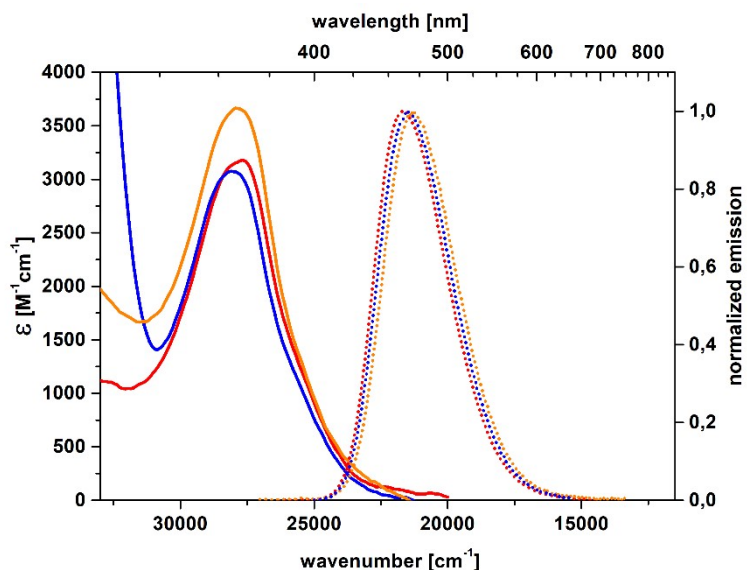


Figure S188: Absorption (solid) and emission (dot) spectra of **2n** in **dichloromethane**, **tetrahydrofuran** and **acetonitrile**

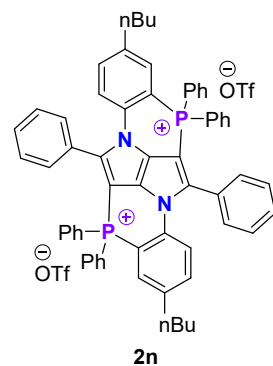
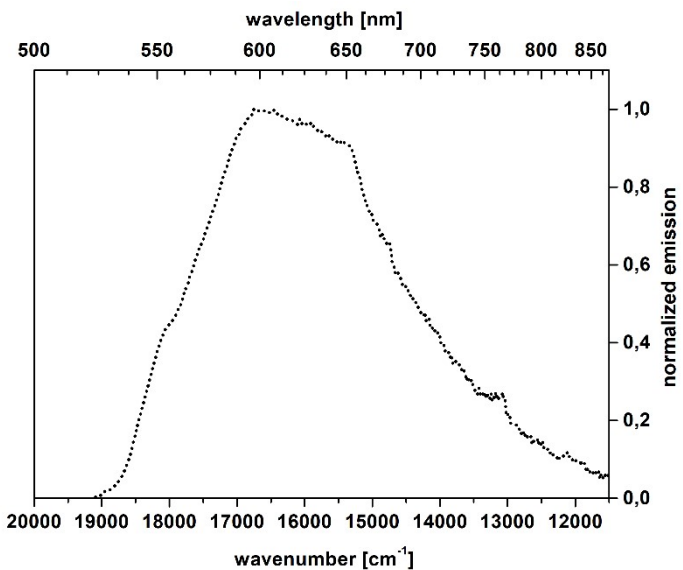


Figure S189: Solid state emission (dot) spectrum of **2n**

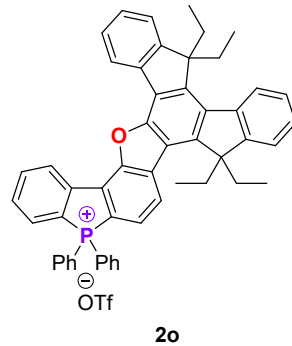
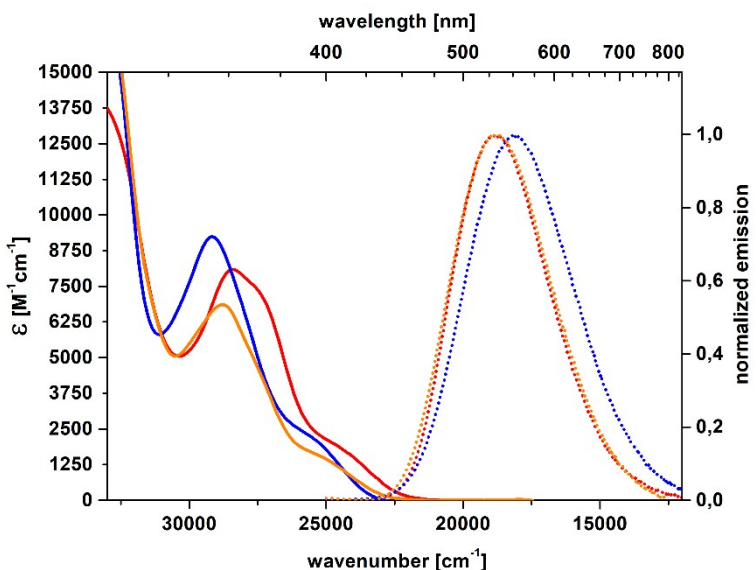


Figure S190: Absorption (solid) and emission (dot) spectra of **2o** in **dichloromethane**, **tetrahydrofuran** and **acetonitrile**

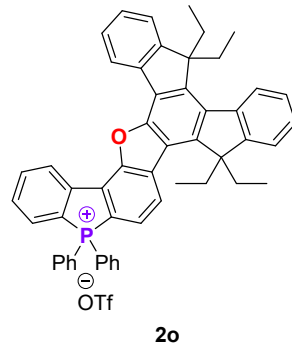
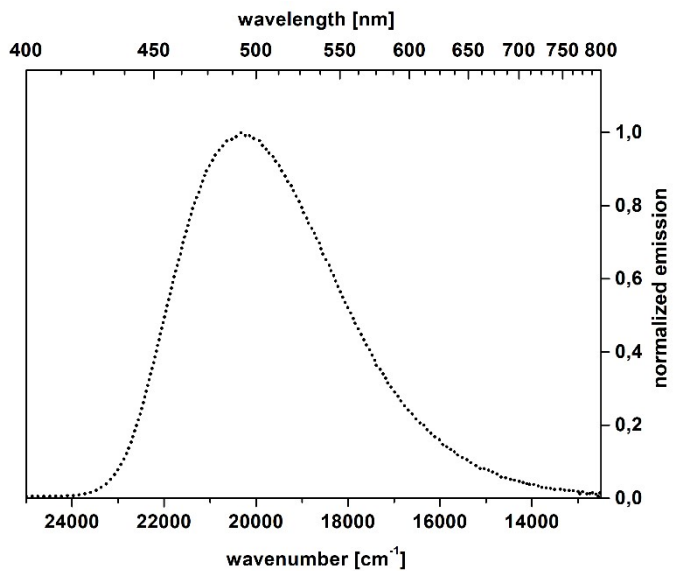


Figure S191: Solid state emission (dot) spectrum of **2o**

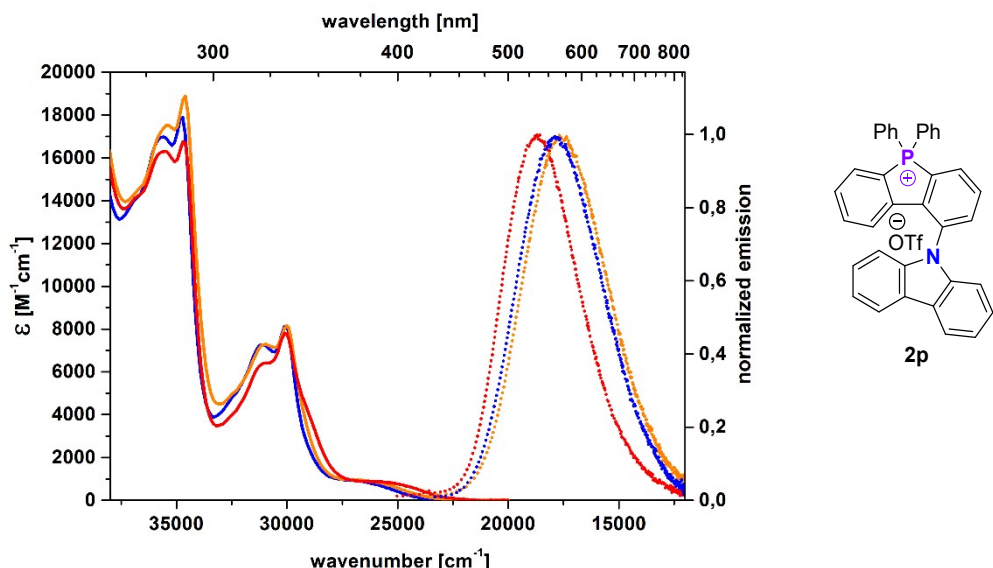


Figure S192: Absorption (solid) and emission (dot) spectra of 2p in dichloromethane, tetrahydrofuran and acetonitrile

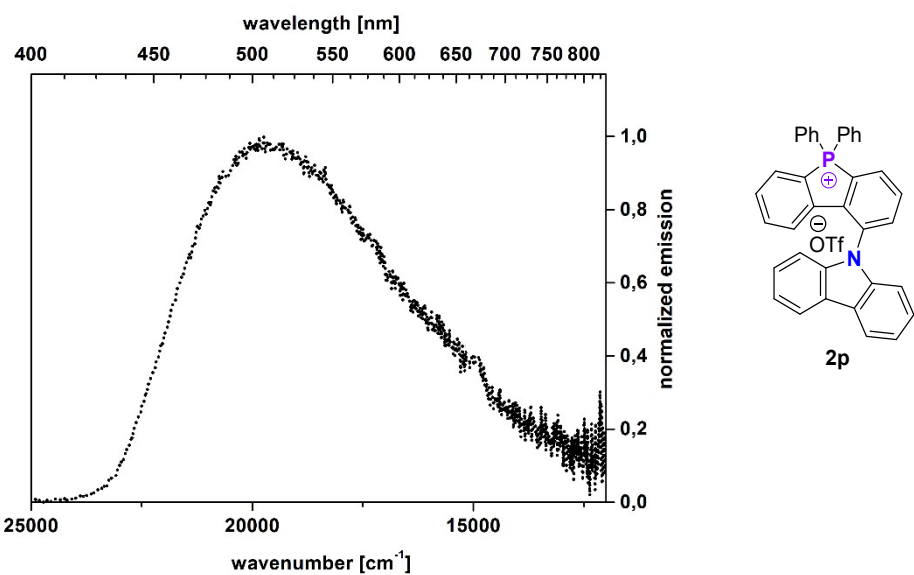


Figure S193: Solid state emission (dot) spectrum of 2p

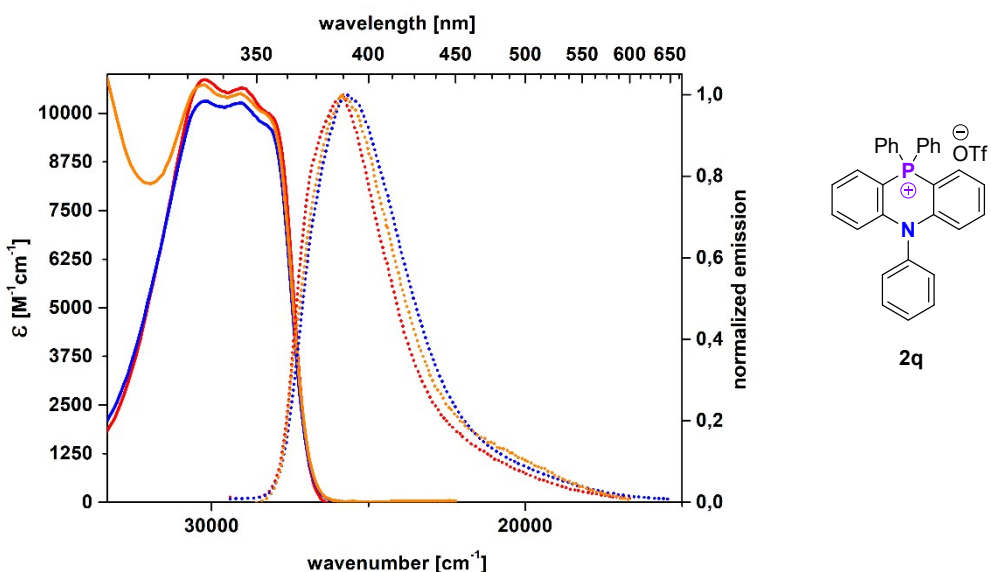


Figure S194: Absorption (solid) and emission (dot) spectra of **2q** in dichloromethane, tetrahydrofuran and acetonitrile

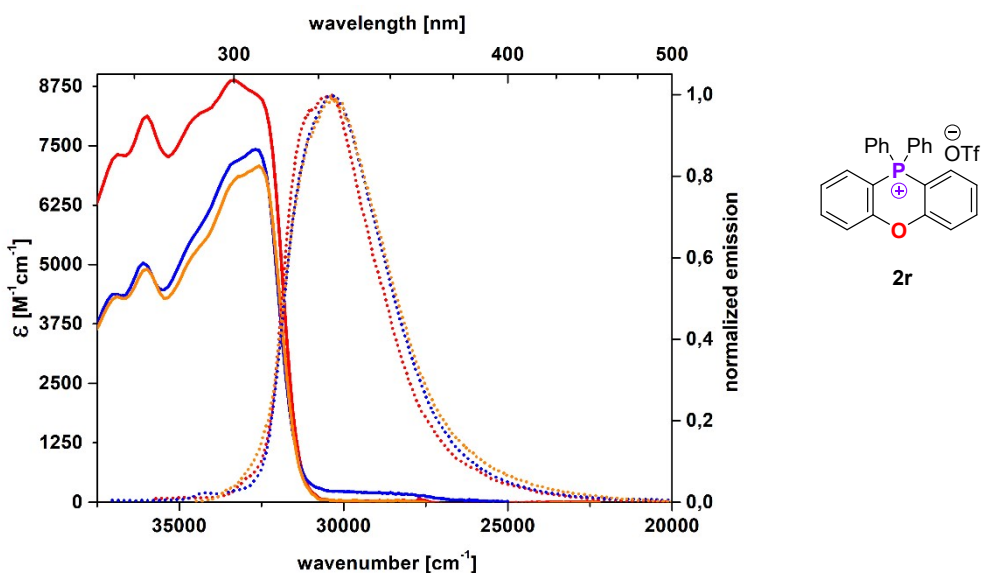


Figure 195: Absorption (solid) and emission (dot) spectra of **2r** in dichloromethane, tetrahydrofuran and acetonitrile

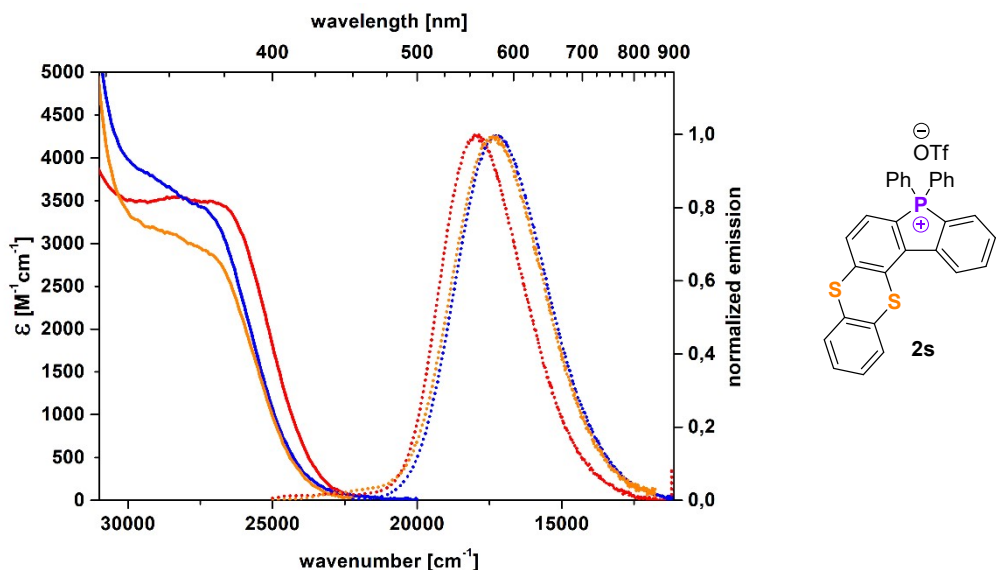


Figure S196: Absorption (solid) and emission (dot) spectra of 2s in dichloromethane, tetrahydrofuran and acetonitrile

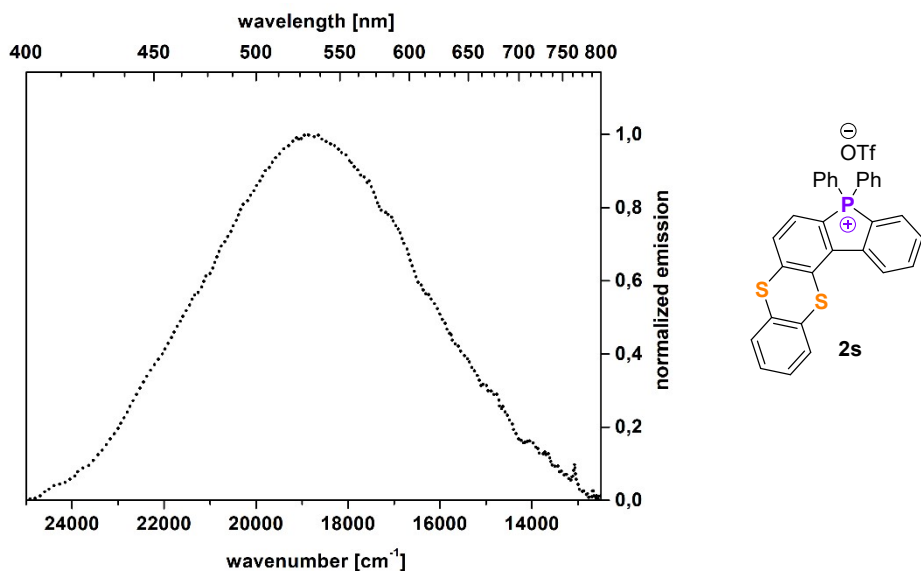


Figure S197: Solid state emission (dot) spectrum of 2s

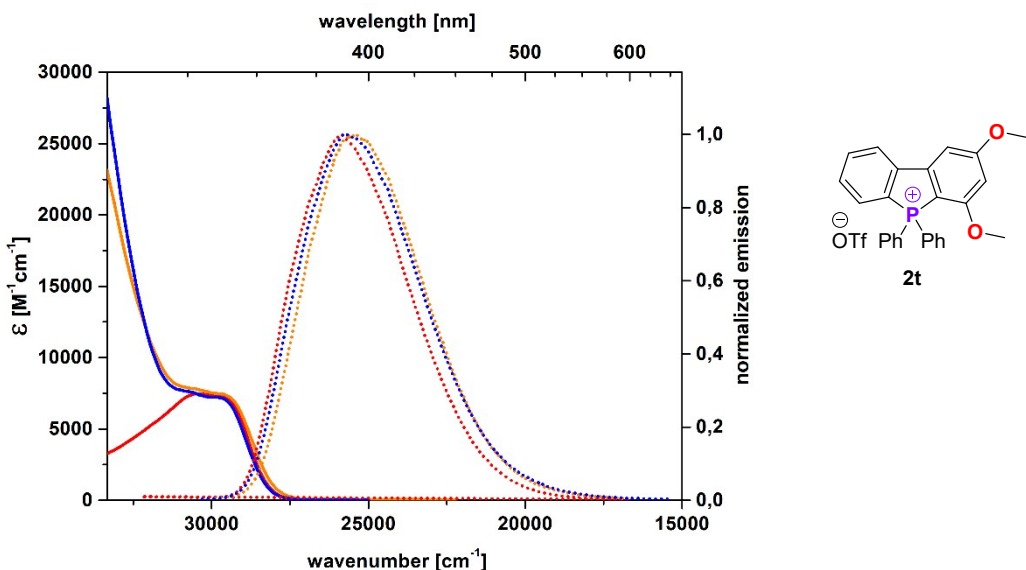


Figure S198: Absorption (solid) and emission (dot) spectra of 2t in dichloromethane, tetrahydrofuran and acetonitrile

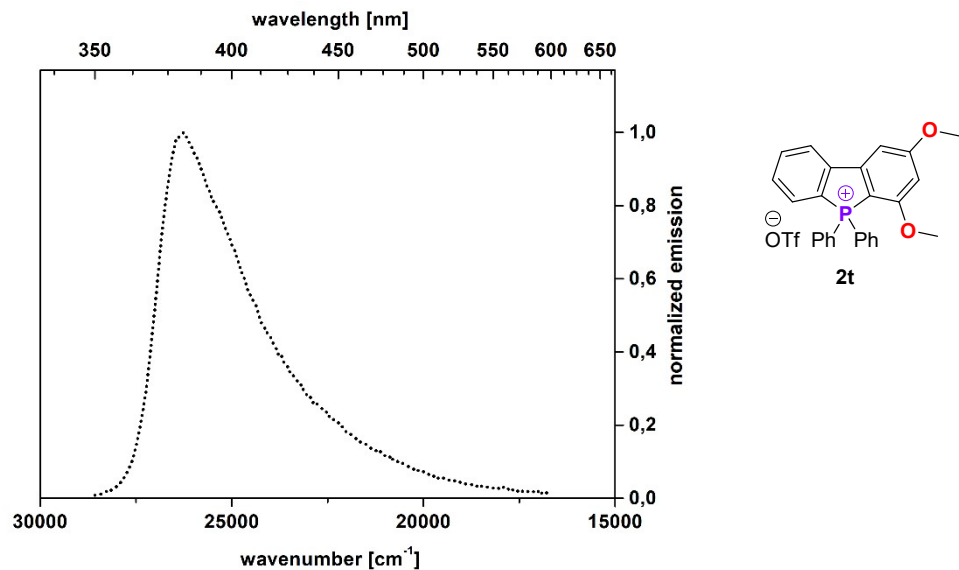


Figure S199: Solid state emission (dot) spectrum of 2t

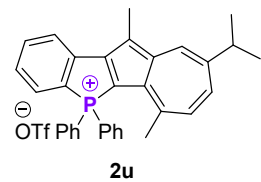
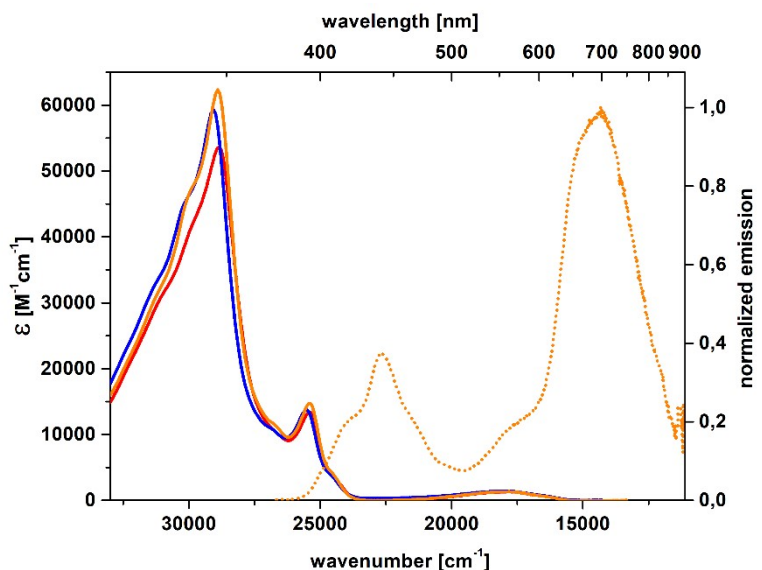


Figure S200: Absorption (solid) and emission (dot) spectra of **2u** in dichloromethane, tetrahydrofuran and acetonitrile

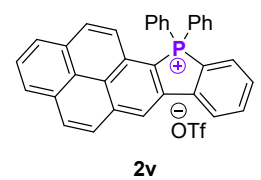
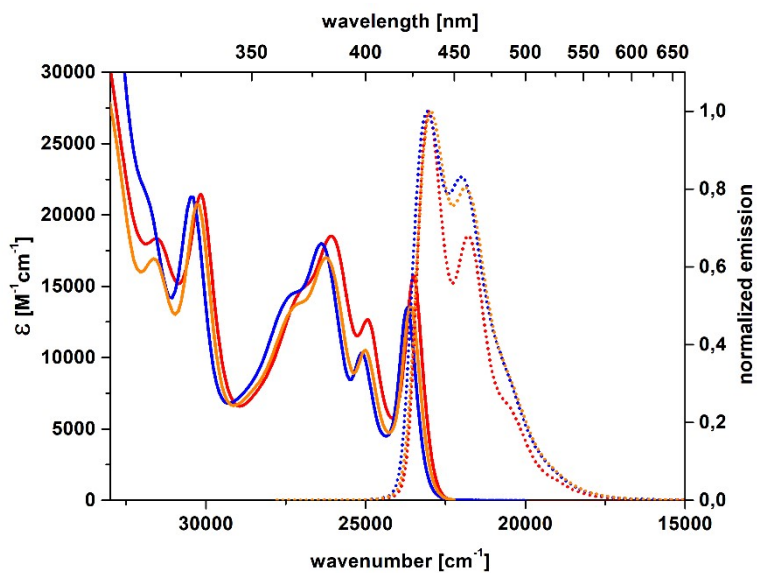


Figure S201: Absorption (solid) and emission (dot) spectra of **2v** in dichloromethane, tetrahydrofuran and acetonitrile

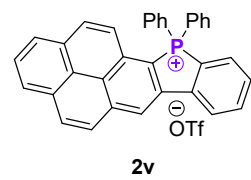
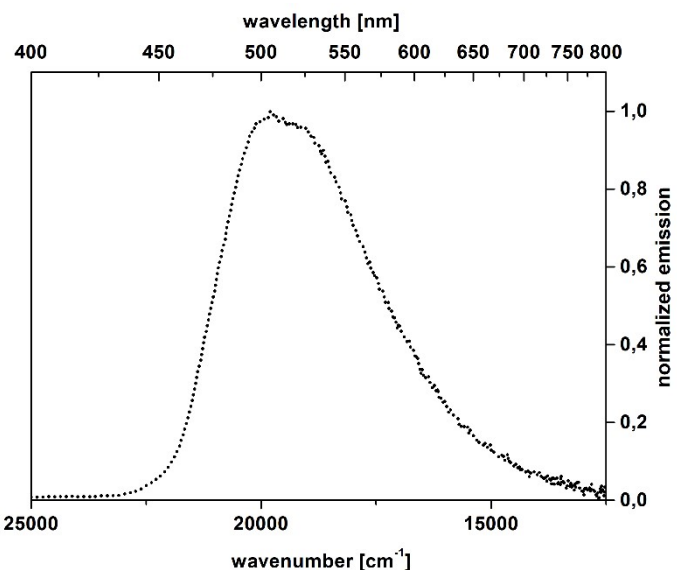


Figure S202: Solid state emission (dot) spectrum of **2v**

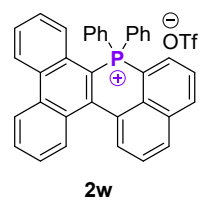
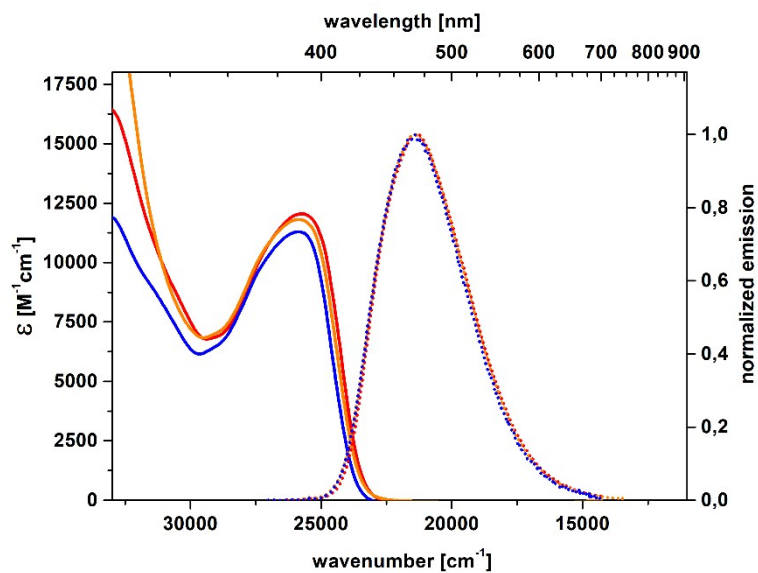


Figure S203: Absorption (solid) and emission (dot) spectra of **2w** in dichloromethane, tetrahydrofuran and acetonitrile

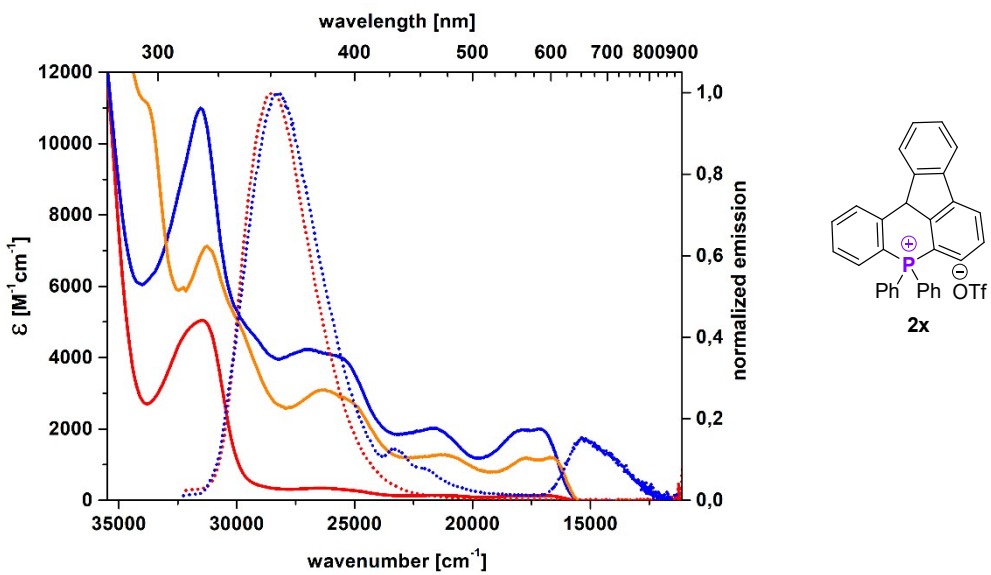


Figure S204: Absorption (solid) and emission (dot) spectra of **2x** in dichloromethane, tetrahydrofuran and acetonitrile

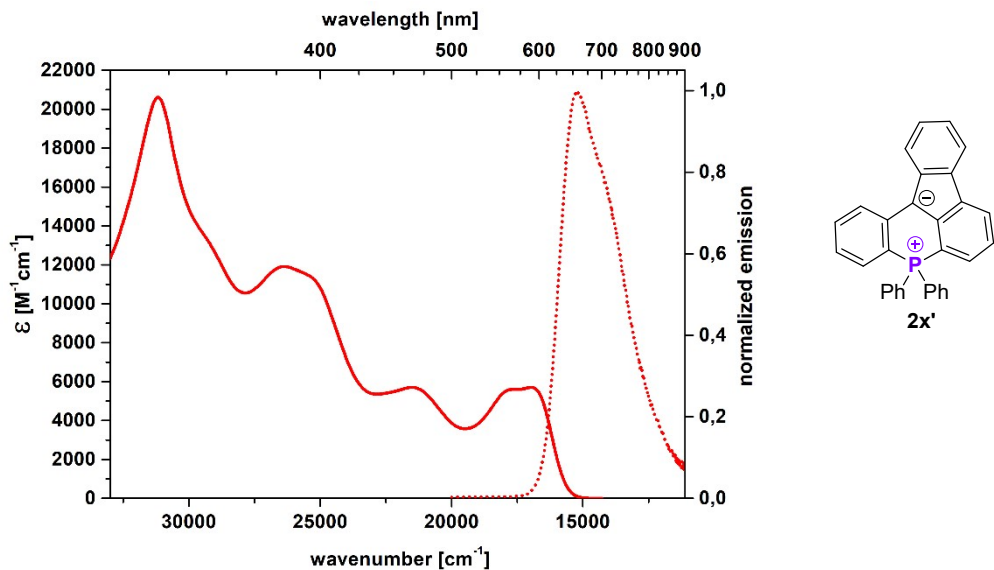


Figure S205: Absorption (solid) and emission (dot) spectra of **2x'** in dichloromethane (measured after the addition of 100 μ l of DBU to **2x** solution)

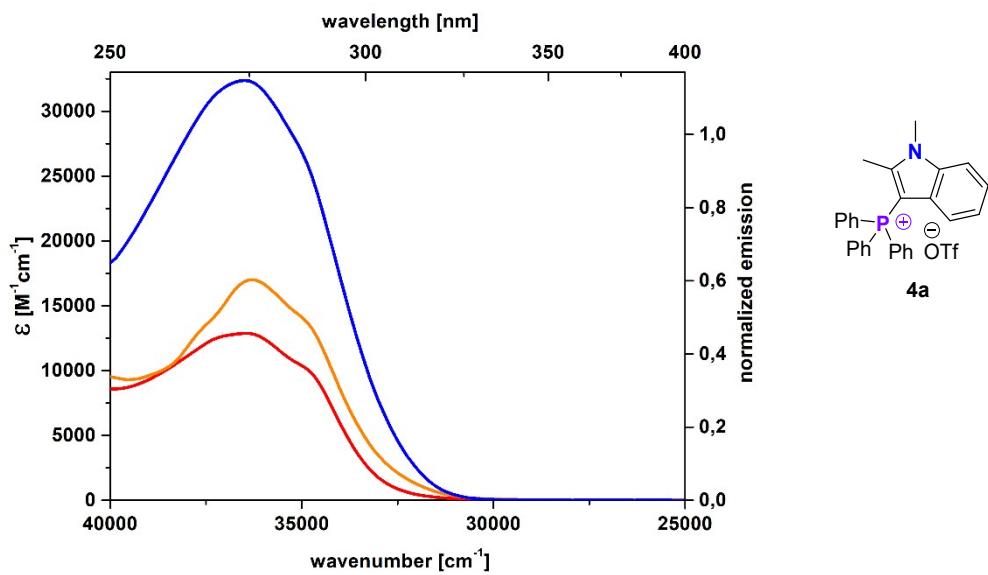


Figure S206: Absorption (solid) spectra of **4a** in dichloromethane, tetrahydrofuran and acetonitrile

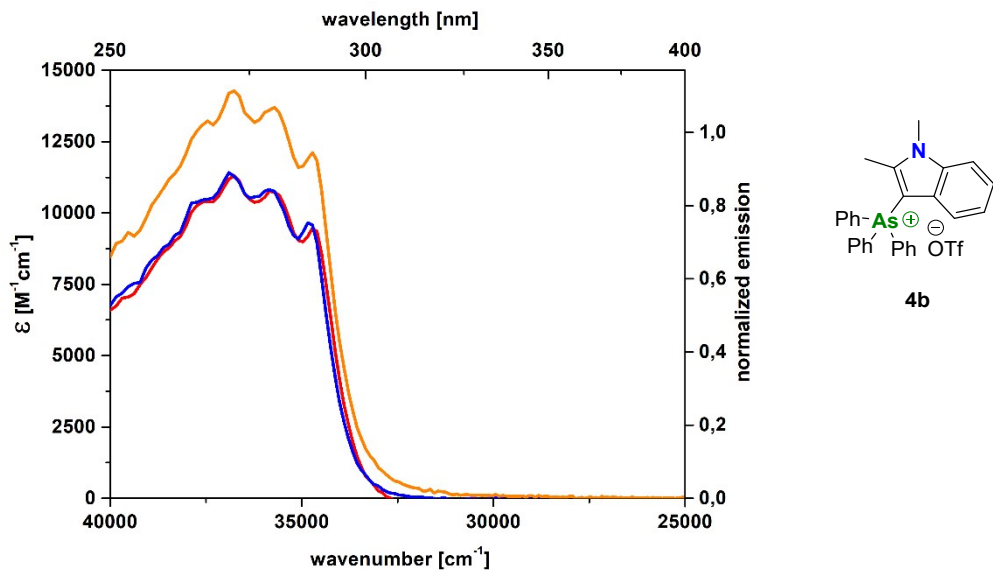


Figure S207: Absorption (solid) spectra of **4b** in dichloromethane, tetrahydrofuran and acetonitrile

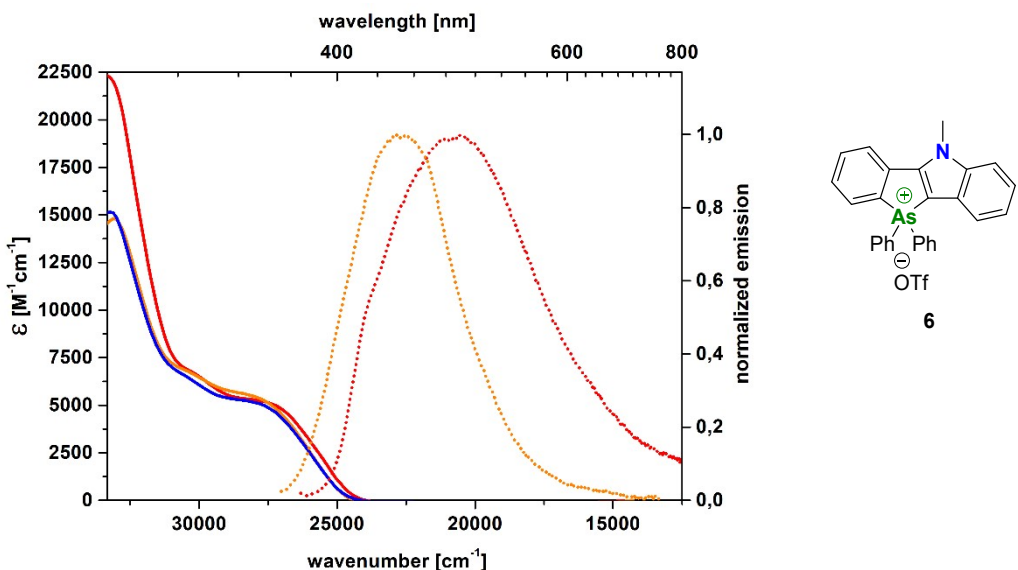


Figure S208: Absorption (solid) and emission (dot) spectra of 6 in dichloromethane, tetrahydrofuran and acetonitrile

$$pK_a = -\log \left(\frac{\left(\frac{A(590)}{l \cdot \varepsilon(590)} \right)^2}{C_0 - \frac{A(590)}{l \cdot \varepsilon(590)}} \right) = 7.05$$

$$A(590) = 0.02104 / \varepsilon(590) = 5704.95101 / l = 1$$

Equation S1: Acidic dissociation equilibrium constant for 2x.

Table S1: Spectroscopic data in dichloromethane (red), tetrahydrofuran (orange), acetonitrile (blue) and solid (bold black) for salts. Redox properties measured in acetonitrile.

salt	$\lambda_{\text{abs}} (\varepsilon \cdot 10^{-3})$ [nm] [$\text{cm}^{-1} \text{M}^{-1}$]	λ_{em} [nm]	$\Delta\nu$ [cm ⁻¹]	Φ_{FL} [%]	$\lambda_{\text{em}}^{\text{S}}$ [nm]	$\Phi_{\text{FL}}^{\text{S}}$ [%]	$E_{\text{ox}}^{\text{onset}}$	$E_{\text{red}}^{\text{onset}}$	E_{HOMO}	E_{LUMO}
2a	341 (1.9)	426	5900	9.7	n.d.	n.d.	1.40	-1.87	-6.17	-2.91
	338 (1.6)	428	6200	15.1						
	336 (1.6)	429	6500	16.9						
2b	350 (3.9)	433	5500	~100	459	43.5	1.48	-1.71	-6.25	-3.06
	349 (3.3)	445	6200	~100						
	348 (3.3)	440	6000	~100						
2c	346 (2.9)	440	6200	72.3	558	14.1	1.47	-1.77	-6.24	-3.00
	343 (2.6)	459	7400	75.0						
	344 (2.9)	448	6700	85.5						
2d	307 (4.9), 340 (3.9), 368 (3.0)	460	5400	60.9	482	18.9	1.53	-1.56	-6.30	-3.21
	306 (4.6), 338 (3.4), 366 (2.5)	464	5800	62.4						
	304 (6.0), 334 (3.6), 364 (2.8)	462	5800	61.0						
2e	360 (5.4)	460	6000	68.5	472	58.3	1.45	-1.59	-6.22	-3.18
	353 (5.7)	467	6900	69.1						
	353 (5.0)	466	6900	67.5						
2f	304 (12.8), 371 (3.7)	490	6500	56.7	483	31.7	1.16	-1.85	-5.93	-2.92
	301 (17.8), 354 (4.4)	493	8000	59.5						
	301 (19.8), 356 (4.9)	491	7700	63.0						
2f^a	315 (19.3)	577	n.d.	2.2	n.d.	n.d.	n.d.	n.d.	-	-
	319 (12.9)	577	n.d.	2.2						
	313 (26.7)	577	n.d.	2.1						

		371 (3.8)	490	6500	89.4							
2g		370 (3.2)	500	7000	~100%	553	77.1	1.14	-1.84	-5.91	-2.93	
		364 (3.7)	500	7500	92.8							
2h		350 (13.2), 363 (11.3)	401	2600	30.0							
		352 (12.7), 364 (11.1)	410	3100	89.1	504	53.3	1.23	-2.00	-6.00	-2.77	
		348 (13.0), 360 (11.4)	410	3400	83.1							
2i		278 (19.2), 300 (15.8)	399	8300	2.4							
		277 (18.7), 301 (15.5)	414	9100	2.6	409	1.4	1.22	-2.23	-5.99	-2.54	
		276 (18.3), 298 (15.3)	426	10100	2.3							
2j		506 (13.5)	633	4000	18.8							
		504 (12.3)	640	4200	27.4	633	0.1	n.d.	n.d.	-	-	
		489 (3.7)	640	4800	18.6							
2k		483 (6.3)	642	5100	0.8							
		485 (6.9)	633	4800	0.4	619	8.8	n.d.	n.d.	-	-	
		463 (3.0)	659	6400	<0.001							
2l		322 (28.7), 427 (15.3)	523	4300	59.7							
		324 (35.3), 429 (17.4)	542	4900	74.8	558	5.2	n.d.	n.d.	-	-	
		321 (25.9), 422 (13.8)	539	5100	51.4							
2m		362 (31.3), 460 (7.0)	672	6900	2.0							
		358 (30.3), 450 (6.7)	672	7300	1.1	639	9.4	0.25	-1.90	-5.02	-2.87	
		355 (31.8), 442 (7.1)	705	8400	0.4							
2n		361 (3.2)	463	6100	61.8							
		358 (3.7)	465	6400	62.0	600	0.6	n.d.	n.d.	-	-	
		356 (3.1)	468	6700	52.1							
2o		352 (8.1), 407 (1.9)	530	5700	16.9							
		347 (6.9), 402 (1.4)	530	6000	15.1	492	10.7	1.05	-1.66	-5.82	-3.11	
		343 (9.2), 391 (2.2)	550	7400	11.4							
2p		323 (6.4), 333 (7.8), 387 (0.9)	535	7100	10.8							
		323 (7.3), 333 (8.2), 375 (1.0)	567	9000	5.4	504	2.2	0.99	-1.66	-5.76	-3.11	
		323 (7.3), 333 (8.2), 371 (0.9)	559	9100	4.3							
2q		331 (10.9), 344 (10.6), 355 (10.0)	388	2400	5.4							
		331 (10.7), 344 (10.5), 355 (9.9)	388	2400	5.2	n.d.	n.d.	1.22	-2.19	-5.99	-2.58	
		331 (10.3), 344 (10.3), 355 (9.6)	390	2500	4.7							
2r		278 (8.1), 300 (8.9), 307 (8.5)	328	2100	3.4							
		278 (4.9), 301 (6.9), 307 (7.1)	329	2200	6.1	n.d.	n.d.	1.37	-2.08	-6.14	-2.69	
		277 (5.0), 300 (7.2), 306 (7.4)	329	2300	3.0							
2s		371 (3.5)	557	9000	8.0							
		366 (2.9)	575	9900	11.1	532	2.0	1.05	-1.63	-5.82	-3.14	
		366 (3.4)	583	10200	9.1							
2t		329 (7.5), 336 (7.4)	387	3900	7.9							
		328 (7.8), 337 (7.4)	390	4000	4.5	381	35.5	1.61	-1.87	-6.38	-2.90	
		328 (7.5), 335 (7.2)	390	4200	3.6							
2u		347 (53.6), 394 (13.4), 562 (1.3)	n.d.	n.d.	n.d.							
		346 (62.3), 394 (14.7), 561 (1.3)	418, 441, 698	3500*	<0.001	n.d.	n.d.	0.96	-1.41	-5.73	-3.36	
		344 (59.4), 392 (13.7), 559 (1.4)	n.d.	n.d.	n.d.							
2v		384 (18.5), 401 (12.7), 425 (15.7)	434, 456	500	91.1							
		381 (17.0), 400 (10.5), 424 (13.6)	434, 458	500	97.3	507	11.4	1.21	-1.55	-5.98	-3.22	
		379 (18.0), 398 (10.3), 422 (13.5)	434, 455	700	92.5							
2w		388 (12.1)	466	4300	9.9							
		387 (11.8)	466	4400	8.6	n.d.	n.d.	1.38	-1.50	-6.15	-3.27	
		387 (11.3)	466	4400	10.0							
2x		318 (5.0), 378 (0.3), 590 (0.1)	351	n.d.	12.9							
		320 (7.1), 379 (3.1), 602 (1.2)	n.d.	n.d.	n.d.	n.d.	n.d.	1.51	-2.05	-6.28	-2.72	
		317 (11.0), 370 (4.2), 582 (2.0)	355, 652	n.d.	5.5*							
2x ^a		379 (11.9), 465 (5.7), 590 (5.7)	657	1700	0.5	n.d.	n.d.	n.d.	n.d.	-	-	
4a		274 (12.9), 287 (10.0)	n.d.	n.d.	n.d.	n.d.	n.d.	1.23	-2.32	-6.00	-2.45	
		275 (17.0), 287 (13.7)	n.d.	n.d.	n.d.	n.d.	n.d.					

	274 (32.4)	n.d.	n.d.	n.d.							
4b	272 (11.3), 279 (10.8), 288 (9.5)	n.d.	n.d.	n.d.							
	272 (14.3), 280 (13.7), 288 (12.1)	n.d.	n.d.	n.d.	n.d.	n.d.					
	271 (11.4), 279 (10.8), 287 (9.7)	n.d.	n.d.	n.d.							
6	361 (5.2)	472, 486	6500	<0.001							
	362 (5.2)	440	4900	0.1	n.d.	n.d.					
	358 (5.1)	n.d.	n.d.	n.d.							

$\lambda_{\text{abs}} / \lambda_{\text{em}}$ – absorption / emission wavelength, ϵ – molar absorption coefficient, Δv – Stokes shift, Φ_{FL} – fluorescence quantum yield in solution, $\lambda_{\text{em}}^{\text{S}}$ – emission wavelength, $\Phi_{\text{FL}}^{\text{S}}$ fluorescence quantum yield in solid, # - determined for transition between S_0 and S_1 states, * – determined for two emission bands, ^a – measured after addition of 100 μ l of DBU, $E_{\text{ox}}^{\text{onset}} / E_{\text{red}}^{\text{onset}}$ – oxidation / reduction potential (vs Fc/Fc⁺ couple) onset, $E_{\text{HOMO}} / E_{\text{LUMO}}$ – HOMO / LUMO energy

Table S2: Spectroscopic data for 2b, 2g, 2m and 2k in different solvents.

	solvent	$\lambda_{\text{abs}} [\text{nm}]$	$\lambda_{\text{flu}} [\text{nm}]$	$\Delta v [\text{cm}^{-1}]$	$\Phi_{\text{FL}} [\%]$
2b	dichloromethane	350	433	5500	≈100
	chloroform	349	441	6000	≈100
	ethyl acetate	347	446	6400	96.0
	tetrahydrofuran	349	445	6200	≈100
	acetone	348	441	6100	91.1
	acetonitrile	348	440	6000	≈100
	dimethylformamide	348	443	6200	≈100
	dimethylsulfoxide	351	449	6200	27.0
2m	toluene	444	637	6800	1.3
	dichloromethane	460	672	6900	2.0
	chloroform	455	666	7000	<0.001
	ethyl acetate	441	670	7800	2.5
	tetrahydrofuran	450	672	7300	1.1
	acetone	447	693	8000	0.8
	acetonitrile	442	705	8400	0.4
	dimethylformamide	443	703	8300	1.6
2k	dimethylsulfoxide	444	701	8300	1.1
	dichloromethane	483	642	5100	0.8
	chloroform	489	641	4800	0.6
	ethyl acetate	486	673	5700	<0.001
	tetrahydrofuran	485	633	4800	0.4
	acetone	480	650	5400	0.7
	acetonitrile	453	659	6400	<0.001
	dimethylformamide	449	603	5700	6.38
2g	dimethylsulfoxide	450	652	6900	0.77
	dichloromethane	371	490	6500	89.4
	chloroform	368	500	7200	93.83
	ethyl acetate	367	508	7600	57.06
	tetrahydrofuran	370	500	7000	≈100
	acetone	367	499	7200	60.06
	acetonitrile	364	500	7500	92.8
	dimethylformamide	367	503	7400	79.50
	dimethylsulfoxide	365	502	7500	91.71

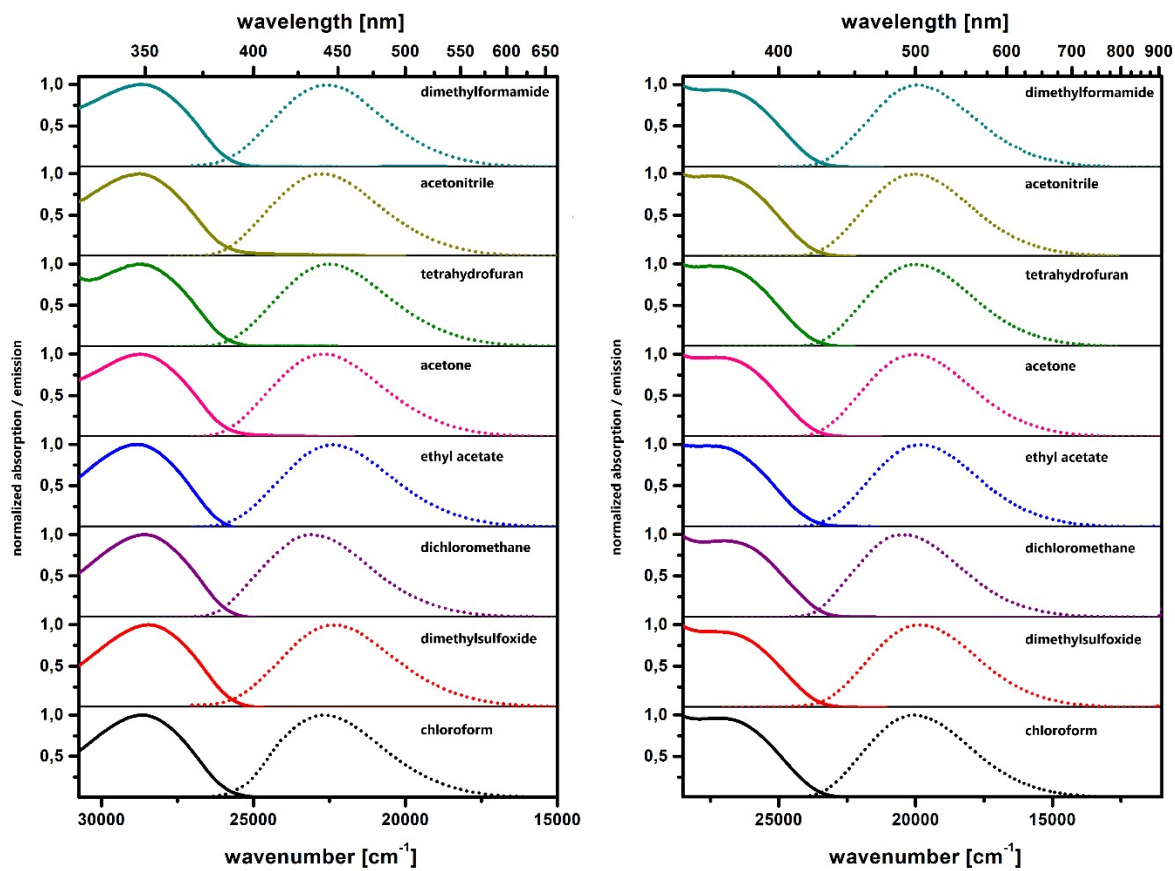


Figure S209: Absorption (solid) and emission (dot) spectra of 2b (left) and 2g (right)

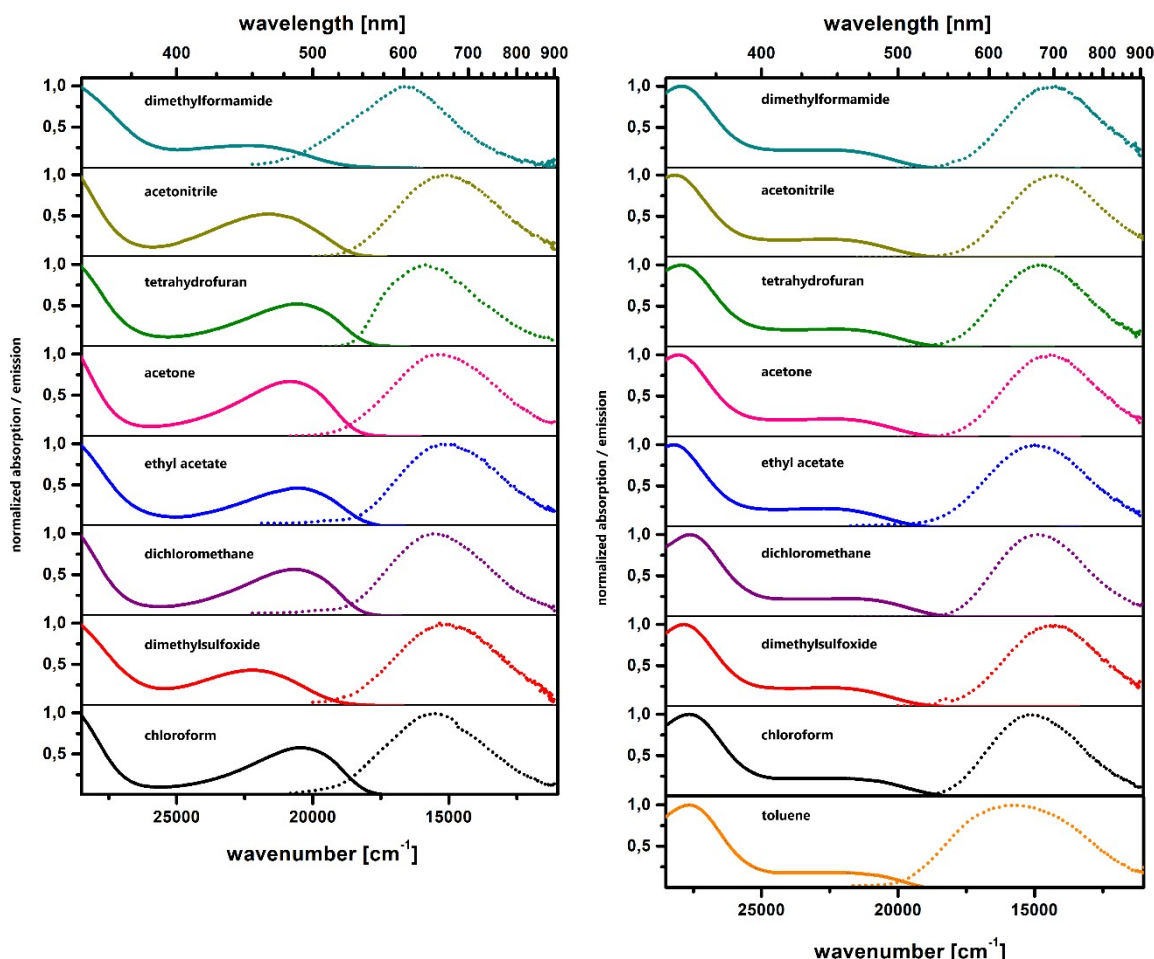


Figure S210: Absorption (solid) and emission (dot) spectra of 2k (left) and 2m (right)

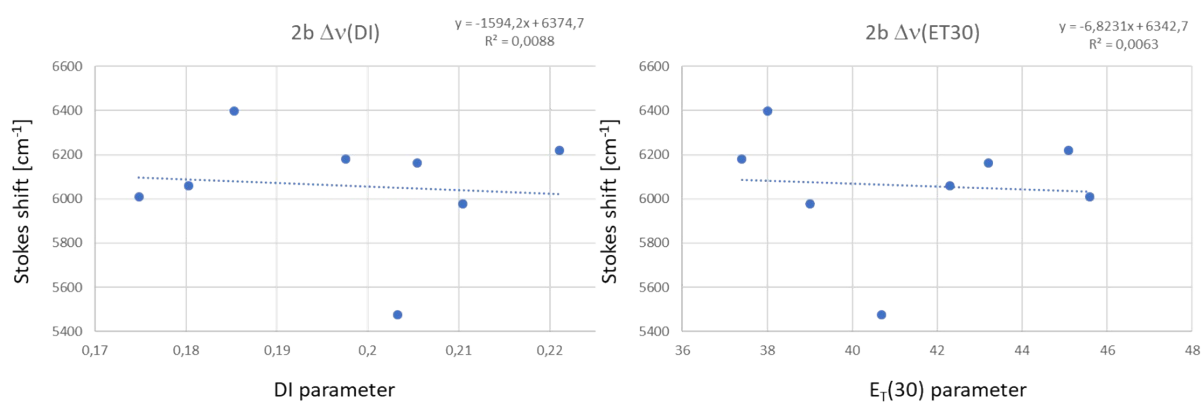


Figure S211: Stokes shift vs $E_T(30)$ solvent parameter plot and linear regression for 2b

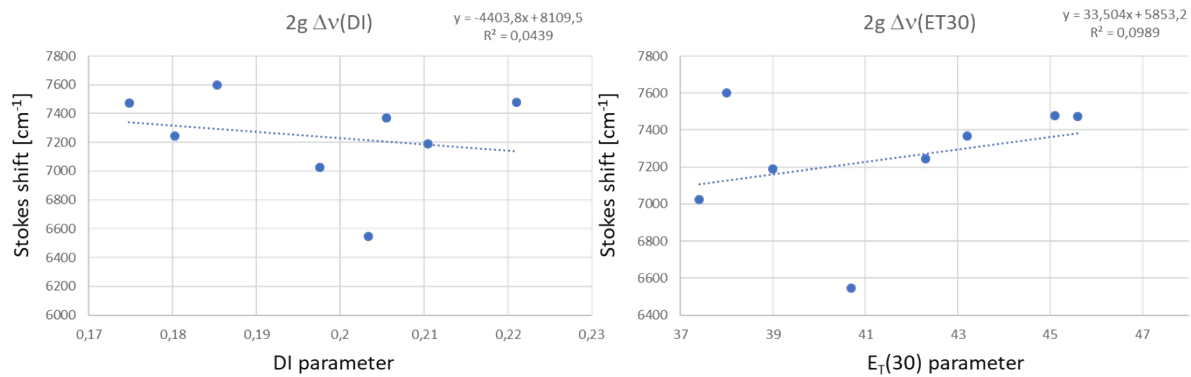


Figure S212: Stokes shift vs E_T(30) solvent parameter plot and linear regression for 2g

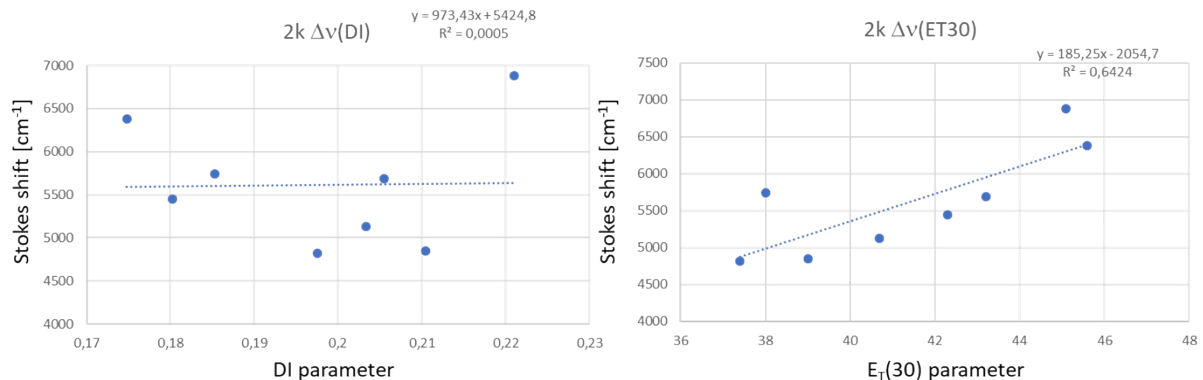


Figure S213: Stokes shift vs E_T(30) solvent parameter plot and linear regression for 2k

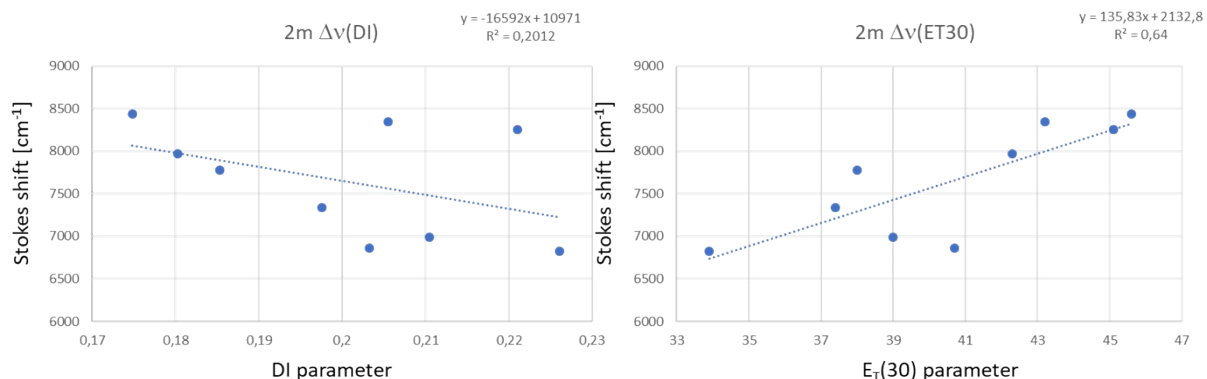


Figure S214: Stokes shift vs E_T(30) solvent parameter plot and linear regression for 2m

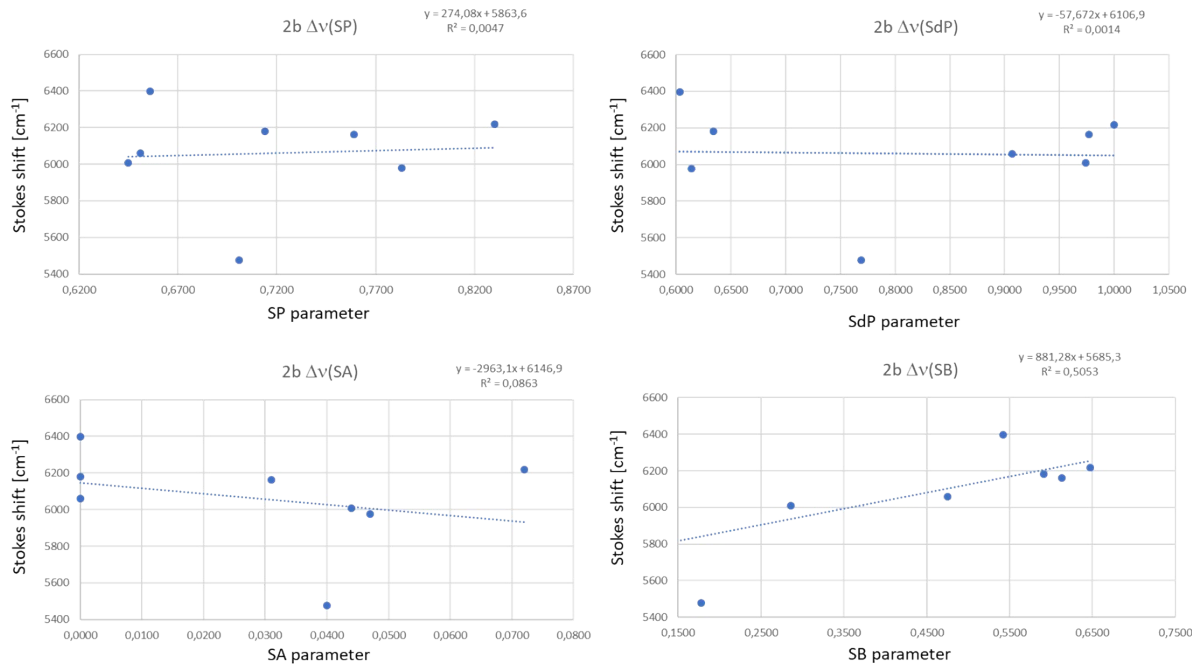


Figure S215: Stokes shift vs SP (solvent polarizability), SdP (solvent dipolarity), SA (solvent acidity), SB (solvent basicity) parameter plot and linear regression for 2b

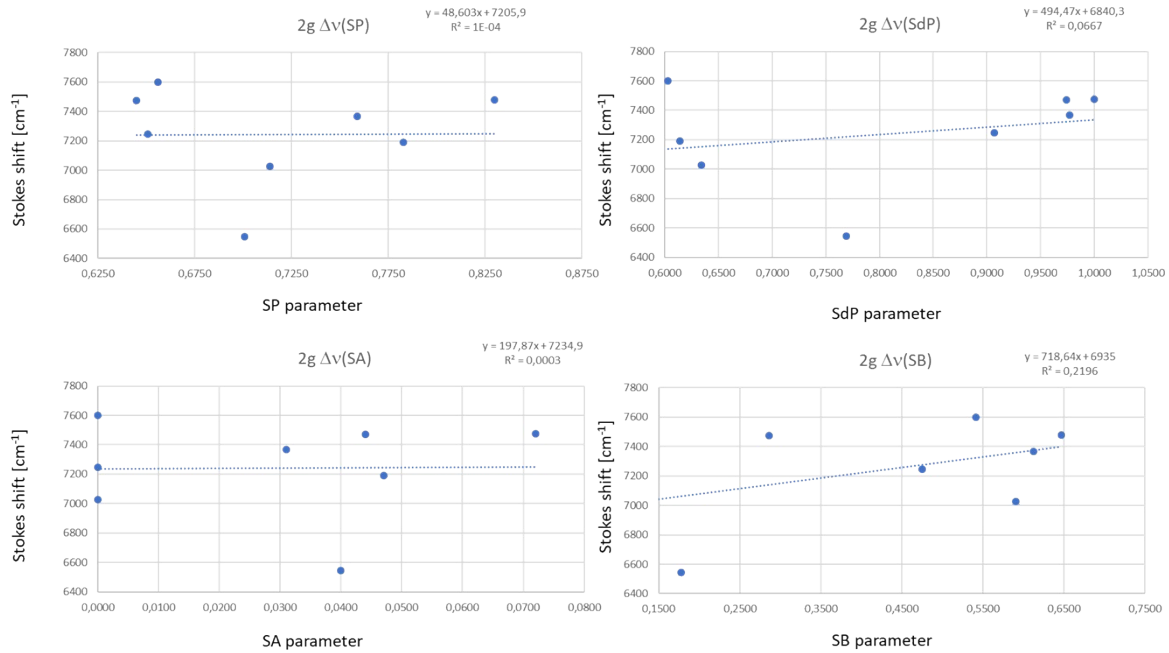


Figure S216: Stokes shift vs SP (solvent polarizability), SdP (solvent dipolarity), SA (solvent acidity), SB (solvent basicity) parameter plot and linear regression for 2g

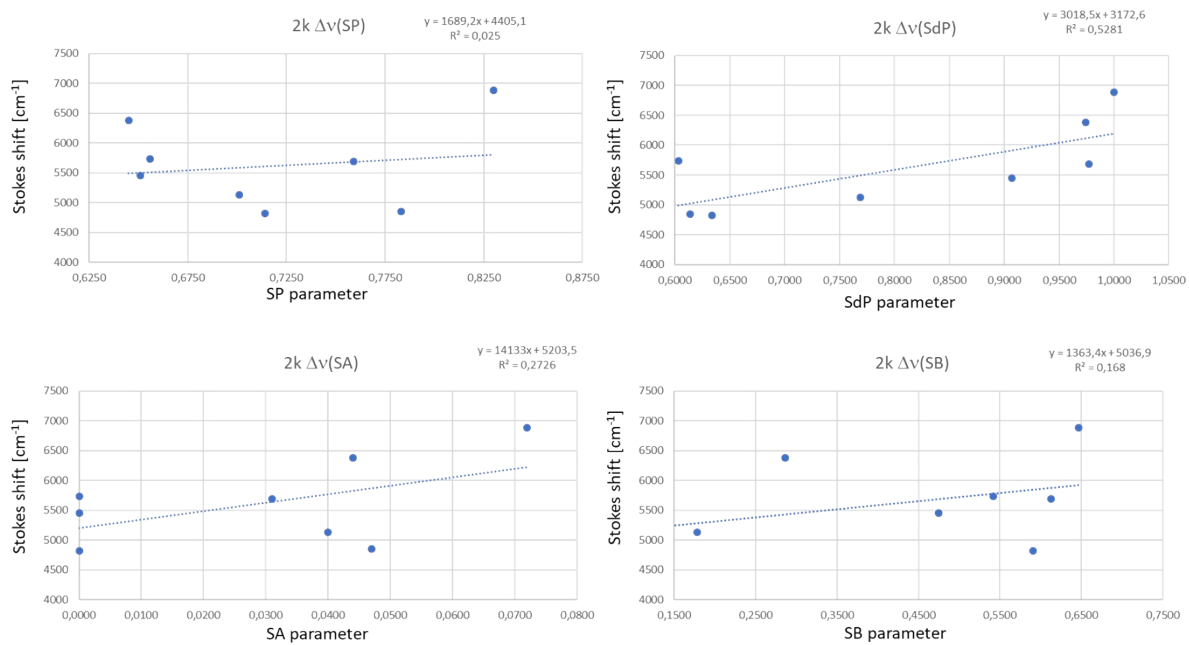


Figure S217: Stokes shift vs SP (solvent polarizability), SdP (solvent dipolarity), SA (solvent acidity), SB (solvent basicity) parameter plot and linear regression for 2k

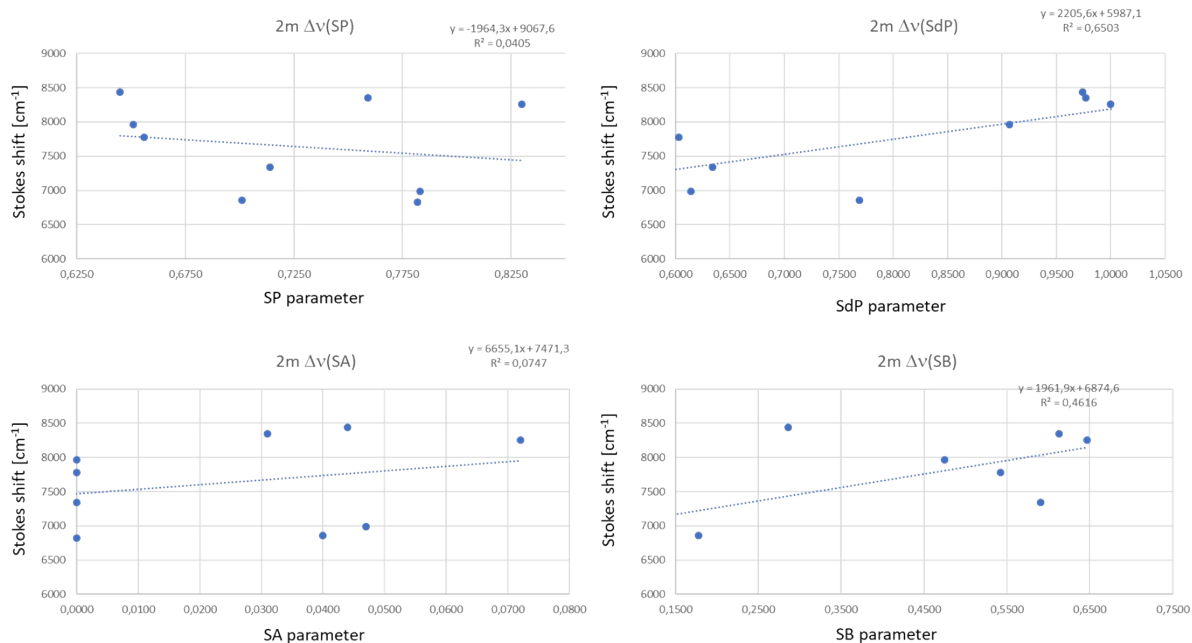


Figure S218: Stokes shift vs SP (solvent polarizability), SdP (solvent dipolarity), SA (solvent acidity), SB (solvent basicity) parameter plot and linear regression for 2m

5. Electrochemistry

All cyclic voltammetry measurements were conducted using Bio-Logic SP-50 potentiostat equipped with 2.25 mm² glassy carbon electrode as a working electrode, Ag/AgCl/NaCl(sat) electrode as a reference electrode and platinum wire as a counter electrode. All measurements were conducted in anhydrous MeCN, in the presence of 0.1 M tetrabutylammonium hexafluorophosphate as a supporting electrolyte. Concentration of the analyte were kept in range of 4-10 mM, and the scan rate was set to 100 mV/s. The direction of potential sweep is indicated with a suffix following the compound symbol on the chart legend (_ox – positive potential first, _red – negative potential first). Before the measurement a cyclic voltammogram of every electrolyte solution was recorded and is presented as a light gray trace on each figure. To check whether reversibility of the reduction peaks could be achieved, additional measurements in DCE and DMF were performed for salt **2g** (Fig. S226 and S227). Unfortunately, only a minute improvement in reversibility was observed in DCE when the potential scan rate was increased to 200 mV/s.

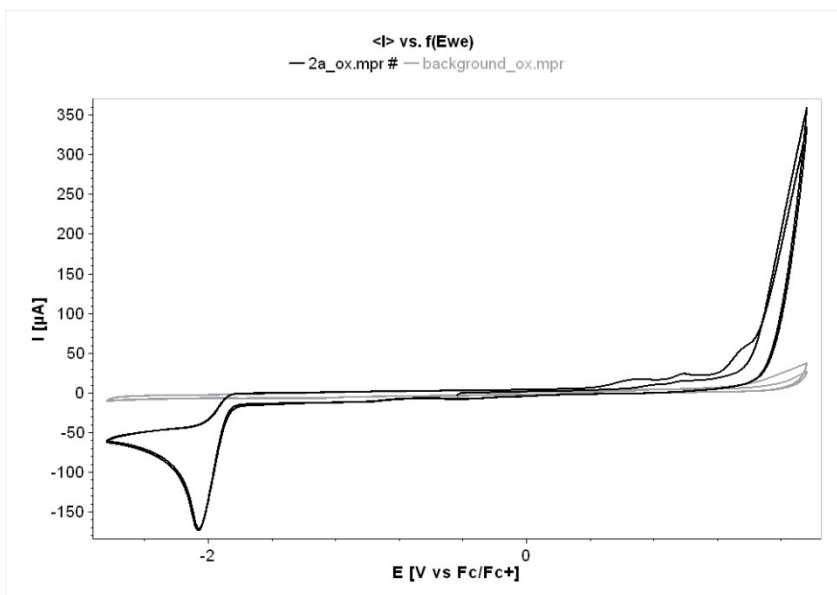


Figure S219: Cyclic voltammogram of **2a** in MeCN

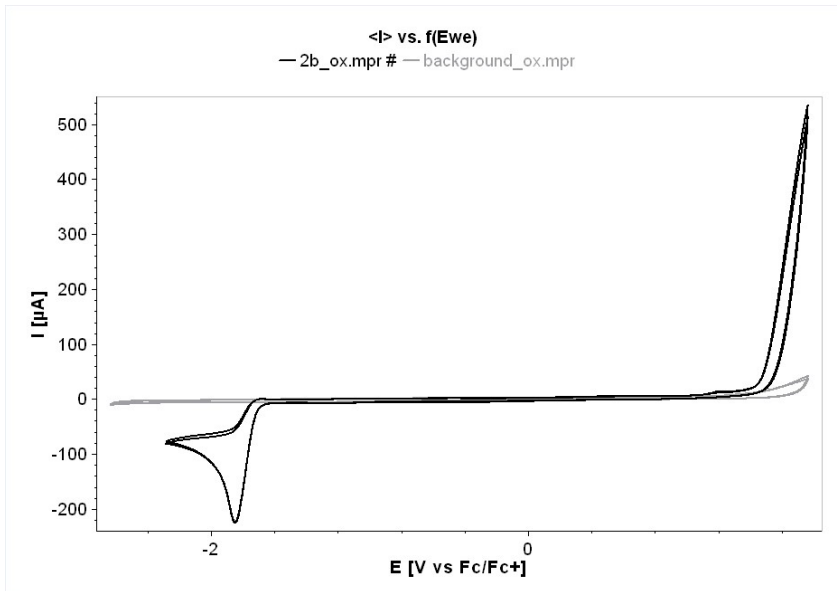


Figure S220: Cyclic voltammogram of **2b** in MeCN

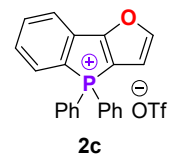
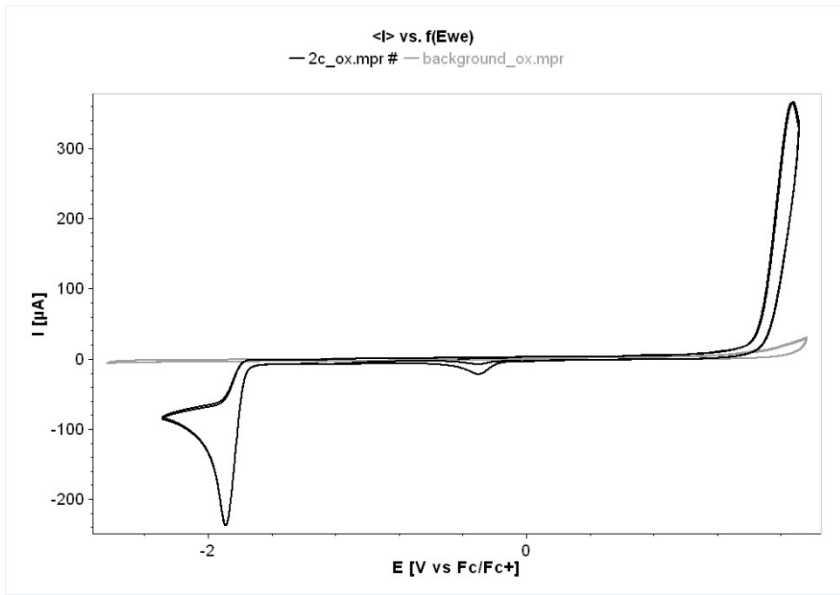


Figure S221: Cyclic voltammogram of 2c in MeCN

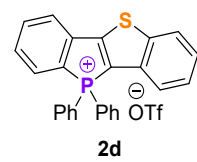
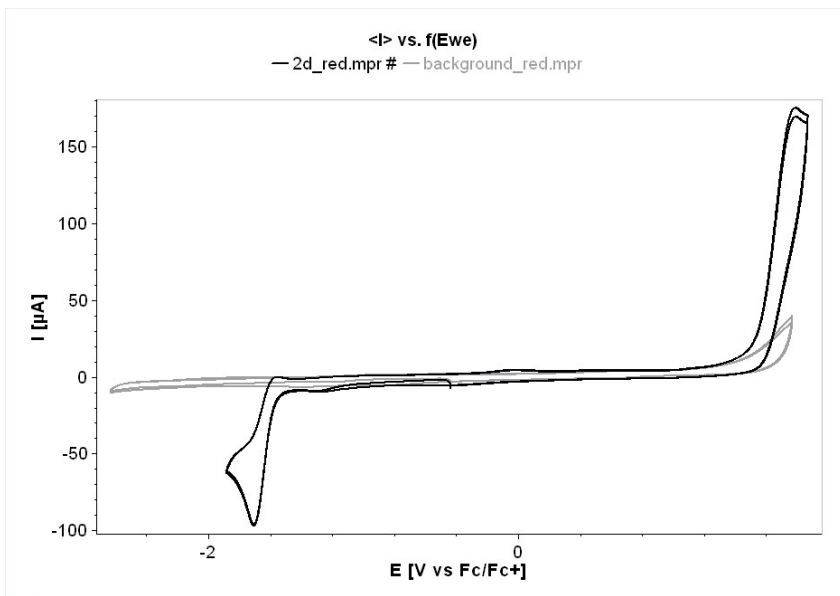


Figure S222: Cyclic voltammogram of 2d in MeCN

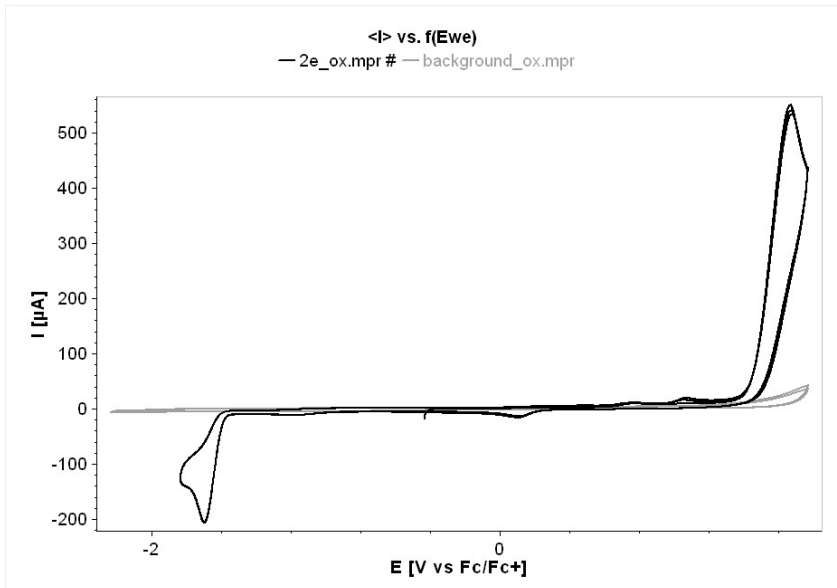


Figure S223: Cyclic voltammogram of **2e** in MeCN

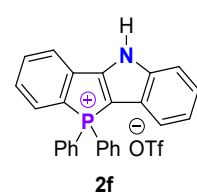
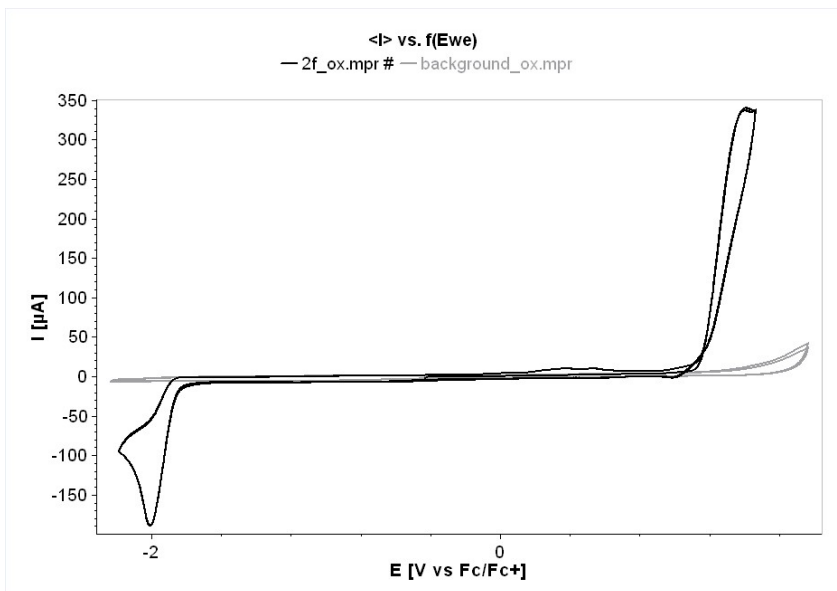


Figure S224: Cyclic voltammogram of **2f** in MeCN

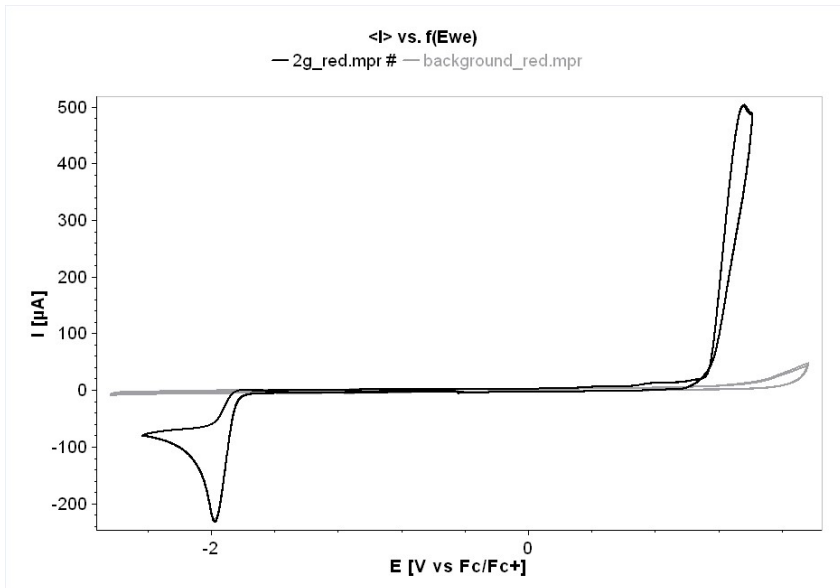


Figure S225: Cyclic voltammogram of 2g in MeCN

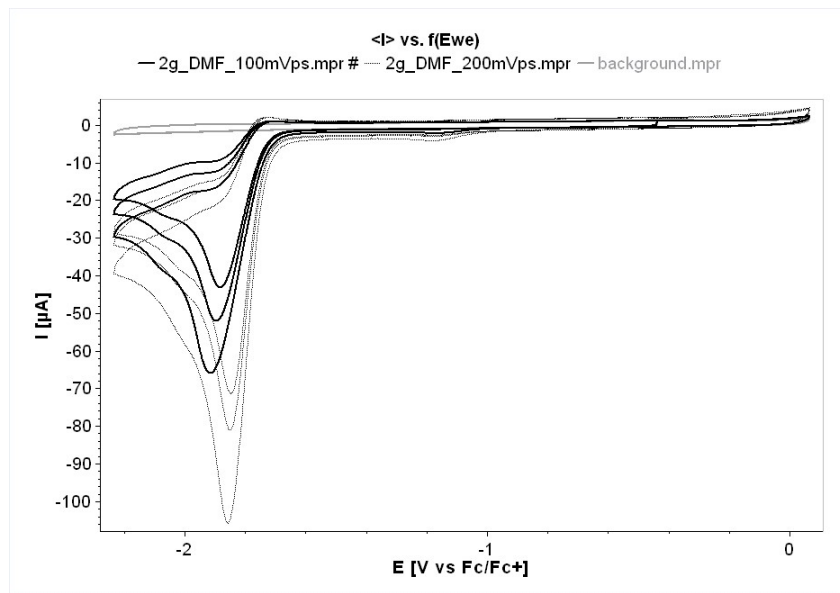


Figure S226: Cyclic voltammogram of 2g in DMF

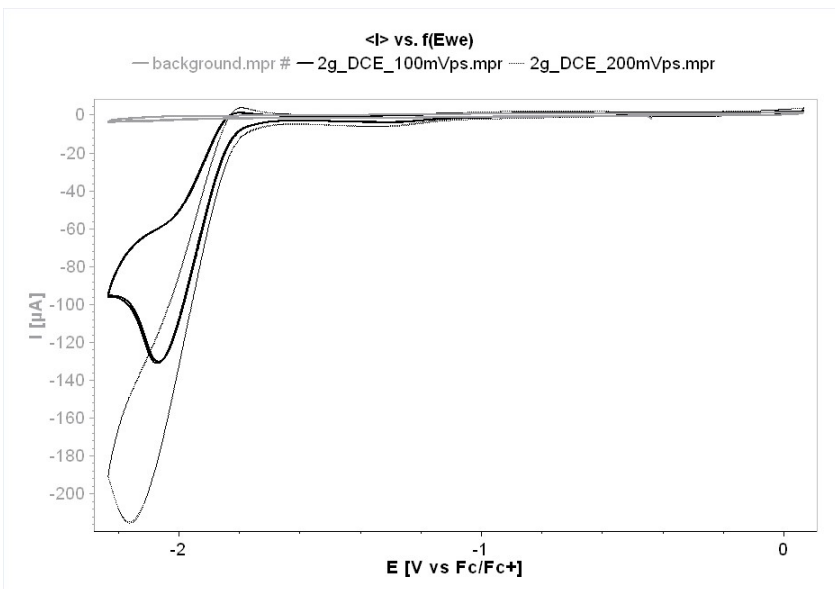


Figure S227: Cyclic voltammogram of **2g** in DCE

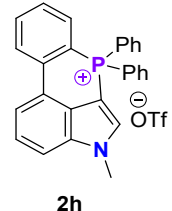
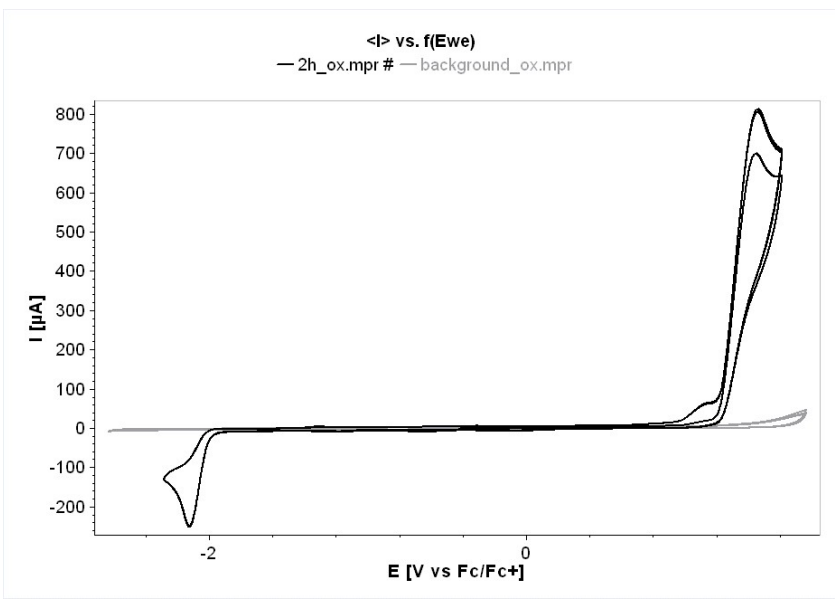
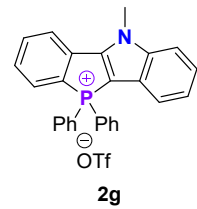


Figure S228: Cyclic voltammogram of **2h** in MeCN

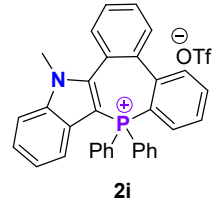
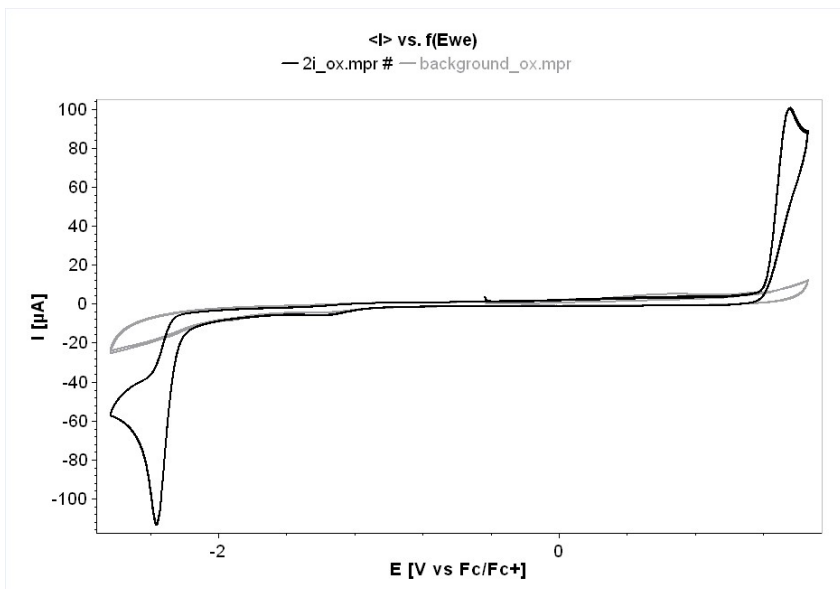


Figure S229: Cyclic voltammogram of 2i in MeCN

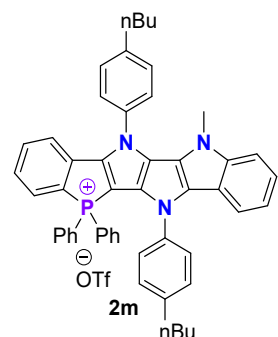
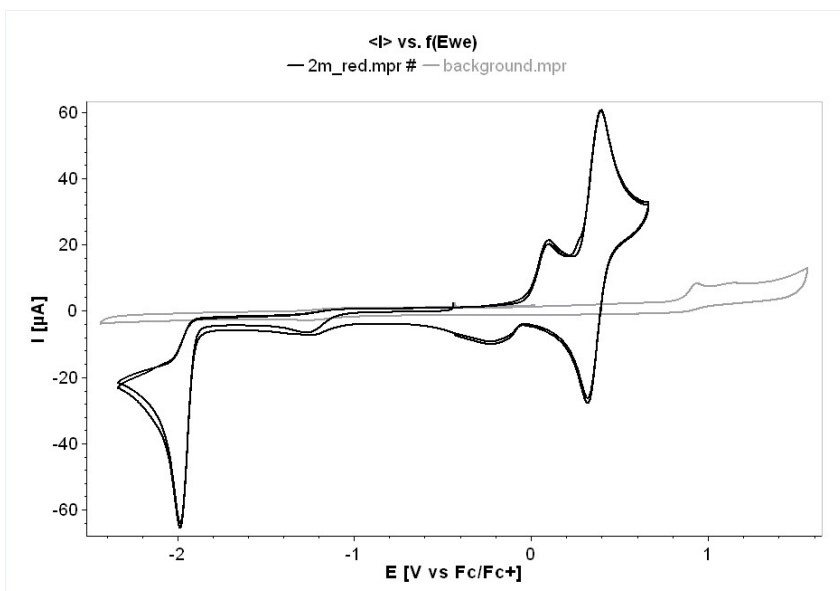


Figure S230: Cyclic voltammogram of 2m in MeCN

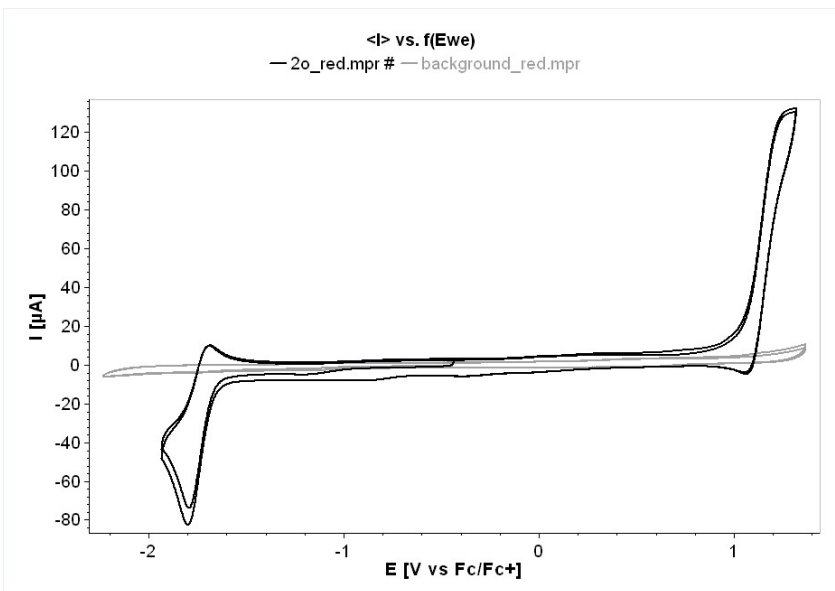


Figure S231: Cyclic voltammogram of 2o in MeCN

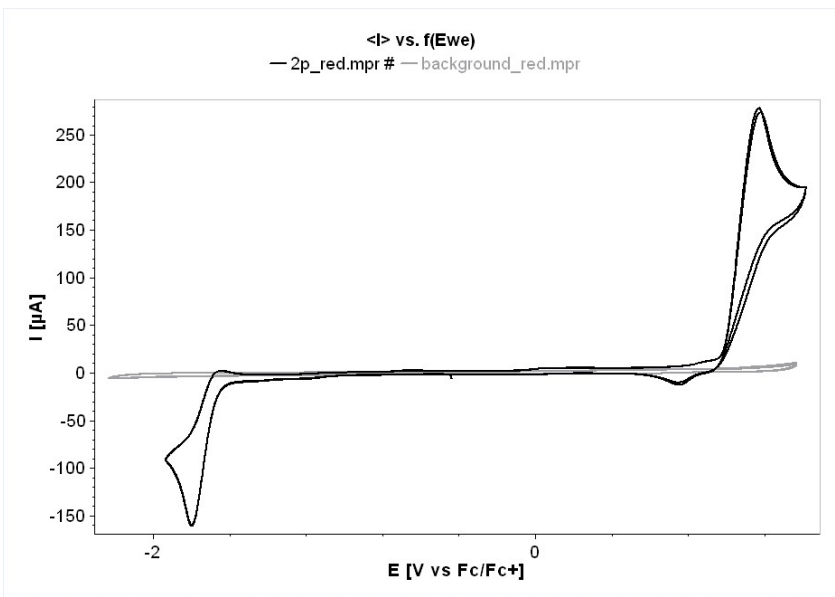


Figure S232: Cyclic voltammogram of 2p in MeCN

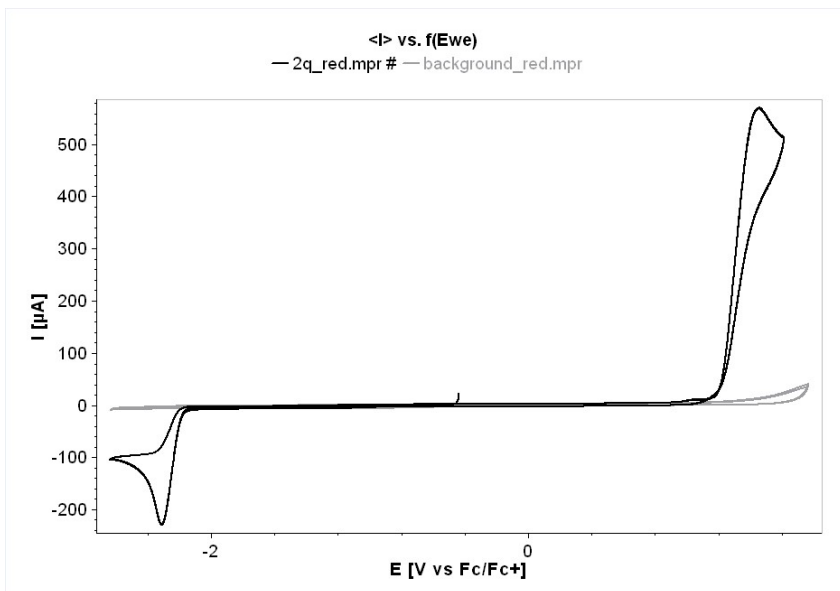
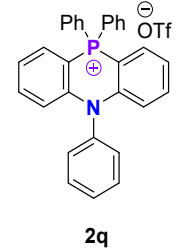
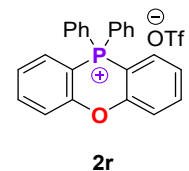
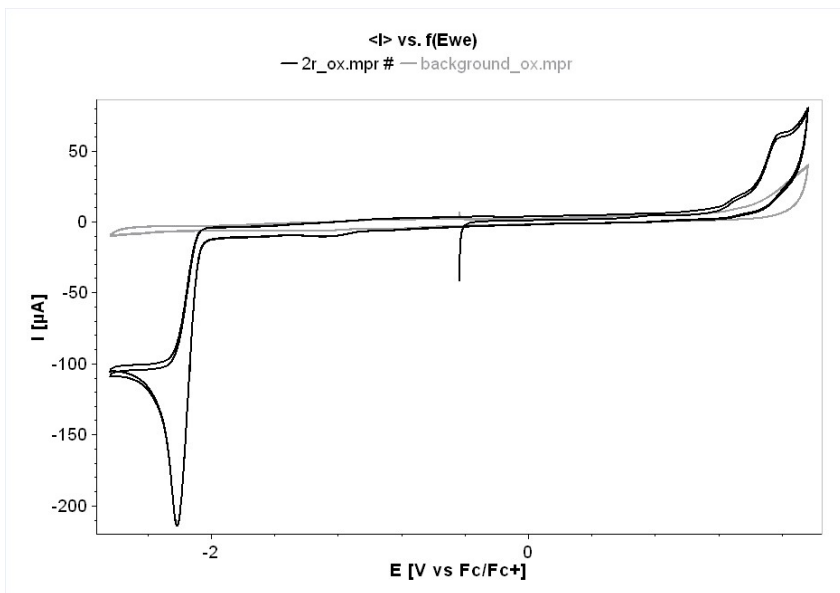


Figure S233: Cyclic voltammogram of 2q in MeCN



2q



2r

Figure 234: Cyclic voltammogram of 2r in MeCN

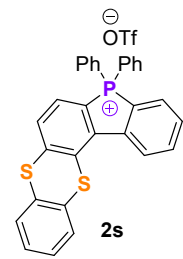
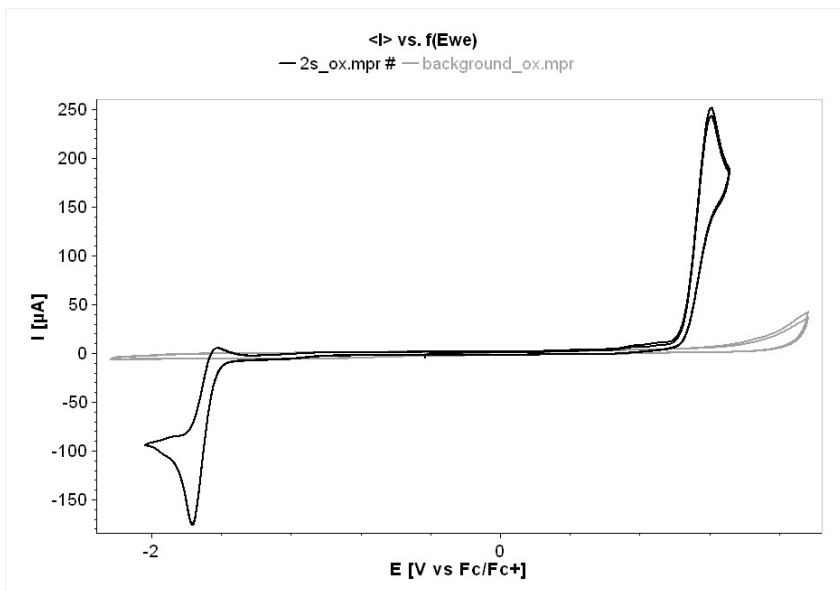


Figure S235: Cyclic voltammogram of 2s in MeCN

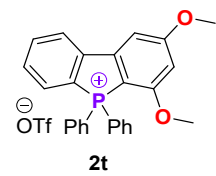
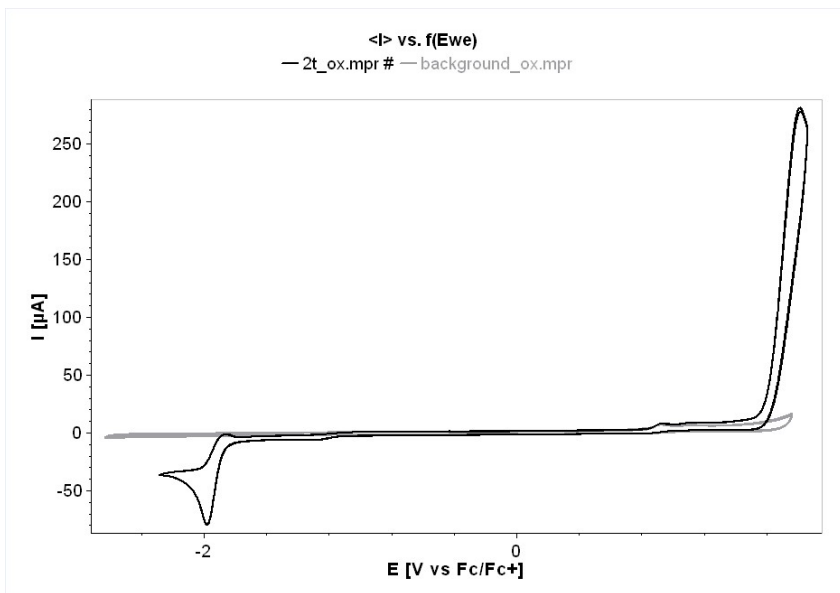


Figure S236: Cyclic voltammogram of 2t in MeCN

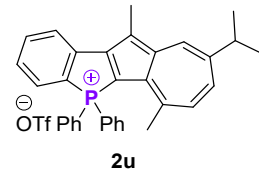
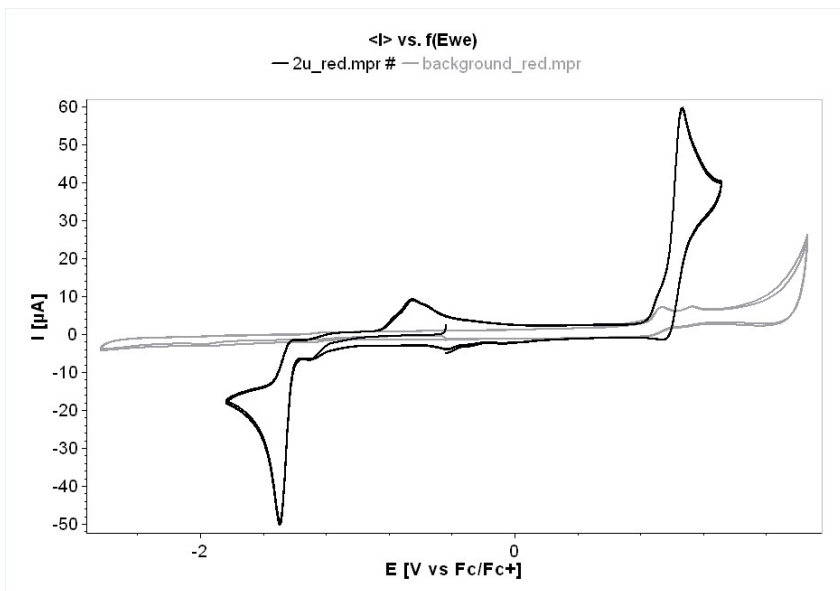


Figure S237: Cyclic voltammogram of 2u in MeCN

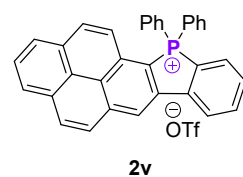
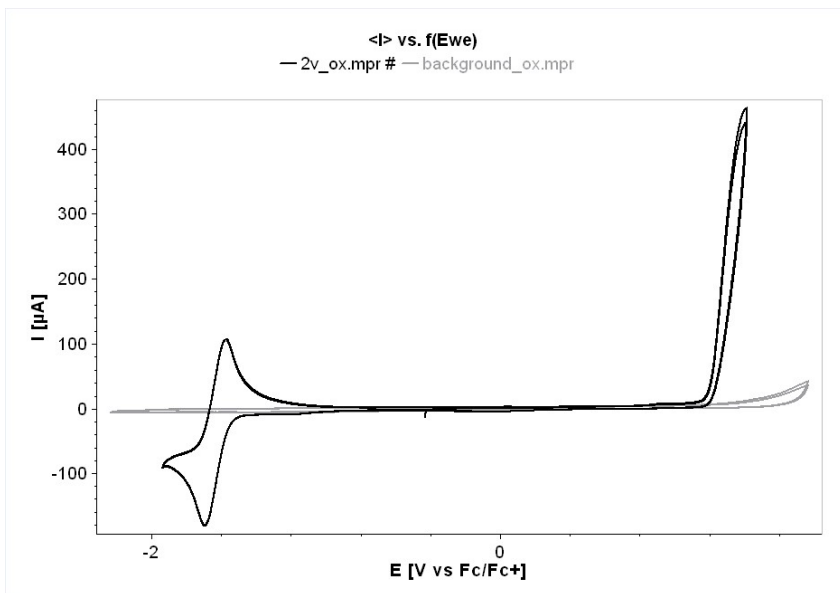


Figure S238: Cyclic voltammogram of 2v in MeCN

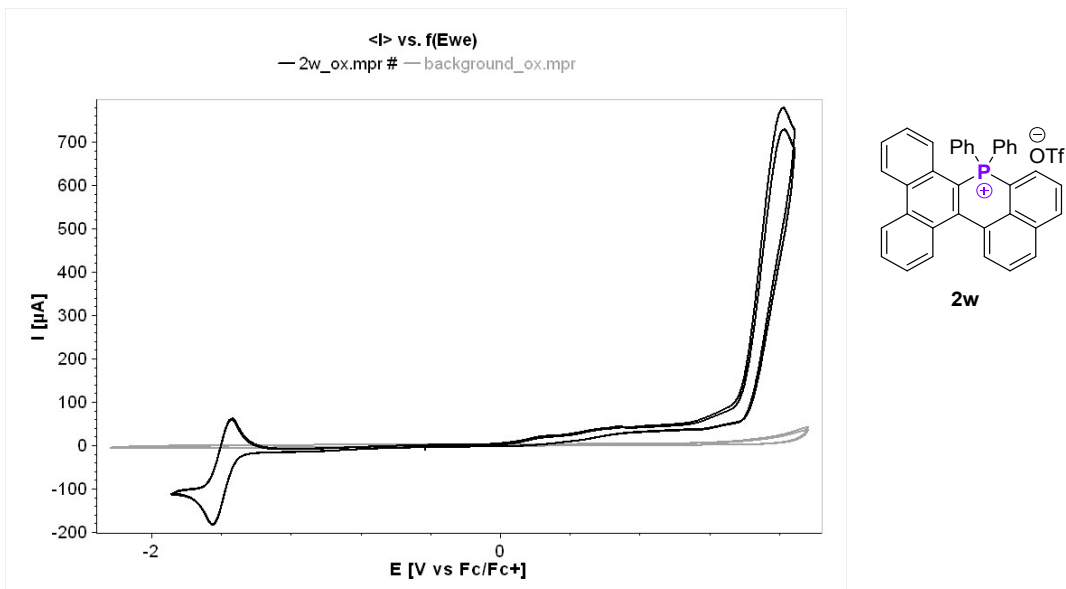


Figure S239: Cyclic voltammogram of 2w in MeCN

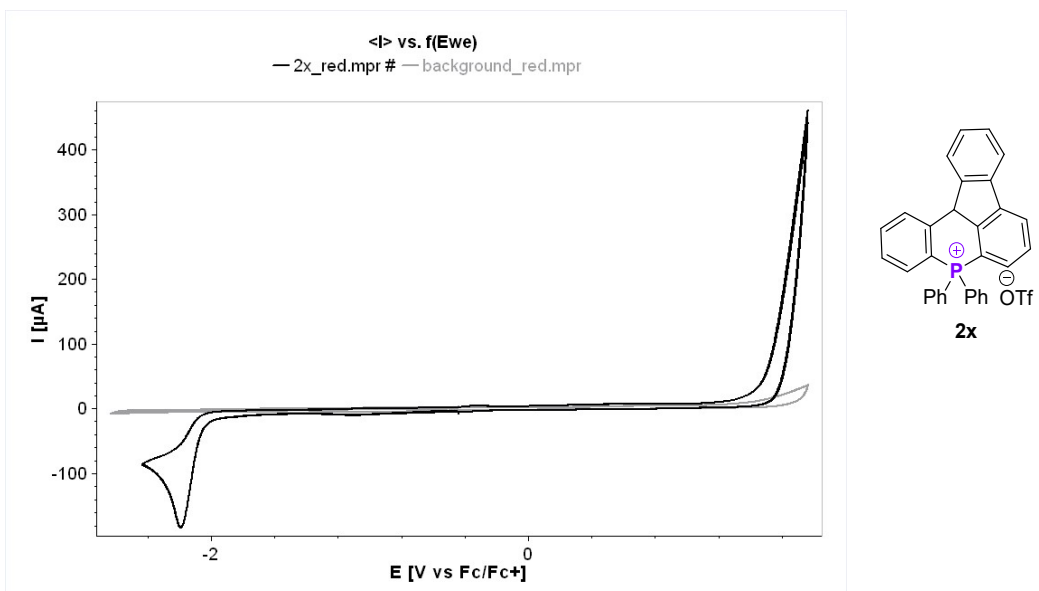


Figure S240: Cyclic voltammogram of 2x in MeCN

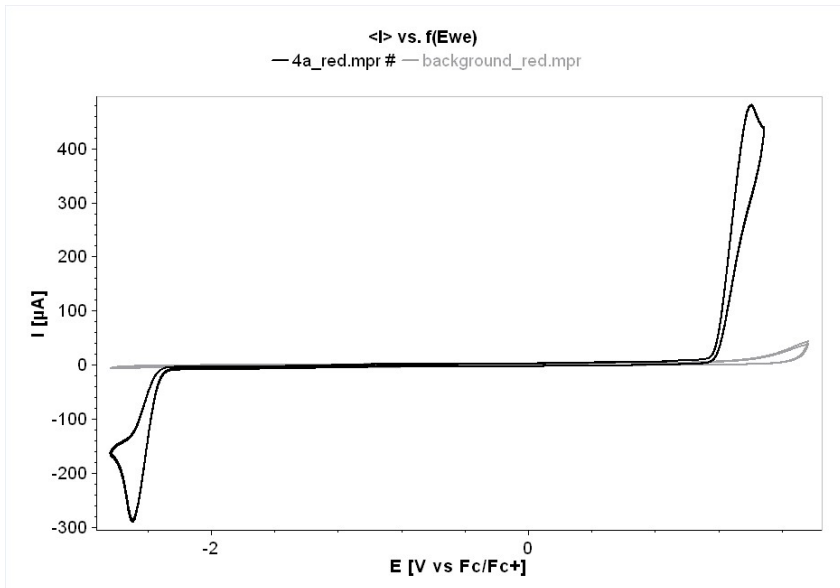


Figure S241: Cyclic voltammogram of 4a in MeCN

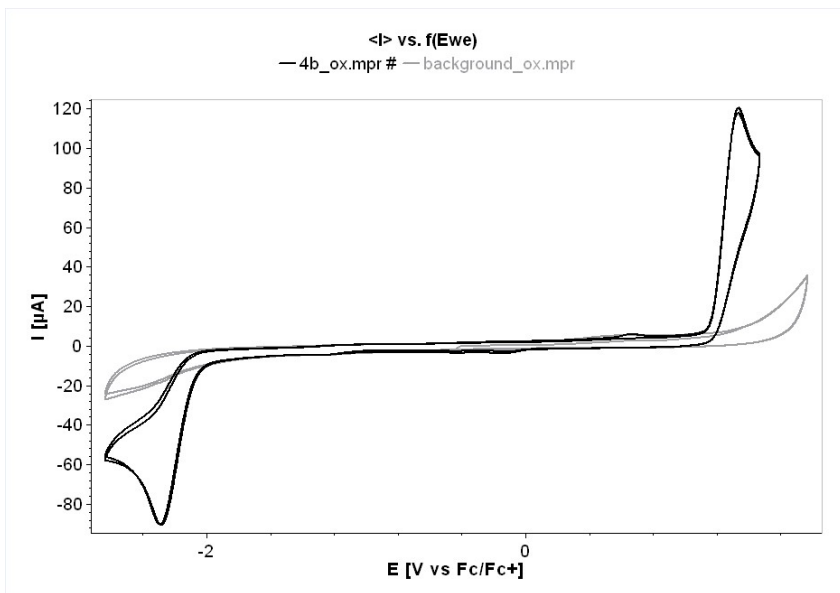


Figure S242: Cyclic voltammogram of 4b in MeCN

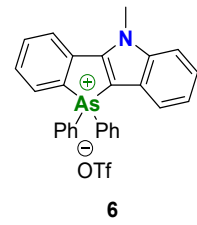
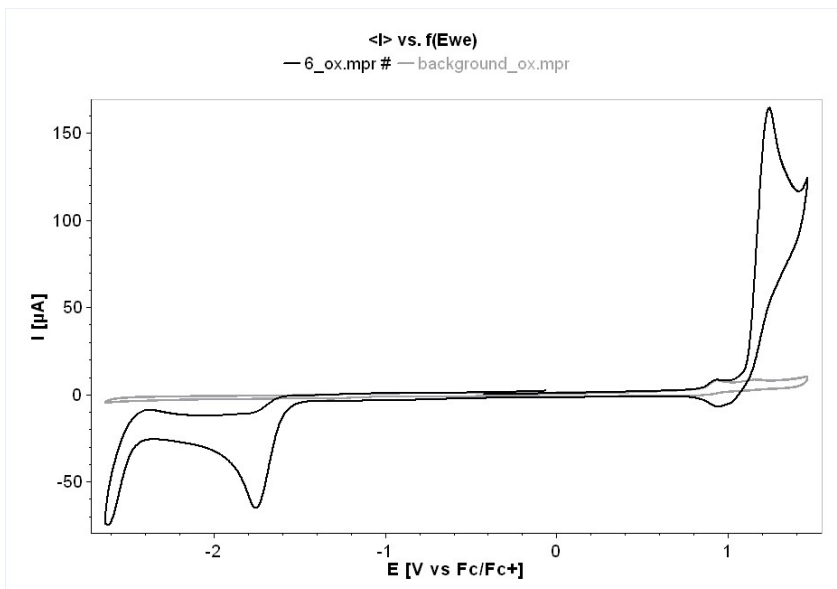


Figure S243: Cyclic voltammogram of 6 in MeCN

6. Computational studies

The ground-state equilibrium geometries of all compounds were optimized using the Møller-Plesset (MP2) method.¹³ Vertical excitation energies of the lowest excited states were computed with the second-order algebraic-diagrammatic construction (ADC(2)) method.^{14¹⁵} The ADC(2) method was also employed to determine the excited state equilibrium geometries.¹⁶ The calculations were performed with the Turbomole 7.3 program package and the valence double-zeta def2-SVP basis set of was used.¹⁷

Discussion and conclusions

A pivotal role of the charge-transfer (CT) states in determining the photophysical properties of the discussed class of compounds is emphasized by quantum-chemical computations. At the equilibrium geometry of the ground state, the vertical energy of these states is well above that of the lowest excited singlet states, which carry oscillator strength for optical excitation. As the absorbing, locally excited (LE) state has an equilibrium geometry similar to that of the ground state, the molecular geometry in the CT state undergoes more drastic changes upon energy relaxation. During relaxation, the electron density, initially distributed over two phenyl moieties, localizes on the phosphorus (or arsenic) atom. Neutralization of the atom changes its hybridization, and the two phenyl rings adopt a perpendicular orientation with respect to the molecular ring. Since the CT state is “dark” with respect to radiative transitions and intersects (or nearly intersects) the ground state, it serves as a pathway for fast nonradiative decay of electronic excitation. Its influence on the fluorescence yield depends on the relative energetics of the LE and CT states and the energetic barrier separating the minima of these states. Both factors are expected to be sensitive to the environment.

Table S3: Absorption ADC(2)/def2-SVP@MP2 geometry for 2b

 el. configuration			
State	E _{abs} /eV	f	el. configuration
S ₁	4.009	0.123	0.92(29a''-30a'')+0.25(28a''-31a'')
S ₂	4.660	0.044	0.53(29a''-31a'')-0.49(26a''-30a'')+0.47(28a''-30a'')
S ₃	5.016	0.008	0.61(27a''-61a')+0.39(28a''-62a')

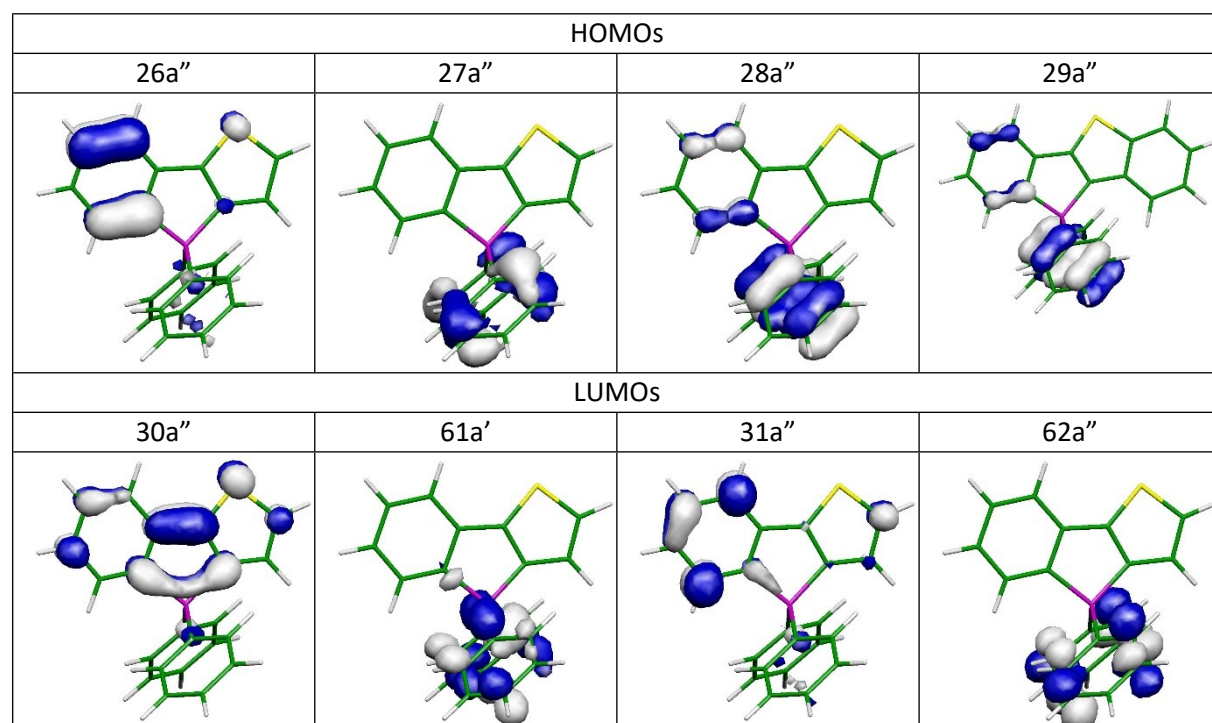


Table S4: Fluorescence ADC(2)/def2-SVP @ ADC(2)/def2-SVP geometry for 2b

State	E_{0-0}/eV	E_{flu}/eV	SOMO1	SOMO2
^1LE	3.586	3.205		
^1CT	3.446	3.205		

Table S5: Absorption ADC(2)/def2-SVP@MP2 geometry for 2c

State	E_{abs}/eV	f	el. configuration
S_1	4.077	0.095	$0.92(28a''-29a'')+0.21(28a''-30a'')$
S_2	4.740	0.050	$0.53(28a''-30a'')-0.51(25a''-29a'')+0.45(27a''-29a'')$
S_3	5.014	0.007	$0.61(26a''-58a')+0.39(27a''-59a')$

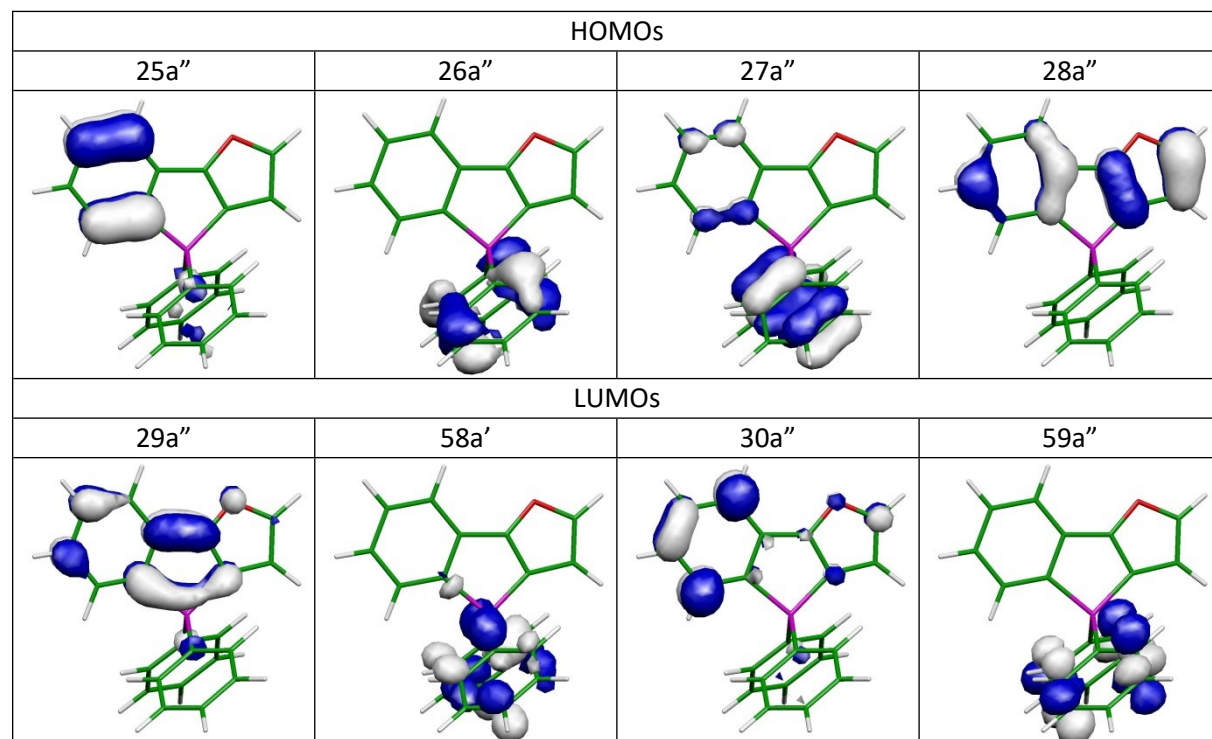


Table S6: Fluorescence ADC(2)/def2-SVP @ ADC(2)/def2-SVP geometry for 2c

State	E_{0-0}/eV	E_{flu}/eV	SOMO1	SOMO2
^1LE	3.618	3.203		
^1CT	3.380	0.543		

Table S7: Absorption ADC(2)/def2-SVP@MP2 geometry for 2d

State	E/eV	f	el. configuration
S_1	3.757	0.176	0.95(31a''-32a'')
S_2	3.991	0.121	0.94(30a''-32a'')
S_3	4.519	0.056	0.55(31a''-33a'')+0.50(27a''-32a'')+0.44(29a''-32a'')
S_4	4.886	0.001	0.86(31a''-72a')

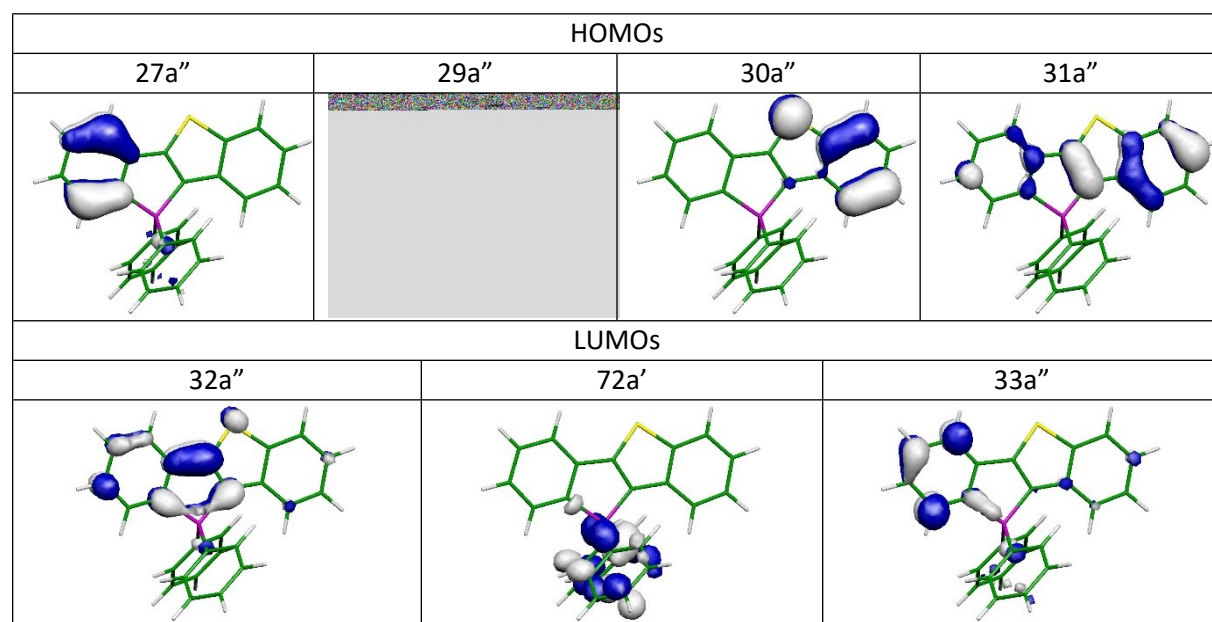


Table S8: Fluorescence ADC(2)/def2-SVP @ ADC(2)/def2-SVP geometry for 2d

State	E_{0-0}/eV	E_{flu}/eV	SOMO1	SOMO2
^1LE	3.317	2.905		
^1CT	2.541	1.823		

Table S9: Absorption ADC(2)/def2-SVP @ MP2/def2-SVP geometry for 2e

State	E/eV	f	el. configuration
S_1	3.826	0.188	0.94(30a''-31a'')
S_2	4.867	0.1055	0.90(29a''-31a'')
S_3	4.566	0.101	0.60(30a''-32a)+0.50(26a''-31a'')
S_4	4.928	0.002	0.82(30a''-69a')
HOMOs			
	26a''	29a''	30a''
LUMOs			
	31a''	69a'	32a''

Table S10: Fluorescence ADC(2)/def2-SVP @ ADC(2)/def2-SVP geometry for 2e

State	E_{0-0}/eV	E_{flu}/eV	SOMO1	SOMO2
^1LE	3.350	2.905		
^1CT	3.258	0.398		

Table S11: Absorption ADC(2)/def2-SVP@MP2 geometry for 2f

State	E/eV	f	el. configuration
S_1	3.742	0.133	0.93(30a''-31a'')
S_2	4.252	0.126	0.92(29a''-31a'')
S_3	4.533	0.172	0.69(30a''-32a'')+0.41(25a''-31a'')
S_4	4.774	0.0	0.91(30a''-69a')

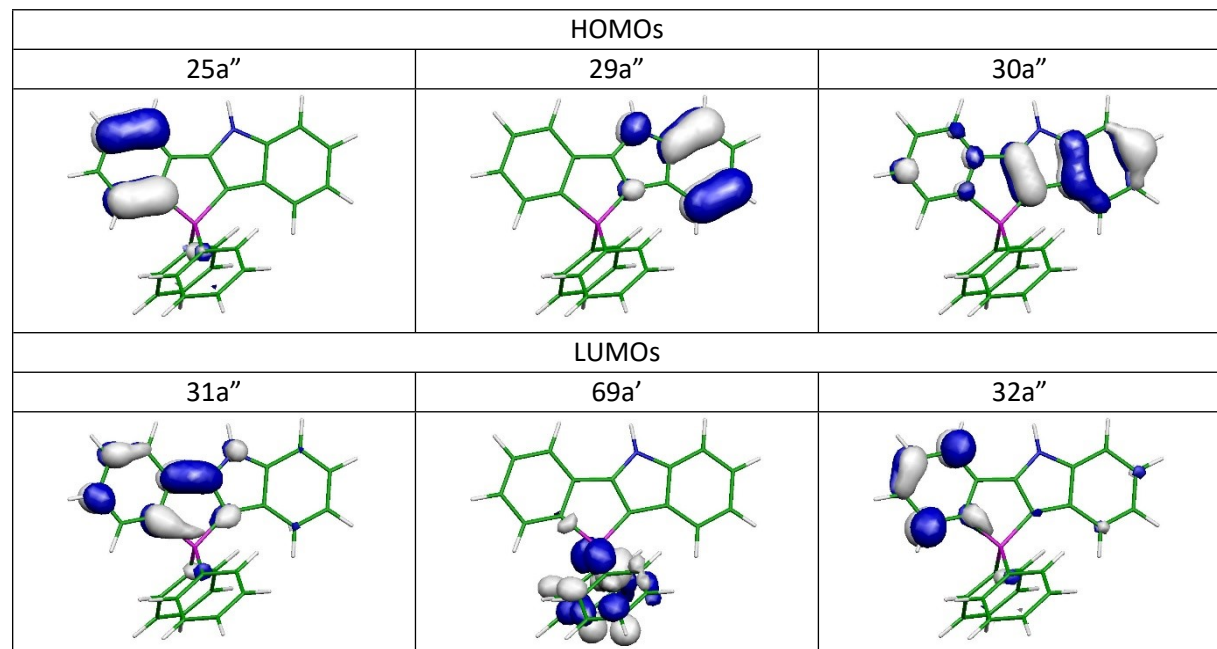


Table S12: Fluorescence ADC(2)/def2-SVP @ ADC(2)/def2-SVP geometry for 2f

State	E_{0-0}/eV	E_{flu}/eV	SOMO1	SOMO2
^1LE	3.286	2.857		
^1CT	3.186	0.271		

Table S13: Absorption ADC(2)/def2-SVP @ MP2/def2-SVP geometry for 2f'

 el. configuration			
State	E/eV	f	el. configuration
S_1	3.141	0.025	$0.85(30\text{a}''-31\text{a}'')+0.43(29\text{a}''-31\text{a}'')$
S_2	3.455	0.001	$0.74(30\text{a}''-69\text{a}')+0.61(29\text{a}''-69\text{a}')$
S_3	3.570	0.146	$0.83(29\text{a}''-31\text{a}'')-0.44(30\text{a}''-31\text{a}'')$
S_4	4.112	0.278	$0.80(30\text{a}''-32\text{a}'')+0.43(29\text{a}''-32\text{a}'')$

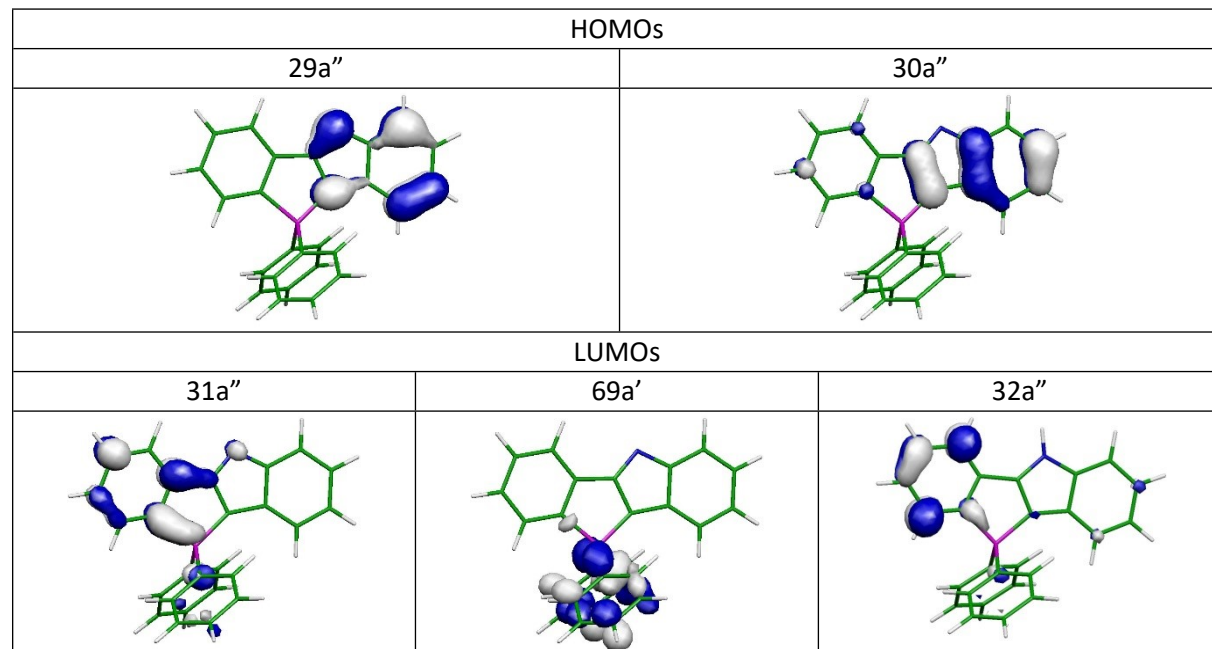


Table S14: Fluorescence ADC(2)/def2-SVP @ ADC(2)/def2-SVP geometry for 2f'

State	E_{0-0}/eV	E_{flu}/eV	SOMO1	SOMO2
^1LE	2.686	2.272		
^1CT	2.201	-1.629		

Table S15: Absorption ADC(2)/def2-SVP@MP2 geometry for 2g in C_1 symmetry

State	E/eV	f	el. configuration
^1LE	3.506	0.084	0.93(102a-103a)
^1LE	3.985	0.182	0.92(101a-103a)
$^1\text{LE}/^1\text{CT}$	4.457	0.177	0.60(102a-104a)-0.35(102a-106a)-0.33(96a-103a)
^1CT	4.626	0.042	0.70(102a-105a)+0.54(102a-104a)

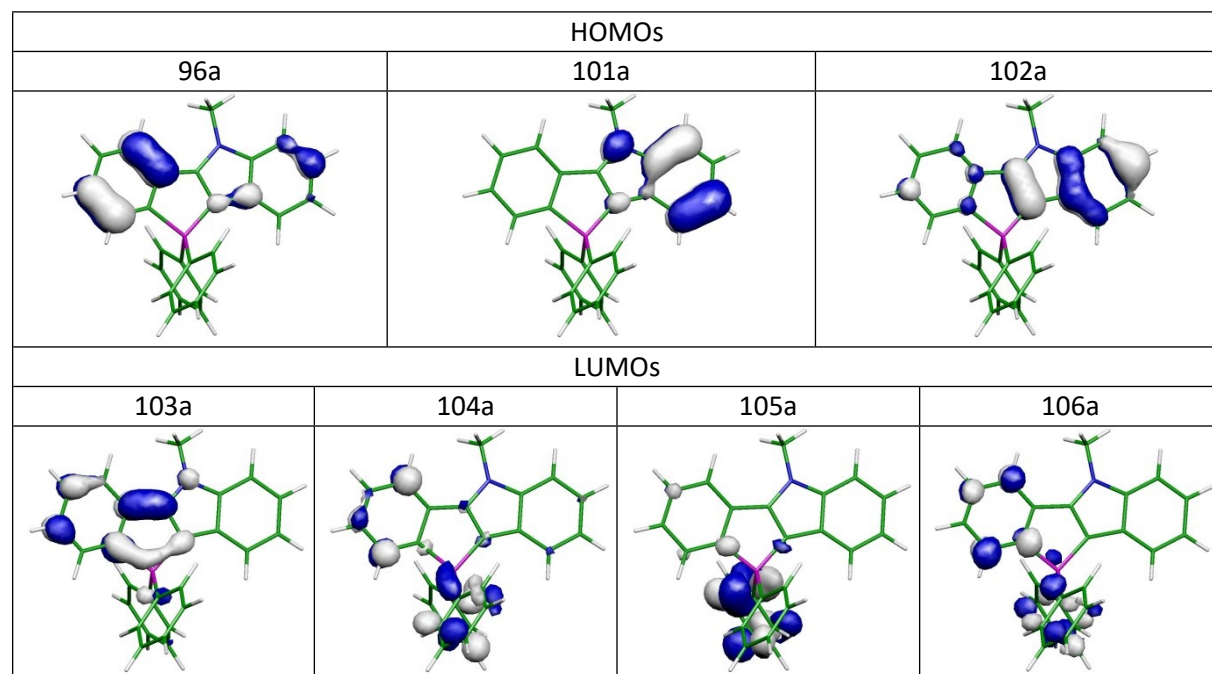
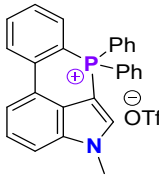


Table S16: Absorption ADC(2)/def2-SVP @ MP2/def2-SVP geometry for 2h

				
State	E/eV	f		el. configuration
S ₁	3.953	0.313		0.95(31a''-32a'')
S ₁	4.370	0.074		0.85(30a''-32a'')
S ₁	4.698	0.0		0.96(31a''-72a')

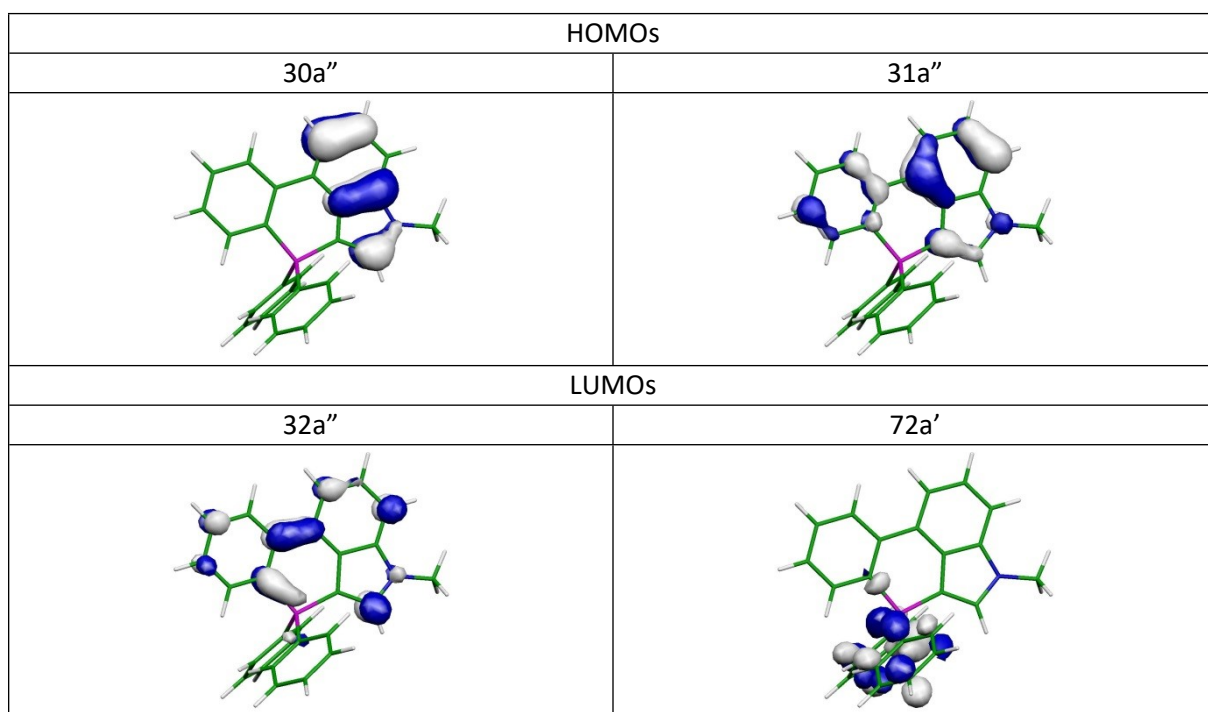


Table S17: Fluorescence ADC(2)/def2-SVP @ ADC(2)/def2-SVP geometry

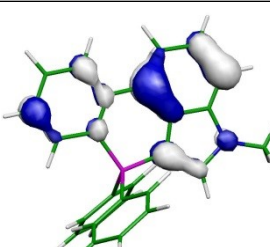
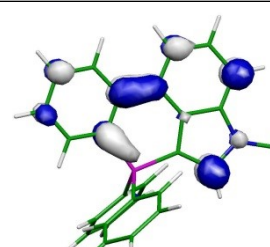
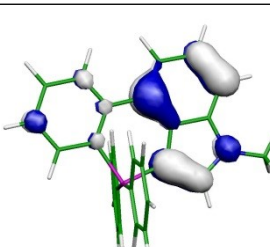
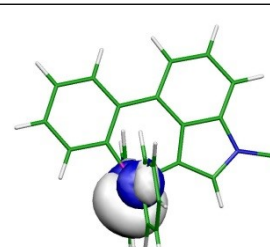
State	E ₀₋₀ /eV	E _{flu} /eV	SOMO1	SOMO2
¹ LE	3.682	3.48		
¹ CT	3.382	0.501		

Table S18: Absorption ADC(2)/def2-SVP @ MP2/def2-SVP geometry for 2i

State	E_{abs}/eV	f	el. configuration
S_1	4.309	0.126	0.82(118a-119a)
S_2	4.397	0.155	0.74(118a-120a)-0.34(118a-119a)+0.30(117a-119a)
S_3	4.498	0.159	0.67(117a-119a)-0.38(117a-120a)-0.32(118a-120a)

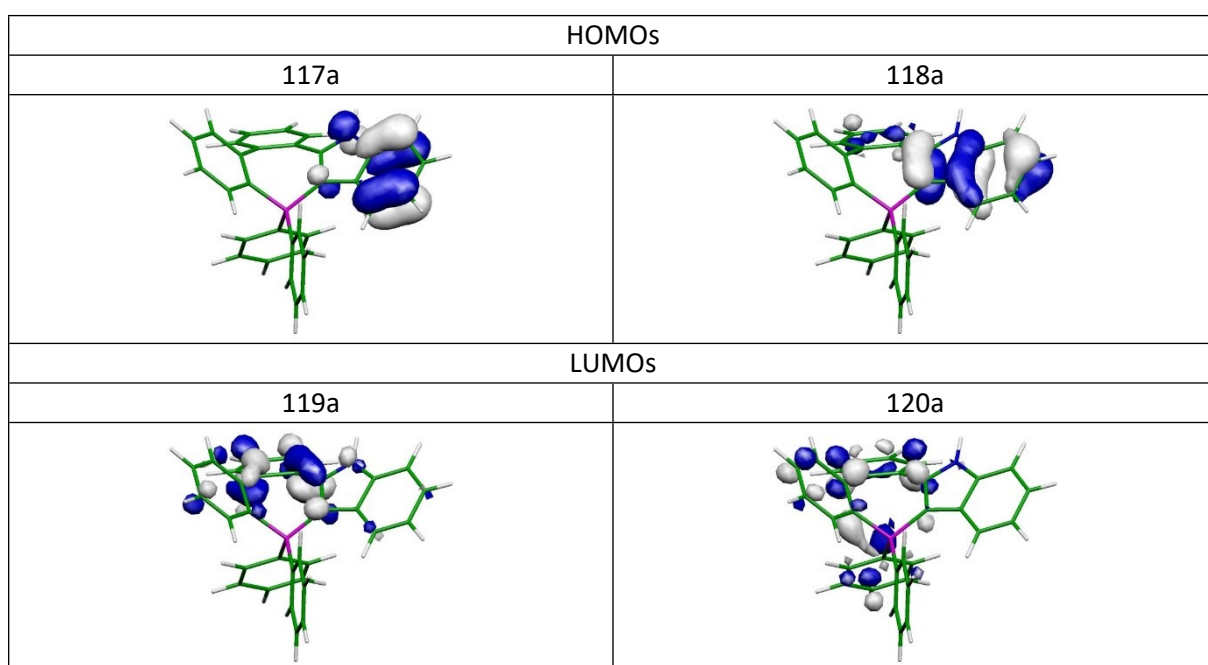


Table S19: Absorption ADC(2)/def2-SVP @ MP2/def2-SVP geometry for 2k

State	E_{abs}/eV	f	el. configuration
S_1	2.802	0.232	0.97(111au-112ag)
S_2	3.883	0.058	0.90(111au-113ag)
S_3	3.197	0.0	0.95(111au-112au)
S_4	3.878	0.0	0.93(111au-113au)
S_5	3.907	0.235	0.66(108au-112ag)+0.41(102au-112ag)-0.37(110au-112ag)

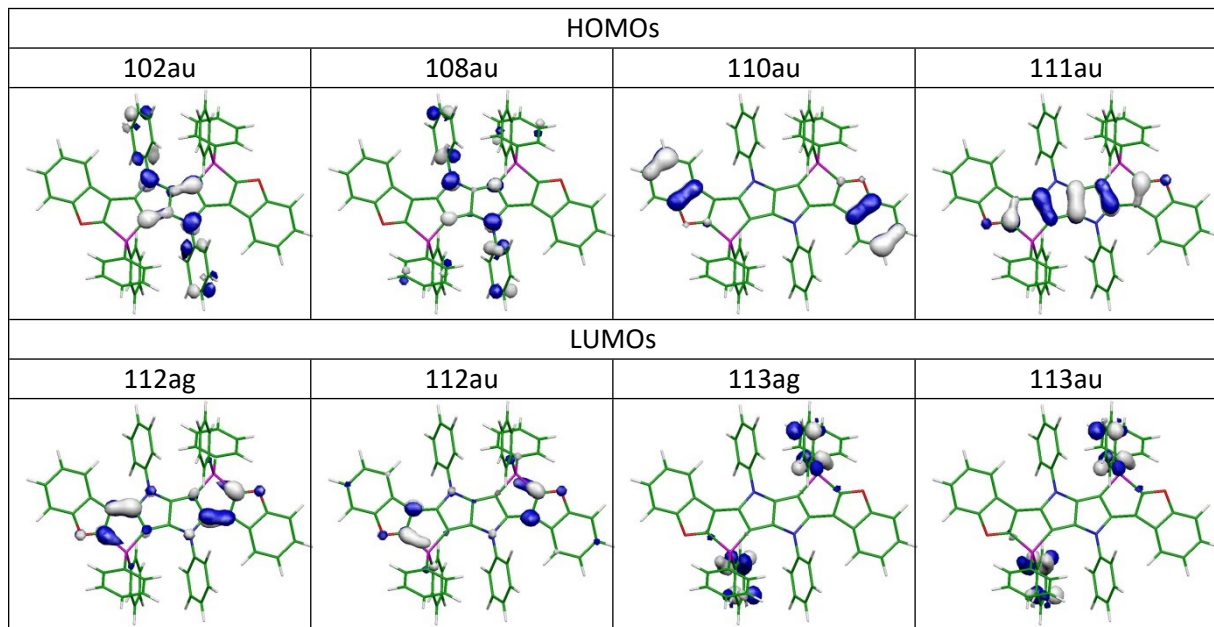
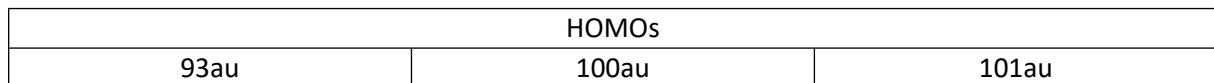


Table S20: Absorption ADC(2)/def2-SVP @ MP2/def2-SVP geometry for 2I

State	E_{abs}/eV	f	el. configuration
S_1	3.177	0.424	0.96(101au-102ag)
S_2	3.526	0.0	0.94(101au-102au)
S_3	3.944	0.194	0.83(100au-102ag)+0.38(93au-102ag)
S_4	4.210	0.350	0.85(101au-103ag)+0.20(100au-102ag)



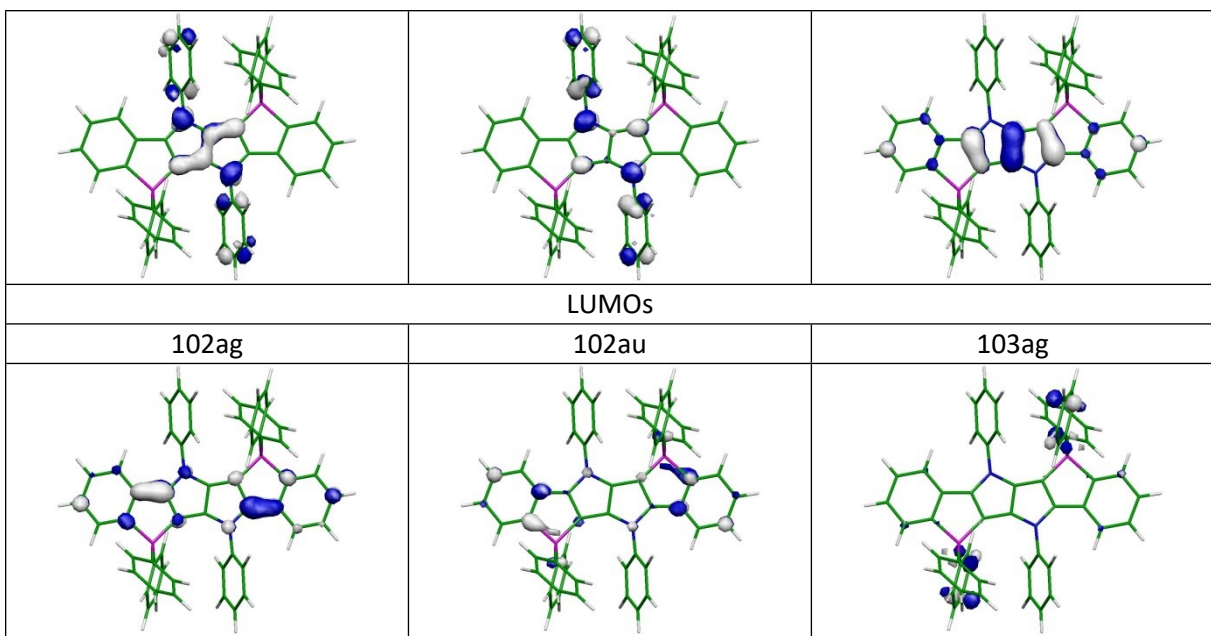


Table S21: Absorption ADC(2)/def2-SVP@MP2 geometry for 6

State	E _{abs} /eV	f	el. configuration
S ₁	3.729	0.136	0.92(34a''-35a'')
S ₂	4.138	0.177	0.92(33a''-35a'')
S ₃	4.536	0.162	0.72(34a''-36a')+0.42(30a''-35a')
S ₄	4.727	0.0	0.89(34a''-78a')

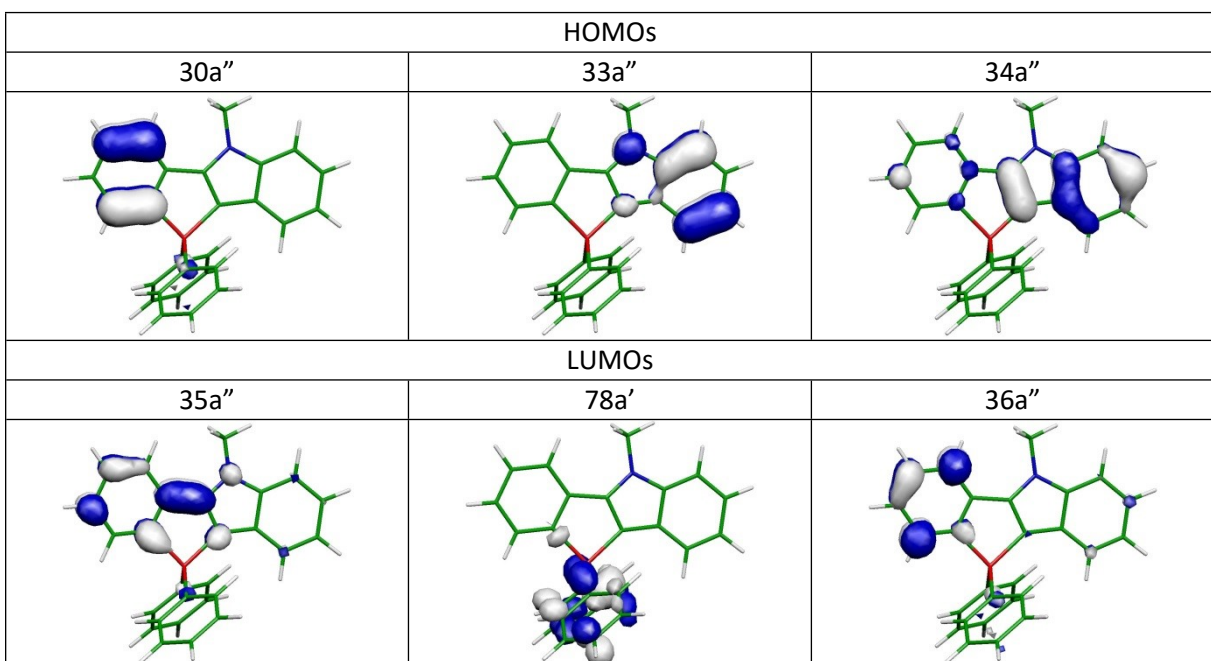


Table S22: Fluorescence ADC(2)/def2-SVP @ ADC(2)/def2-SVP geometry for 6

State	E_{0-0}/eV	E_{flu}/eV	SOMO1	SOMO2
^1LE	3.280	2.864		
^1CT	2.592	-0.164		

Table S23: Absorption ADC(2)/def2-SVP@MP2 geometry for 6 in C_1 symmetry

 State E/eV f el. configuration			
^1LE	3.595	0.106	0.93(111a-112a)
^1LE	4.037	0.189	0.92(110a-112a)
^1CT	4.501	0.198	0.48(111a-113a)+0.47(111a-114a)-0.36(111a-115a)-0.34(105a-112a)

HOMOs			
105a		110a	111a
LUMOs			
112a	113a	114a	115a

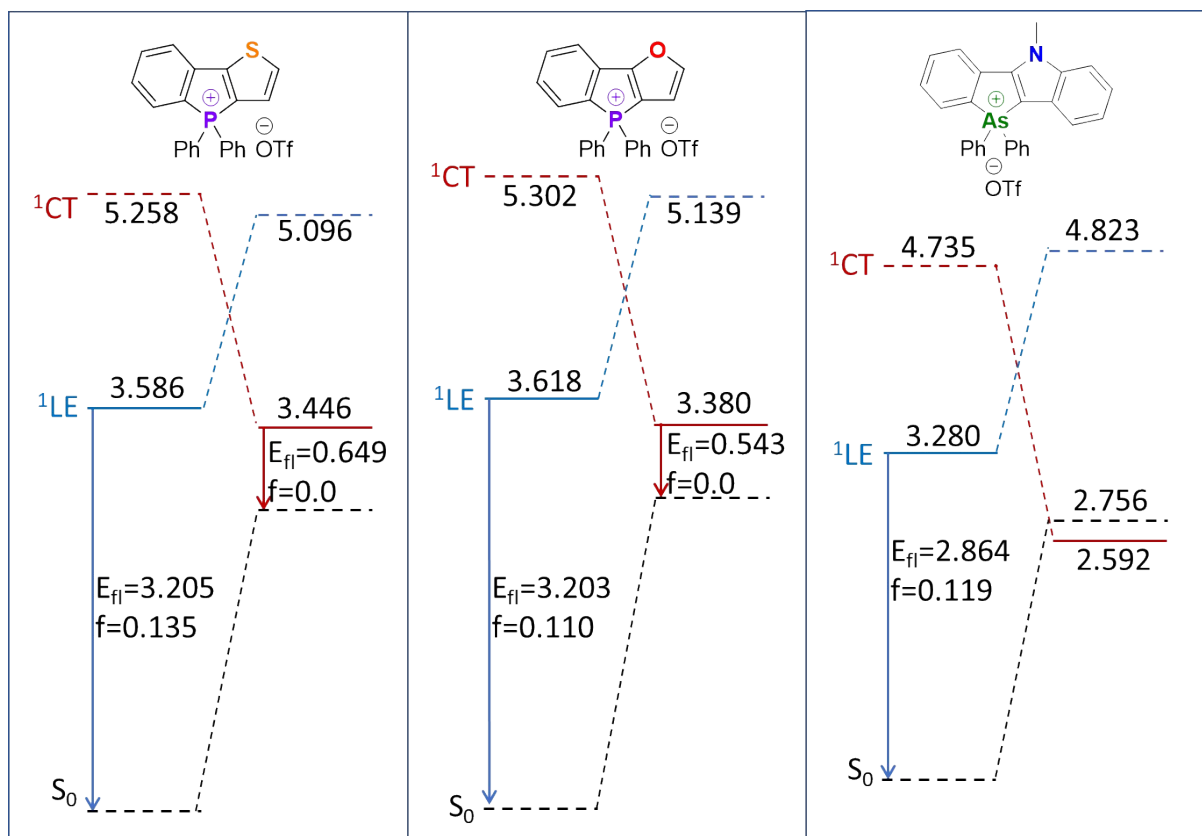
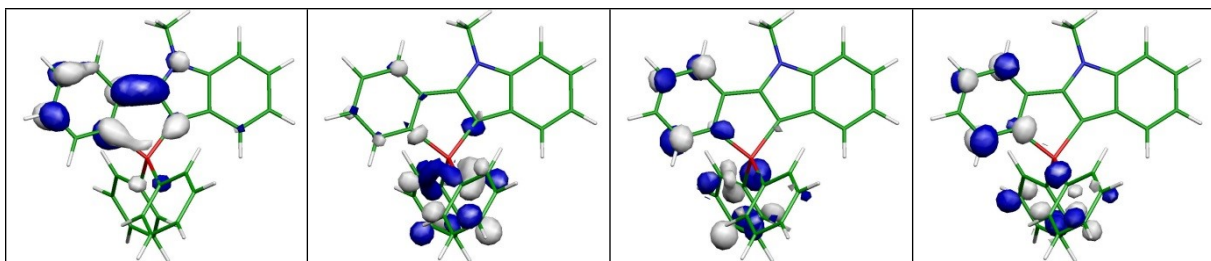


Figure S244: Relative energies of ^1LE and ^1CT in the ground and excited states optimized geometries for 2b,c and 6

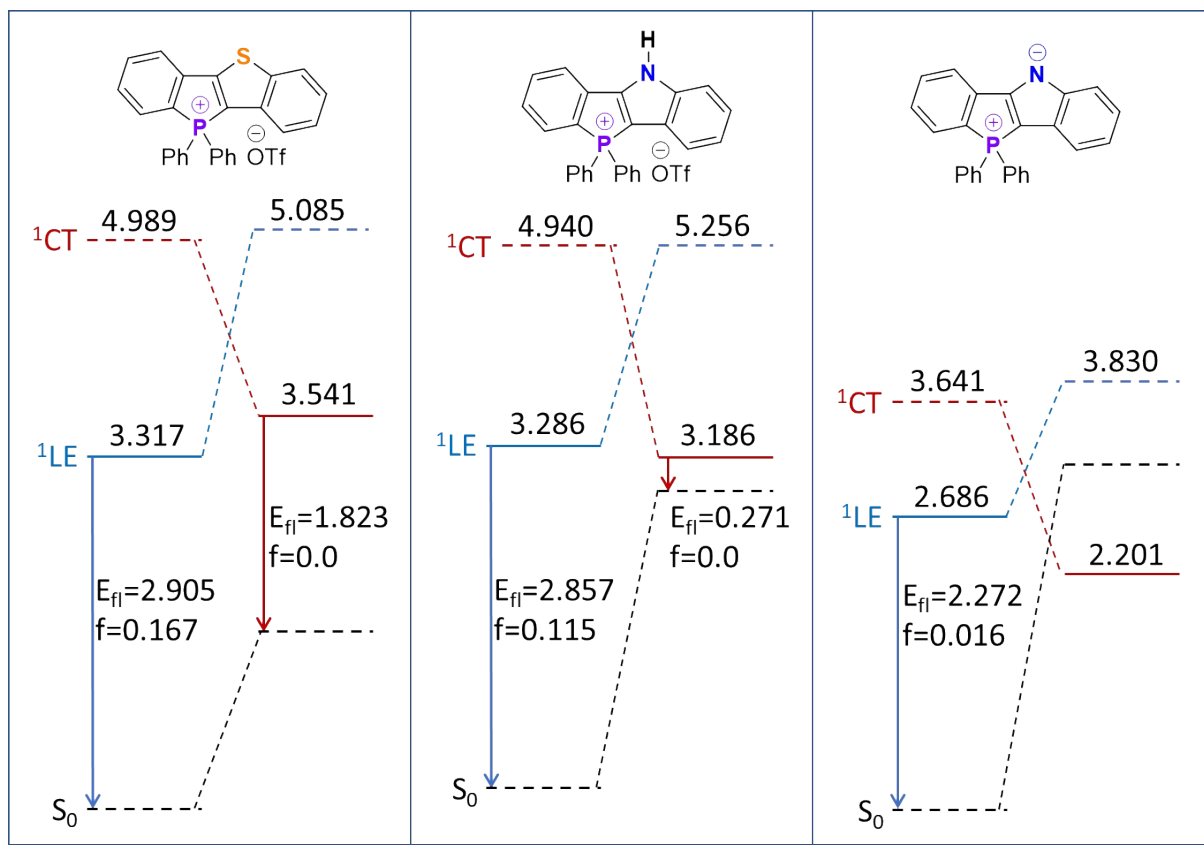


Figure S245: Relative energies of ^1LE and ^1CT in the ground and excited states optimized geometries for 2d,f,f'

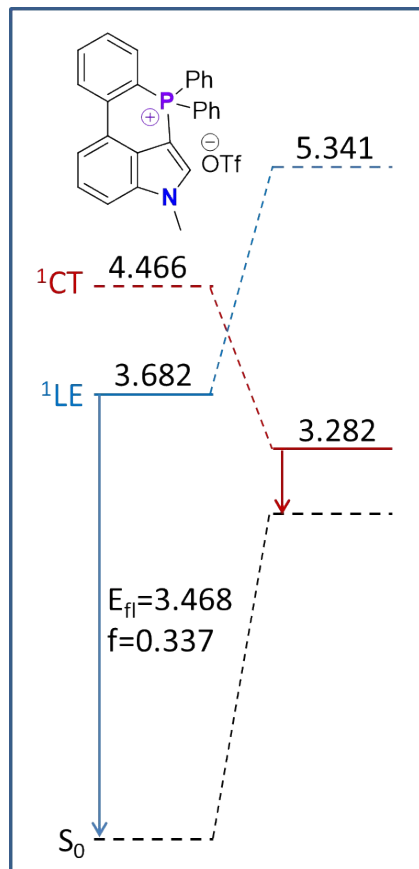


Figure S246: Relative energies of ^1LE and ^1CT in the ground and excited states optimized geometries for 2h

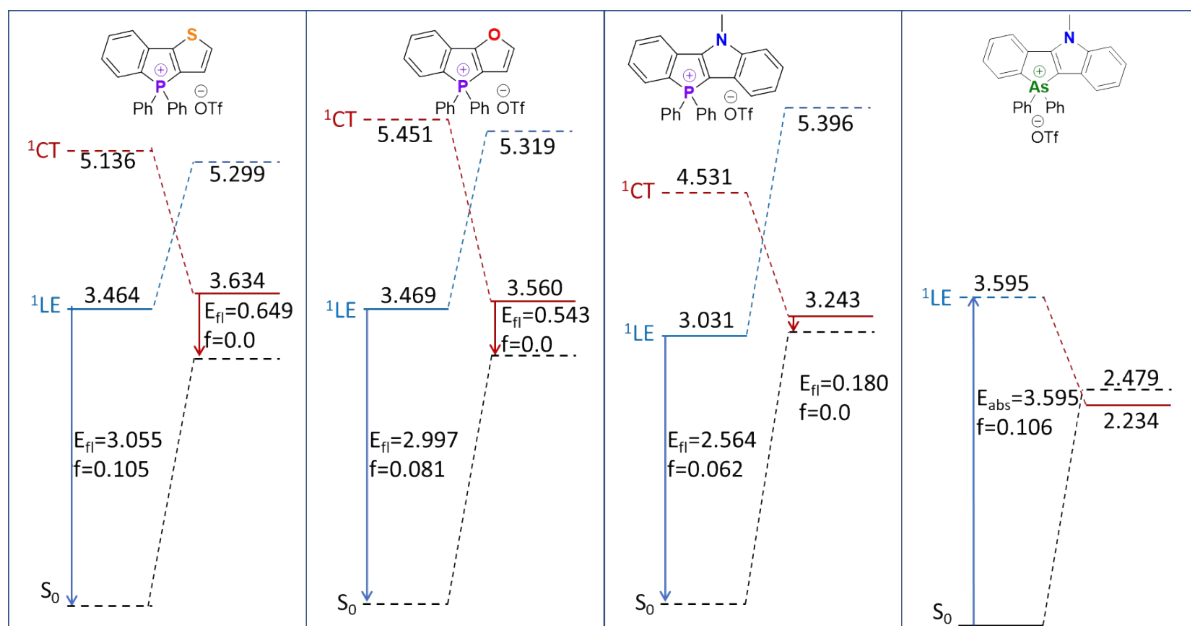


Figure S247: Relative energies of ^1LE and ^1CT in the ground and excited states optimized geometries for **2b,c,g** and **6** in C_1 symmetry

2f ^1GS MP2/def2-SVP geometry coordinates

FINAL HEAT OF FORMATION = -1393.419080

N	-3.341936	-0.233183	-0.011243
C	-3.297885	1.151637	0.028806
C	-1.925997	1.557933	0.049505
C	-1.172248	0.344590	0.030277
C	-2.077014	-0.725578	-0.010805
C	-4.350871	2.079384	0.044736
C	-4.007287	3.427887	0.086903
C	-2.655044	3.848836	0.109815
C	-1.609214	2.931788	0.093098
H	-5.395205	1.759275	0.027117
H	-4.799351	4.179707	0.100812
H	-2.433383	4.917793	0.140963
H	-0.568638	3.265686	0.107897
P	0.460082	-0.312086	-0.003835
C	-0.101418	-2.035391	-0.039590
C	-1.521421	-2.075083	-0.044479
C	1.405992	0.084695	1.462665
C	1.415013	0.082822	-1.467449
C	0.663554	-3.201780	-0.054948
C	-0.003531	-4.436657	-0.079039
C	-1.405387	-4.486195	-0.084383
C	-2.173871	-3.312795	-0.063980
H	1.756349	-3.161396	-0.047841
H	0.572472	-5.364358	-0.091907

H	-1.908554	-5.455624	-0.101494
H	-3.265305	-3.373103	-0.065491
C	2.766870	-0.272567	1.531966
C	3.475674	-0.027080	2.711626
C	2.834524	0.566063	3.808365
C	1.481556	0.921036	3.730839
C	0.755343	0.676893	2.560343
H	3.271496	-0.721314	0.671667
H	4.531877	-0.297861	2.775429
H	3.395166	0.758285	4.725821
H	0.988809	1.389280	4.585689
H	-0.300671	0.951570	2.492283
C	2.266878	1.203912	-1.458267
C	2.927137	1.567864	-2.636317
C	2.732648	0.828486	-3.810554
C	1.878384	-0.282530	-3.813925
C	1.208445	-0.658583	-2.645799
H	2.422336	1.778277	-0.541165
H	3.594309	2.432618	-2.637749
H	3.253113	1.116643	-4.726540
H	1.732216	-0.857569	-4.730878
H	0.539967	-1.523603	-2.647319
H	-4.194879	-0.783584	-0.034719

2f 1LE MP2/def2-SVP geometry coordinates

FINAL HEAT OF FORMATION = -1393.304400

N	-3.349623	-0.635894	0.017361
C	-3.400157	0.765213	0.053170
C	-2.045657	1.266080	0.042854
C	-1.205465	0.143947	-0.020063
C	-2.070427	-1.053971	-0.016414
C	-4.495086	1.605810	0.105627
C	-4.237893	2.996852	0.135671
C	-2.927483	3.514996	0.121353
C	-1.822366	2.665763	0.072463
H	-5.519333	1.226062	0.117217
H	-5.084959	3.685809	0.174957
H	-2.781015	4.596548	0.145696
H	-0.803191	3.059660	0.065388
P	0.500421	-0.347111	-0.018487
C	0.049968	-2.061871	0.041098
C	-1.394047	-2.279942	-0.075197
C	1.499725	0.099497	1.419744
C	1.339501	0.402271	-1.441326
C	0.913109	-3.184846	0.022595
C	0.368693	-4.462082	-0.053210
C	-1.039963	-4.678011	-0.163550
C	-1.909438	-3.601738	-0.160055
H	1.997208	-3.053059	0.092519
H	1.036643	-5.327605	-0.045837

H	-1.425555	-5.696284	-0.244759
H	-2.988773	-3.764324	-0.241911
C	1.491921	-0.747666	2.544531
C	2.164655	-0.356257	3.706406
C	2.800086	0.891412	3.768121
C	2.780428	1.746036	2.657575
C	2.127888	1.359410	1.482081
H	0.976167	-1.710777	2.498696
H	2.182722	-1.022054	4.572347
H	3.314878	1.196700	4.681860
H	3.274860	2.719018	2.707565
H	2.127537	2.021859	0.612333
C	2.739596	0.296860	-1.557635
C	3.369914	0.740206	-2.725908
C	2.614591	1.271758	-3.779003
C	1.220077	1.362360	-3.665428
C	0.576295	0.909015	-2.510137
H	3.335132	-0.110379	-0.735507
H	4.456315	0.666122	-2.815433
H	3.111940	1.615672	-4.688588
H	0.631176	1.773895	-4.488628
H	-0.513294	0.961507	-2.430165
H	-4.166620	-1.241429	0.044921

2f 1CT MP2/def2-SVP geometry coordinates

FINAL HEAT OF FORMATION = -1393.297250

N	-2.712100	-0.000995	0.000000
C	-2.589249	1.390558	0.000000
C	-1.186027	1.715934	0.000000
C	-0.493030	0.501125	0.000000
C	-1.484245	-0.553790	0.000000
C	-3.573984	2.368463	0.000000
C	-3.134501	3.704449	0.000000
C	-1.762307	4.054356	0.000000
C	-0.777784	3.075800	0.000000
H	-4.638747	2.125893	0.000000
H	-3.882355	4.501018	0.000000
H	-1.483649	5.109566	0.000000
H	0.284731	3.328482	0.000000
P	1.208404	-0.198843	0.000000
C	0.452233	-1.886673	0.000000
C	-0.976039	-1.886738	0.000000
C	1.327590	-0.050945	1.938532
C	1.327590	-0.050945	-1.938532
C	1.147172	-3.098669	0.000000
C	0.418991	-4.296052	0.000000
C	-0.992729	-4.300137	0.000000
C	-1.698629	-3.102260	0.000000
H	2.239923	-3.114815	0.000000
H	0.954073	-5.248993	0.000000

H -1.529697 -5.250918 0.000000
H -2.792350 -3.104857 0.000000
C 2.367202 0.762822 2.420209
C 2.492636 0.993853 3.796966
C 1.587173 0.414363 4.695231
C 0.556442 -0.403214 4.213748
C 0.419629 -0.638811 2.837873
H 3.081477 1.206560 1.719161
H 3.305298 1.622579 4.170134
H 1.689943 0.591177 5.768107
H -0.144885 -0.867182 4.912746
H -0.383516 -1.294793 2.488227
C 2.367202 0.762822 -2.420209
C 2.492636 0.993853 -3.796966
C 1.587173 0.414363 -4.695231
C 0.556442 -0.403214 -4.213748
C 0.419629 -0.638811 -2.837873
H 3.081477 1.206560 -1.719161
H 3.305298 1.622579 -4.170134
H 1.689943 0.591177 -5.768107
H -0.144885 -0.867182 -4.912746
H -0.383516 -1.294793 -2.488227
H -3.596080 -0.504718 0.000000

7. Bioimaging

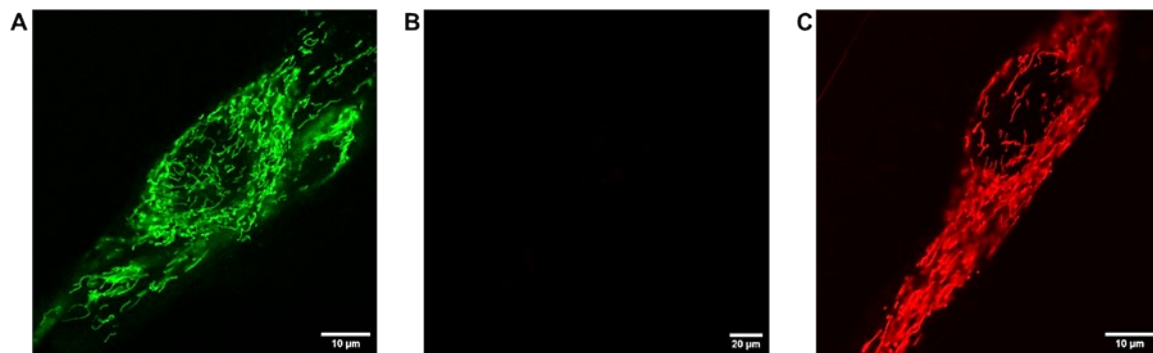


Figure S248: Intracellular localization of 2g compound and Mito Red as detected using confocal fluorescence microscopy. (A; B). the fluorescence of 2g compound excitation wavelength 405 nm and (A) emission wavelength 510±50 nm and (B) excitation wavelength 559 nm and emission wavelength 594±30 nm. (C) the fluorescence of Mito Red recorded with 559 nm excitation wavelength and emission wavelength 594±30 nm. Scale bar 10 µm for (A) and (C) and 20 µm for (B)

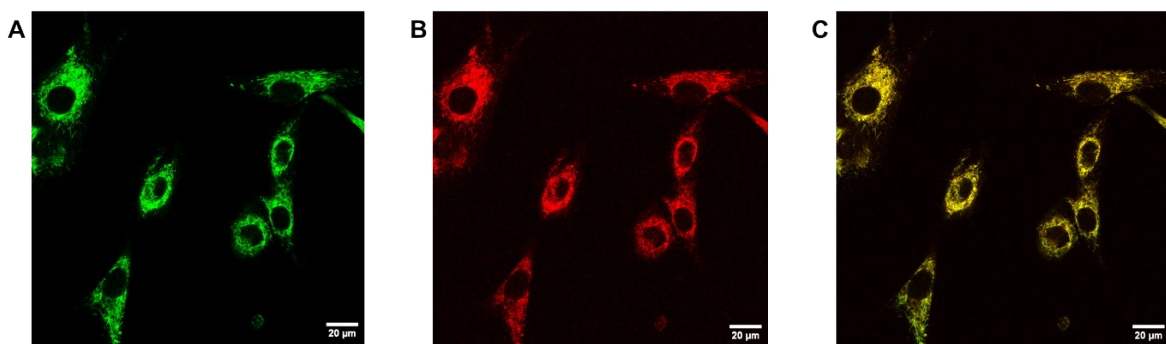


Figure S249: Intracellular localization of 2g compound and Mito Red as detected using confocal fluorescence microscopy. (A) fluorescence of 2g compound excitation wavelength 405 nm emission wavelength 500±50 nm, (B) fluorescence of Mito Red compound excitation wavelength 405 nm emission wavelength 594±50 nm nm . (C) overlay picture recorded sequentially as at (A) and (B) parameters for two fluorophores in living cells U-87. Scale bar 20 µm.

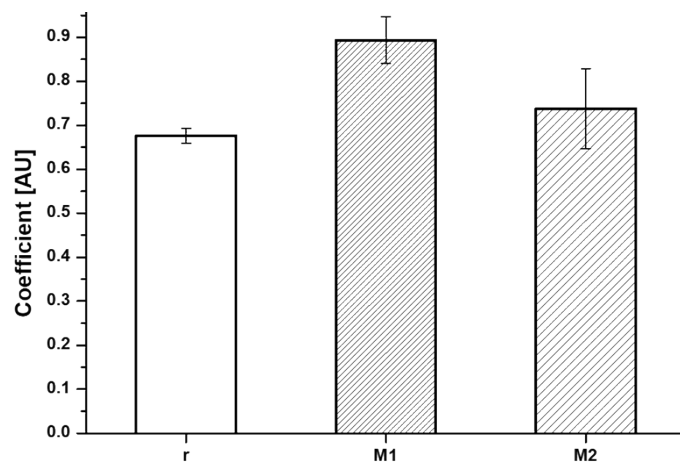


Figure S250: Pearson's coefficient r and Manders' coefficients M1 and M2 of colocalization 2g compound and Mito Red. Columns represent the coefficient value and bars ±SEM, n value 9 cells from 3 independent experiments.

Cell culture conditions

The U-87 cell line was cultured at 37°C in a humidified atmosphere containing 5% CO₂ in DMEM supplemented with 10% fetal bovine serum, 2 mM glutamine, 100 U/ml penicillin, and 100 µg/ml streptomycin.

Fluorescence of **2g and Mito Red in U87 cell line**

Fluorescence localization of **2g** within the cells. The U-87 cells were loaded with fluorophores in DMEM medium supplemented with 10% fetal bovine serum, 2 mM glutamine, 100 U/ml penicillin, and 100 µg/ml streptomycin at 37°C in a humidified atmosphere containing 5% CO₂ for 15 to 30 minutes with the **4a** compound at the final concentration ranging from 500 nM. The final concentration of the Mito Red was 100 nM and Pluronic 127 was added to reach the final concentration in medium 0.2%. Both fluorophores were dissolved in DMSO. Before measurements, the incubation medium was replaced with FluoroBrite™ DMEM. The measurements were performed with the use of Olympus IX83 confocal microscope with the water objective 60x UPLSAPO 60XW. Registered data were transferred to the Image and analyzed for presentation.

8. X-ray analysis

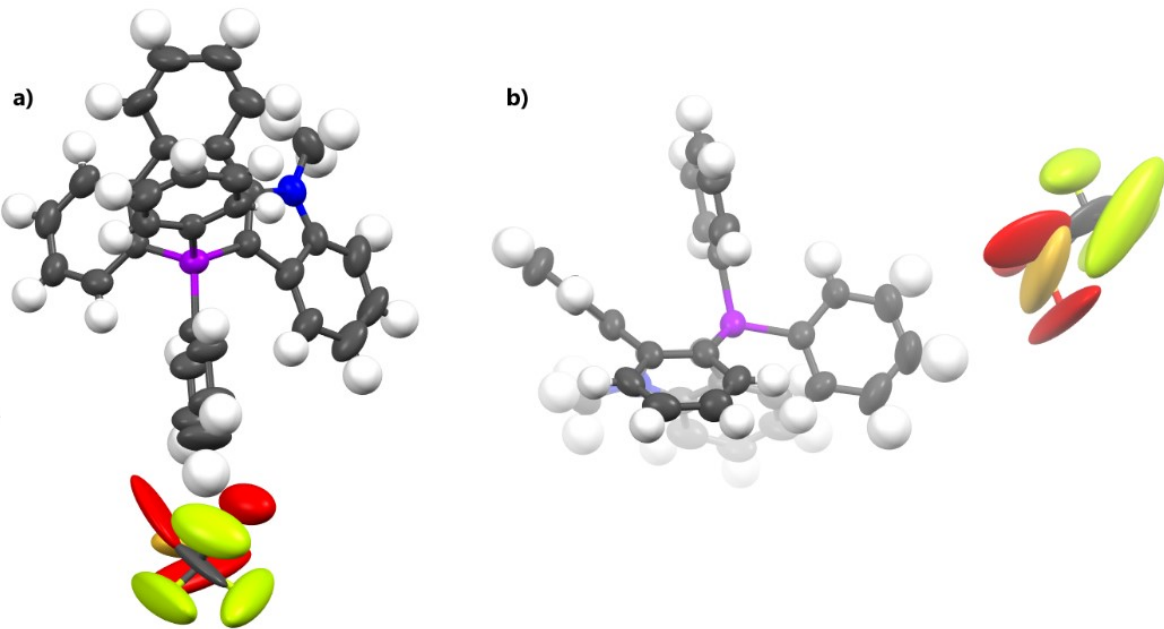


Figure S251: X-ray crystal structure of **2i** shown with 50% probability ellipsoids. a) – top view, b) side view with applied depth cue

A colorless needle-like specimen of $C_{34}H_{25}F_3NO_3PS$ (**2i**), approximate dimensions 0.128 mm x 0.298 mm x 0.310 mm, was used for the X-ray crystallographic analysis.

Table S24: Sample and crystal data for **2i**

Chemical formula	$C_{34}H_{25}NO_3PS$
Formula weight	615.58 g/mol
Temperature	296(2) K
Wavelength	1.54178 Å
Crystal size	0.128 x 0.298 x 0.310 mm
Crystal habit	Colorless needle
Crystal system	monoclinic
Space group	$P_{1}21/c\ 1$
Unit cell dimensions	$a = 12.7109(7)$ Å / $\alpha = 90^\circ$ $b = 27.0146(15)$ Å / $\beta = 108.653(4)^\circ$ $c = 9.0263(6)$ Å / $\gamma = 90^\circ$
Volume	2936.6(3) Å ³
Z	4
Density (calculated)	1.392 g/cm ³
Absorption coefficient	1.392 mm ⁻¹
F(000)	1272

Table S25: Data collection and structure refinement for **2i**

Theta range for data collection	3.27 to 69.07 °
Index ranges	-14≤h≤14, -24≤k≤30, -10≤l≤7
Reflections collected	13897
Independent reflections	3614 [R(int) = 0.0752]
Coverage of independent reflections	66.0%

Absorption correction	numerical
Max. and min. transmission	0.7860 and 0.5800
Structure solution technique	direct methods
Structure solution program	SHELXL-2014 (Sheldrick, 2014)
Refinement method	Full-matrix least-squares on F^2
Refinement program	SHELXL-2014 (Sheldrick, 2014)
Function minimized	$\sum w(F_o^2 - F_c^2)^2$
Data / restraints / parameters	3614 / 16 / 390
Goodness-of-fit on F^2	1.057
$\Delta/\sigma_{\text{max}}$	0.008
Final R indices	2119 data; $I > 2\sigma(I)$ $R_1 = 0.1489$, $wR_2 = 0.3481$ all data $R_1 = 0.2149$, $wR_2 = 0.3921$ $w = 1/[\sigma^2(F_o^2) + (0.1516P)^2 + 22.6325P]$ where $P = (F_o^2 + 2F_c^2)/3$
Weighting scheme	
Extinction coefficient	0.0008(4)
Largest diff. peak and hole	1.231 and -1.049 e \AA^{-3}
R.M.S. deviation from mean	0.104 e \AA^{-3}

Table S26: Atomic coordinates and equivalent isotropic atomic displacement parameters (\AA^2) for 2i. $U(\text{eq})$ is defined as one third of the trace of the orthogonalized U_{ij} tensor.

	x/a	y/b	z/c	U(eq)
P1	0.3817(2)	0.37959(9)	0.6041(4)	0.0540(10)
N2	0.1491(7)	0.2971(3)	0.6640(11)	0.060(2)
C26	0.2230(8)	0.4166(4)	0.3421(13)	0.059(3)
C17	0.5380(9)	0.4106(4)	0.8854(16)	0.064(3)
C22	0.3625(9)	0.4740(4)	0.4839(16)	0.070(3)
C33	0.0535(9)	0.2890(5)	0.7201(15)	0.081(4)
C15	0.3430(8)	0.4245(3)	0.8576(14)	0.049(3)
C1	0.2063(9)	0.2596(4)	0.6237(14)	0.060(3)
C2	0.1895(12)	0.2080(4)	0.6217(15)	0.082(4)
C3	0.2591(13)	0.1776(5)	0.5775(17)	0.085(4)
C6	0.2951(9)	0.2783(4)	0.5841(14)	0.064(3)
C4	0.3429(14)	0.1964(4)	0.5294(17)	0.091(4)
C5	0.3634(10)	0.2468(4)	0.5338(14)	0.073(3)
C8	0.2005(8)	0.3408(4)	0.6573(13)	0.056(3)
C7	0.2907(8)	0.3317(3)	0.6079(13)	0.056(3)
C9	0.1562(8)	0.3892(4)	0.6818(13)	0.055(3)
C10	0.2214(8)	0.4279(4)	0.7687(14)	0.058(3)
C11	0.1699(11)	0.4721(4)	0.7777(16)	0.080(4)
C14	0.0431(9)	0.3983(5)	0.6039(16)	0.078(4)
C16	0.4238(8)	0.4073(3)	0.7916(13)	0.051(3)
C19	0.4906(11)	0.4456(4)	0.0962(15)	0.073(4)
C20	0.3800(10)	0.4436(4)	0.0103(15)	0.065(3)
C18	0.5694(10)	0.4296(4)	0.0318(17)	0.071(4)
C21	0.3179(8)	0.4273(4)	0.4675(13)	0.052(3)
C25	0.1746(9)	0.4544(5)	0.2353(15)	0.075(4)
C24	0.2201(10)	0.5004(5)	0.2548(17)	0.078(4)
C23	0.3123(11)	0.5106(4)	0.3777(18)	0.082(4)
C27	0.4985(9)	0.3551(4)	0.5620(16)	0.063(3)
C28	0.5702(10)	0.3226(5)	0.6674(16)	0.083(4)
C32	0.5139(10)	0.3656(5)	0.4187(18)	0.080(4)
C31	0.6001(12)	0.3436(6)	0.3828(19)	0.108(5)

C29	0.6592(12)	0.3022(6)	0.625(3)	0.115(6)
C30	0.6740(14)	0.3131(8)	0.486(3)	0.133(7)
F1	0.8098(11)	0.3844(5)	0.920(2)	0.280(10)
C13	0.9945(10)	0.4429(6)	0.6162(19)	0.094(5)
C12	0.0589(11)	0.4790(5)	0.7031(19)	0.097(5)
C34	0.8845(10)	0.3586(6)	0.020(2)	0.183(13)
S1	0.8500(10)	0.3389(6)	0.1817(15)	0.456(15)
O1	0.7278(11)	0.3221(4)	0.0913(19)	0.182(6)
O2	0.914(2)	0.3065(9)	0.270(2)	0.51(3)
F3	0.9843(10)	0.3749(6)	0.048(3)	0.57(3)
F2	0.8870(12)	0.3095(6)	0.9498(18)	0.375(17)
O3	0.8487(13)	0.3895(5)	0.200(3)	0.320(18)

Table S27: Bond lengths (Å) for 2i

P1-C7	1.743(10)	P1-C27	1.774(11)
P1-C16	1.769(11)	P1-C21	1.790(11)
N2-C8	1.360(12)	N2-C1	1.362(13)
N2-C33	1.475(13)	C26-C25	1.404(15)
C26-C21	1.396(14)	C26-H26	0.93
C17-C18	1.354(15)	C17-C16	1.430(14)
C17-H17	0.93	C22-C21	1.371(14)
C22-C23	1.381(16)	C22-H22	0.93
C33-H33A	0.96	C33-H33B	0.96
C33-H33C	0.96	C15-C20	1.405(15)
C15-C16	1.421(13)	C15-C10	1.499(14)
C1-C6	1.383(14)	C1-C2	1.409(15)
C2-C3	1.357(18)	C2-H2	0.93
C3-C4	1.369(18)	C3-H3	0.93
C6-C5	1.392(15)	C6-C7	1.462(14)
C4-C5	1.386(16)	C4-H4	0.93
C5-H5	0.93	C8-C7	1.377(14)
C8-C9	1.469(14)	C9-C10	1.408(14)
C9-C14	1.406(14)	C10-C11	1.378(14)
C11-C12	1.367(17)	C11-H11	0.93
C14-C13	1.375(17)	C14-H14	0.93
C19-C20	1.373(15)	C19-C18	1.379(17)
C19-H19	0.93	C20-H20	0.93
C18-H18	0.93	C25-C24	1.358(16)
C25-H25	0.93	C24-C23	1.359(17)
C24-H24	0.93	C23-H23	0.93
C27-C28	1.397(15)	C27-C32	1.398(16)
C28-C29	1.416(18)	C28-H28	0.93
C32-C31	1.373(16)	C32-H32	0.93
C31-C30	1.37(2)	C31-H31	0.93
C29-C30	1.36(2)	C29-H29	0.93
C30-H30	0.93	F1-C34	1.285(13)
C13-C12	1.351(18)	C13-H13	0.93
C12-H12	0.93	C34-F3	1.289(13)
C34-S1	1.737(16)	C34-F2	1.476(16)
S1-O2	1.283(13)	S1-O3	1.379(15)
S1-O1	1.573(14)		

Table S28: Bond angles (°) for 2i

C7-P1-C27	109.5(5)	C7-P1-C16	107.1(5)
C27-P1-C16	110.2(5)	C7-P1-C21	113.0(5)
C27-P1-C21	110.3(5)	C16-P1-C21	106.6(5)
C8-N2-C1	109.1(8)	C8-N2-C33	127.2(10)
C1-N2-C33	123.5(9)	C25-C26-C21	118.7(10)
C25-C26-H26	120.6	C21-C26-H26	120.6
C18-C17-C16	121.8(11)	C18-C17-H17	119.1
C16-C17-H17	119.1	C21-C22-C23	119.9(11)
C21-C22-H22	120.0	C23-C22-H22	120.0
N2-C33-H33A	109.5	N2-C33-H33B	109.5
H33A-C33-H33B	109.5	N2-C33-H33C	109.5
H33A-C33-H33C	109.5	H33B-C33-H33C	109.5
C20-C15-C16	118.2(10)	C20-C15-C10	117.9(9)
C16-C15-C10	123.7(10)	N2-C1-C6	110.3(9)
N2-C1-C2	130.3(11)	C6-C1-C2	119.5(12)
C3-C2-C1	119.4(13)	C3-C2-H2	120.3
C1-C2-H2	120.3	C4-C3-C2	121.1(12)
C4-C3-H3	119.4	C2-C3-H3	119.5
C5-C6-C1	120.4(10)	C5-C6-C7	135.1(11)
C1-C6-C7	104.5(10)	C3-C4-C5	120.9(13)
C3-C4-H4	119.6	C5-C4-H4	119.6
C4-C5-C6	118.6(12)	C4-C5-H5	120.7
C6-C5-H5	120.7	N2-C8-C7	108.8(9)
N2-C8-C9	123.5(9)	C7-C8-C9	127.3(9)
C8-C7-C6	107.3(9)	C8-C7-P1	120.1(8)
C6-C7-P1	132.2(8)	C10-C9-C14	118.3(10)
C10-C9-C8	124.0(9)	C14-C9-C8	117.5(10)
C9-C10-C11	118.1(10)	C9-C10-C15	125.1(9)
C11-C10-C15	116.8(10)	C12-C11-C10	121.6(12)
C12-C11-H11	119.2	C10-C11-H11	119.2
C13-C14-C9	121.9(12)	C13-C14-H14	119.1
C9-C14-H14	119.1	C17-C16-C15	117.7(10)
C17-C16-P1	122.1(8)	C15-C16-P1	120.1(8)
C20-C19-C18	120.0(12)	C20-C19-H19	120.0
C18-C19-H19	120.0	C19-C20-C15	122.0(11)
C19-C20-H20	119.0	C15-C20-H20	119.0
C19-C18-C17	120.3(12)	C19-C18-H18	119.9
C17-C18-H18	119.9	C22-C21-C26	120.0(10)
C22-C21-P1	120.5(9)	C26-C21-P1	119.5(8)
C24-C25-C26	120.1(12)	C24-C25-H25	120.0
C26-C25-H25	120.0	C25-C24-C23	120.7(12)
C25-C24-H24	119.6	C23-C24-H24	119.6
C24-C23-C22	120.5(12)	C24-C23-H23	119.7
C22-C23-H23	119.7	C28-C27-C32	120.3(11)
C28-C27-P1	119.9(10)	C32-C27-P1	119.7(8)
C27-C28-C29	117.6(14)	C27-C28-H28	121.2
C29-C28-H28	121.2	C31-C32-C27	119.2(13)
C31-C32-H32	120.4	C27-C32-H32	120.4
C30-C31-C32	121.8(15)	C30-C31-H31	119.1
C32-C31-H31	119.1	C28-C29-C30	121.7(15)
C28-C29-H29	119.1	C30-C29-H29	119.2
C31-C30-C29	119.4(14)	C31-C30-H30	120.3

C29-C30-H30	120.3	C12-C13-C14	118.3(12)
C12-C13-H13	120.8	C14-C13-H13	120.8
C13-C12-C11	121.8(12)	C13-C12-H12	119.1
C11-C12-H12	119.1	F3-C34-F1	114.4(14)
F3-C34-S1	115.9(15)	F1-C34-S1	115.3(12)
F3-C34-F2	103.6(13)	F1-C34-F2	107.5(14)
S1-C34-F2	97.5(11)	O2-S1-O3	129.1(15)
O2-S1-C34	116.8(13)	O3-S1-C34	79.2(18)
O2-S1-O1	116.8(16)	O3-S1-O1	107.5(8)
C34-S1-O1	97.2(9)		

Table S29: Torsion angles (°) for 2i

C8-N2-C1-C6	-2.1(13)	C33-N2-C1-C6	-176.7(10)
C8-N2-C1-C2	176.1(12)	C33-N2-C1-C2	1.5(19)
N2-C1-C2-C3	-179.5(12)	C6-C1-C2-C3	-1.5(19)
C1-C2-C3-C4	-2.(2)	N2-C1-C6-C5	-177.9(10)
C2-C1-C6-C5	3.7(18)	N2-C1-C6-C7	1.7(13)
C2-C1-C6-C7	-176.7(10)	C2-C3-C4-C5	4.(2)
C3-C4-C5-C6	-2.(2)	C1-C6-C5-C4	-2.2(19)
C7-C6-C5-C4	178.5(13)	C1-N2-C8-C7	1.6(13)
C33-N2-C8-C7	175.9(10)	C1-N2-C8-C9	175.1(10)
C33-N2-C8-C9	-10.5(17)	N2-C8-C7-C6	-0.5(13)
C9-C8-C7-C6	-173.7(10)	N2-C8-C7-P1	-174.1(7)
C9-C8-C7-P1	12.7(17)	C5-C6-C7-C8	178.7(13)
C1-C6-C7-C8	-0.7(13)	C5-C6-C7-P1	-9.(2)
C1-C6-C7-P1	171.8(9)	C27-P1-C7-C8	172.0(10)
C16-P1-C7-C8	52.5(11)	C21-P1-C7-C8	-64.6(11)
C27-P1-C7-C6	0.2(14)	C16-P1-C7-C6	-119.3(12)
C21-P1-C7-C6	123.6(11)	N2-C8-C9-C10	138.5(11)
C7-C8-C9-C10	-49.2(18)	N2-C8-C9-C14	-46.5(16)
C7-C8-C9-C14	125.8(13)	C14-C9-C10-C11	2.6(16)
C8-C9-C10-C11	177.6(11)	C14-C9-C10-C15	-179.6(11)
C8-C9-C10-C15	-4.6(17)	C20-C15-C10-C9	-134.1(11)
C16-C15-C10-C9	51.9(15)	C20-C15-C10-C11	43.7(14)
C16-C15-C10-C11	-130.3(11)	C9-C10-C11-C12	-1.0(18)
C15-C10-C11-C12	-179.0(12)	C10-C9-C14-C13	-3.0(18)
C8-C9-C14-C13	-178.3(12)	C18-C17-C16-C15	-0.4(15)
C18-C17-C16-P1	-176.7(9)	C20-C15-C16-C17	0.1(14)
C10-C15-C16-C17	174.0(9)	C20-C15-C16-P1	176.4(7)
C10-C15-C16-P1	-9.7(13)	C7-P1-C16-C17	122.3(9)
C27-P1-C16-C17	3.2(10)	C21-P1-C16-C17	-116.5(8)
C7-P1-C16-C15	-53.9(9)	C27-P1-C16-C15	-172.9(8)
C21-P1-C16-C15	67.4(9)	C18-C19-C20-C15	1.4(17)
C16-C15-C20-C19	-0.6(15)	C10-C15-C20-C19	-174.9(10)
C20-C19-C18-C17	-1.8(18)	C16-C17-C18-C19	1.3(17)
C23-C22-C21-C26	1.0(17)	C23-C22-C21-P1	-179.9(9)
C25-C26-C21-C22	-0.4(15)	C25-C26-C21-P1	-179.5(8)
C7-P1-C21-C22	158.1(9)	C27-P1-C21-C22	-79.0(10)
C16-P1-C21-C22	40.7(10)	C7-P1-C21-C26	-22.8(10)
C27-P1-C21-C26	100.1(9)	C16-P1-C21-C26	-140.2(8)
C21-C26-C25-C24	0.0(17)	C26-C25-C24-C23	-0.4(19)
C25-C24-C23-C22	1.(2)	C21-C22-C23-C24	-1.4(19)

C7-P1-C27-C28	-64.4(11)	C16-P1-C27-C28	53.1(11)
C21-P1-C27-C28	170.6(10)	C7-P1-C27-C32	111.1(10)
C16-P1-C27-C32	-131.4(10)	C21-P1-C27-C32	-13.9(11)
C32-C27-C28-C29	1.6(19)	P1-C27-C28-C29	177.1(11)
C28-C27-C32-C31	0.(2)	P1-C27-C32-C31	-175.4(11)
C27-C32-C31-C30	-3.(2)	C27-C28-C29-C30	-1.(2)
C32-C31-C30-C29	3.(3)	C28-C29-C30-C31	-1.(3)
C9-C14-C13-C12	2.(2)	C14-C13-C12-C11	0.(2)
C10-C11-C12-C13	0.(2)	F3-C34-S1-O2	-54.(2)
F1-C34-S1-O2	168.9(18)	F2-C34-S1-O2	55.5(17)
F3-C34-S1-O3	74.8(15)	F1-C34-S1-O3	-62.6(16)
F2-C34-S1-O3	-176.0(11)	F3-C34-S1-O1	-178.6(13)
F1-C34-S1-O1	43.9(16)	F2-C34-S1-O1	-69.5(10)

Table S30: Anisotropic atomic displacement parameters (\AA^2) for 2i. The anisotropic atomic displacement factor exponent takes the form: $-2\pi^2 [h^2 a^{*2} U_{11} + \dots + 2 h k a^* b^* U_{12}]$

	U₁₁	U₂₂	U₃₃	U₂₃	U₁₃	U₁₂
P1	0.0553(16)	0.0461(16)	0.066(2)	0.0053(16)	0.0272(13)	0.0040(11)
N2	0.059(5)	0.060(6)	0.064(7)	0.005(5)	0.022(4)	-0.012(4)
C26	0.061(7)	0.050(6)	0.069(9)	-0.010(6)	0.027(6)	0.004(5)
C17	0.060(7)	0.052(7)	0.084(10)	0.008(7)	0.028(6)	0.007(5)
C22	0.061(7)	0.053(7)	0.096(10)	-0.005(7)	0.025(6)	-0.007(5)
C33	0.071(8)	0.092(9)	0.078(10)	0.005(8)	0.024(6)	-0.026(6)
C15	0.061(6)	0.036(6)	0.055(8)	-0.006(6)	0.026(5)	-0.002(4)
C1	0.065(7)	0.045(7)	0.064(9)	0.005(6)	0.014(6)	-0.014(5)
C2	0.114(11)	0.055(8)	0.070(10)	-0.003(7)	0.019(8)	-0.022(7)
C3	0.144(13)	0.036(7)	0.080(11)	-0.006(7)	0.042(9)	-0.001(8)
C6	0.083(8)	0.045(7)	0.064(9)	0.000(6)	0.024(6)	0.000(6)
C4	0.154(14)	0.043(8)	0.081(12)	0.006(8)	0.045(10)	0.007(8)
C5	0.102(9)	0.051(7)	0.069(10)	-0.002(7)	0.032(7)	0.001(6)
C8	0.056(6)	0.053(7)	0.061(8)	0.008(6)	0.022(5)	-0.005(5)
C7	0.059(6)	0.041(6)	0.071(9)	0.000(6)	0.025(5)	-0.004(4)
C9	0.053(6)	0.052(7)	0.065(8)	0.009(6)	0.028(5)	0.003(5)
C10	0.058(6)	0.049(6)	0.075(9)	-0.004(6)	0.034(6)	0.000(5)
C11	0.093(9)	0.060(8)	0.108(12)	-0.021(8)	0.061(8)	0.004(6)
C14	0.060(7)	0.079(8)	0.096(11)	0.019(8)	0.025(6)	0.003(6)
C16	0.058(6)	0.041(6)	0.058(8)	-0.004(6)	0.022(5)	-0.005(4)
C19	0.102(10)	0.056(7)	0.052(9)	-0.007(7)	0.011(7)	-0.010(6)
C20	0.094(9)	0.048(7)	0.065(9)	0.000(7)	0.042(7)	-0.005(6)
C18	0.080(8)	0.060(8)	0.066(10)	-0.014(7)	0.013(7)	-0.004(6)
C21	0.054(6)	0.050(6)	0.059(8)	-0.002(6)	0.030(5)	-0.005(5)
C25	0.064(7)	0.074(9)	0.084(10)	0.002(8)	0.019(6)	0.010(6)
C24	0.069(8)	0.076(9)	0.092(11)	0.013(8)	0.031(7)	0.018(7)
C23	0.094(10)	0.050(7)	0.109(12)	0.004(8)	0.042(9)	0.003(7)
C27	0.066(7)	0.058(7)	0.072(10)	0.008(7)	0.031(6)	0.012(5)
C28	0.088(9)	0.083(9)	0.079(10)	0.013(8)	0.028(7)	0.035(7)
C32	0.088(9)	0.089(9)	0.075(11)	0.015(8)	0.043(7)	0.033(7)
C31	0.108(11)	0.143(14)	0.090(12)	0.005(11)	0.057(9)	0.039(10)
C29	0.085(10)	0.124(13)	0.133(17)	-0.005(12)	0.032(10)	0.046(9)
C30	0.108(13)	0.189(19)	0.126(17)	0.013(15)	0.068(12)	0.064(12)
F1	0.174(13)	0.261(17)	0.41(3)	0.202(18)	0.096(15)	0.051(12)
C13	0.051(7)	0.105(11)	0.127(13)	0.009(10)	0.030(8)	0.018(7)

C12	0.068(9)	0.085(10)	0.144(15)	0.013(10)	0.044(9)	0.027(8)
C34	0.018(7)	0.137(17)	0.34(4)	0.12(2)	-0.016(12)	-0.006(8)
S1	0.266(14)	0.70(4)	0.37(2)	-0.12(2)	0.061(14)	0.29(2)
O1	0.134(11)	0.124(10)	0.301(19)	0.049(11)	0.087(12)	0.023(8)
O2	0.64(5)	0.66(5)	0.162(16)	0.05(2)	0.05(2)	0.60(5)
F3	0.105(11)	0.195(16)	1.35(9)	-0.19(3)	0.12(3)	-0.035(10)
F2	0.31(2)	0.30(2)	0.33(2)	-0.199(18)	-0.157(17)	0.203(18)
O3	0.101(12)	0.24(2)	0.45(4)	0.10(2)	-0.158(18)	-0.069(13)

Table S31: Hydrogen atomic coordinates and isotropic atomic displacement parameters (\AA^2) for 2i.

	x/a	y/b	z/c	U(eq)
H26	0.1924	0.3850	0.3296	0.07
H17	0.5922	0.3993	0.8446	0.077
H22	0.4264	0.4811	0.5664	0.084
H33A	-0.0122	0.2837	0.6324	0.121
H33B	0.0432	0.3177	0.7771	0.121
H33C	0.0671	0.2606	0.7874	0.121
H2	0.1311	0.1949	0.6504	0.099
H3	0.2498	0.1435	0.5799	0.102
H4	0.3866	0.1750	0.4934	0.109
H5	0.4217	0.2594	0.5037	0.087
H11	0.2115	0.4980	0.8359	0.096
H14	-0.0001	0.3735	0.5422	0.094
H19	0.5124	0.4578	1.1979	0.088
H20	0.3279	0.4553	1.0545	0.078
H18	0.6444	0.4319	1.0892	0.085
H25	0.1113	0.4479	0.1511	0.09
H24	0.1879	0.5252	0.1832	0.093
H23	0.3418	0.5424	0.3905	0.099
H28	0.5600	0.3146	0.7620	0.1
H32	0.4663	0.3873	0.3485	0.096
H31	0.6084	0.3496	0.2857	0.129
H29	0.7087	0.2809	0.6937	0.138
H30	0.7340	0.2999	0.4615	0.16
H13	-0.0809	0.4482	0.5660	0.113
H12	0.0270	0.5093	0.7125	0.116

9. References

- 1 J. Desroches, A. Gilbert, C. Houle and J.-F. Paquin, *Synthesis (Stuttg.)*, 2017, **49**, 4827–4844.
- 2 C. Baillie and J. Xiao, *Tetrahedron*, 2004, **60**, 4159–4168.
- 3 X.-L. Huang, C. Li, J. Wang and S.-D. Yang, *Synthesis (Stuttg.)*, 2022, **54**, 4711–4720.
- 4 K. Górski, J. Mech-Piskorz, K. Noworyta, B. Leśniewska and M. Pietraszkiewicz, *New J. Chem.*, 2018, **42**, 5844–5852.
- 5 C. Fan, F. Zhao, P. Gan, S. Yang, T. Liu, C. Zhong, D. Ma, J. Qin and C. Yang, *Chem. – A Eur. J.*, 2012, **18**, 5510–5514.
- 6 Y. Okuda, T. Sato, S. Takebe, M. Mori, M. Fujimoto, K. Masuda, T. Sabato, K. Wakamatsu, H. Akashi and A. Orita, *J. Org. Chem.*, 2024, **89**, 7747–7757.
- 7 C. Han, Z. Zhang, H. Xu, G. Xie, J. Li, Y. Zhao, Z. Deng, S. Liu and P. Yan, *Chem. – A Eur. J.*, 2013, **19**, 141–154.
- 8 D. N. Coventry, A. S. Batsanov, A. E. Goeta, J. A. K. Howard, T. B. Marder and R. N. Perutz, *Chem. Commun.*, 2005, 2172.
- 9 WO 2010/038956 A2, .
- 10 T. Iwai, R. Tanaka and M. Sawamura, *Organometallics*, 2016, **35**, 3959–3969.
- 11 H. Gross, *Chem. Ber.*, 1962, **95**, 2270–2275.
- 12 P. Boontiem and S. Kiatisevi, *Inorganica Chim. Acta*, 2020, **506**, 119538.
- 13 C. Møller and M. S. Plesset, *Phys. Rev.*, 1934, **46**, 618–622.
- 14 J. Schirmer, *Phys. Rev. A*, 1982, **26**, 2395–2416.
- 15 A. B. Trofimov and J. Schirmer, *J. Phys. B At. Mol. Opt. Phys.*, 1995, **28**, 2299–2324.
- 16 C. Hättig, in *Advances in Quantum Chemistry*, 2005, vol. 50, pp. 37–60.
- 17 TURBOMOLE GmbH, TURBOMOLE V7.0, a development of University of Karlsruhe and Forschungszentrum Karlsruhe GmbH, 1989-2007, <https://www.turbomole.org/>.